# Functional dissection of transcriptional regulation during normal and malignant T-cell development

An integrative (epi)genomic approach

Kaat Durinck

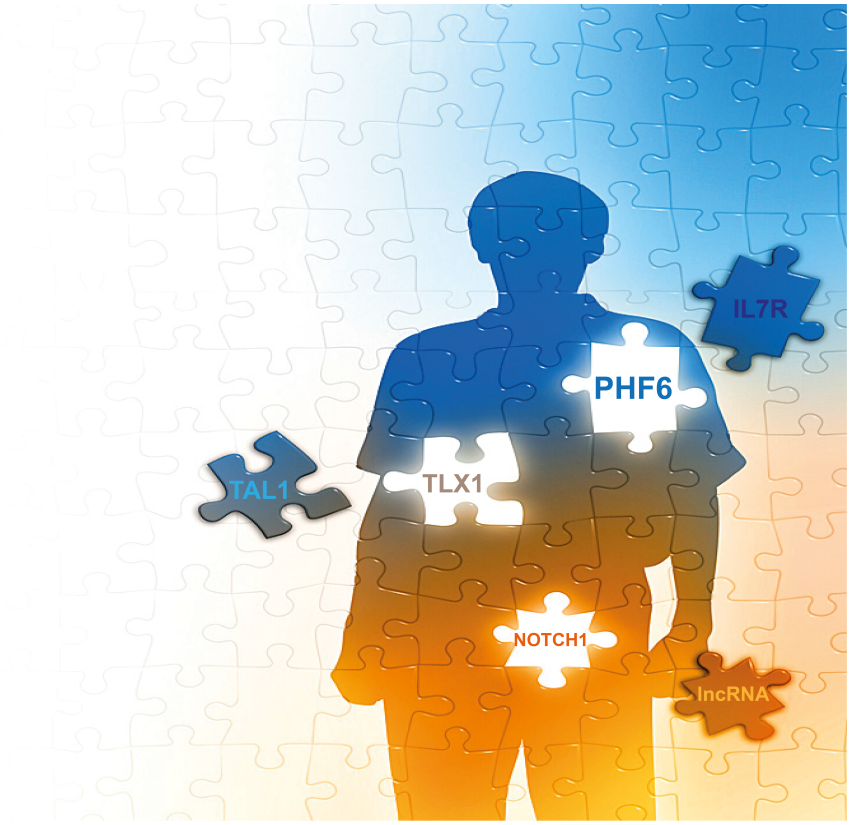

Ghent University, Faculty of Medicine and Health Sciences

# Functional dissection of transcriptional regulation during normal and malignant T-cell development

## An integrative (epi)genomic approach

This thesis is submitted as fulfillment of the requirements for the degree of Doctor in Medical Sciences by Kaat Durinck, 2016

Promotor
prof. dr. Frank Speleman

Co-promotors
prof. dr. ir. Pieter van Vlierberghe
prof. dr. Tom Taghon

Thesis submitted to fulfill the requirements for the degree of Doctor in Medical Sciences

Promotor: prof. dr. Frank Speleman
Ghent University, Belgium

Co-promotors: prof. dr. ir. Pieter van Vlierberghe
Ghent University, Belgium

prof. dr. Tom Taghon
Ghent University, Belgium

Members of the examination committee:

prof. dr. Panagiotis Ntziachristos
Feinberg School of Medicine, Chicago, USA

prof. dr. Marc Mansour
University College London, UK

prof. dr. Kim De Keersmaecker
KULeuven, Belgium

prof. dr. Jan Philippé
Ghent University, Belgium

prof. dr. Katleen De Preter
Ghent University, Belgium

prof. dr. Pieter Mestdagh
Ghent University, Belgium

dr. Morgan Thénoz
Ghent University, Belgium

The research described in this thesis was conducted at the Center for Medical Genetics, Ghent University, Ghent, Belgium.

This work was supported by the Fund for Innovation, Science and Technology (IWT) Flanders (PhD grant to Kaat Durinck); the Fund for Scientific Research (FWO) Flanders (project grant); the Flemisch League against Cancer (VLK) (PhD grant to Kaat Durinck and project grant); the Belgian Program of Interuniversity Poles of Attraction (IUAP).

# Table of Contents

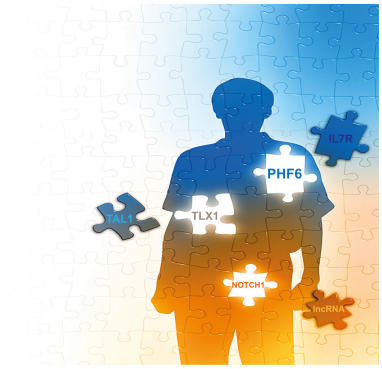


# CHAPTER 1

## Introduction

# PART I: General introduction

## 1. The role of the (epi)genetic landscape in normal development

*1.1 Deciphering the 'code' of the epigenome*

The revolutionary concept of the 'epigenetic landscape', raised by Conrad Waddington more than fifty years ago, was fundamental in the understanding of the processes controlling and driving the development of a multicellular organism, consisting of a large diversity of different cell types that arise from the pool of pluripotent stem cells, exerting distinct cellular functions while harboring a (nearly) identical genetic program. The transition from stem cells to a fully differentiated cell type requires orchestration and fine-tuning of transcriptional programs conveyed by transcription factors interacting with various DNA regulatory elements embedded in a specific epigenetic constellation, whereas mutations affecting the genetic information of the cell would rewire or distort the cellular differentiation path[1,2]. The epigenetic landscape therefore plays a crucial role in the spatio-temporal regulation of gene expression to safeguard normal development and homeostasis. Important phenomena such as X-chromosome inactivation and paternal/maternal imprinting of loci are classic examples of epigenetically controlled processes required for accurate gene dosage regulation[3-5]. X-chromosome inactivation in females is a process that randomly silences one of the two X-chromosomes during early embryogenesis and involves coating of the chromosome by the non-coding RNA *XIST* as well as DNA and histone methylation[5].

The epigenetic code is a constellation of DNA methylation patterns in combination with a variety of post-translational modifications on the N-terminal tails of the core histone proteins H2A, H2B, H3 and H4. The core histones assemble into octamers to form nucleosomes covered with stretches of genomic DNA of about 147bp in size. The nucleosome is a repeating unit within the chromatin fiber and this structural organization allows DNA compaction[6]. Along the chromatin template, domains of euchromatin and heterochromatin can be distinguished, delineating active and transcriptionally silent regions respectively[5], as demarcated by specific epigenetic

modifications and nucleosome positioning at these sites. The chemical modification of the DNA backbone by cytosine methylation forms the basis of the epigenetic landscape. Methyl-binding domain (MBD) proteins (MBD1, MBD2, MD3, MBD4 and MecP2) mediate transcriptional silencing by recruiting histone deacetylases and histone methyltransferases that mediate the formation of a compact chromatin structure[7]. In mammals, DNA-methylation patterns are newly established by the DNA methyltransferase 3 (DNMT3) family members and maintained over mitotic divisions by DNMT1[8]. DNA methylation occurs at about 70-80% of all CpG dinucleotides genome-wide[8]. Clusters of CpG sites mainly occur at promoter regions, termed CpG islands. Unmethylated CpG islands, together with gene body methylation, mark regions of active gene expression[9]. For a long time, cytosine methylation was considered as a stable modification[10]. Instead, it is now known that also DNA demethylation plays an important role in normal development and cancer, underlying genomic instability[11]. Demethylation of the DNA template can occur either actively or passively. Passive DNA demethylation can occur during DNA replication. Instead, active DNA demethylation is a consequence of the catalytic activity of the 'Ten Eleven Translocation' (TET) protein family (TET1, TET2, TET3). These TET enzymes convert 5-methylcytosine (5mC) to the intermediate 5-hydroxymethylcytosine (5hmC), which can be further oxidized to 5-formylcytosine and 5-carboxylcytosine[12]. These oxidation products can then be efficiently removed from the DNA template by the activity of the 'thymine DNA glycosylase' (TDG) enzyme and replaced by an unmethylated cytosine residue during DNA repair (base excission repair). In addition, active DNA demethylation can also be the consequence of the conversion of 5hmC to 5-hydroxymethyluridine by the 'activation-induced cytidine deaminase' (AID) enzymes and coupled DNA repair[12]. Passive DNA-demethylation by TET enzymes is rather a consequence of the conversion they mediate of 5mC to 5hmC, which inhibits the DNA maintenance methyltransferase DNMT1 from further DNA association[13].

The second layer of the epigenetic landscape is embedded within a series of post-translational modifications (PTMs) that are displayed at the N-terminal tails of the core histone proteins to form the so-called 'histone code'[14]. In addition, a variety of

histone variants can replace the canonical ones, such as the H2A variant H2AX, which is incorporated into the nucleosomes at sites where DNA double-strand breaks occur[15] (**Figure 1A**). There are at least eight different types of PTMs possible on histone tails such as lysine acetylation, lysine and arginine methylation, serine and threonine phosphorylation amongst others, that can be of different forms (eg di- or tri-methylation)[16]. Particular modifications can mark regions of active/inactive transcription. For example, active genes are marked by lysine acetylation at the histone H3 and H4 tails, tri-methylation of lysine 4 of histone H3 (H3K4me3) and lysine 36 of histone H3 (H3K36me3) amongst others. In contrast, transcriptionally silent regions carry high levels of tri-methylation of H3 lysine 9 (H3K9me3) and 27 (H3K27me3)[17]. Moreover, histone modifications are also specific in demarcating various functional elements in the genome such as enhancers or transcribed regions[18]. For example, H3K4me3 deposition is highly correlated to the presence of unmethylated CpG islands at active promoter regions[17] (**Figure 1B**).

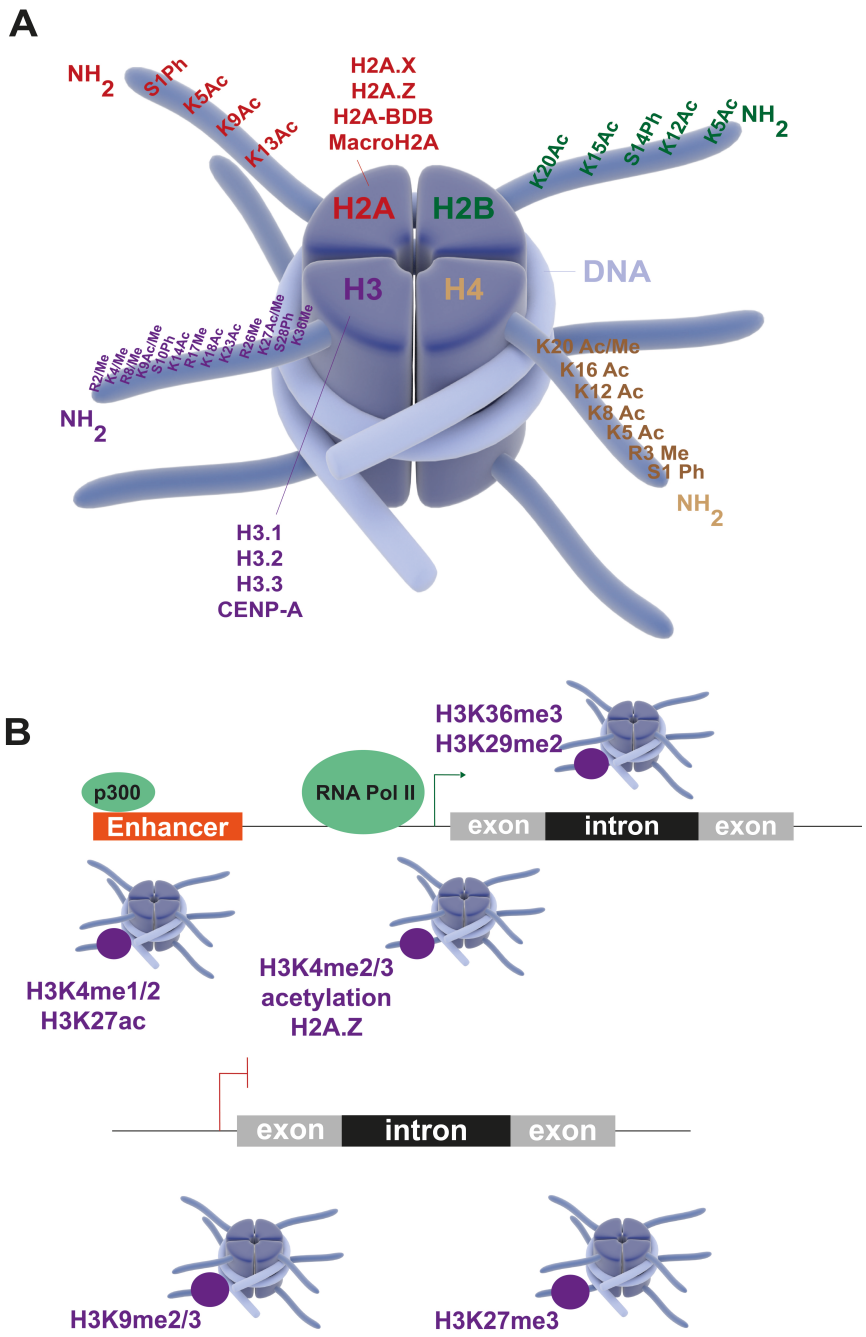


**Figure 1**: Histone PTMs (eg. methylation, acetylation, phosphorylation, …) and variants (eg. H3.3, H2AZ, …) (**A**) demarcate various functional elements in the genome (**B**): specific constellations of histone modifications discriminate inactive/active promoter and enhancer regions. Adapted from Tollervey et al. (Epigenetics, 2012)[3] and Zhou et al. (Nature Reviews Genetics, 2011)[18].

Histone modifications are dynamic in nature and a plethora of histone modifier enzymes have been identified in the last decades that are involved in the deposition ('writers') or removal of the histone PTMs ('erasers') (**Figure 2**). For example, the Polycomb group protein complex 2 (PRC2) component EZH2 is a key regulatory

entity involved in gene silencing during normal differentiation by catalyzing the deposition of the H3K27me3 mark[19]. A third class of proteins can dock to certain histone modifications through a specific binding domain, but have no intrinsic enzymatic activity ('readers') and therefore recruit writers and erasers to control the expression state of their targets. For example, the plant homeodomain (PHD) and chromodomain are the two most commonly found histone methyl-lysine binding domains[20,21].

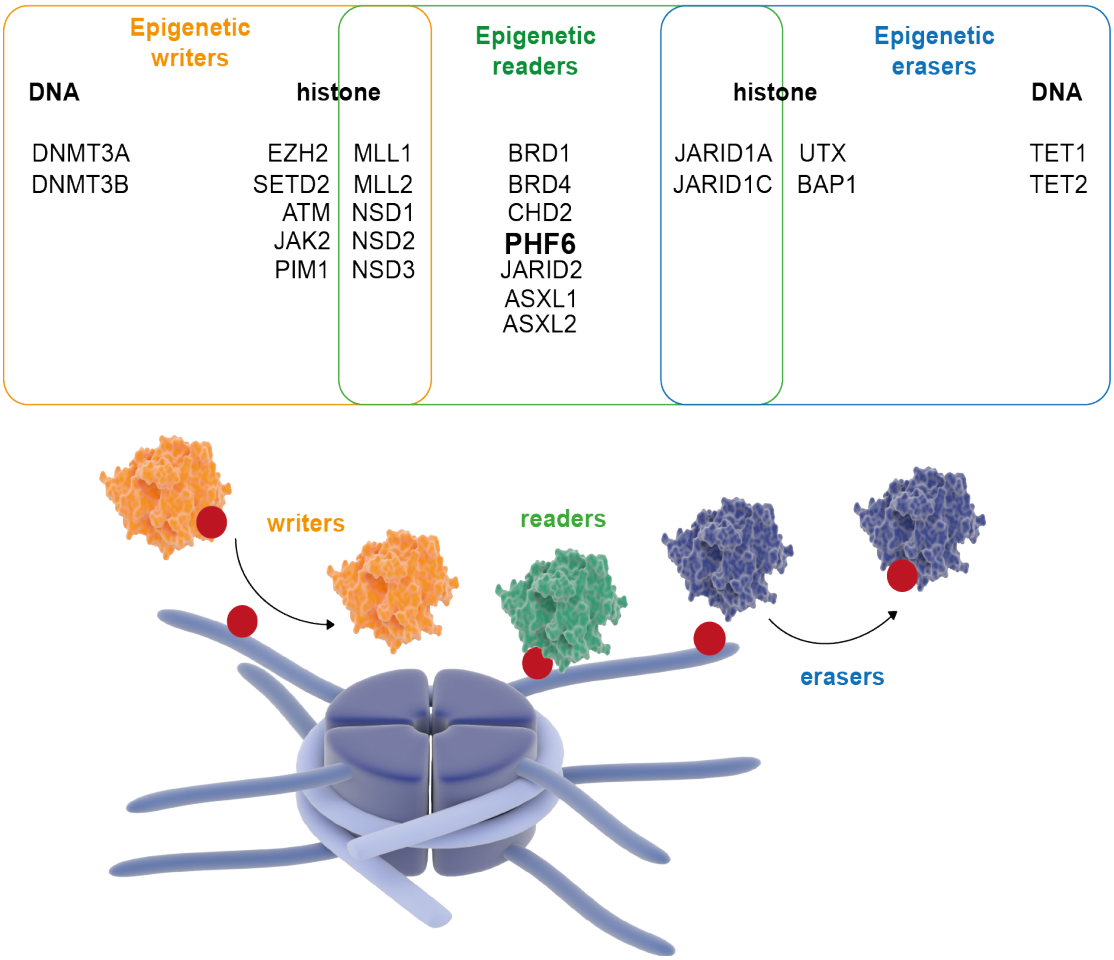


**Figure 2**: Histone modifier enzymes can be classified as epigenetic writers, readers and erasers. 'Writers' and 'erasers' are chromatin modifiers that have intrinsic catalytic activity and can deposit or remove specific histone modifications respectively. Epigenetic 'reader' proteins lack the capability of catalyzing the deposition of post-translational modifications on the N-terminal histone tails, but can recognize and bind to a specific histone PTM through a specialized binding domain. Adapted from Fong et al. (Haematologica, 2014)[21].

## Chapter 1: Introduction

Dynamic regulation of the chromatin template is important at the level of transcription, translation and DNA-repair[22]. Depending on the constellation or cross-talk between the different histone modifications at a specific site, different chromatin modifiers or chromatin remodelers are recruited or occluded for binding to the chromatin template[16]. Chromatin remodeling complexes are a specific class of chromatin regulators that catalyze the eviction or deposition of nucleosomes coupled to ATP-hydrolysis. Four major chromatin remodeler complexes are currently known: the 'Switching defective/Sucrose Non-Fermenting' (SWI/SNF) family, 'Inositol requiring 80' (INO80), 'Imitation Switch' (ISWI) and the 'Chromodomain helicase' (CHD) family[23]. Each of these chromatin remodeler complexes can exert diverse functions during normal human development. For example, INO80 complexes are known to be involved in cellular processes such as chromosome segregation and cell cycle checkpoint control[24]. Also SWI-SNF complexes are crucial in mammalian development, with evidence for a role in various tissues such as in development of heart and muscles, neuronal development and hematopoiesis[25].

### *1.2 Coordinated activity of hematopoietic master regulators within a dynamic epigenomic landscape is essential for normal hematopoietic lineage development*

Epigenetic gene expression regulation is very crucial in the context of a plethora of normal developmental programs, including the process of hematopoiesis[26]. During normal hematopoietic lineage specification, a series of gene expression programs are strictly orchestrated and fine-tuned to direct cell potential in a hierarchical manner to generate a specialized set of effector cells (**Figure 3**). For example, generation of the T-cell repertoire requires homing of bone marrow derived hematopoietic progenitor cells to the thymus microenvironment with subsequent proliferation and differentiation across different developmental phases involving the pool of early T-cell progenitors (ETP) that enter the thymus, over the double negative stages DN2a/2b and DN3a/3b towards the development of double positive ($CD4^+CD8^+$, DP) T-cells expressing a functional alpha-beta T-cell receptor ($\alpha\beta$ $TCR^+$). Survival and proliferation of DN1 and DN2 cells is supported by the interleukin-7 receptor (IL7R). During the DN3 stage, a functional pre-TCR complex is generated

that leads to the generation of DN4 stage cells. These DN4 cells will express both CD4 and CD8 molecules at their surface to become DP stage T-cells. These DP cells will eventually undergo further TCR-rearrangements, leading to the expression of a mature TCR αβ receptor, which triggers the maturation towards single positive CD4 or CD8 T-cells[27]. Naïve $CD4^+$ and $CD8^+$ single positive lymphocytes emigrate from the thymus to the secondary lymphoid organs. There, $CD4^+$ T-cells will either differentiate into T-helper (Th) type 1 or 2 cells, whereas $CD8^+$ cells will evolve to cytotoxic effector T-cells.

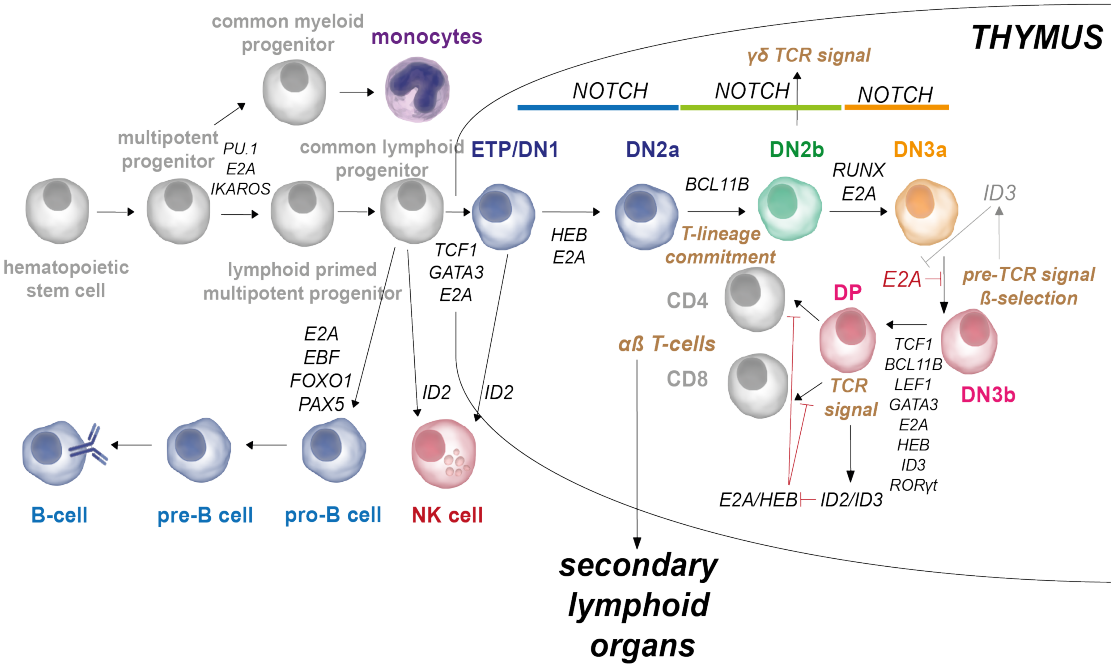


**Figure 3**: Diagram of normal hematopoietic lineage development focusing on thymocyte progenitors entering the thymus microenvironment with indication of the key transcriptional regulators involved in different phases of lineage commitment. Blood lineage development is a hierarchical differentiation process starting from the hematopoietic stem cell (HSC) that gives rise to the branches of the lymphoid and myeloid lineages. From the common myeloid progenitor, amongst others monocytes (purple) arise that take part in the innate immune response. Increased PU.1 transcription factor activity will favor monocytic commitment. In contrast, the common lymphoid progenitor will give rise to the T-, B- and NK-cell lineages. The transcription factor E2A for example will trigger the initiation of B-lymphopoiesis. In mammals, TCF1 is exclusively expressed in T-lymphocytes and is a critical gatekeeper of the T-cell fate from the stage of thymus seeding to the development of effector T-cells. Adapted from Yui and Rothenberg (Nature Reviews Immunology, 2014)[27].

## Chapter 1: Introduction

The most important factor controlling entrance of the T-cell developmental program is NOTCH1[28]. In humans, NOTCH1 belongs to a family of four transmembrane receptors (NOTCH1-4) that are activated by ligands that either belong to the Serrate-like (Jagged 1 or 2) or the Delta-like ligand (DLL1, DLL3 and DLL4) families[29]. Briefly, NOTCH1 signaling is triggered by activation of the receptor by one of the previously mentioned ligands, which subsequently results in successive receptor cleavages by ADAM-metalloproteases and the γ-secretase complex, ultimately leading to the formation and release of the intracellular NOTCH1 fragment (ICN1) (**Figure 4**). Next, ICN1 will translocate to the nucleus and act as a transcriptional regulator in concert with co-factors such as 'Mastermind-like' (MAML), 'Suppressor of Hairless' (CSL) and 'Recombination Signal binding Protein for Immunoglobulin Kappa J region' (RBPJκ) to regulate the expression of canonical targets such as *c-MYC*, *DTX1*, *HES1*, *CCND3*[30,31] and *IL7R*[32,33]. The E3 ubiquitin ligase 'F-box and WD repeat domain containing 7' (FBXW7) is required for NOTCH1 receptor turnover as it targets the receptor for proteasomal degradation. In this respect, the PEST domain of the NOTCH1 receptor tags the protein for FBXW7 mediated proteasomal degradation[34]. A 'PEST' sequence is composed of a stretch of proline, glutamic acid, serine and threonine amino acid residues that will target a protein for proteolytic degradation[35]. This signaling cascade is strongly evolutionary conserved and mutations that affect this pathway occur in a variety of human malignancies[36]. For the NOTCH1 receptor itself, both the heterodimerization domain as well as the PEST domain are hotspots for gain-of-function mutations[37]. NOTCH1 signaling is crucial to drive hematopoietic progenitors into the T-cell lineage at the expense of development towards other blood lineages. Moreover, it also assists in TCR-mediated selection, lineage commitment and final T-cell differentiation[38].

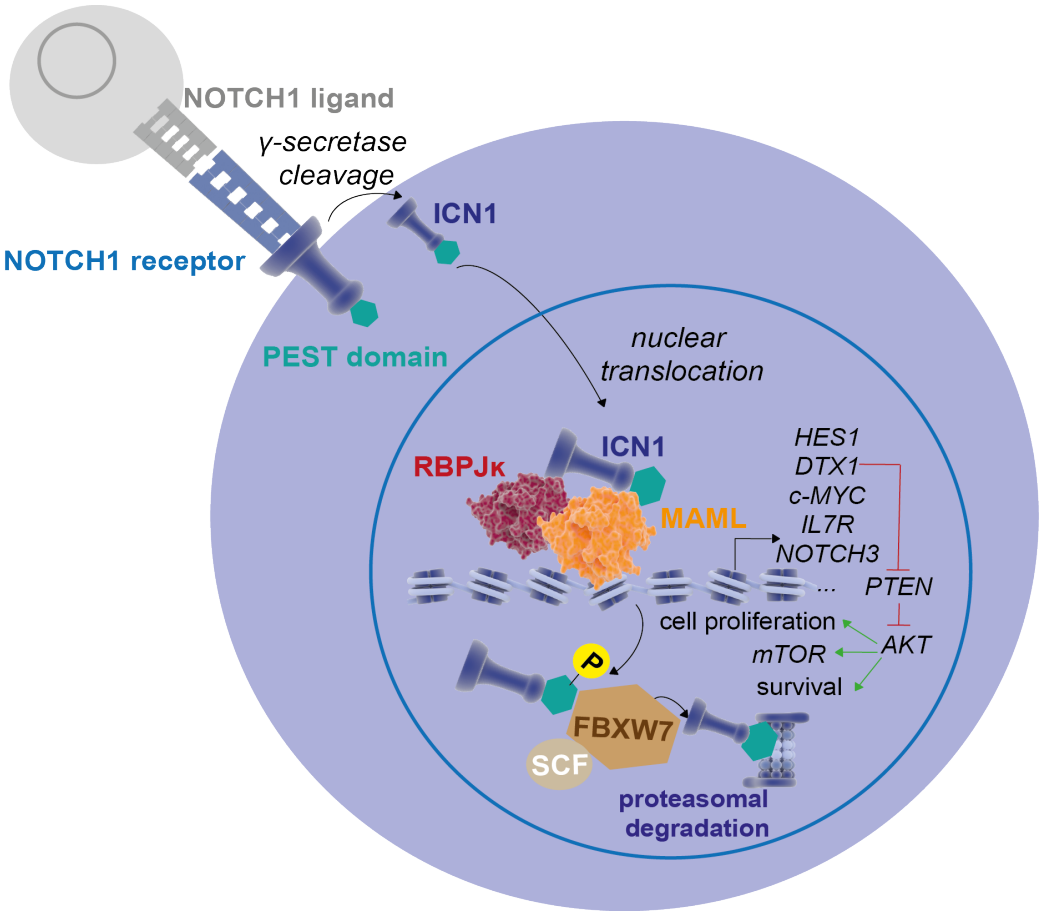


**Figure 4**: The NOTCH1 signaling pathway is an evolutionary conserved pathway in multicellular organisms. In brief, upon association of a suitable ligand (Delta or Serrate like family) to the transmembrane NOTCH1 receptor, successive proteolytic cleavage reactions are initiated that eventually lead to the formation of the intracellular NOTCH1 fragment (ICN1). This ICN1 component can translocate to the nucleus and assembles towards a transcriptonal regulatory complex by association with its co-factors RBPJκ and MAML, thereby activating the expression of amongst others canonical target genes such as *HES1*, *DTX1*, *NOTCH3*, *CCND3*, … The ICN1 fragment also contains a PEST domain (green) which targets this protein for proteolytic degradation upon recognition and association with the FBXW7 E3 ubiquitin ligase. Adapted from Palomero and Ferrando (Clinical Cancer Research, 2008)[33].

In concert with NOTCH1, other master regulators are essential to guide the expression programs required for specification and maintenance of T-cell identity. Several key transcriptional regulators are required across different T-cell developmental phases and a specific active constellation of transcription factors is required to establish the correct gene expression network for each stage. Three main transcriptional regulators are required to ensure correct T-cell specification:

BCL11B plays a crucial role in T-cell lineage commitment, while GATA3 and TCF-1 are essential drivers in the T-cell differentiation process. GATA3 exerts at least three major roles in normal T-cell development: specification of precursors cells to the T-cell lineage, during TCR-αβ dependent positive selection and in the maturation of Th2 effector cells[28]. The key factors required at the final stages of T-cell differentiation and T-cell maturation are the transcriptional regulators HEB, E2A and LEF1 amongst others in concert with BCL11B, TCF-1 and GATA3[27]. Both E2A and HEB belong to the E protein family, binding to the E-box elements that are present in regulatory elements of many genes encoding key T-cell factors[39].

Gene expression regulation in the hematopoietic system not only involves the assembly of these transcriptional complexes on gene regulatory elements, but also depends on the accessibility of these regulators to their docking sites within the chromatin template. Coordinated interaction between lineage-specific transcription factors and the epigenetic landscape is thus required to secure correct checkpoint regulation[40]. At the level of DNA-methylation, DNMT1 has an essential role in T-cell maturation, as deletion of *Dnmt1* in double negative T-cells in a conditional knock-out mouse model, leads to massive de-methylation and a large reduction in cell numbers of double positive and more mature T-cell stages[41]. Lineage commitment also involves changes at the level of DNA-methylation. It has been shown that myeloid lineage commitment involves less global DNA-methylation in comparison to the lymphoid lineage[42]. For example, at the level of T-cell development, the TCR-loci of double-negative stage T-cells are methylated, while de-methylation of these sites is required to allow recombination for the formation of a functional pre-TCR complex[7]. In addition, also integrity of the chromatin structure is essential in support of normal T-cell development. This is nicely illustrated by the study of Gebuhr and co-workers[43] showing that deficiency for the SWI-SNF ATPase subunit Brg1 in mice leads to a block at the DN to DP stage transition and impairs processes downstream of pre-TCR signaling. In addition, it has been shown that loss of Snf5, another core component of the SWI-SNF complex, leads to development of mature $CD8^+$ T-cell lymphoma in 100% of the Snf5 deficient mice within a couple of weeks after knock-out[44].

# Chapter 1: Introduction

## 2. The epigenetic basis of cancer

### *2.1. The hallmarks of cancer*

The 'Hallmarks of Cancer' concept as proposed by Hanahan and Weinberg has provided a framework to understand the principles of cancer biology. The authors were among the first to make a synopsis starting from a bewildering and rapidly growing amount of genetic and biological data on the causes of cancer and behavior of tumor cells[45]. The initially proposed six biological features acquired along the multi-step process of tumor formation allow cancer cells to breech multiple cellular safeguards allowing for proliferation and cell renewal, unlimited growth, angiogenesis, invasion and metastasis and evasion of cell death[46]. Ten years after the initial publication and thousands of citations later, the authors added a number of further essential cellular traits acquired by most if not all cancer cells i.e. maintenance of genomic stability, sustained energy supply related to the rewired metabolic cancer cell circuitry and tumor promoting inflammation[45]. In addition, tumor cells are not isolated but are in continuous communication to their immediate surrounding thus inducing the formation of a tumor microenvironment. This microenvironment is constituted of the tumor cells, the tumoral stroma, blood vessels, inflammatory cells and associated tissue cells[47] and plays a crucial role both locally to escape from immunological defense mechanisms as well as to settle distal metastasis[48]. Since the tumor microenviroment plays a crucial role in oncogenesis and metastasis, this now also forms a novel target for cancer prevention and therapy[47].

### *2. 2. Genetic and epigenetic alterations as drivers of the cancer hallmarks*

The field of cancer genomics has rapidly evolved as a consequence of recent advances in sequencing technologies. Over the past decades, a comprehensive catalogue of somatic mutations has been established and underscored tumor heterogeneity across different tumor types and within a single tumor[49]. Tumors typically acquire a series of mutations over time. 'Gatekeeper' mutations arise first

and confer a growth advantage to normal cells at the start of malignant transformation. Uncontrolled proliferation of the established tumor cells is eventually supported by so-called 'driver' mutations. In keeping with the concept that cancer arises through (epi-)genetic alterations driving most if not all cancer hallmarks, the vast majority of tumor entities harbour multiple of these driver mutations. In addition, genomically unstable tumors and/or tumor cells arising through exposure to carcinogens (eg. smoke, UV-rays, …) like in lung cancer or melanoma development, can exhibit hundreds or more additional mutations which have no immediate obvious cellular advantage and are called passenger mutations[50]. Most of the driver mutations can be assigned to twelve critical signaling pathways, such as the RAS-signaling, the MAPK cascade and the NOTCH pathway. Cancer cells not only display mutations but also exhibit a variety of chromosomal aberrations, such as aneuploidy, chromosomal deletions, inversions and translocations resulting in the aberrant activation of cellular proto-oncogenes, generation of novel fusion oncogenes or the silencing of tumor suppressor genes.

During recent years, a new dimension has been added to the field of cancer research. It is now clear that aberrant DNA-methylation patterns and changes in histone modification significantly contribute to tumorigenesis besides genetic mutations and genomic rearrangements. Bernstein and Vogelstein discovered the first epigenetic aberration in cancer cells: loss of DNA methylation[9,51] (**Figure 5**). Indeed, CpG islands of many oncogenes become hypomethylated, leading to their aberrant activation. Moreover, DNA hypomethylation is intricately linked to genomic instability[52]. In addition, hypermethylation occurs leading to epigenetic silencing of a range of tumor suppressor genes, mainly those implicated in cell cycle regulation (eg *p16*) and DNA repair (eg *MHL1* and *BRCA1*)[53]. Aberrant methylation might be directly caused by previous genetic alterations. This is nicely illustrated by the aberrant expression of the fusion protein PML-RARA in some types of leukemia, leading to recruitment of DNA-methyltransferases and histone deacetylases. In addition, changes in the DNA-methylation pattern are correlated to aberrations in the histone modification profile. As such, CpG island hypermethylation is often accompanied by loss of acetylation and lysine trimethylation of histone H3 and gain of trimethylation of lysine 9 and 27.

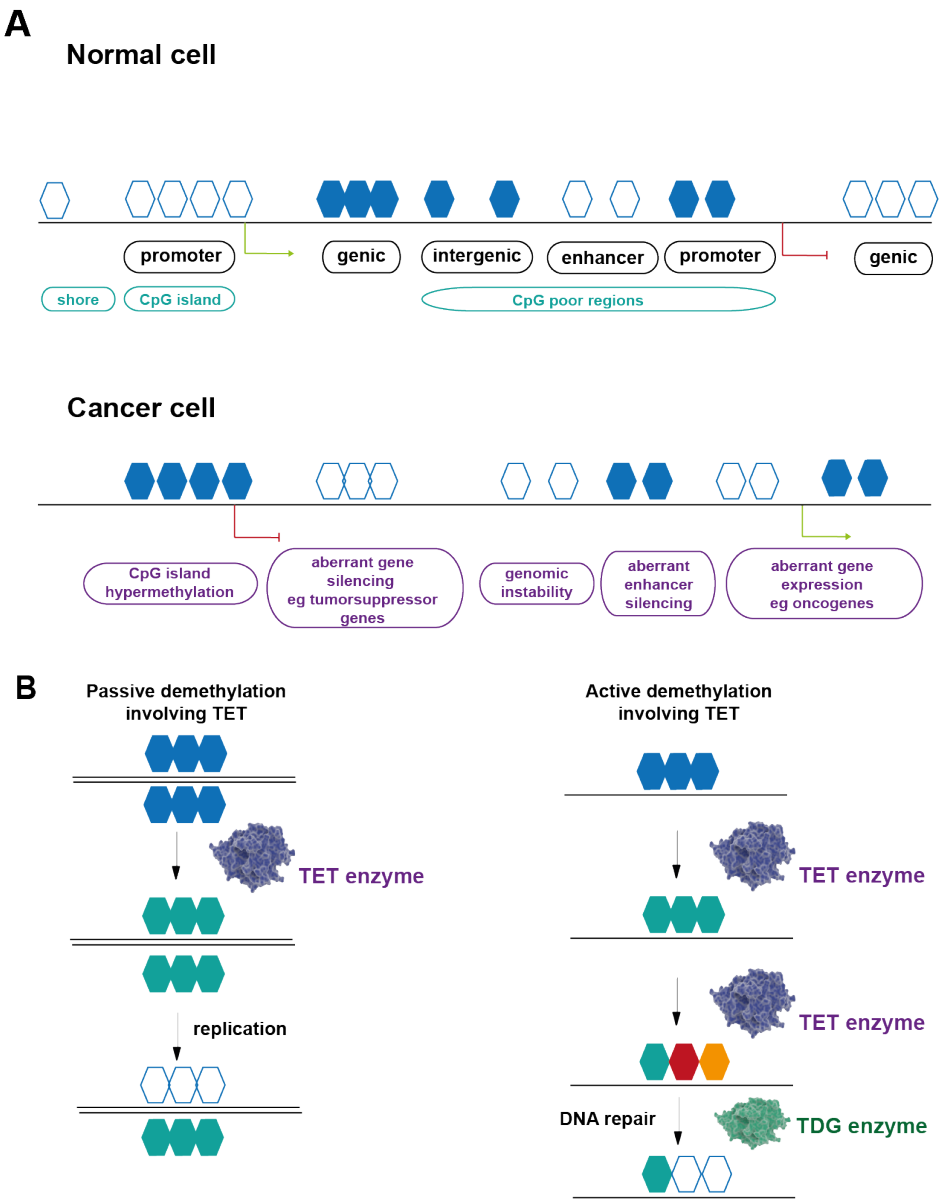


**Figure 5**: (**A**) DNA methylation patterns under normal and malignant conditions[9], **white hexagons**: unmethylated CpG sites, **blue hexagons**: methylated CpG sites. (**B**) Passive and active DNA demethylation involving TET-enzymatic activity: (**left**) passive demethylation involves the conversion of 5-methylcytosine residues (blue hexagons) to 5-hydroxymethylcytosine (green hexagons) by TET-enzymes, which will inhibit DNMT1 from cytosine methylation upon replication, eventually resulting in replacement of 5-hydroxymethylcytosine to unmethylated cytosine residues (white hexagons); (**right**) Active DNA demethylation involves consecutive action of the TET enzyme family to convert 5-methylcytosine (blue hexagon) to 5-hydroxymethylcytosine and subsequent conversion towards further oxidative products 5-formylcytosine (red hexagon) and 5-carboxylcytosine (orange hexagon). The latter cytosine derivatives will be the substrate for the 'thymine DNA glycosylase' enzyme and coupled base excision repair to remove these oxidation products and replace them by unmethylated cytosine residues (white hexagons)[12].

## Chapter 1: Introduction

DNA methylation drew most of the attention in the epigenetic cancer research field. For a long time, 5mC was the only epigenetic modification recognized for the DNA template. Now, the role of 5hmC is also firmly established in the context of differentiation of various tissues, for example with strong enrichment of this modification in neuronal tissue[54] and high levels in pluripotent cells[55]. Interestingly, a recent study by Hon et al.[56] showed that 5hmC is especially enriched at enhancer sites, thereby revealing a role for DNA demethylation in dynamic enhancer regulation during differentiation. Given the recent amazing discovery that nearly 20% of all mutations across cancer types target various epigenetic regulators impacting on not only DNA methylation but also all aspects of chromatin modification and even upstream metabolic pathways the interest in the study of cancer epigenetics was further boosted. Moreover, an increasing number of epigenetic drugs are under development or being tested, further fueling interest from academic research and pharma[57]. Among the recently described mutations are those affecting *DNMT1* and *DNMT3*, with a high frequency of *DNMT3A* mutations in AML (30%). Genetic changes in histone modifiers are rather cancer-specific[58]. In leukemia, recurrent translocations affecting histone acetyltransferases/deacetylases and histone methyltransferase/demethylase enzymes underscored their importance in this pathology[59]. For example, translocations involving the histone methyltransferase 'mixed lineage leukemia' (MLL) frequently occur in acute leukemia and lead to the generation of a variety of fusion proteins that cause aberrant H3K4me3 methylation[60]. In myeloid leukemia, recurrent mutations and deletions are identified, affecting the genes encoding the epigenetic modifiers *ASXL1*, *DNMT3A*, *EZH2*, *IDH1/2*, *MLL1/2* and *TET2*[61].

Genome-wide changes in 5hmC contribute to malignant transformation in hematological cancers as well as in solid tumors (breast cancer, colon cancer, prostate cancer, melanoma)[11]. From all TET family members, mainly TET2 fulfills a key role in normal hematopoietic development[62]. The function of TET2 is hampered by recurrent inactivating mutations both in myeloid and lymphoid hematological cancer types[63]. Recently, cooperative *DNMT3A* mutations were described to be cooperative with *TET2* inactivation, required for full-blown leukemogenesis[64].

While most of the mutations in the above mentioned genes cause loss-of-function, the Polycomb group repressive complex 2 catalytic component *EZH2* is frequently overexpressed in many cancer types such as breast, lung and prostate cancer, while acting as tumor suppressor in the context of some hematological malignancies characterized by *EZH2* inactivating mutations[65]. Identifying the dependency of many cancer types on somatic alterations in various chromatin modifiers has triggered the generation of targeted epigenetic therapeutic strategies such as EZH2 inhibitors.

## 3. Genetic and epigenetic deregulation in T-cell acute lymphoblastic leukemia

*3.1 The molecular-cytogenetic profile of T-cell acute lymphoblastic leukemia*

T-cell acute lymphoblastic leukemia originates from thymocytes that are developmentally arrested at a specific maturation stage with concomitant aberrant clonal expansion of these blasts. Leukemic transformation of thymocyte progenitor cells is a paradigm for the multi-step nature of tumor formation in which a plethora of genetic aberrations collectively contribute to the formation of a full-blown leukemia. Various cellular processes are being affected such as cell cycle regulation, differentiation and cell survival, coupling back to the capabilities that need to be acquired for tumor formation[66]. From a molecular perspective, T-ALL patients can be classified into genetic subtypes that are defined by the aberrant expression of a specific driver oncogene and are characterized by a unique gene expression signature[67,68]. Structural chromosomal aberrations are identified in about 50% of all T-ALL patients. Translocations involving the TCR loci on 14q11 (TCR-α/δ) and 7q34 (TCR-β) occur in 35% of all T-ALLs. This results in the juxtaposition of control elements of the T-cell receptor (TCR) loci with oncogenes such as *TAL1*, *LMO1/2*, *LYL1*, *TLX1*, *TLX3*, *MYB* and *HOXA*[69]. Each of these translocations induce a developmental arrest of progenitor T-cells at a specific developmental stage that define the major T-ALL subtypes. Both *LYL1* and *TAL1* are ectopically expressed in the thymus in T-ALL and interfere with normal T-cell development by binding EA and HEB[70]. *LYL1* expression defines the immature T-ALL subtype 'early T-cell precursor acute lymphoblastic leukemia' (ETP-ALL). Additional genetic lesions marking ETP-ALL

are found in *RUNX1*, *GATA3*, *ETV6* and *MEF2C* amongst others[71]. The latter T-ALL subtype is associated with a poor prognosis (see also Part II[72]). Aberrant expression of *LMO1* and *LMO2* occurs in 45% of T-ALL driven by their juxtaposition to the TCR-α locus. The aberrant activation of *HOXA* genes in T-ALL occurs due a cryptic inversion inv(7) or the translocation t(7;7). The homeobox transcription factors TLX1 and TLX3 cause a T-cell developmental arrest at the early cortical stage. Aberrant *TLX1* expression occurs in about 10% of pediatric and 30% of adult T-ALL[67,73-75] and is mainly driven through a t(10;14)(q24;q11) or t(7;10)(q34;q24) translocation, with juxtaposition to the TCR-α and TCR-β locus respectively. TLX1-driven leukemia is characterized by a more favorable prognosis than all other T-ALL subtypes. TLX1-expressing T-ALL presents with specific genetic alterations that only rarely occur in other genetic subgroups, such as *PTPN2* deletion[76] or mutations in *PHF6*[77]. Overexpression of *TLX3* in T-ALL is driven by the translocation t(5;14)(q35;q32), juxtaposing *TLX3* to the distal region of *BCL11B* and occurs in 25% of pediatric and 5% of adult T-ALL. Also the formation of fusion genes such as *CALM-AF10* and *MLL-ENL* further contribute to deregulated T-cell differentiation through aberrant activation of *HOXA* expression. The *CALM-AF10* fusion occurs in about 10% of T-ALL patients and is associated with a poor prognosis[78]. As previously mentioned, the *MLL* locus participates in many translocations in leukemia, which are also found in about 4-8% of T-ALL. They represent a T-ALL molecular subtype that is associated with commitment to the γδ-lineage[69]. Other genetic abnormalities occur across the different T-ALL genetic subgroups and will interfere with cell cycle regulation (eg *CDKN2A* deletion), contribute to unlimited self-renewal capacity (eg mutations in *NOTCH1*, *FBXW7*, *PTEN*), deregulate crucial signaling pathways (eg *IL7R*, *RAS, PI3K-AKT*), affect translation (eg mutations of *RPL5*, *RPL10*), etc. Deletion of the *CDKN2A* locus, including both tumor suppressor genes *p14* and *p16* occurs in 70% of all T-ALL patients[66].

*3.2 The role of NOTCH1 signaling in T-ALL*

As previously described, NOTCH1 is important in both T-cell lineage commitment and pre-TCR signaling[38]. Ablation of this signaling pathway results in a complete differentiation block of thymocytes at the earliest phases of thymocyte development[79]. Hyperactivation of *NOTCH1* is the oncogenic hallmark of T-ALL that occurs across different genetic subgroups and is either established through mutations (>60% of all cases) or translocation of the TCR-β enhancer with the *NOTCH1* locus (1% of T-ALLs). Activating mutations are either found in the heterodimerization domain of the receptor (44%) or in the PEST-domain (30%) or both (17% of all cases). The E3 ubiquitin ligase FBXW7 is required for NOTCH1 receptor turnover by targeting for proteasomal degradation and *FBXW7* inactivating mutations, which occur in about 15% of all T-ALLs, can thus further contribute to hyperactivation of the NOTCH1 pathway in T-ALL. The exceptional high prevalence of *NOTCH1* aberrations in T-ALL provides opportunities for therapeutic targeting. Gamma-secretase inhibitors (GSI) are a classical example of small molecules that block oncogenic NOTCH1 by interfering with the activity of the gamma-secretase complex and thus preventing the formation of ICN1. The clinical applicability of GSI compounds has been hampered by induction of gastro-intestinal toxicity as a major side effect, as a consequence of NOTCH1 inhibition in the gut. Interestingly, combination therapy of GSIs and glucocorticoids have shown to improve the therapeutic efficacy of GSI treatment (allow for reduced dosing) and diminish the toxic side-effects to the gastro-intestinal system[80,81]. Recently, Pinell and co-workers proposed that therapeutic targeting of ZMIZ1, an important NOTCH1 co-factor, could provide opportunities to interfere with hyperactive NOTCH1 signaling, while circumventing interference with intestinal homeostasis[82].

It was shown that aberrant NOTCH1 signaling also interferes with normal gene regulation at the level of the epigenome, as constitutive signaling through the NOTCH1 receptor triggers global H3K27me3 demethylation by antagonizing PRC2 activity[83]. Moreover, the histone demethylase JMJD3 facilitates part of the NOTCH1 transcriptional program through its direct interaction with ICN1[84] (see also 3.4). On the other hand, upstream mechanisms that control NOTCH1 activity could also be

exploited for therapeutic purposes. For example, the cyclin C-CDK8 complex is known to be involved in transcriptional regulation, but more importantly is capable to control ICN1 levels through phosphorylation, which subsequently promotes its degradation by FBXW7. To study the role of cyclin C (*CCNC* gene) in T-ALL, Li et al.[85] developed an *in vivo* conditional knockout model and crossed it with an *Mx1-Cre* line to ablate cyclin C expression specifically in the hematopoietic lineage. The resulting progeny was characterized by an enlarged thymus, due to an increased number of thymocytes. Moreover, higher levels of ICN1 were present in both precursor T-cells and bone marrow cells compared to those of the wild-type mice. Primary T-ALLs show heterozygous loss in *CCCNC*, with the remaining allele being unaffected, suggesting that cyclin C acts as a novel haploinsufficient tumor suppressor in T-ALL. Finally, point mutations affecting the cyclin C-CDK phosphorylation sites of ICN1 were found as another mechanism by which these hematological neoplasms can escape phosphorylation triggered ICN1 degradation.

*3.3 The genomic landscape of TLX1 driven leukemia*

Besides NOTCH1, also '*T-cell leukemia homeobox 1*' (*TLX1* or *HOX11*) and *TLX3* are key T-ALL transcription factor oncogenes. Physiologically, the TLX1 protein has a role in splenogenesis[86] and neuronal development[87]. In T-ALL patients however, as previously mentioned, TLX1 is ectopically expressed in thymic progenitor cells due to translocations that juxtaposes *TLX1* to the T-cell receptor (TCR)-δ or TCR-β associated regulatory elements respectively (**Figure 6**)[67]. This genetic aberration eventually results in aneuploidy (defective mitotic checkpoint activation) and causes an arrest of developing thymocytes at the early cortical stage of T-cell development[88-90]. Dadi and co-workers[91] have elegantly shown that this maturation block involves a physical association between TLX1 and the ETS1 protein, forming a repressive complex that blocks the activity of the TCR alpha enhancer region, eventually interfering with correct TCR rearrangements (**Figure 6**). In another study, Della Gatta and colleagues[92] could show that besides ETS1, RUNX1 also acts as a crucial regulator within the TLX1 transcriptional network. From this study, RUNX1 emerged as the most interconnected hub in the TLX1-TLX3 network, identifying this

factor as a key regulator of TLX1-TLX3 driven transcriptional programs. Moreover, *RUNX1* is most significantly downregulated in TLX1-positive leukemia and recurrently mutated in T-ALL (about 5%), underscoring RUNX1 as an important tumor suppressor in this T-ALL subtype[92]. TLX1 driven tumors show, in comparison to other T-ALL subtypes, a gene expression signature that is primarily characterized by gene repression, indicative for the role of TLX1 as a transcriptional repressor in T-ALL. Many of these targets, such as *BRCA2* and *CHEK1*, are involved in well-defined key tumor suppressor activities and their repression by TLX1 converges towards loss of mitotic checkpoint control and chromosomal missegregation. In murine TLX1-driven leukemia, 78% of all tumors are aneuploid. Murine models of TLX1-induced leukemias exhibited a very long latency of leukemia onset (>30 weeks), indicative that cooperating mutations are required to establish overt leukemia[93].

Hyper-activating *NOTCH1* mutations occur in over 50% of all T-ALL patients while intriguingly they are present in more than 90% of all TLX1-positive cases[94] suggesting a very strong interrelationship between TLX1 driven leukemia formation and the cooperative *NOTCH1* mutations. In this thesis, we provide an explanation through an unusual transcriptional antagonism of both T-ALL oncogenes at pre-leukemic stages of T-ALL development. More specifically, TLX1 downregulates most of the core components of the NOTCH1 signaling pathway and therefore requires additional oncogenic NOTCH1 activation in order for full-blown T-ALL development to occur (see **paper 1, Chapter 3**).

As indicated above, while unexpectedly repressing NOTCH1 signaling, TLX1 represses a plethora of T-ALL associated tumor suppressor genes, driving TLX1 positive leukemia to a fully malignant state[95]. Inactivating mutations affect the expression of several tumor suppressor genes such as *BCL11B*[93], *PTPN2*[76], *WT1*[96] and *PHF6*[77] amongst others. Moreover, focal deletions of *Bcl11b*, *Pten* and *Cdkn2a/b* are often found in TLX1-driven mouse models of T-ALL[93,95].

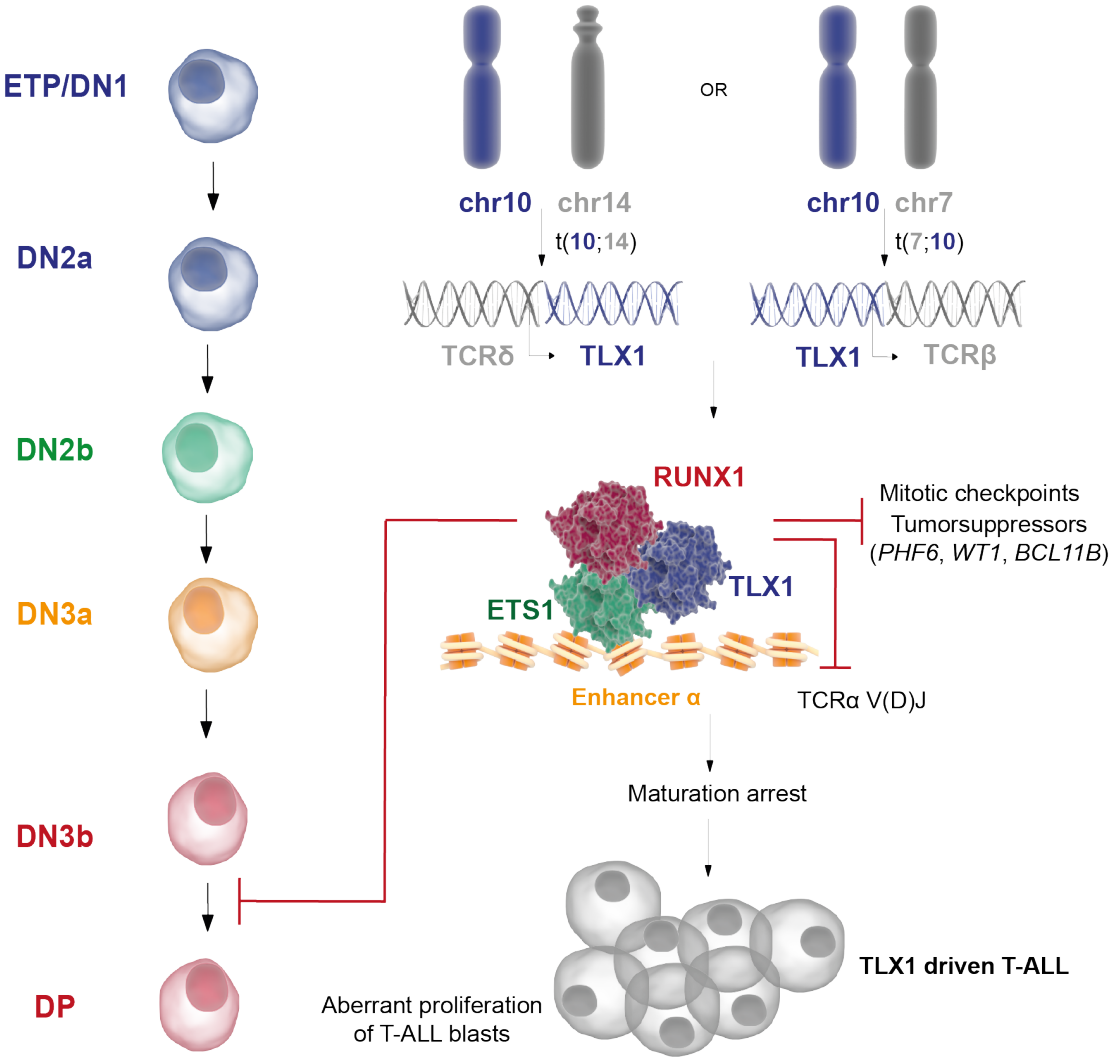


**Figure 6**: TLX1 is ectopically expressed in developing thymocytes due to a t(10;14) or t(7;10) translocation. TLX1 forms a repressor complex with RUNX1 and ETS1 at the TCR-α enhanceosome, thereby inducing a developmental arrest at the DN-DP T-cell stage transition and interferes with normal TCR-rearrangements ultimately leading to T-ALL blast formation. Adapted from Dadi et al. (Cancer Cell, 2012)[91]

### *3.4 The T-ALL epigenome*

Huether and co-workers have shown that T-cell acute lymphoblastic leukemia (T-ALL), is characterized by one of the highest mutational frequencies in chromatin modifiers across a large panel of pediatric cancer entities[97] and thus present a novel pool of oncogenes and tumor suppressors in this malignancy.

Like in other cancer types, the T-ALL epigenome is affected both at the level of DNA methylation and chromatin modifications. Global methylation profiles have been shown relevant in the classification of leukemia subtypes[98]. In T-ALL, transcriptional silencing of tumor suppressors such as *CDKN1A/2B*, *SYK* and *C/EBPA* is associated with CpG island hypermethylation[99]. Moreover, adult T-ALL cases show a high frequency (18%) of *DNMT3A* mutations that are especially enriched in the ETP subtype[100] and are associated with a poor prognosis. Active DNA-demethylation involves the action of the 'ten-eleven-translocation' (TET) protein family required for the conversion of 5-methylcytosine to 5-hydroxymethylcytosine. While *TET2* mutations are recurrent in hematological malignancies such as AML, so far only *TET1* genetic lesion could be identified in about 14% of all T-ALL cases[101]. TET enzymes require 2-oxoglutarate for their action, which can be produced by isocitrate dehydrogenase enzymes (IDH). Both *IDH1* and *IDH2* mutations have been identified in adult T-ALL[102,103]. Notably, like 5mC, also the oxidative products 5hmC, 5-formylcytosine and 5-carboxylcytosine are involved in gene expression regulation. For example, Wang and co-workers could show that the levels of 5-formylcytosine and 5-carboxylcytosine can affect the rate of RNA Polymerase II driven transcription, through their direct interaction with the polymerase enzyme[104]. In addition, the role of these cytosine (oxidative) methylation products is ever expanding, with a proven role as an epigenetic marker in DNA damage response[105] and CTCF-dependent splicing[106].

Epigenetic regulatory proteins such as CREBBP, EED, p300, EZH2, PHF6 and SETD2 are most recurrently mutated in pediatric ALL[97]. Both CREBBP and p300 are co-factors of histone acetyltransferases and are mutated in T-ALL[107]. The histone methyltransferase SETD2 specifically catalyzes methylaton of lysine 36 of histone H3 and is mutated in T-ALL, with 48% of ETP-ALL cases harboring mutations in epigenetic regulators, including SETD2[71]. Besides histone acetylation, also aberrations interfering at the level of histone methylation play a crucial role in the pathogenesis of T-ALL. Ntziachristos and co-workers recently described the identification of inactivating mutations and deletions in *EZH2* and *SUZ12*, both core components of the PRC2 complex in 25% of T-ALL cases[83]. These loss-of-function

mutations have been shown to be cooperative with hyperactivity of the NOTCH1 signaling pathway in T-ALL, since abrogration of the PRC2 complex function enhances the NOTCH1 driven transcriptional program, in addition to global H3K27me3 loss upon oncogenic NOTCH1 signaling. In addition, also histone demethylation has been shown to contribute to oncogenic transformation. Somatic mutations in the lysine-specific demethylase 6A (*KDM6A* or *UTX*) have already been identified in a plethora of other cancers, such as renal cell carcinoma and multiple myeloma[108]. Recently, In T-ALL, *UTX* loss-of-function mutations were identified in 5% of T-ALL cases, with a skewed gender distribution towards males[109], escaping X-inactivation in female T-ALL and normal T-cells. Remarkably, whereas UTX acts as a tumor suppressor in T-ALL, the histone demethylase 6B (*KDM6B* or *JMJD3*) was shown to exhibit oncogenic properties in T-ALL, crucial in both establishment and maintenance of the leukemic phenotype[84], partially through its direct interaction with NOTCH1 and its downstream transcriptional program. While these genes superficially seem to act in similar epigenetic processes (histone lysine demethylation), there seems to be strong context dependent action for the great diversity of epigenetic regulators as reflected from specific occurrence of either gain or loss-of-function mutations in well-defined cancer entities.

*3.5 PHF6 as a novel epigenetic regulator in T-ALL*

In 2010, inactivating mutations and deletions were identified in the X-linked gene *PHF6* (Xq26.3) (**Figure 7**) in 16% of pediatric and 38% of adult T-ALLs and were shown to be exclusively present in male patients[77]. Later studies provided evidence that *PHF6* mutations also occur in females[110-112]. Given the 3:1 male to female ratio in which T-ALL occurs, the identification of an X-linked tumor suppressor is of particular interest. Notably, these *PHF6* aberrations were predominantly associated with the *TLX1*$^{+}$ and *TLX3*$^{+}$ T-ALL subgroups, adding *PHF6* as an additional and critical tumor suppressor in this T-ALL subtype. In addition, it was shown that repression of *PHF6* may also, at least in part, be the result of activation of oncogenic miRNAs *miR-20a*, *miR-26a* and *miR-128b* in T-ALL[113,114]. Activating *NOTCH1* mutations are present in more than 80% of *PHF6* mutated cases[112]. Furthermore, also *JAK1* mutations (>30%)

and *SET-NUP214* translocations (>40%) were significantly enriched within *PHF6* associated T-ALLs. Later, *PHF6* lesions were also identified, although to a minor extent, in other (hematological) tumor entities[111] such as acute myeloid leukemia (AML, 3%), hepatocellular carcinoma en chronic myeloid leukemia (CML)[115], with *PHF6* mutations seven times more prevalent in males than females in case of AML. Furthermore, this places *PHF6* aberrations amongst other genetic defects such as the *SET-NUP214* and *CALM-AF10* translocations or *FLT3* mutations that are shared between T-ALL and AML[116]. So far, *PHF6* lesions have not been observed in B-cell acute lymphoblastic leukemia (B-ALL). In this context, it is of interest that Meacham and colleagues could actually demonstrate that PHF6 deficiency impaired growth of B-ALL cells through the use of a genome-wide *in vivo* loss-of-function screen[117], thus mimicking a similar duality in leukemia formation as mentioned above for NOTCH1. In line with these notions, work presented in this thesis shows that PHF6 acts as an important regulatory component in controlling lineage-specificity during normal hematopoietic development and ontogeny of hematological cancers (see **paper 2**, **Chapter 3**).

While PHF6 is expressed in the thymus, this protein also plays a key role in brain development. Historically, *PHF6* germline mutations were shown to be the causal event of the Börjeson-Forssman-Lehmann syndrome (BFLS), an X-linked mental retardation syndrome, with patients presenting features such as tapered fingers, gynaecomastia and intellectual disability amongst others[118-120]. It is presumed that PHF6 is implicated in BFLS through its involvement in neuronal migration in concert with the PAF1 transcription elongation complex[121].

BFLS affects predominantly males, while female carriers usually do not present clear phenotypic effects. However, *de novo PHF6* mutations were recently found in seven females presenting a BFLS phenotype[122]. Importantly, a case study by Chao[123] and co-workers described a BFLS patient that also developed T-ALL thus suggesting that PHF6 can be involved in early stages of T-ALL oncogenesis and can predispose to leukemia formation.

The *PHF6* gene comprises 11 exons (**Figure 7**) and produces an mRNA transcript of 4.5 kb, with an alternative splice variant that can be formed due to inclusion of intron 10[118]. *PHF6* is highly conserved amongst different species, but absent in non-vertebrates. During embryonic, fetal and post-natal phases of life, high levels of PHF6 are present in the brain, which are reduced again during adulthood. During these phases in life, also the intracellular location of the protein is shifted, with expression both in the nucleus and the cytoplasm during development and finally towards an exclusive nuclear expression[124]. The PHF6 protein (365 amino acids) is structurally characterized by four nuclear localization sequences (NLS) (**Figure 7**), which target PHF6 towards the nucleus, with an enrichment of the protein in the nucleolar compartments. Given that the nucleoli are the main sites of ribosome biogenesis, the subcellular localization of PHF6 at these compartments is suggestive for a role in the regulation of rDNA transcription[118,125]. Indeed, Wang and co-workers recently showed that PHF6 directly interacts with the transcription factor UBF, known to be involved in RNA polymerase I mediated rRNA generation. Interaction of PHF6 with UBF leads to stabilized UBF expression and finally results in rDNA transcriptional silencing. Moreover, Wang et al could show that PHF6 deficiency results in increased DNA-damage at the rDNA loci, which subsequently induces a cell cycle arrest at the G2/M phase[125]. Interestingly, Van Vlierberghe et al. previously suggested that PHF6 deficiency leads to increased γ-H2AX levels that are indicative for DNA double strand breaks[77]. Moreover, the role of PHF6 in the cell cycle and DNA-damage response (DDR) is further supported by the observation that the PHF6 protein itself is also subjected to phosphorylation, both during mitosis[126] and during DDR by ATM and ATR kinases[127]. The role of PHF6 in the process of DDR could be an interesting entry point for therapy. One of the hallmarks of cancer involves the acquisition of limitless replicative potential[45]. When the control mechanisms of faithful DNA replication are hampered, a phenomenon called 'replicative stress'[128] is induced with concomitant accumulation of DNA damage. This makes the DDR an ideal target for therapeutic intervention[129]. This is nicely illustrated by a recent study of Hähnel et al.[130] focusing on *KRAS*-mutated T-ALL. It was previously shown[131] that over half of all these cases harbour activating *NOTCH1* mutations and thus benefit from treatment with GSI alone or combination strategies. Hähnel and colleagues

now show that targeting the non-homologous end-joining pathway (NHEJ), which is markedly upregulated in *KRAS*-mutated T-ALLs by e.g. use of PARP inhibitors is a sensitization strategy for evoking a therapeutic response to chemotherapy in these cases[130]. A more recent study, conducted by Sarmento and co-workers[132], provides evidence for the pharmacological inhibition of the checkpoint kinase 1 (CHK1) as a novel therapeutic target for T-ALL patients. CHK1 is a crucial factor in genomic surveillance and regulation of the cell cycle at the G2/M checkpoint. In T-ALL lymphoblasts, CHK1 is one of the major factors that protects them from replicative stress induced upon massive proliferation and is overexpressed in 60% of primary T-ALLs. Pharmacological inhibition of CHK1 shows anti-tumorigenic potential as it induces cell cycle arrest and cell death of T-ALL cells, with the response being dependent on ATM and caspase-3 activity.

Besides NLS motifs, PHF6 also harbours two imperfect plant homeodomain (PHD) zinc fingers (**Figure 7**)[77]. So far, about 14 members of the PHD-finger protein family have been identified in yeast, 50 members in *Drosophila* and more than 100 members in the human genome[133]. These PHD domains are about 50-80 amino acids in size and are found in many transcriptional regulators such as the family of '*mixed lineage leukemia*' (MLL) proteins and the '*inhibitor of growth family member*' (ING) protein family[134]. These PHD modules can recognize the N-terminal tail of histone H3 and more in particular is targeted to the methylation on lysine (K) four (K4), methylation of arginine two (R2) or the acetylation of K14. The specificity towards the substrate can be different amongst various PHD-containing chromatin-associating factors. The two PHD zinc fingers in the protein structure of PHF6 deviate in composition from the standard $Cys_4$-His-$Cys_3$ motif. The terminal cysteine in the consensus motif is in PHF6 replaced by histidine and only 8 amino acids separate the cysteine residues at position two and three[118]. Chromatin-associating proteins that can only recognize specific post-translational modified (PTM) histone residues and do not have intrinsic enzymatic activity are referred to as 'readers'[135]. Besides the PHD-motif, also other domains are known that allow recognition of a specific type of PMT on core histone proteins. A well-known example is the bromodomain, which allows proteins to recognize acetylated histone lysine residues[136]. Bromodomain

containing proteins, such as the well-known example 'bromodomain containing 4' (BRD4), are currently successfully targeted in acute leukemia and across many other malignancies[137]. Two other classes of chromatin interacting proteins, referred to as 'writers' (generate these PTMs) or 'erasers' (remove these PTMs), are distinguished from reader proteins by the additional capacity of placing or removing chemical modification on core histone proteins[138]. This capacity requires the presence of a catalytic domain in the protein structure, such as the SET domain of the protein *'Enhancer of Zeste homolog 2*' (EZH2), which enables it to catalyze methylation of K27 residues of the core histones to establish transcriptional silencing[139]. The PHF6 protein can thus be classified as a 'reader', since it has no intrinsic enzymatic activity, but is hypothesized to rather be capable of recognizing specific histone modifications (or combinations thereof) through its PHD domains[133]. In general these reader proteins then recruit 'writer' or 'erasers' to alter the chromatin structure at their target site. Interestingly, PHF8 is another PHD-finger protein that shows commonalities with PHF6 in various aspects. Amongst others, PHF8 is involved in regulation of rDNA transcription[140], control of cell cycle progression (in particular the G2-M phase transition)[141] and is a mutated in X-linked mental retardation. In contrast to PHF6, the PHF8 protein is classified as 'eraser' protein, as it can act as H4K20me1 demethylase through the presence of a 'Jumonji C' (JmjC) domain, after docking to H3K4me3 sites through its PHD-domains, to activate transcription[142]. Although PHF8 has a known role in various cancer types[143,144], the potential implication of PHF8 in hematological malignancies is thus far unknown. Notably, a recent proteomics study by Yatim et al.[145] identified PHF8 as a component of the NOTCH1 transcriptional complex in T-ALL cells promoting the expression of several NOTCH1 downstream target genes, providing a hint for potential implications of PHF8 in T-ALL as well.

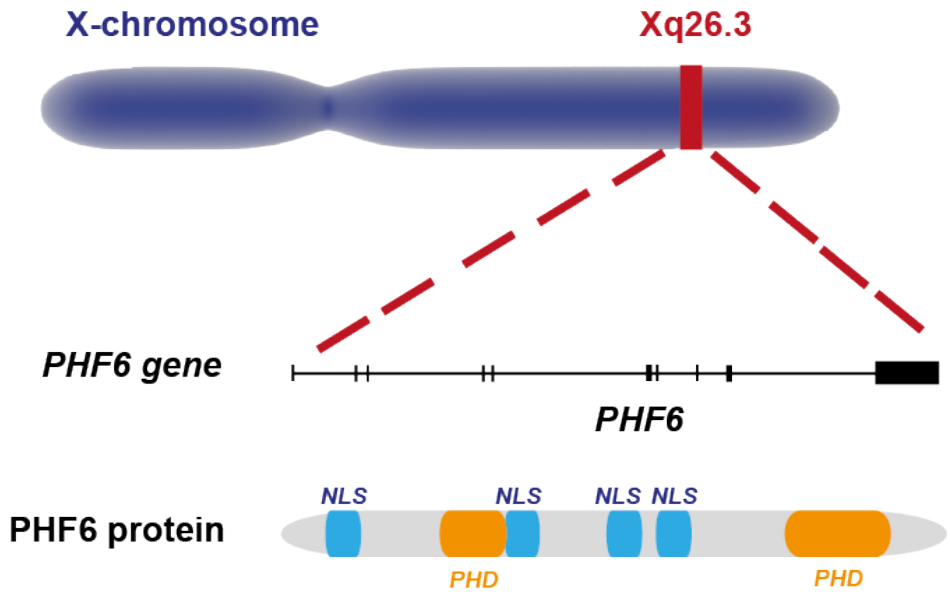


**Figure 7**: The PHF6 gene resides on the X-chromosome (Xq26.3) and is transcribed into a transcript containing 11 exons. The protein structure of PHF6 contains 4 nuclear localisation signals (NLS) and 2 imperfect plant homeodomain (PHD) zinc fingers allowing the protein to dock to specific (yet unknown) post-translational modifications on the N-termini of the histone tails.

Transcriptional regulation at the level of chromatin also involves more profound architectural changes besides post-translational modification of core histone proteins and methylation of DNA CpG sites. These conformational shifts are induced by chromatin remodeling complexes. ATP-hydrolysis provides the energetic driving force for these multi-protein scaffolds to force nucleosome sliding, removal or exchange[146]. Well-known examples of these ATP-driven chromatin remodelers are the 'SWItch/Sucrose Non-Fermentable' (SWI-SNF) and the 'Nucleosome Remodeling and Deacetylase' (Mi-2/NurD) complexes (**Figure 8**)[147]. Both complexes have a known role in transcriptional regulation within the hematopoietic compartment, such as in normal T-cell development[148,149]. The SWI-SNF complex members are mutated in many different cancer types, such as colorectal and lung cancer[150]. Besides well-established members of the complex such as SMARCA4 (BRG1) and ARID1A, novel subunits such as BCL11B and BRD9 were recently described[122]. Interestingly, *PHF6* mutations were recently associated with Coffin-Siris (CSS) and Nicolaides-Baraitser (NCBRS) syndromes, two congenital disorders with associated

intellectual disability[151,152]. These syndromes were previously marked by *de novo* mutations in several members of the SWI-SNF nucleosome-remodeling complex. Notably, like PHF6, also other X-linked epigenetic modifiers have been associated in the past with mental retardation syndromes, such as *ATRX* and *MECP2* (besides PHF8)[133]. These findings further support the hypothesis that PHF6 can be an important epigenetic modulator of gene expression in concert with NurD and/or SWI-SNF complexes, in keeping with the recent identification of a physical association between PHF6 and members of the NurD complex[153]. Moreover, as the NurD complex has known roles in both brain[154] function and lymphopoiesis[149], their interaction is suggestive for functional cooperation in these tissue types.

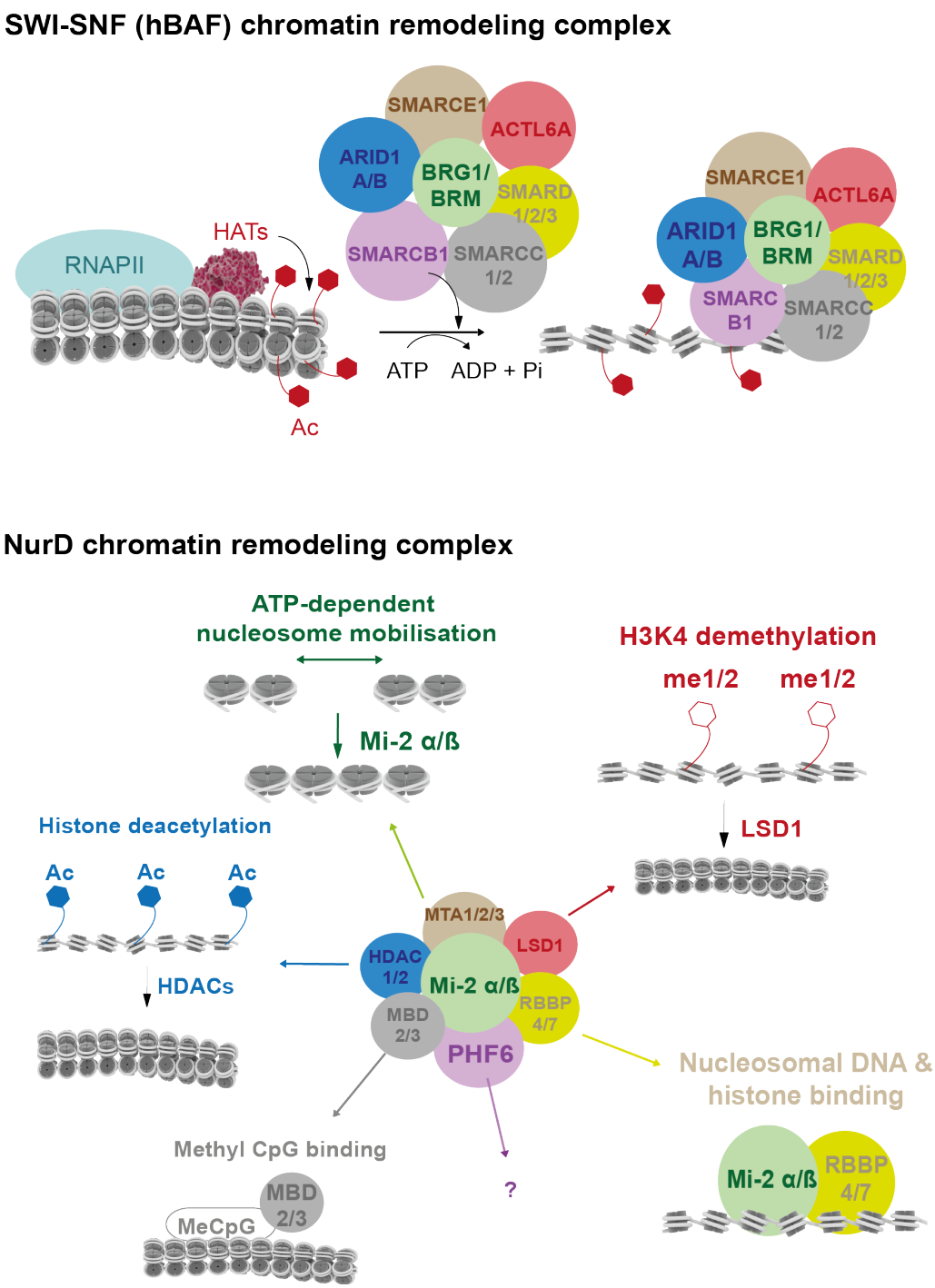


**Figure 8**: The ATP-dependent SWI-SNF and NurD chromatin remodeling complexes[147] (sp.uconn.edu) are involved in ATP-hydrolysis coupled reshaping of the chromatin structure, supporting the formation of either a hetero- (closed) or euchromatin (open) conformation: (**upper panel**) the catalytic component of the SWI-SNF complex is BRG1 (SMARCA4) and the remainder constellation of this complex is context-specific; (**lower panel**) it is already shown that PHF6 is part of the NurD remodeling complex[153] in which several core compontens mediate the transition from an open to closed chromatin conformation eventually resulting in gene silencing. The exact role of PHF6 in the function of this complex is unknown thus far.

## 4. The role of long non-coding RNAs in normal development and cancer

Besides the multiple protein complexes that are involved in modulation of the epigenome, either through chromatin chemical modification (PTMs) or structural remodeling, an additional key layer of regulatory complexity should be taken into account to fully understand the network that controls correct epigenetic gene expression regulation. Recent technological advances in high-throughput sequencing have revolutionized the discovery of many non-coding RNA species throughout the genome. Although the function for the majority of long non-coding RNAs (lncRNAs) is still unknown, it is now clear that these RNA-species comprise the major part of the non-coding transcriptome and show a high versatility in their mechanism-of-action to regulate gene expression (**Figure 9**)[155]. The diversity of their folding or structure is crucial to support the interaction with protein complexes and the specific functions that lncRNAs are able to execute[156]. In addition, recent discoveries have proven their cell-type specific expression, with important implications both in normal development and malignant transformation[157] (see also **Chapter I**, **Part II**) and thereby influencing various processes such as genomic stability, cell proliferation and survival[158]. There is currently no general way to assign the functional contribution of a particular lncRNA, given both our increased knowledge that transcriptional regulation is very complex and that the functional diversity that RNA molecules display is huge. The potential importance of lncRNAs (and ncRNAs as a whole) in development is further supported by the intriguing observation that organism complexity is strongly correlated to the proportion of the genome that is non-coding[159]. A prototypical example is the lncRNA *HOTTIP*, expressed from the HOX loci and implicated in anatomic patterning[160].

To exert their function, lncRNAs mainly interact with chromatin regulatory complexes[161]. The 'polycomb repressive complex 2' (PRC2) is known to interact with many lncRNAs. One particular notorious lncRNA that interacts with PRC2 is *XIST*[162,163], the key regulator controlling X-inactivation[164]. Yet another example is lncRNA *HOTAIR*[165], transcribed from the *HOXC* locus, which plays a role in gastric and metastatic breast cancer amongst others[166]. Besides the interaction of lncRNAs with

proteins, their interaction with other RNA species also plays a crucial role in the diversity of functions they execute and control of their actions. For instance, it is known that lncRNAs can be bound by miRNAs. In this way, lncRNAs can act as miRNA sponges[167], thereby sequestering the miRNA away from its endogenous target and act as a 'competing endogenous RNA' (ceRNA), as nicely illustrated for the *PTENP1* transcript interacting with miRNAs belonging to the *miR-17-92* cluster[168] or interaction of the lncRNA *HULC* with *miR-372*[169].

Given tissue-specific expression of many lncRNAs, they may represent important and powerful biomarkers in diagnosis and monitoring of disease and are currently being scrutinzed to that end. This has been illustrated in prostate cancer where researchers identified lncRNA *PCA3* as being highly prostate-specific[170]. Moreover, certain lncRNAs for the same reason can act as suitable therapeutic targets as their specific expression will avoid unwanted toxic side-effects in normal tissues[171]. This was nicely illustrated by a recent study of Gutschner and colleagues showing that *in vivo* perturbation of the lncRNA *MALAT1* in a lung cancer mouse xenograft model using anti-sense oligonucleotides (ASO) prevented metastasis[172] and also in the unpublished work in melanoma (Mestdagh P et al., personal communication, paper under review). Taken together, a better understanding of the previously so-called 'dark matter' of the genome will have a profound impact on our understanding of the complex regulation of various cellular processes such as replication, transcription, splicing, DNA repair, chromatin conformation and so on. Together with steadily evolving opportunities for genome editing and RNA therapeutics, a new era of revolutionized targeted therapy is now emerging.

An important feature of lncRNAs that will also be crucial to tackle in the near future is the issue of lncRNA conservation. We do not only need to account for their sequence conservation across species, but also their positional conservation, given that positionally conserved lncRNAs which are expressed can be often found in proximity of protein coding genes that have a crucial role in development. On the other hand, if a particular lncRNA is neither positionally nor sequence conserved, this does not imply that this lncRNA lacks any important funtionality or therapeutic potential. It might be that the function of the lncRNA is rather dictated by its RNA

structural conformation and that structure is therefore the main parameter to be evaluated in terms of evolutionary conservation[173,174].

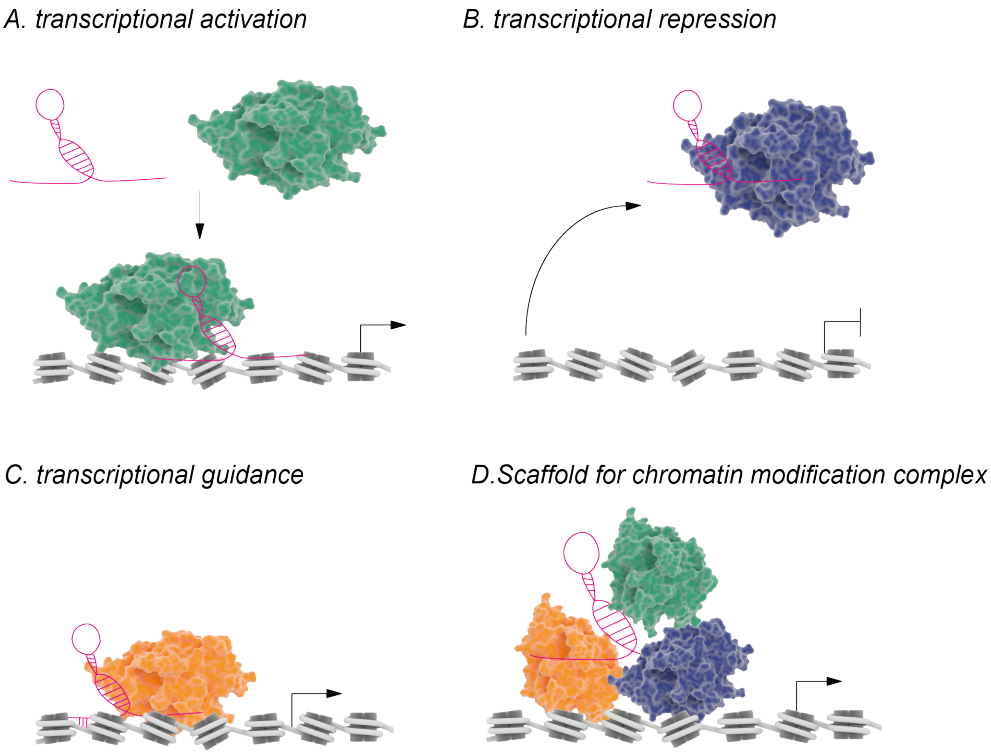


**Figure 9**: Mechanistic diversity of transcriptional control mechanisms by lncRNAs in concert with chromatin remodeling complexes comprises four main modes-of-action: (**A**) lncRNA transcripts can induce conformational/allosteric changes that lead to the activation of interacting proteins, (**B**) lncRNAs can be a decoy to titrate the chromatin remodeling complex away from the DNA template and thereby interfere with its action, (**C**) lncRNAs can guide interacting transcriptional regulators to their site-of-action either *in cis* or *in trans* to distal sites, (**D**) lcnRNAs can act as a scaffold facilitating the formation of a multiprotein complex. Adapted from Yang et al. (Biochim and Biophys Acta, 2014)[155]

A more detailed review concerning T-ALL genetics and development of novel state-of-the-art targeted therapies are described in the review 'Novel biological insights in T-cell acute lymphoblastic leukemia' (see **Chapter I**, **Part II**).

## Chapter 1: Introduction

## References


1. Slack, J.M. Conrad Hal Waddington: the last Renaissance biologist? *Nat Rev Genet* **3**, 889-895 (2002).

2. Holliday, R. Epigenetics: a historical overview. *Epigenetics* **1**, 76-80 (2006).

3. Tollervey, J.R. & Lunyak, V.V. Epigenetics: judge, jury and executioner of stem cell fate. *Epigenetics* **7**, 823-840 (2012).

4. Cantone, I. & Fisher, A.G. Epigenetic programming and reprogramming during development. *Nat Struct Mol Biol* **20**, 282-289 (2013).

5. Li, E. Chromatin modification and epigenetic reprogramming in mammalian development. *Nat Rev Genet* **3**, 662-673 (2002).

6. Li, B., Carey, M. & Workman, J.L. The role of chromatin during transcription. *Cell* **128**, 707-719 (2007).

7. Wilson, C.B., Makar, K.W., Shnyreva, M. & Fitzpatrick, D.R. DNA methylation and the expanding epigenetics of T cell lineage commitment. *Semin Immunol* **17**, 105-119 (2005).

8. Law, J.A. & Jacobsen, S.E. Establishing, maintaining and modifying DNA methylation patterns in plants and animals. *Nat Rev Genet* **11**, 204-220 (2010).

9. Stirzaker, C., Taberlay, P.C., Statham, A.L. & Clark, S.J. Mining cancer methylomes: prospects and challenges. *Trends Genet* **30**, 75-84 (2014).

10. Sadakierska-Chudy, A., Kostrzewa, R.M. & Filip, M. A comprehensive view of the epigenetic landscape part I: DNA methylation, passive and active DNA demethylation pathways and histone variants. *Neurotox Res* **27**, 84-97 (2015).

11. Jeschke, J., Collignon, E. & Fuks, F. Portraits of TET-mediated DNA hydroxymethylation in cancer. *Curr Opin Genet Dev* **36**, 16-26 (2016).

12. Delatte, B., Deplus, R. & Fuks, F. Playing TETris with DNA modifications. *EMBO J* **33**, 1198-1211 (2014).

13. Pastor, W.A., Aravind, L. & Rao, A. TETonic shift: biological roles of TET proteins in DNA demethylation and transcription. *Nat Rev Mol Cell Biol* **14**, 341-356 (2013).

14. Strahl, B.D. & Allis, C.D. The language of covalent histone modifications. *Nature* **403**, 41-45 (2000).

15. van Attikum, H. & Gasser, S.M. Crosstalk between histone modifications during the DNA damage response. *Trends Cell Biol* **19**, 207-217 (2009).

16. Kouzarides, T. Chromatin modifications and their function. *Cell* **128**, 693-705 (2007).

17. Zhang, T., Cooper, S. & Brockdorff, N. The interplay of histone modifications - writers that read. *EMBO Rep* **16**, 1467-1481 (2015).

18. Zhou, V.W., Goren, A. & Bernstein, B.E. Charting histone modifications and the functional organization of mammalian genomes. *Nat Rev Genet* **12**, 7-18 (2011).

19. Khan, A.A., Lee, A.J. & Roh, T.Y. Polycomb group protein-mediated histone modifications during cell differentiation. *Epigenomics* **7**, 75-84 (2015).

20. Swygert, S.G. & Peterson, C.L. Chromatin dynamics: interplay between remodeling enzymes and histone modifications. *Biochim Biophys Acta* **1839**, 728-736 (2014).

21. Fong, C.Y., Morison, J. & Dawson, M.A. Epigenetics in the hematologic malignancies. *Haematologica* **99**, 1772-1783 (2014).

22. Wang, G.G., Allis, C.D. & Chi, P. Chromatin remodeling and cancer, Part I: Covalent histone modifications. *Trends Mol Med* **13**, 363-372 (2007).

23. Clapier, C.R. & Cairns, B.R. The biology of chromatin remodeling complexes. *Annu Rev Biochem* **78**, 273-304 (2009).

24. Morrison, A.J. & Shen, X. Chromatin remodelling beyond transcription: the INO80 and SWR1 complexes. *Nat Rev Mol Cell Biol* **10**, 373-384 (2009).

25. Wu, J.I. Diverse functions of ATP-dependent chromatin remodeling complexes in development and cancer. *Acta Biochim Biophys Sin (Shanghai)* **44**, 54-69 (2012).

26. Cedar, H. & Bergman, Y. Epigenetics of haematopoietic cell development. *Nat Rev Immunol* **11**, 478-488 (2011).

27. Yui, M.A. & Rothenberg, E.V. Developmental gene networks: a triathlon on the course to T cell identity. *Nat Rev Immunol* **14**, 529-545 (2014).

28. Rothenberg, E.V. Transcriptional drivers of the T-cell lineage program. *Curr Opin Immunol* **24**, 132-138 (2012).

29. Van de Walle, I.*, et al.* Specific Notch receptor-ligand interactions control human TCR-alphabeta/gammadelta development by inducing differential Notch signal strength. *J Exp Med* **210**, 683-697 (2013).

30. Joshi, I.*, et al.* Notch signaling mediates G1/S cell-cycle progression in T cells via cyclin D3 and its dependent kinases. *Blood* **113**, 1689-1698 (2009).

31. Choi, Y.J.*, et al.* The requirement for cyclin D function in tumor maintenance. *Cancer Cell* **22**, 438-451 (2012).

32. Wang, H.*, et al.* NOTCH1-RBPJ complexes drive target gene expression through dynamic interactions with superenhancers. *Proc Natl Acad Sci U S A* **111**, 705-710 (2014).

33. Palomero, T. & Ferrando, A. Oncogenic NOTCH1 control of MYC and PI3K: challenges and opportunities for anti-NOTCH1 therapy in T-cell acute lymphoblastic leukemias and lymphomas. *Clin Cancer Res* **14**, 5314-5317 (2008).

34. Gianfelici, V. Activation of the NOTCH1 pathway in chronic lymphocytic leukemia. *Haematologica* **97**, 328-330 (2012).

35. Rechsteiner, M. & Rogers, S.W. PEST sequences and regulation by proteolysis. *Trends Biochem Sci* **21**, 267-271 (1996).

36. Lobry, C., Oh, P. & Aifantis, I. Oncogenic and tumor suppressor functions of Notch in cancer: it's NOTCH what you think. *J Exp Med* **208**, 1931-1935 (2011).

37. Weng, A.P.*, et al.* Activating mutations of NOTCH1 in human T cell acute lymphoblastic leukemia. *Science* **306**, 269-271 (2004).

38. Taghon, T., Waegemans, E. & Van de Walle, I. Notch signaling during human T cell development. *Curr Top Microbiol Immunol* **360**, 75-97 (2012).

39. Tremblay, M., Herblot, S., Lecuyer, E. & Hoang, T. Regulation of pT alpha gene expression by a dosage of E2A, HEB, and SCL. *J Biol Chem* **278**, 12680-12687 (2003).

40. Rothenberg, E.V. The chromatin landscape and transcription factors in T cell programming. *Trends Immunol* **35**, 195-204 (2014).

41. Lee, P.P.*, et al.* A critical role for Dnmt1 and DNA methylation in T cell development, function, and survival. *Immunity* **15**, 763-774 (2001).

42. Ji, H.*, et al.* Comprehensive methylome map of lineage commitment from haematopoietic progenitors. *Nature* **467**, 338-342 (2010).

43. Gebuhr, T.C.*, et al.* The role of Brg1, a catalytic subunit of mammalian chromatin-remodeling complexes, in T cell development. *J Exp Med* **198**, 1937-1949 (2003).

44. Roberts, C.W., Leroux, M.M., Fleming, M.D. & Orkin, S.H. Highly penetrant, rapid tumorigenesis through conditional inversion of the tumor suppressor gene

Snf5. *Cancer Cell* **2**, 415-425 (2002).

45. Hanahan, D. & Weinberg, R.A. Hallmarks of cancer: the next generation. *Cell* **144**, 646-674 (2011).

46. Hanahan, D. & Weinberg, R.A. The hallmarks of cancer. *Cell* **100**, 57-70 (2000).

47. Albini, A. & Sporn, M.B. The tumour microenvironment as a target for chemoprevention. *Nat Rev Cancer* **7**, 139-147 (2007).

48. Chen, F.*, et al.* New horizons in tumor microenvironment biology: challenges and opportunities. *BMC Med* **13**, 45 (2015).

49. Yates, L.R. & Campbell, P.J. Evolution of the cancer genome. *Nat Rev Genet* **13**, 795-806 (2012).

50. Vogelstein, B.*, et al.* Cancer genome landscapes. *Science* **339**, 1546-1558 (2013).

51. Feinberg, A.P. & Vogelstein, B. Hypomethylation distinguishes genes of some human cancers from their normal counterparts. *Nature* **301**, 89-92 (1983).

52. Feinberg, A.P. & Tycko, B. The history of cancer epigenetics. *Nat Rev Cancer* **4**, 143-153 (2004).

53. Esteller, M. Cancer epigenomics: DNA methylomes and histone-modification maps. *Nat Rev Genet* **8**, 286-298 (2007).

54. Hahn, M.A.*, et al.* Dynamics of 5-hydroxymethylcytosine and chromatin marks in Mammalian neurogenesis. *Cell Rep* **3**, 291-300 (2013).

55. Choi, I., Kim, R., Lim, H.W., Kaestner, K.H. & Won, K.J. 5-hydroxymethylcytosine represses the activity of enhancers in embryonic stem cells: a new epigenetic signature for gene regulation. *BMC Genomics* **15**, 670 (2014).

56. Hon, G.C.*, et al.* 5mC oxidation by Tet2 modulates enhancer activity and timing of transcriptome reprogramming during differentiation. *Mol Cell* **56**, 286-297 (2014).

57. Baylin, S.B. & Jones, P.A. A decade of exploring the cancer epigenome - biological and translational implications. *Nat Rev Cancer* **11**, 726-734 (2011).

58. Ozdag, H.*, et al.* Differential expression of selected histone modifier genes in human solid cancers. *BMC Genomics* **7**, 90 (2006).

59. Greenblatt, S.M. & Nimer, S.D. Chromatin modifiers and the promise of epigenetic therapy in acute leukemia. *Leukemia* **28**, 1396-1406 (2014).

60. Krivtsov, A.V. & Armstrong, S.A. MLL translocations, histone modifications and leukaemia stem-cell development. *Nat Rev Cancer* **7**, 823-833 (2007).

61. Chung, Y.R., Schatoff, E. & Abdel-Wahab, O. Epigenetic alterations in hematopoietic malignancies. *Int J Hematol* **96**, 413-427 (2012).

62. Nakajima, H. & Kunimoto, H. TET2 as an epigenetic master regulator for normal and malignant hematopoiesis. *Cancer Sci* **105**, 1093-1099 (2014).

63. Ko, M.*, et al.* TET proteins and 5-methylcytosine oxidation in hematological cancers. *Immunol Rev* **263**, 6-21 (2015).

64. Scourzic, L.*, et al.* DNMT3A mutant and Tet2 inactivation cooperate in the deregulation of DNA methylation control to induce lymphoid malignancies in mice. *Leukemia* (2016).

65. Lund, K., Adams, P.D. & Copland, M. EZH2 in normal and malignant hematopoiesis. *Leukemia* **28**, 44-49 (2014).

66. Van Vlierberghe, P., Pieters, R., Beverloo, H.B. & Meijerink, J.P. Molecular-genetic insights in paediatric T-cell acute lymphoblastic leukaemia. *Br J Haematol* **143**, 153-168 (2008).

67. Ferrando, A.A.*, et al.* Gene expression signatures define novel oncogenic pathways in T cell acute lymphoblastic leukemia. *Cancer Cell* **1**, 75-87 (2002).

68. Meijerink, J.P. Genetic rearrangements in relation to immunophenotype and outcome in T-cell acute lymphoblastic leukaemia. *Best Pract Res Clin Haematol* **23**, 307-318 (2010).

69. Graux, C., Cools, J., Michaux, L., Vandenberghe, P. & Hagemeijer, A. Cytogenetics and molecular genetics of T-cell acute lymphoblastic leukemia: from thymocyte to lymphoblast. *Leukemia* **20**, 1496-1510 (2006).

70. Goodings, C.*, et al.* Enforced expression of E47 has differential effects on Lmo2-induced T-cell leukemias. *Leuk Res* **39**, 100-109 (2015).

71. Zhang, J.*, et al.* The genetic basis of early T-cell precursor acute lymphoblastic leukaemia. *Nature* **481**, 157-163 (2012).

72. Durinck, K.*, et al.* Novel biological insights in T-cell acute lymphoblastic leukemia. *Exp Hematol* **43**, 625-639 (2015).

73. Ferrando, A.A.*, et al.* Prognostic importance of TLX1 (HOX11) oncogene expression in adults with T-cell acute lymphoblastic leukaemia. *Lancet* **363**, 535-536 (2004).

74. Kees, U.R.*, et al.* Expression of HOX11 in childhood T-lineage acute lymphoblastic leukaemia can occur in the absence of cytogenetic aberration at 10q24: a study from the Children's Cancer Group (CCG). *Leukemia* **17**, 887-893 (2003).

75. Berger, R.*, et al.* t(5;14)/HOX11L2-positive T-cell acute lymphoblastic leukemia. A collaborative study of the Groupe Francais de Cytogenetique Hematologique (GFCH). *Leukemia* **17**, 1851-1857 (2003).

76. Kleppe, M.*, et al.* Deletion of the protein tyrosine phosphatase gene PTPN2 in T-cell acute lymphoblastic leukemia. *Nat Genet* **42**, 530-535 (2010).

77. Van Vlierberghe, P.*, et al.* PHF6 mutations in T-cell acute lymphoblastic leukemia. *Nat Genet* **42**, 338-342 (2010).

78. Asnafi, V.*, et al.* CALM-AF10 is a common fusion transcript in T-ALL and is specific to the TCRgammadelta lineage. *Blood* **102**, 1000-1006 (2003).

79. Ferrando, A.A. The role of NOTCH1 signaling in T-ALL. *Hematology Am Soc Hematol Educ Program*, 353-361 (2009).

80. Real, P.J.*, et al.* Gamma-secretase inhibitors reverse glucocorticoid resistance in T cell acute lymphoblastic leukemia. *Nat Med* **15**, 50-58 (2009).

81. Tosello, V. & Ferrando, A.A. The NOTCH signaling pathway: role in the pathogenesis of T-cell acute lymphoblastic leukemia and implication for therapy. *Ther Adv Hematol* **4**, 199-210 (2013).

82. Pinnell, N.*, et al.* The PIAS-like Coactivator Zmiz1 Is a Direct and Selective Cofactor of Notch1 in T Cell Development and Leukemia. *Immunity* **43**, 870-883 (2015).

83. Ntziachristos, P.*, et al.* Genetic inactivation of the polycomb repressive complex 2 in T cell acute lymphoblastic leukemia. *Nat Med* **18**, 298-301 (2012).

84. Ntziachristos, P.*, et al.* Contrasting roles of histone 3 lysine 27 demethylases in acute lymphoblastic leukaemia. *Nature* **514**, 513-517 (2014).

85. Li, N.*, et al.* Cyclin C is a haploinsufficient tumour suppressor. *Nat Cell Biol* **16**, 1080-1091 (2014).

86. Kanzler, B. & Dear, T.N. Hox11 acts cell autonomously in spleen development and its absence results in altered cell fate of mesenchymal spleen precursors. *Dev Biol* **234**, 231-243 (2001).

87. Guo, Z*., et al.* Tlx1/3 and Ptf1a control the expression of distinct sets of transmitter and peptide receptor genes in the developing dorsal spinal cord. *J Neurosci* **32**, 8509-8520 (2012).

88. Heidari, M., Rice, K.L., Phillips, J.K., Kees, U.R. & Greene, W.K. The nuclear oncoprotein TLX1/HOX11 associates with pericentromeric satellite 2 DNA in leukemic T-cells. *Leukemia* **20**, 304-312 (2006).

89. Owens, B.M., Hawley, T.S., Spain, L.M., Kerkel, K.A. & Hawley, R.G. TLX1/HOX11-mediated disruption of primary thymocyte differentiation prior to the CD4+CD8+ double-positive stage. *Br J Haematol* **132**, 216-229 (2006).

90. Riz, I., Hawley, T.S., Johnston, H. & Hawley, R.G. Role of TLX1 in T-cell acute lymphoblastic leukaemia pathogenesis. *Br J Haematol* **145**, 140-143 (2009).

91. Dadi, S*., et al.* TLX homeodomain oncogenes mediate T cell maturation arrest in T-ALL via interaction with ETS1 and suppression of TCRalpha gene expression. *Cancer Cell* **21**, 563-576 (2012).

92. Della Gatta, G*., et al.* Reverse engineering of TLX oncogenic transcriptional networks identifies RUNX1 as tumor suppressor in T-ALL. *Nat Med* **18**, 436-440 (2012).

93. De Keersmaecker, K*., et al.* The TLX1 oncogene drives aneuploidy in T cell transformation. *Nat Med* **16**, 1321-1327 (2010).

94. Asnafi, V*., et al.* NOTCH1/FBXW7 mutation identifies a large subgroup with favorable outcome in adult T-cell acute lymphoblastic leukemia (T-ALL): a Group for Research on Adult Acute Lymphoblastic Leukemia (GRAALL) study. *Blood* **113**, 3918-3924 (2009).

95. De Keersmaecker, K. & Ferrando, A.A. TLX1-induced T-cell acute lymphoblastic leukemia. *Clin Cancer Res* **17**, 6381-6386 (2011).

96. Tosello, V*., et al.* WT1 mutations in T-ALL. *Blood* **114**, 1038-1045 (2009).

97. Huether, R*., et al.* The landscape of somatic mutations in epigenetic regulators across 1,000 paediatric cancer genomes. *Nat Commun* **5**, 3630 (2014).

98. Figueroa, M.E*., et al.* Integrated genetic and epigenetic analysis of childhood acute lymphoblastic leukemia. *J Clin Invest* **123**, 3099-3111 (2013).

99. Kraszewska, M.D*., et al.* DNA methylation pattern is altered in childhood T-cell acute lymphoblastic leukemia patients as compared with normal thymic subsets: insights into CpG island methylator phenotype in T-ALL. *Leukemia* **26**, 367-371 (2012).

100. Neumann, M.*, et al.* Whole-exome sequencing in adult ETP-ALL reveals a high rate of DNMT3A mutations. *Blood* **121**, 4749-4752 (2013).

101. Kalender Atak, Z.*, et al.* High accuracy mutation detection in leukemia on a selected panel of cancer genes. *PLoS One* **7**, e38463 (2012).

102. Zhang, Y.*, et al.* Mutation analysis of isocitrate dehydrogenase in acute lymphoblastic leukemia. *Genet Test Mol Biomarkers* **16**, 991-995 (2012).

103. Hao, Z.*, et al.* Idh1 mutations contribute to the development of T-cell malignancies in genetically engineered mice. *Proc Natl Acad Sci U S A* **113**, 1387-1392 (2016).

104. Wang, L.*, et al.* Molecular basis for 5-carboxycytosine recognition by RNA polymerase II elongation complex. *Nature* **523**, 621-625 (2015).

105. Kafer, G.R.*, et al.* 5-Hydroxymethylcytosine Marks Sites of DNA Damage and Promotes Genome Stability. *Cell Rep* **14**, 1283-1292 (2016).

106. Marina, R.J.*, et al.* TET-catalyzed oxidation of intragenic 5-methylcytosine regulates CTCF-dependent alternative splicing. *EMBO J* **35**, 335-355 (2016).

107. Mullighan, C.G.*, et al.* CREBBP mutations in relapsed acute lymphoblastic leukaemia. *Nature* **471**, 235-239 (2011).

108. van Haaften, G.*, et al.* Somatic mutations of the histone H3K27 demethylase gene UTX in human cancer. *Nat Genet* **41**, 521-523 (2009).

109. Van der Meulen, J.*, et al.* The H3K27me3 demethylase UTX is a gender-specific tumor suppressor in T-cell acute lymphoblastic leukemia. *Blood* **125**, 13-21 (2015).

110. De Keersmaecker, K.*, et al.* Exome sequencing identifies mutation in CNOT3 and ribosomal genes RPL5 and RPL10 in T-cell acute lymphoblastic leukemia. *Nat Genet* **45**, 186-190 (2013).

111. Yoo, N.J., Kim, Y.R. & Lee, S.H. Somatic mutation of PHF6 gene in T-cell acute lymphoblatic leukemia, acute myelogenous leukemia and hepatocellular carcinoma. *Acta Oncol* **51**, 107-111 (2012).

112. Wang, Q.*, et al.* Mutations of PHF6 are associated with mutations of NOTCH1, JAK1 and rearrangement of SET-NUP214 in T-cell acute lymphoblastic leukemia. *Haematologica* **96**, 1808-1814 (2011).

113. Mavrakis, K.J.*, et al.* A cooperative microRNA-tumor suppressor gene network in acute T-cell lymphoblastic leukemia (T-ALL). *Nat Genet* **43**, 673-678 (2011).

114. Mets, E.*, et al.* MicroRNA-128-3p is a novel oncomiR targeting PHF6 in T-cell acute lymphoblastic leukemia. *Haematologica* **99**, 1326-1333 (2014).

115. Li, X.*, et al.* Somatic mutations of PHF6 in patients with chronic myeloid leukemia in blast crisis. *Leuk Lymphoma* **54**, 671-672 (2013).

116. Van Vlierberghe, P.*, et al.* PHF6 mutations in adult acute myeloid leukemia. *Leukemia* **25**, 130-134 (2011).

117. Meacham, C.E.*, et al.* A genome-scale in vivo loss-of-function screen identifies Phf6 as a lineage-specific regulator of leukemia cell growth. *Genes Dev* **29**, 483-488 (2015).

118. Lower, K.M.*, et al.* Mutations in PHF6 are associated with Borjeson-Forssman-Lehmann syndrome. *Nat Genet* **32**, 661-665 (2002).

119. Turner, G.*, et al.* The clinical picture of the Borjeson-Forssman-Lehmann syndrome in males and heterozygous females with PHF6 mutations. *Clin Genet* **65**, 226-232 (2004).

120. Visootsak, J.*, et al.* Clinical and behavioral features of patients with Borjeson-Forssman-Lehmann syndrome with mutations in PHF6. *J Pediatr* **145**, 819-825 (2004).

121. Zhang, C.*, et al.* The X-linked intellectual disability protein PHF6 associates with the PAF1 complex and regulates neuronal migration in the mammalian brain. *Neuron* **78**, 986-993 (2013).

122. Zweier, C.*, et al.* A new face of Borjeson-Forssman-Lehmann syndrome? De novo mutations in PHF6 in seven females with a distinct phenotype. *J Med Genet* **50**, 838-847 (2013).

123. Chao, M.M.*, et al.* T-cell acute lymphoblastic leukemia in association with Borjeson-Forssman-Lehmann syndrome due to a mutation in PHF6. *Pediatr Blood Cancer* **55**, 722-724 (2010).

124. Voss, A.K.*, et al.* Protein and gene expression analysis of Phf6, the gene mutated in the Borjeson-Forssman-Lehmann Syndrome of intellectual disability and obesity. *Gene Expr Patterns* **7**, 858-871 (2007).

125. Wang, J.*, et al.* PHF6 regulates cell cycle progression by suppressing ribosomal RNA synthesis. *J Biol Chem* **288**, 3174-3183 (2013).

126. Dephoure, N.*, et al.* A quantitative atlas of mitotic phosphorylation. *Proc Natl Acad Sci U S A* **105**, 10762-10767 (2008).

127. Matsuoka, S.*, et al.* ATM and ATR substrate analysis reveals extensive protein networks responsive to DNA damage. *Science* **316**, 1160-1166 (2007).

128. Hills, S.A. & Diffley, J.F. DNA replication and oncogene-induced replicative stress. *Curr Biol* **24**, R435-444 (2014).

129. Weber, A.M. & Ryan, A.J. ATM and ATR as therapeutic targets in cancer. *Pharmacol Ther* **149**, 124-138 (2015).

130. Hahnel, P.S.*, et al.* Targeting components of the alternative NHEJ pathway sensitizes KRAS mutant leukemic cells to chemotherapy. *Blood* **123**, 2355-2366 (2014).

131. Kindler, T.*, et al.* K-RasG12D-induced T-cell lymphoblastic lymphoma/leukemias harbor Notch1 mutations and are sensitive to gamma-secretase inhibitors. *Blood* **112**, 3373-3382 (2008).

132. Sarmento, L.M.*, et al.* CHK1 overexpression in T-cell acute lymphoblastic leukemia is essential for proliferation and survival by preventing excessive replication stress. *Oncogene* **34**, 2978-2990 (2015).

133. Baker, L.A., Allis, C.D. & Wang, G.G. PHD fingers in human diseases: disorders arising from misinterpreting epigenetic marks. *Mutat Res* **647**, 3-12 (2008).

134. Sanchez, R. & Zhou, M.M. The PHD finger: a versatile epigenome reader. *Trends Biochem Sci* **36**, 364-372 (2011).

135. Falkenberg, K.J. & Johnstone, R.W. Histone deacetylases and their inhibitors in cancer, neurological diseases and immune disorders. *Nat Rev Drug Discov* **13**, 673-691 (2014).

136. Sanchez, R. & Zhou, M.M. The role of human bromodomains in chromatin biology and gene transcription. *Curr Opin Drug Discov Devel* **12**, 659-665 (2009).

137. Basheer, F. & Huntly, B.J. BET bromodomain inhibitors in leukemia. *Exp Hematol* **43**, 718-731 (2015).

138. Simo-Riudalbas, L. & Esteller, M. Targeting the histone orthography of cancer: drugs for writers, erasers and readers. *Br J Pharmacol* **172**, 2716-2732 (2015).

139. Kuzmichev, A., Nishioka, K., Erdjument-Bromage, H., Tempst, P. & Reinberg, D. Histone methyltransferase activity associated with a human multiprotein complex containing the Enhancer of Zeste protein. *Genes Dev* **16**, 2893-2905 (2002).

140. Sun, L*., et al.* Cyclin E-CDK2 protein phosphorylates plant homeodomain finger protein 8 (PHF8) and regulates its function in the cell cycle. *J Biol Chem* **290**, 4075-4085 (2015).

141. Lim, H.J*., et al.* The G2/M regulator histone demethylase PHF8 is targeted for degradation by the anaphase-promoting complex containing CDC20. *Mol Cell Biol* **33**, 4166-4180 (2013).

142. Qi, H.H*., et al.* Histone H4K20/H3K9 demethylase PHF8 regulates zebrafish brain and craniofacial development. *Nature* **466**, 503-507 (2010).

143. Zhu, G*., et al.* Elevated expression of histone demethylase PHF8 associates with adverse prognosis in patients of laryngeal and hypopharyngeal squamous cell carcinoma. *Epigenomics* **7**, 143-153 (2015).

144. Ma, Q*., et al.* The histone demethylase PHF8 promotes prostate cancer cell growth by activating the oncomiR miR-125b. *Onco Targets Ther* **8**, 1979-1988 (2015).

145. Yatim, A*., et al.* NOTCH1 nuclear interactome reveals key regulators of its transcriptional activity and oncogenic function. *Mol Cell* **48**, 445-458 (2012).

146. Hargreaves, D.C. & Crabtree, G.R. ATP-dependent chromatin remodeling: genetics, genomics and mechanisms. *Cell Res* **21**, 396-420 (2011).

147. Ramirez, J. & Hagman, J. The Mi-2/NuRD complex: a critical epigenetic regulator of hematopoietic development, differentiation and cancer. *Epigenetics* **4**, 532-536 (2009).

148. Chi, T.H*., et al.* Sequential roles of Brg, the ATPase subunit of BAF chromatin remodeling complexes, in thymocyte development. *Immunity* **19**, 169-182 (2003).

149. Dege, C. & Hagman, J. Mi-2/NuRD chromatin remodeling complexes regulate B and T-lymphocyte development and function. *Immunol Rev* **261**, 126-140 (2014).

150. Kadoch, C*., et al.* Proteomic and bioinformatic analysis of mammalian SWI/SNF complexes identifies extensive roles in human malignancy. *Nat Genet* **45**, 592-601 (2013).

151. Kosho, T., Miyake, N. & Carey, J.C. Coffin-Siris syndrome and related disorders involving components of the BAF (mSWI/SNF) complex: historical review and recent advances using next generation sequencing. *Am J Med Genet C Semin Med Genet* **166C**, 241-251 (2014).

152. Wieczorek, D*., et al.* A comprehensive molecular study on Coffin-Siris and Nicolaides-Baraitser syndromes identifies a broad molecular and clinical spectrum converging on altered chromatin remodeling. *Hum Mol Genet* **22**, 5121-5135 (2013).

153. Todd, M.A. & Picketts, D.J. PHF6 interacts with the nucleosome remodeling and deacetylation (NuRD) complex. *J Proteome Res* **11**, 4326-4337 (2012).

154. Sun, Y.E., Cheng, L. & Hu, K. With NuRD, HDACs Go "Nerdy". *Dev Cell* **30**, 9-10 (2014).

155. Yang, G., Lu, X. & Yuan, L. LncRNA: a link between RNA and cancer. *Biochim Biophys Acta* **1839**, 1097-1109 (2014).

156. Yan, K.*, et al.* Structure Prediction: New Insights into Decrypting Long Noncoding RNAs. *Int J Mol Sci* **17**(2016).

157. Haemmerle, M. & Gutschner, T. Long non-coding RNAs in cancer and development: where do we go from here? *Int J Mol Sci* **16**, 1395-1405 (2015).

158. Huarte, M. The emerging role of lncRNAs in cancer. *Nat Med* **21**, 1253-1261 (2015).

159. Liu, G., Mattick, J.S. & Taft, R.J. A meta-analysis of the genomic and transcriptomic composition of complex life. *Cell Cycle* **12**, 2061-2072 (2013).

160. Wang, K.C.*, et al.* A long noncoding RNA maintains active chromatin to coordinate homeotic gene expression. *Nature* **472**, 120-124 (2011).

161. Rinn, J.L. & Chang, H.Y. Genome regulation by long noncoding RNAs. *Annu Rev Biochem* **81**, 145-166 (2012).

162. Lee, J.T. & Jaenisch, R. Long-range cis effects of ectopic X-inactivation centres on a mouse autosome. *Nature* **386**, 275-279 (1997).

163. Panning, B., Dausman, J. & Jaenisch, R. X chromosome inactivation is mediated by Xist RNA stabilization. *Cell* **90**, 907-916 (1997).

164. Brockdorff, N. Noncoding RNA and Polycomb recruitment. *RNA* **19**, 429-442 (2013).

165. Rinn, J.L.*, et al.* Functional demarcation of active and silent chromatin domains in human HOX loci by noncoding RNAs. *Cell* **129**, 1311-1323 (2007).

166. Hajjari, M. & Salavaty, A. HOTAIR: an oncogenic long non-coding RNA in different cancers. *Cancer Biol Med* **12**, 1-9 (2015).

167. Guil, S. & Esteller, M. RNA-RNA interactions in gene regulation: the coding and noncoding players. *Trends Biochem Sci* **40**, 248-256 (2015).

168. Poliseno, L.*, et al.* A coding-independent function of gene and pseudogene

mRNAs regulates tumour biology. *Nature* **465**, 1033-1038 (2010).

169. Wang, J.*, et al.* CREB up-regulates long non-coding RNA, HULC expression through interaction with microRNA-372 in liver cancer. *Nucleic Acids Res* **38**, 5366-5383 (2010).

170. Ronnau, C.G., Verhaegh, G.W., Luna-Velez, M.V. & Schalken, J.A. Noncoding RNAs as novel biomarkers in prostate cancer. *Biomed Res Int* **2014**, 591703 (2014).

171. Gloss, B.S. & Dinger, M.E. The specificity of long noncoding RNA expression. *Biochim Biophys Acta* (2015).

172. Gutschner, T.*, et al.* The noncoding RNA MALAT1 is a critical regulator of the metastasis phenotype of lung cancer cells. *Cancer Res* **73**, 1180-1189 (2013).

173. Mohammadin, S., Edger, P.P., Pires, J.C. & Schranz, M.E. Positionally-conserved but sequence-diverged: identification of long non-coding RNAs in the Brassicaceae and Cleomaceae. *BMC Plant Biol* **15**, 217 (2015).

174. Johnsson, P., Lipovich, L., Grander, D. & Morris, K.V. Evolutionary conservation of long non-coding RNAs; sequence, structure, function. *Biochim Biophys Acta* **1840**, 1063-1071 (2014).

## Chapter 1: Introduction

# PART II: Review

## Novel biological insights in T-cell acute lymphoblastic leukemia

Kaat Durinck[1], Steven Goossens[2,3,4], Sofie Peirs[1], Annelynn Wallaert[1], Wouter Van Loocke[1], Filip Matthijssens[1], Tim Pieters[1,2,3], Gloria Milani[1], Tim Lammens[5], Pieter Rondou[1], Nadine Van Roy[1], Barbara De Moerloose[5], Yves Benoit[5], Jody Haigh[4], Frank Speleman[1], Bruce Poppe[1*] and Pieter Van Vlierberghe[1*]

[1]*Center for Medical Genetics, Department for Pediatrics, Ghent, Belgium*

[2]*Department for Biomedical Molecular Biology, Ghent University, Ghent, Belgium*

[3]*Unit for Molecular Oncology, VIB Inflammation Research Center, Ghent, Belgium*

[4]*Mammalian Functional Genetics Laboratory, Division of Blood Cancers, Australian Centre for Blood Diseases, Monash University, Melbourne, Victoria, Australia*

[5]*Department of Pediatric Hematology-Oncology and Stem Cell Transplantation, Ghent University Hospital, Ghent, Belgium*

**Exp Hematol. 2015 Aug;43(8):625-39.**

## Chapter 1: Introduction

## Abstract

T-cell acute lymphoblastic leukemia (T-ALL) is an aggressive type of blood cancer that accounts for about 15% of paediatric and 25% of adult ALL cases and is considered a paradigm for the multistep nature of cancer initiation and progression. Genetic and epigenetic reprogramming events, which transform T-cell precursors into malignant T-ALL lymphoblasts, have been extensively characterized over the past decade.

Despite our comprehensive understanding of the genomic landscape of human T-ALL, leukemia patients are nowadays still treated by high-dose multi-agent chemotherapy potentially followed by hematopoietic stem cell transplantation. Even with such aggressive treatment regimens, which are often associated with considerable acute and long-term side effects, about 15% of paediatric and 40% of adult T-ALL patients still relapse due to acquired therapy resistance and present with very dismal survival perspectives. Unfortunately, the molecular mechanisms by which residual T-ALL tumor cells survive chemotherapy and act as a reservoir for leukemic progression and hematological relapse remain poorly understood.

Nevertheless, it is expected that enhanced molecular understanding of T-ALL disease biology will ultimately facilitate a targeted therapy driven approach that can reduce chemotherapy associated toxicities and improve survival of refractory T-ALL patients through personalized salvage therapy. In this review, we summarize recent biological insights in the molecular pathogenesis of T-ALL and speculate how the genetic landscape of T-ALL could trigger the development of novel therapeutic strategies for the treatment of human T-ALL.

# Chapter 1: Introduction

## Introduction

Normal T-cell development is a strictly regulated, multi-step process in which hematopoietic progenitor cells differentiate into functionally diverse T-lymphocyte subsets after their migration into the thymus microenvironment. The different checkpoints, covering thymic colonization, lineage commitment and definitive differentiation[1] are orchestrated by diverse transcriptional regulatory networks and transitions between epigenetic states[2,3] in response to cytokine receptor activation. During this fine-tuned developmental process, inappropriate activation of T-cell acute lymphoblastic leukemia (T-ALL) T-ALL oncogenes and loss of tumor suppressor gene activity will coordinately push thymic precursors into uncontrolled clonal expansion and cause T-ALL.

T-ALL is an aggressive hematological cancer that arises from the malignant transformation of T-cell progenitors and occurs in about 15% of pediatric and 25% of adult ALL cases. High-dose multi-agent chemotherapy serves as the current standard of care for this tumor entity and is highly effective in the majority of childhood leukemia patients with overall survival rates reaching 85% in most pediatric protocols. Nevertheless, these aggressive treatment regimens are often associated with severe acute toxicities and long-term side effects, including the development of secondary tumors later in life. Notably, the situation for older leukemia patients is less favorable as compared to children with at least 40% of adult T-ALL patients failing current therapy. Despite the introduction of hematopoietic stem cell transplantations for refractory leukemias, the clinical outcome of these high-risk, primary resistant tumors remains extremely poor[4-6].

Different studies have collectively shown that T-ALL can be divided in molecular genetic subgroups that are characterized by unique gene expression signatures and aberrant activation of specific T-ALL transcription factor oncogenes, including *MEF2C*, *HOXA*, *TLX1*, *NKX2.1*, *TLX3*, *TAL1*, *LMO1* and *LMO2*[6-10]. Moreover, whole-genome T-ALL profiling has provided a fairly complete and comprehensive list of additional genetic defects that are shared amongst the different genetic subclasses

and activate a plethora of oncogenic signaling cascades including interleukin 7 receptor (IL7R)/Janus Kinase (JAK)/Signal transducer and activator of transcription (STAT)[11], phosphatidylinositol 3-kinase (PI3K)/AKT[12-14] and Ras/mitogen extracellular-signal-related kinase (MEK)/extracellular signal-regulated kinase (ERK)[15] signaling. In addition, some of these cooperative genetic lesions also coordinately target more general cellular pathways, as exemplified by aberrant activation of anti-apoptotic effector pathways and enhanced cap-dependent translation activity in human T-ALL. Notably, this conversion towards aberrant activation of a discrete set of common cellular or signaling pathways provides unique opportunities for the development of targeted therapies in the context of human T-ALL[16, 17].

Now that we acquired a detailed molecular understanding of the genetic defects that drive human T-ALL at the coding level of the genome, we face a number of interesting challenges that will hopefully be addressed in the near future. First, we need to better understand how specific T-ALL oncogenes and tumor suppressors actually cooperate to drive overt disease and full leukemic transformation. Indeed, we lack a thorough understanding of the genetic interactions between genetic defects that preferentially co-occur in primary human T-ALL samples. Secondly, the potential contribution of the exact order in which genetic lesions are acquired during disease initiation, progression and/or maintenance should be further investigated. In addition, it is still unclear whether the exact cell of origin for T-cell transformation is truly different for the distinct molecular genetic subtypes of human T-ALL. Moreover, the existence of long-lived pre-leukemic stem cells (pre-LSCs) in the context of T- ALL is still under debate and the molecular mechanism that could regulate pre-LSC activity of thymic precursors remains poorly characterized. Finally, epigenetic mechanisms and the non-coding part of the human genome provide an additional layer of complexity and we are currently only starting to understand the putative oncogenic contributions of deregulated microRNAs (miRNAs), long non-coding RNAs (lncRNAs), enhancer activities, chromatin remodeling and/or epigenetic changes in the context of malignant T-cell transformation.

In this review, we summarize recent biological insights in the molecular pathogenesis

of T- ALL and discuss the impact of these findings on some of the intriguing challenges mentioned above. Moreover, we speculate on how the genetic landscape of T-ALL could trigger the development of novel therapeutic strategies for the treatment of human T-ALL.

## Genetic heterogeneity of immature T-ALL subtypes

More than a decade ago, attempts were made to classify human T-ALL into different tumor entities based on their transcriptional signature. Indeed, depending on the expression of specific T-ALL transcription factor oncogenes, T-cell leukemia was classified into molecular genetic subgroups reflecting distinct stages of arrest during T-cell development[7].

In these initial studies, early immature T-ALLs were recognized as a transcriptionally distinct leukemic entity with high expression of the basic Helix-Loop-Helix (bHLH) transcription factor' lymphoblastic leukemia associated hematopoiesis regulator' (*LYL1*) and the 'LIM domain–only protein' (*LMO2*)[7]. In addition, leukemic blasts from these so-called *LYL1*$^{+}$ T-ALLs collectively expressed early lymphoid/myeloid markers including CD13, CD33 and/or CD34, and mostly lacked CD4 or CD8 proteins at their surface. Although no unifying molecular alterations could be identified in *LYL1*$^{+}$ T-ALLs, these leukemias were characterized by a high frequency of deletions on the long arm of chromosome 5 and often lacked deletions on the short arm of chromosome 9 targeting the *CDKN2A/CDKN2B* tumor suppressor locus[7].

Absence of these 9p deletions, which occur in more than 70% of other T-ALL subtypes[18], is an intriguing feature of immature T-ALL that might be linked to the epigenetic state of the *cdkn2a* locus during tumor progression. In primitive hematopoietic precursor cells, the polycomb repressive complex 2 (PRC2) mediates silencing of the *Ink4a-Arf* locus[19, 20], suggesting that leukemias that originate from hematopoietic progenitors lack the selective pressure for genomic *cdkn2a* deletion during T-cell transformation[21, 22]. In contrast, this permanent silencing is not present in early thymocytes in which the *Ink4a-Arf* locus can be re-activated in response to

oncogenic signaling[21]. In such model, engagement of *cdkn2a* expression during tumor initiation creates a strong selective pressure for rare cells to bypass tumor suppression by deleting *cdkn2a* and eventually, to emerge as clonal malignancies[22]. Altogether, these studies might provide an explanation for the unequal distribution of *CDKN2A/CDKN2B* deletions between immature and mature T-ALLs, supporting the view that the cell of origin for some early immature leukemias might have features of a very early hematopoietic progenitor. More recent efforts have further enhanced our molecular understanding of immature T-ALLs and provided a comprehensive overview of genetic alterations that occur in this particular subtype of human T-ALL. These studies showed that the genetic landscape of immature T- ALL is highly heterogeneous with aberrant expression of the *MEF2C* gene[23, 24], genetic alterations in hematopoietic transcription factors such as *RUNX1*, *GATA3*, *BCL11B*, *PU.1* and *ETV6*[24], activating mutations in critical mediators of cytokine receptor and Ras signaling, including *NRAS*, *KRAS*, *FLT3*, *IL7R*, *JAK1*, *JAK3*, *SH2B3* and *BRAF*; mutations in the epigenetic regulators *EZH2*, *EED*, *SUZ12*, *MLL2*, *BMI1*, *SETD2* and *EP300*; and mutations in the dynamin coding gene *DNM2*[8, 25]. In addition, immature T-ALLs present with lower frequencies of the prototypical *NOTCH1* mutations, which occur in the majority of mature T- ALL patient samples and are considered one of the hallmarks of human T-cell transformation.

For reasons not well understood, the relative percentage of immature T-ALLs in adults seems to be significantly higher as compared with children[26] and some molecular alterations are exclusively present in adult immature T-ALLs[26]. For example, genetic lesions that were initially identified in acute myeloid leukemia and target genes implicated in DNA methylation, such as *DNMT3A*, *IDH1* and *IDH2* are uniquely present in adult immature T-ALL and have not been reported in pediatric patients. In that context, it was recently shown that *DNMT3A* mutations in primary human acute myeloid leukemias (AMLs) occur in both pre-leukemic hematopoietic stem cells (HSCs) and committed T-cells, suggesting that *DNMT3A* mutant pre-leukemic HSCs retain the ability to differentiate into multiple cell types[27]. Therefore, *DNMT3A* mutations could act as an early leukemogenic event that enables the establishment of a pre-leukemic reservoir. Such *DNMT3A* mutant pre-HSCs could

remain quiescent over a certain period in life and eventually progress towards malignant transformation in the myeloid and/or early T-cell lineage depending on the spectrum of acquired secondary hits. Notably, such hierarchical model in which pre-leukemic stem cells precede full malignant transformation has been previously proposed in the context of T-ALL[28]. The concept of *DNMT3A* mutant pre-leukemic HSCs, which emerge in ageing adults, could partially explain why *DNMT3A* mutations are not identified in pediatric early T-cell precursor ALL (ETP-ALL)[25], but are mainly present in early immature adult T-ALLs [26, 29]. Nevertheless, it is currently unknown whether a similar model could be applied for other lesions that target the DNA methylation machinery, including *IDH1* and *IDH2* mutations.

## Thymocyte self renewal and pre-leukemic stem cells in T-ALL development

Pre-leukemic stem cells (pre-LSC) are a population of progenitor cells that harbour a few mutations, but not the entire complement of genetic alterations necessary to become a leukemia. In contrast to these fully transformed leukemic cells, pre-LSCs retain the ability to differentiate into the full spectrum of mature daughter cells. In addition, their stem cell properties allow clonal expansion and subsequent acquisition of extra oncogenic driver mutations, eventually leading to the onset of a fully transformed tumor.

McCormack and colleagues initially described a population of long-term self-renewing thymocytes many months prior to the generation of leukemia in the *CD2-LMO2*$^{tg}$ transgenic mouse model[30] that spontaneously develops T-ALL with an expression profile similar to that of immature T-ALL patients. Unlike the thymus of normal mice, which is continually replenished by progenitors from the bone marrow, the pre-leukemic thymus of *CD2-LMO2*$^{tg}$ transgenic mice was self-sustaining from a young age. The self-renewal capacity of *CD2- LMO2*$^{tg}$ thymocytes was restricted to the $CD4^-CD8^-$ double negative precursor T-cells, specifically the $CD4^-CD8^-CD44^-CD25^+$ (DN3) subpopulation. In addition, it was demonstrated that the bHLH transcription

factor *Lyl1* is an essential but not a sufficient factor to reprogram *Lmo2* overexpressing DN3 cells into pre-LSCs[31]. More work will need to be done to decipher the exact molecular mechanism explaining how LMO2 controls thymocyte self-renewal. LMO2 itself has no DNA binding capacity and depends on LYL1 for its transcriptional activity. LYL1 as well requires binding with other helix-loop-helix proteins, including E2A, E47 or 'transcription factor 12' (TCF12, HEB), to form heterodimers, which can recognize E-box sequences in specific target gene promoters. Recently, it was suggested that LMO2 and 'LIM domain binding 1' (LDB1) are essential co-factors to bridge two of these heterodimer complexes as a prerequisite for binding at tandem E-boxes throughout the genome[32].

More recently, it was shown that these pre-LSCs are Notch1 dependent and supra-physiological levels of Notch1 expanded the pool of pre-LSC and rendered them independent of the thymic microenvironment[33, 34]. Nevertheless, It remains to be determined whether gain of pre-leukemic self-renewal capacity is a true obligatory trait for human T-ALL development. Moreover, it would be interesting to know whether other T-ALL specific transcription factor oncogenes, including NKX2.1, MEF2C, TLX1, TLX3 or HOXA, also possess the intrinsic capacity to induce self-renewal in T cell progenitors[28].

Finally, the pre-LSCs discussed above are more chemo/radioresistant and could reflect the population that would eventually give rise to tumor relapse after chemotherapy. Recent studies indicate that pre-LSC radioresistance and self-renewal capacity are regulated via distinct molecular pathways[35]. Although *Kit* is not essential for *LMO2* mediated leukemia development, *Lmo2* transgenic thymocytes utilize Kit-dependent signaling pathways to enable radioresistance.

## Prognostic relevance of immature subtypes of human T-ALL

From a clinical perspective, early work suggested that *LYL1*$^{+}$ T-ALLs could be associated with reduced survival rates and this notion was further supported by the

identification of early T- cell specific 'V-Ets avian erythroblastosis virus E26 oncogene homolog' (*ERG*) and 'brain and acute leukemia cytoplasmic' (*BAALC*) expression as poor prognostic markers in adult T-ALL[36]. In addition, absence of bi-allelic deletion of T-cell receptor γ, a marker for early arrest during T-cell differentiation, was associated with induction failure and poor clinical outcome in pediatric T-ALL[37]. Some studies have suggested that *RUNX1*[38], *DNMT3A*[26], *IDH1*[26] or *IDH2*[26] mutations might confer poor prognosis within the immature subtype of adult T-ALL. Further, specific immature subtypes characterized by aberrant *HOXA* gene activation, including *SET-NUP214* and *CALM-AF10* positive leukemias, were associated with higher levels of corticosteroid resistance[39] or dismal survival rates[40]. Finally, in an attempt to start integrating these molecular genetic findings into the clinic, the Group for Research in Adult Acute Lymphoblastic Leukemia (GRAALL) implemented a *NOTCH1/FBXW7/RAS/PTEN*-based oncogenetic risk classification, in which patients with mutated *NOTCH1* or *FBXW7* who present with a wild-type *RAS* and *PTEN* are considered low-risk, whereas all other adult T-ALLs are categorized in a high-risk category[41]. Notably, this new risk classification strategy was strongly associated with higher cumulative incidence of relapse and shorter relapse-free and overall survival in the multicenter GRAALL-2003 and GRAALL-2005 clinical trials[42]. Additional inclusion of poor prognostic genetic markers, such as mutational status of *DNMT3A*, *IDH1* and *IDH2* mutations, should be considered to further improve this novel risk stratification approach for adult T-ALL. Moreover, it should be noted that the prognostic value of this novel risk classification strategy might not be applicable in pediatric treatment protocols given the high overall survival rates for T-ALL in children.

More recently, early T-cell precursor ALL (ETP-ALL) was identified as a specific sub-entity within immature T-ALL with unique immunophenotypic properties, including lack of CD1a and CD8 expression, weak CD5 positivity and expression of one of the stem cell/myeloid markers CD13, CD117, CD33, 'major histocompatibility, Class II, DR-Beta (HLA-DR) and/or CD34. Most importantly, the initial study that defined ETP-ALL as a novel immature subtype of pediatric human T-ALL, reported an extremely poor clinical course for these patients with 10-year overall survival rates of 19% for

ETP-ALL patients as compared with 84% for other T-ALL subtypes[43]. Although the poor clinical characteristics of this leukemic subtype were subsequently validated in a variety of independent patient series from different international pediatric T-ALL treatment protocols[24, 43-46], more recent work has started to question the prognostic relevance of this aggressive T-ALL subtype[23,47]. In that context, a recent and large study on 1,144 pediatric T-ALL patients enrolled in the Children's Oncology Group (COG) Study AALL0434 suggested that, despite significantly higher rates of induction failure, pediatric ETP-ALL patients as defined by flow cytometry in a single reference laboratory, show 5-year event-free and overall survival rates identical to those of non-ETP-ALLs[48]. These discrepant results suggest that subtle differences in treatment protocols or particular challenges associated with accurate assessment of the ETP-ALL immunophenotype might ultimately affect the therapeutic response for ETP-ALL observed in different studies, institutions and/or treatment protocols. Nevertheless, given the size of the patient population included in the COG Study, it seems unlikely that the ETP-ALL immunophenotype, as originally defined by Coustan-Smith et al.[43], will eventually be implemented as a useful prognostic marker to guide treatment decisions for pediatric T-ALL.

## Novel drivers of T-ALL oncogenesis

*ZEB2 as a novel transcription factor oncogene in early immature T-ALL*

Although immature T-ALL has been identified as a separate T-ALL disease entity, this genetic subtype is relatively heterogeneous; only few oncogenic transcription factors implicated in immature T-ALL disease biology have been identified to date.

The zinc finger E-box binding homeobox 2 protein (*ZEB2*/*SIP1*) has an established role in the process of epithelial-mesenchymal transition (EMT) and is implicated in both normal embryonic development and tumorigenesis[49] such as melanoma[50], breast[51] and gastric cancer[52]. ZEB2 is also abundantly expressed in the hematopoietic system and is essential for differentiation and mobilization of hematopoietic stem cells during embryonic development[53]. However, the role of ZEB2 in normal T-cell

development and hematological malignancies has not been thoroughly investigated. Recently, Goossens et al.[54] identified the translocation, t(2;14)(q22;q32), as a rare but recurrent genetic event in immature T-ALL. Detailed cytogenetic analysis allowed mapping of the translocation breakpoint at 14q32 within the *BCL11B* locus and within close vicinity of the *ZEB2* gene at chromosomal band 2q22. Notably, juxtaposition of *BCL11B* near putative oncogenes has been previously reported for a number of T-ALL oncogenes including *TLX3*, *NKX2-5* and *PU.1*[55, 56]. Therefore, this work suggested that sustained expression of the EMT regulator ZEB2 could act as a molecular driver of immature T-ALL development. It is also interesting to note that *BCL11B* haplo-insufficiency has also been implicated in T-cell leukemogenesis, as exemplified by loss-of-function *BCL11B* deletions and mutations identified in primary T-ALLs[57, 58]. Therefore, this particular chromosomal translocation might execute a dual function towards malignant T-cell transformation with concomitant loss of *BCL11B* and gain of *ZEB2*, a concept that also applies for the other *BCL11B*-driven translocations mentioned above.

Using a conditional ROSA26-based *Zeb2* gain-of-function mouse model, Goossens et al.[54] showed that hematopoietic overexpression of *Zeb2* resulted in spontaneous thymic lymphoma development starting at 5 months of age, indicating that *Zeb2* can act as a *bona fide* oncogene in hematologic T cell malignancies. Furthermore, breeding of this tumor model in a tumor-prone p53 null background revealed that *Zeb2* overexpression shortens tumor latency and drives a gene expression profile that resembles immature T-ALL, including the early T-cell/stem cell markers *c-Kit*, *Baalc* and *Lyl1*. Similar activation of a stem cell-like transcriptional program has previously been described in a *CD2-Lmo2*$^{tg}$ mouse model[59], in which pre-leukemic thymocytes acquired *Lmo2* driven self-renewal capacity as a prerequisite of full clonal T cell transformation[30]. Similarly, transplantation experiments using *Zeb2* overexpressing lymphoblasts in immunodeficient mice showed that *Zeb2* driven tumors contained a higher fraction of leukemia-initiating cells as compared with controls, suggesting some putative communalities between the *Zeb2* and *Lmo2* driven tumor models as described above. Interestingly, ZEB proteins also bind tandem E-boxes[60] suggesting a potential overlap or competition for the same

regulatory sequences with the above described LYL1/LMO2 transcriptional regulatory complex[32].

*Zeb2* tumors were also characterized by enhanced JAK/STAT signaling through transcriptional activation of *IL7R*. This association between ZEB2 and IL7R/JAK/STAT activation is in line with other recent studies that reported alternative *in vivo* models for immature T-ALL. Indeed, bone marrow transplantation of precursor cells expressing gain-of- function *IL7R*[61] or *JAK3*[62] mutations resulted in the development of a transplantable murine immature T-ALL, reminiscent of the human disease. Altogether, this study convincingly identified *ZEB2* as a novel oncogene implicated in immature T-ALL, but the molecular mechanisms by which ZEB2 regulates leukemic stem cell activity, in addition to the spectrum of direct ZEB2 target genes that modulate disease initiation or progression remain to be established.

*The role of non-coding RNAs in T-ALL*

Over the last years, genome wide profiling studies have extensively characterized oncogenic gene expression signatures of molecular genetic subtypes in human T-ALL[7-10]. It has become clear that protein-coding genes only constitute about 2% of the entire genome, suggesting that the human transcriptome is predominantly composed of non-coding RNAs[63]. Besides those RNA species carrying out some of the main housekeeping functions (such as rRNAs, snoRNAs and tRNAs), diverse classes such as miRNAs, lncRNAs and circular RNAs constitute novel functional effectors and are crucial regulators of diverse gene expression programs.

**MicroRNAs in the pathogenesis of T-ALL**

MicroRNAs (miRNAs) are a well-known class of small non-coding RNAs, important in both normal development and cancer[64]. The regulatory functions of miRNAs are essential to all levels of hematopoietic development[65]. With respect to T-ALL, a landmark study by Mavrakis et al.[66] identified a set of five microRNAs (*miR-19b*, *miR-*

*20a*, *miR-26a*, *miR-92* and *miR-223*) that cooperatively suppress a network of tumor suppressor genes including *PHF6*, *PTEN*, *BIM* and *FBXW7*. Notably, each of these onco-miRNAs were able to accelerate leukemia onset in a *Notch1*-induced murine bone marrow transplant model of T-ALL, confirming their *in vivo* potential. This study was in line with other work that identified the *miR-17-92* cluster as one of the most prominent oncogenic miRNA clusters able to induce overt T-cell leukemia in concert with activated *NOTCH1*[67, 68]. The role of *miR-223* in oncogenic T-ALL signaling was also emphasized by others[69] and could be further validated through the identification of *miR-223* as a direct target gene of the T-ALL oncogenes *NOTCH1*[70] and *TAL1*, which contributes to T-ALL development by repression of the tumor suppressor gene *FBXW7*[71]. Finally, another study identified *miR-128-3p* as a novel oncogenic miRNA in T- ALL that negatively regulates the expression of the tumor suppressor *PHF6*[72] and cooperates with activated NOTCH1 signaling to accelerate T-ALL formation *in vivo*[72].

In addition to oncogenic miRNAs that contribute to T-cell transformation by inactivation of specific tumor suppressor genes, Sanghvi and co-workers[73] were able to identify a set of so-called tumor suppressor miRNAs (*miR-29*, *miR-31*, *miR-150*, *miR-155* and *miR-200*) in T-ALL. These miRNAs converged towards post-transcriptional activation of the *MYB* and *HBP1* oncogenes. Another recent T-ALL study identified *miR-193b* as an additional tumor suppressor miRNA that also regulated the *MYB* oncogene expression as well as expression of the anti-apoptotic factor *MCL1*[74].

Altogether, it is clear that a small subset of miRNAs has oncogenic or tumor suppressive properties in the context of malignant T-cell transformation (**Figure 1**). Nevertheless, a comprehensive overview of differential miRNA expression between the different molecular genetic subgroups in human T-ALL remains to be established.

### Long non-coding RNAs in the pathogenesis of T-ALL

Long non-coding RNAs (lncRNAs) are defined as transcripts with a length of at least 200 nucleotides that lack protein-coding potential and evolutionary conservation[75]. They are positionally located as antisense, intronic, intergenic or overlapping transcripts with protein coding genes[76]. The functional repertoire of lncRNAs can be very diverse, acting mainly in concert with chromatin modifier enzymes. They can serve as *scaffolds* bridging between multiple proteins, *guides* to target chromatin remodelers to their target sites or *control devices* which can induce protein conformational changes and thereby activate/inactivate the interacting protein complex[77]. Unlike miRNAs, the role of lncRNAs in normal and malignant T-cell development is only starting to be fully explored.

Last year, Trimarchi and colleagues published a pioneering study on the identification of a set of lncRNAs under control of aberrant NOTCH1 signaling in T-ALL[78]. They identified *LUNAR1* as an oncogenic lncRNA, localized in the nucleus, that is overexpressed in primary T-ALLs with higher expression in T-ALL cases that harbor activating *NOTCH1* mutations. *LUNAR1* is located *in cis* to the *IGF1R* locus and promotes its expression through a direct interaction between *LUNAR1* and an intronic *IGF1R* enhancer element, as shown by chromosome conformation capture analysis (Hi-C). Moreover, *in vitro* knockdown of *LUNAR1* significantly affected leukemic cell growth due to decreased 'insulin-like growth factor 1 receptor' (*IGF1R*) signaling. In addition, the *in vivo* oncogenic capacity of the *LUNAR1* transcript was further supported by xenograft assays, in which tumor cells that lost *LUNAR1* expression were outcompeted by the leukemic control population. Importantly, these initial findings were subsequently confirmed by a parallel study[79] in which *LUNAR1* was identified as the top-candidate of NOTCH1 regulated lncRNAs in T-ALL and normal T-cell development. These studies collectively show that lncRNAs act as an additional layer of complexity in T-ALL disease biology and warrant a further in-depth analysis of lncRNA profiles in an extensive series of disease specimens.

## Chapter 1: Introduction

*Aberrant enhancer activity in malignant T-cell development*

Enhancers are gene regulatory elements that can act *in cis* or *trans* and ensure correct spatiotemporal gene expression. It is estimated that there are over one million active enhancers present in all human cells[80]. Hallmark epigenetic features of enhancers include the presence of H3K4me1 and binding by p300, with the absence or presence of H3K27ac further distinguishing between inactive and active enhancers[81]. Context and time-dependent binding of a diversity of transcription factors to these enhancer elements is crucial to ensure proper development and homeostasis[82]. Enhancer activity may act on genes *in cis*, but are often also implicated in long-range interactions through chromatin looping[83].

Recent studies have comprehensively mapped large enhancer regions that are marked by a high occupancy of 'bromodomain containing 4' (BRD4), p300, H3K27ac and the Mediator complex; these are termed the super-enhancers[84]. These large enhancers resemble previously identified locus control regions and associate with lineage specific transcription factors to establish a correct transcriptional cell identity program[85]. Moreover, given that these large enhancers are often aberrantly acquired at oncogenic driver genes, accurate localization and identification of these super-enhancers can help in identifying relevant cancer genes for a variety of tumor entities[86].

Two parallel T-ALL studies conducted by Mansour et al.[87] and Navarro et al.[88] nicely illustrated the putative role of aberrant enhancer activity in the context of T-cell transformation. Notably, these landmark publications identified a new mechanism for oncogene activation in human T-ALL[87, 88], namely, somatic insertions in a regulatory element upstream of the transcriptional start site of the *TAL1* oncogene[87, 88]. Indeed, small acquired heterozygous alterations targeting a non-coding region of the human genome introduced a *de novo* recognition site for 'V-myb avian myeloblastosis viral oncogene homolog' (*MYB*) near the *TAL1* locus[87]. Interestingly, MYB binding at this particular locus resulted in the creation of a somatically acquired super-enhancer and a concomitant epigenetic switch from H3K27me3 to H3K27ac occupancy, which eventually caused increased and mono-allelic *TAL1* expression[87].

Therefore, these studies identified a novel genetic mechanism for the generation of oncogenic super-enhancers in malignant T cells[87, 88] and their results suggest a general role for MYB in the regulation of T-cell specific super-enhancer activity[87]. Additional research will be required to verify if similar mechanisms are also involved in other tumor entities and/or activation of other T-ALL oncogenes.

In T-ALL, it was previously shown that a proportion of relevant NOTCH1 target genes are also under control of long-range enhancers[89]. One interesting example is the massive binding of NOTCH1 at a distal enhancer near the *MYC* locus, which was recently described by Herranz et al.[90] and subsequently independently validated by others[91]. Most notably, conditional deletion of this single, NOTCH1 controlled, *MYC* enhancer site (N-Me) abolished the initiation and maintenance of NOTCH1 induced leukemia *in vivo*[90]. Moreover, recurrent and focal duplications of the *N-Me* locus were found in 5% of T-ALLs, providing an alternative example of genetic alterations that target oncogenic enhancer activity in T-ALL[90].

*Epigenetic modulation in T-ALL*

Genome-wide or candidate-approach based studies recently identified recurrent genomic lesions in a variety of genes involved in DNA methylation or post-translational histone modifications in T-ALL. Therefore, disruption of the epigenetic state and changes in the chromatine structure of normal thymocytes probably represent crucial mediators of malignant T cell transformation. The reversible nature of epigenetic modifications makes these DNA methyltransferases and histone modifier enzymes attractive targets for therapeutic intervention.

The PRC2 complex functions as a methyltransferase that regulates H3K27me3 levels at specific target genes throughout the genome. Notably, the core components of this complex, including *EZH2*, *EED* and *SUZ12*, were identified as tumor suppressor genes in T- ALL, with mutations in about 25% of adult T-ALL cases. Loss of PRC2 activity resulted in reduced levels of H3K27me3 and further enhanced the NOTCH1

driven oncogenic transcriptional program during malignant T-cell transformation[92].

'Lysine-speficic (K) demethylase 6A' (*KDM6A*, *UTX*) is a H3K27 demethylase that exerts an opposite function on gene transcription as compared to the PRC2 complex. By contrast, some studies have reported loss-of- function mutations targeting *UTX* in human T-ALL[93-95], suggesting that both chromatin remodelers can exert tumor suppressor functions during T-cell transformation. Interestingly, Van der Meulen et al.[95] exclusively identified *UTX* mutations in male T-ALL patients and showed that *UTX* escapes chromosome X inactivation in female T-ALL blasts, providing a possible explanation for the skewed gender distribution observed in T-ALL. These findings are also clinically relevant given that T-ALL driven by *UTX* inactivation exhibits collateral sensitivity to pharmacological H3K27me3 inhibition[95]. Finally, the critical role of unbalanced H3K27me3 levels in the initiation and maintenance of T-ALL was further exemplified by a recent study that identified an essential oncogenic role for the H3K27 demethylase 'Lysine-speficic (K) demethylase 6B' (*KDM6B*, *JMJD3*) in the pathogenesis of T-ALL[94]. Indeed, JMJD3 was critically required for the maintenance of oncogenic NOTCH1 signaling during T-cell transformation and was overexpressed in primary T-ALL. JMJD3 inhibition by the small molecule GSKJ4 could restrain T-ALL tumor growth and suggest that this epigenetic inhibitor could serve as another promising therapeutic strategy for the treatment of T- ALL[94].

## Opportunities for targeted therapy in T-ALL

*The NOTCH1 signaling pathway*

T-ALL is a genetically heterogeneous disorder in which multiple oncogenic and loss-of- function mutations cooperate to establish leukemia. Nevertheless, the concept of 'oncogene addiction' supports the idea that targeting single oncogenes should be sufficient to develop effective oncogene-based therapeutic opportunities[96].

The prototype example in the context of T-ALL is the inhibition of the proteolytic cleavage of the transmembrane NOTCH1 receptor by the presenilin/γ-secretase

complex using γ-secretase inhibitors (GSI). Problematically, the accumulation of goblet cells in the digestive system, induced by GSI-treatment through upregulation of 'Kruppel-like factor 4' (*KLF4*) levels, leads to gastro-intestinal toxicity. Combination therapy with glucocorticoid administration effectively reduces the toxic effects in the gut[97]. It was recently shown that GSI-resistant T-ALLs could benefit from a combination of vincristine and GSI treatment, since GSIs were shown to enhance the apoptotic effect induced by the chemotherapeutic agent[98]. Similarly, a preclinical study using a clinically relevant GSI in combination with dexamethasone showed synergistic results in glucocorticoid- resistant leukemias[99].

Alternative strategies to target the NOTCH1 pathway are still being developed and include specific NOTCH1 inhibitory antibodies and stapled peptides that target the NOTCH1 transcriptional complex[100, 101]. For example, the synthetic peptide SAHM1 that directly interferes at the level of protein-protein interactions required for the NOTCH1 transcriptional complex shows a higher potency to inhibit NOTCH1 signaling in comparison to GSI[100].

Other strategies involve therapeutic targeting of downstream signaling components of the NOTCH pathway. For example, pharmacological inhibition or genetic ablation of *IGF1R*, a direct NOTCH1 target gene, inhibits growth and viability of T-ALL cells and might influence the leukemia-initiating cell activity of NOTCH1 induced tumors[102]. Additionally, an elegant high-throughput compound screening approach identified the sarco/endoplasmic reticulum calcium ATPase (SERCA) channels as novel therapeutic targets in NOTCH1 induced T-ALL[103]. SERCA inhibition by the small molecule thapsigargin selectively impaired NOTCH signaling and demonstrated antileukemic activity in both *in vitro* and *in vivo* model systems[103]. Finally, Schnell and colleagues confirmed the critical role of HES1 as downstream component of NOTCH1 signaling in T-ALL and revealed that perhexiline could evoke a strong *in vitro* and *in vivo* anti-leukemic response by reverting the HES1-driven gene expression signature, providing a new lead for targeted T-ALL treatment linked to hyperactive NOTCH1.

*The IL7R-JAK-STAT pathway as a therapeutic target*

The IL7R-signaling pathway is strictly regulated during normal T-cell development, because it is required for proliferation and survival of progenitor T-cells. Binding of IL7 to its heterodimeric receptor (IL7R) will induce phosphorylation of JAK1 and JAK3 as well as subsequent migration of dimerized STAT5 to the nucleus where it will regulate target gene expression[104]. The anti-apoptotic effects of this pathway are mainly mediated through the suppression of downstream 'B-cell CLL/lymphoma 2' (BCL-2) expression[105], whereas IL-7 induced cell cycle progression requires down-regulation of *p27*.

Two independent studies described somatic gain-of-function mutations in *IL7R* that caused cytokine-independent receptor activation[106, 107]. These mutations were found in about 10% of all T-ALL cases and are specifically associated with the *TLX1/3* T-ALL genetic subgroup. Alternatively, activation of JAK/STAT signaling can also be achieved by somatic *JAK1* or *JAK3* gain-of-function mutations[25, 108], or a rare translocation, t(9;12)(p24;p13), that drives expression of a chimeric ETV6-JAK2 fusion protein[109, 110]. Finally, inactivation of the 'protein tyrosine phosphatase non-receptor type 2' (*PTPN2*) gene has been observed in ~5% of T-ALL cases. Loss of *PTPN2* in leukemic T-cells resulted in increased proliferation upon IL7 stimulation with corresponding activation of JAK1 and STAT5[111, 112].

This genetic evidence combined with the transcriptional regulation of *IL7R* by activated NOTCH signaling[113] and/or sustained ZEB2 activity[54], marks this signaling axis as a highly attractive target for molecular therapy and therefore provides a strong rational for the use of clinical-stage JAK- or STAT-specific small molecule inhibitors in a significant fraction of human T-ALL patients (**Figure 2**). Indeed, Goossens et et al. demonstrated that increased IL7R in Zeb2 driven immature T-ALL is associated with increased cell survival and secondary leukemia initiating potential upon xenotransplantation, which could be perturbed by administration of an IL7R blocking antibody[48].

Recent efforts have been made to interfere with JAK-STAT signaling by chemical inhibitions and currently the JAK1/2 inhibitor ruxolitinib and the JAK3 inhibitor

tofacitinib are already in clinical use for rheumatoid arthritis[114] and myelofibrosis[115]. In the context of T-ALL, Maude et al.[116] nicely demonstrated aberrant activation of JAK/STAT signaling in ETP-ALL lymphoblasts as compared with more mature T-ALLs. Most notably, JAK/STAT pathway activation was found to be a universal feature of immature leukemias irrespective of *IL7R*, *JAK1* or *JAK3* mutation status, suggesting that these tumors are strongly addicted to IL7 signaling. Indeed, the broad therapeutic applicability of JAK inhibition in immature T-ALLs was confirmed by in vivo drug treatment experiments in which anti-tumoral effects for ruxolitinib were found in six ETP-ALL patient derived xenografts[116].

*Pharmacological BCL-2 inhibition in T-ALL*

As mentioned earlier, immature T-ALLs are often characterized by aberrant IL7R/JAK/STAT activation and this signaling cascade will eventually converge towards STAT5-mediated activation of the anti-apoptotic factor BCL-2[117]. In addition, anti-apoptotic genes show a spatiotemporal expression pattern during T-cell differentiation with the highest levels of BCL-2 in early T-cell precursors[118].

Given this, pharmacological inhibition of BCL-2 has been suggested as a promising new therapeutic strategy in immature subtypes of human T-ALL. Indeed, three independent studies[118-120] recently showed that immature T-ALLs display an increased sensitivity towards the highly specific BCL-2 inhibitor ABT-199[121]. In addition, synergistic effects were reported between ABT-199 and conventional chemotherapeutics that are currently used in T-ALL treatment schedules. Finally, preclinical models of patient derived xenografts confirmed ABT-199 sensitivity in specific T-ALL subtypes providing additional rationale for including T-ALL patients in clinical trials using this particular drug[118-120].

## Chapter 1: Introduction

*The PI3K-AKT-mTOR pathway*

The PI3K/AKT/'mammalian target of rapamycin' (mTOR) pathway controls multiple cellular responses including metabolic regulation, cell growth and survival. Activation of PI3K by growth factor stimuli results in the generation of phospatidylinositol triphosphate (PIP3) in the plasma membrane and subsequent activation of the Akt kinase and downstream target proteins including mTOR. Importantly, the 'phosphatase and tensin homologue' (*PTEN*) tumorsupressor negatively regulates PI3K/AKT/mTOR signaling by dephosporylation of PIP3[122].

In human T-ALL, constitutive activation of the PI3K/AKT/mTOR signal transduction pathway is achieved by deletions or mutations targeting *PTEN* in about 15% of cases[123, 124] and sporadic gain-of-function mutations in *AKT*, *PIK3R1* or *PIK3CA*[124-126]. Moreover, normal and malignant thymocytes rapidly activate the PI3K/AKT/mTOR pathway in response to IL7 stimulation[127, 128]. Therefore, *IL7R* gain-of-functions mutations[106, 107] serve as an alternative route for enhanced PI3K/AKT/mTOR signaling in leukemic T-cells. Finally, aberrant NOTCH1 signaling will further enhance PI3K/AKT/mTOR activation through NOTCH1-mediated transcriptional upregulation of the IL7R[113] and HES1-mediated transcriptional repression of *PTEN*[123]. Notably, in some T-ALL cases, loss of *PTEN* can occur during disease progression and switch the oncogene addiction from NOTCH1 towards constitutive AKT signaling[123]. However, *PTEN* inactivation can also be important at early stages of leukemogenesis where it regulates the initial survival of the leukemia initiating cells[129, 130]. Blackburn and colleagues used zebrafish as an *in vivo* model to show that the Akt pathway is critically involved in expansion of the pool of leukemia propagating cells that may ultimately give rise to hematological relapse[131].

Given the aberrant activation of the PI3K/AKT/mTOR pathway, this signaling cascade has been evaluated as novel therapeutic target in T-ALL. The mTOR inhibtor rapamycin showed promising results in pre-clinical models[132] and might modulate glucocorticoid resistance in T-ALL[133]. However, inhibition of mTOR can hyperactivate AKT by a feedback loop between mTOR, PI3K and AKT[134]. Therefore, dual PI3K/mTOR small molecule inhibitors have been developed[135]. They show strong cytotoxic

activity against T-ALL cell lines and lymphoblasts obtained from primary human leukemia patients[136]. In addition, direct AKT inhibition leads to rapid cell death in some T-ALL cell lines and primary patient samples[123, 137]. At the level of PI3Ks, elegant work recently showed that the p110δ and p110γ isoforms of PI3K are both critically required to sustain T-ALL development in a mouse model induced by conditional loss of *Pten* in T-cells[138]. Moreover, a specific p110δ/p110γ dual inhibitor prolonged the survival of *Pten* null mice and showed promising effects in *PTEN* deificient primary human T-ALL tumor cells[138]. Therapeutic targeting of cancer cells by exploiting their addiction to specific PI3K isoforms might be particularly relevant in the context of limiting toxicities that would be associated with pan-PI3K inhibitors.

*Targeting general transcription machinery in T-ALL*

Impacting on the activity of large enhancers may provide unique opportunities for intervention with oncogenic transcriptional networks, a concept that has now been firmly established by the use of the BRD4 inhibitor JQ1 in a variety of pre-clinical tumor models, including T-ALL. Interestingly, chemical inhibition of CDK7, an important component of the transcription factor IIH complex (TFIIH) which regulates transcription elongation activity[139], has recently been achieved by the development of a novel CDK7 inhibitor named THZ1. This molecule directly impacts on CDK7 kinase activity, which is required for regulation of the TFIIH complex and therefore globally dampens mRNA transcription of a small set of critical genes involved in T-ALL tumorigenesis[140]. Besides the remarkable *in vitro* and *in vivo* anti- tumor activity observed in T-ALL[140], the anti-cancer effectiveness of the THZ1 compound was also shown for other tumor entities such as MYCN-driven neuroblastoma[141] and small cell lung cancer[142]. Nevertheless, the actual transcriptional response downstream of CDK7 inhibition still needs to be further characterized for most tumors and the degree of overlap with JQ1 driven BRD4 inhibition remains largely unexplored.

*Targeting cap-dependent translation in the biology T-ALL*

Translation of most cellular mRNAs is mediated by a cap structure at the 5' end of mRNAs. The initiation of this process, which is termed cap-dependent translation initiation, involves a tightly controlled multi-protein initiation complex that consists of omnipresent eukaryotic initiating factors, including the cap-binding protein eIF4E and the RNA helicase eIF4A.

Notably, two recent key publications showed that T-ALL cells strictly depend on cap-dependent translation for their survival[143, 144]. Indeed, sustained expression of eIF4A or eIF4E was shown to accelerate tumor development *in vivo* and strong anti-leukemic/apoptotic effects were observed using eIF4A (silvestrol) or eIF4E (4EGI-1) specific inhibitors[143, 144]. This critical dependency for leukemic survival could (at least in part) be explained by a variety of signaling cascades that eventually converge towards enhanced cap-dependent translation activity in human T-ALL through aberrant activation of mTORC1 and mTORC2[145]. Examples of such signaling pathways include aberrant NOTCH1 activation, enhanced PI3K/Akt signaling through *PTEN* inactivation and aberrant receptor tyrosine kinase activity through *IL7R* or *JAK* mutations[145]. Moreover, enhanced cap-dependent translation in T-ALL will eventually result in more efficient translation of specific mRNAs with previously established roles in the pathogenesis of T-ALL and unique structural 5’ untranslated region (UTR) features[143, 144].

## Mechanisms of disease relapse in T-ALL

The biological basis for disease relapse in T-ALL is poorly understood. The identification and characterization of leukemia stem cells might provide novel insights into the mechanisms that mediate disease recurrence in T-ALL and will have important implications for drug development and pre-clinical disease modeling.
Initial studies have shown that multiple different leukemic T-cell subpopulations at diagnosis have intrinsic repopulation capacity in immunodeficient recipient mice[146-149]. More importantly, pairwise genetic comparison of human T-ALL samples at

diagnosis with corresponding leukemic cells obtained after *in vivo* engraftment, showed that the xenograft leukemias often contained additional genetic defects targeting known T-ALL oncogenes and tumor suppressors including *PTEN*, *MYC*, *MYB* and *CDKN2A*[150]. Interestingly, these genetic abnormalities were present in minor leukemic subclones at diagnosis, suggesting a clonal relationship between the relapse clone and a chemoresistant subpopulation at diagnosis. Competitive engraftment experiments using genetically modified primary leukemia cells showed that, for example, loss of *PTEN* is able to drive enhanced leukemia- initiating capacity in a primary human T-ALL patient samples[150].

These genomic analyses[151] suggest that relapse in T-ALL is mainly mediated by oncogenic hits that are already present in minor leukemic subclones at diagnosis and does not simply result from mutations of specific drug-resistance genes. However, this idea has recently been challenged by the identification of mutations targeting the cytosolic *5'-nucleotidase II* (*NT5C2*) gene in about 20% of relapsed T-cell ALL patients[152, 153]. *NT5C2* encodes a 5'- nucleotidase enzyme that can dephosphorylate thiopurine nucleotides, thereby inactivating the purine analogues 6-mercaptopurine (6-MP) and 6-thioguanine (6-TG) which are routinely used in T- ALL maintenance therapy. *NT5C2* mutations probably represent gain-of-function alleles, since they are clustered in specific regions of the NT5C2 protein. Indeed, recombinant NT5C2 mutant protein showed higher enzymatic activity and expression of *NT5C2* mutations in human T-ALL cell lines conferred resistance to the nucleoside analogues 6-MP and 6-TG[152]. Together, these studies document an important role for nucleoside analogue metabolism in the progression and chemoresistance of T-ALL.

With the discovery of the chemo/radioresistant pre-leukemic stem cells, it is becoming increasingly clear that treatment of the bulk leukemic cells may not be sufficient to discard the cell of origin. Although the remaining pre-LSCs are not able to cause immediate overt leukemia, their clonal expansion would allow an accumulation of extra oncogenic hits, causing relapse over time. Therefore it will be important to further study how pre-LSCs are controlled and can be therapeutically targeted. Since pre-LSCs appear to be dependent on Notch1[33], inhibition of NOTCH

signaling could serve as an attractive approach for targeting pre-LSCs more effectively and preventing relapse, irrespective of the *NOTCH1* mutation status of the bulk tumor at diagnosis[34]. Alternatively, targeting the Kit signaling pathway may abolish their chemo/radioresistance and facilitate the eradication of leukemia-initiating cells in immature T-cell leukemias[35].

## Conclusion

T-ALL originates from T-cell precursors at different stages of their development and is characterized by distinct and well-characterized molecular genetic subtypes. Children affected by this disease respond fairly well to high-dose chemotherapy regimens. Unfortunately, the clinical response in adults remains problematic and therapeutic options for relapsed T-ALL patients remain scarce.

Notably, the high survival rates reported in pediatric T-ALL protocols could result from overtreatment of a significant fraction of children. Therefore, and given the long-term side effects associated with intensive chemotherapy, risk stratification in future pediatric T-ALL treatment protocols should be further optimized based on our enhanced understanding of T-ALL disease biology. On the other hand, further reduction of chemotherapy can also be achieved by translation of our molecular genetic findings into novel targeted therapies for the treatment of human T-ALL. In that context, a variety of pre-clinical studies have reported promising therapeutic effects for particular small molecule inhibitors targeting specific oncogenic pathways (**Table 1**). Hopefully, some of these novel therapeutic strategies can be implemented in daily clinical practice in complement with low dose chemotherapy. This will require an accurate definition of the specific T-ALL patient population that might benefit from these novel targeted therapies.

## Acknowledgements

This work is supported by: the Fund for Scientific Research Flanders (FWO) (research projects G.0202.09, G.0869.10N to F.S. and G065614, 3GA00113N and G.0C47.13N to P.V.V; Postdoc grant to S.G.; PhD grant to S.P. and A.W; B.P. is a senior clinical investigator; P.V.V is the recipient of an Odysseus Grant), IWT Vlaanderen (PhD grant to KD), the Belgian Foundation against Cancer, the Flemish Liga against Cancer (VLK) (Postdoc grant to F.M.); Ghent University (GOA grant 12051203 to F.S), the Cancer Plan from the Federal Public Service of Health (F.S. and Y.B.), the Children Cancer Fund Ghent (F.S and Y.B.) and the Belgian Program of Interuniversity Poles of Attraction (365O9110 to F.S.). Additional funding is provided by an Australian NH & MRC grant APP1047995 to J.H.

## Author contributions

KD wrote the manuscript and made the figures, SG-FS-PV supervised the review process and writing of this manuscript, SP made the figures. The other co-authors of this manuscript assisted in editing of the manuscript.

## Figures

## Figure 1. miRNAs implicated in T-ALL disease biology

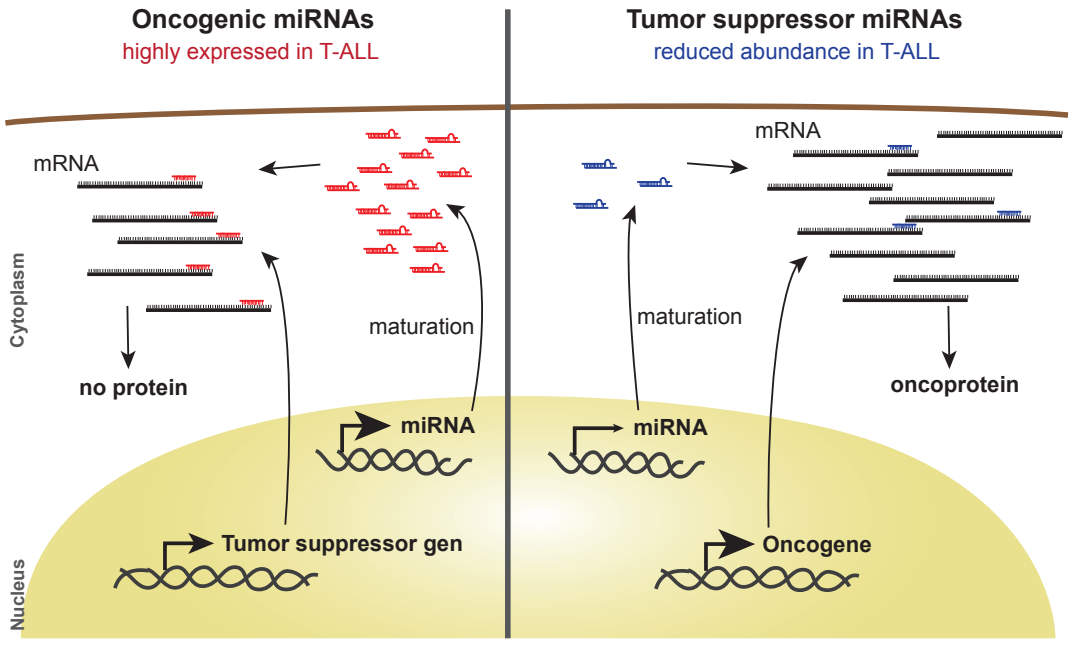


| OncomiR | Tumor suppressor |
|---|---|
| miR-26a | PTEN, PHF6 |
| miR-19b | PTEN, BIM |
| miR-92 | PTEN, BIM, IKZF1, NF1, FBXW7 |
| miR-20a | PTEN, PHF6, BIM |
| miR-148/152 | PTEN, BIM, IKZF1 |
| miR-27 | BIM, IKZF1, NF1, FBXW7 |
| miR-223 | FBXW7 |
| miR-128-3p | PHF6 |

| Tumor suppressor miRNA | Oncogene |
|---|---|
| miR-150 | MYB |
| miR-155 | MYB, HBP1 |
| miR-200 | MYB, HBP1 |
| miR-29 | HBP1 |
| miR-31 | HBP1 |
| miR-193b | MYB, MCL1 |

**Figure 1**: Graphical illustration of miRNAs involved in the pathogenesis of T-ALL with tumor suppressor miRNAs targeting oncogenes and oncomiRs targeting tumor suppressor genes.

## Figure 2. Molecular mechanisms for IL7R/JAK/STAT activation in T-ALL

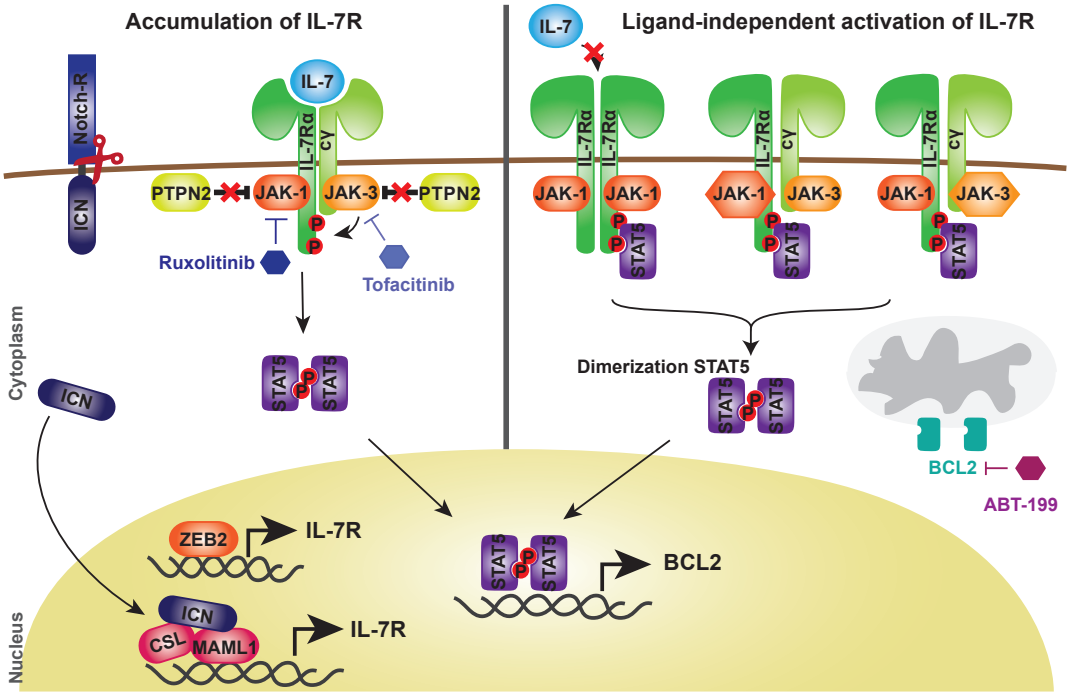


**Figure 2**: Graphical overview of oncogenic mechanisms that can drive aberrant IL7R/JAK/STAT signaling in human T-ALL. The left panel illustrates indirect mechanisms, which will eventually result in enhanced IL7R expression and ligand-dependent pathway activation, including aberrant NOTCH1 signaling or sustained expression of ZEB2. The right panel documents direct mechanisms of pathway activation, which result in ligand independent stimulation, including activating *IL7*R, *JAK1* or *JAK3* mutations. Therapeutic targeting of this oncogenic signaling pathway could be achieved by the JAK1/2 inhibitor ruxolitinib or the JAK3 inhibitor tofacitinib. Moreover, aberrant IL7R/JAK/STAT activation will eventually converge towards STAT5-mediated activation of the anti-apoptotic factor BCL-2. Activation of this anti-apoptotic factor could also be exploited by the BH3 mimetic BCL-2 inhibitor ABT-199.

## Chapter 1: Introduction

## Tables

### Table 1. Opportunities for targeted therapy in T-ALL.

| Pathway | Relevance | Therapies |
|---|---|---|
| NOTCH1 | Activating mutations in the *NOTCH1* gene are present in over 50% of T-ALL cases [6]. | - NOTCH1 inhibitory antibodies and stapled peptides (ex. SAHM1)<br>- γ-secretase inhibitors (ex. compound E)<br>- IGF1R inhibitors (ex. BMS-536924)<br>- SERCA inhibitors (ex. thapsigargin)<br>- HES1-signature antagonists (ex. perhexiline) |
| IL7R-JAK-STAT | Activation of pathway in T-ALL by:<br>- Gain-of-function mutations in IL7R, JAK1, JAK3 and STAT5B or loss of PTPN2<br>- Overexpression of ZEB2<br>- Activation of NOTCH1 pathway | - JAK1/JAK2 inhibitors (ex. ruxolitinib)<br>- JAK3 inhibitors (ex. tofacitinib)<br>- STAT5 inhibitors |
| Mitochondrial apoptosis | Overexpression of BCL-2 is typical for immature T-ALL. IL7R-JAK-STAT signaling also leads to BCL-2 upregulation | - BCL-2 inhibitors (ex. ABT-199) |
| PI3K-Akt-mTOR | Activation of pathway in T-ALL by:<br>- Deletions or mutations in PTEN<br>- Gain-of-function mutations in AKT, PIK3R1 or PIK3CA<br>- IL7 stimulation | - mTOR inhibitors (ex. rapamycin)<br>- PI3Kγ/δ inhibitors (ex. CAL-130)<br>- dual PI3K/mTOR inhibitors (ex. PI-103)<br>- AKT inhibitors (ex. A443654) |
| H3K27 demethylation | JMJD3 is overexpressed and oncogenic in T-ALL | - JMJD3 inhibitors (ex. GSKJ4) |
| General transcription | Oncogenic driver genes are often associated with super-enhancers and are very strongly transcribed | - BRD4 inhibitors (ex. JQ1)<br>- CDK7 inhibitors (ex. THZ1) |
| Cap-dependent translation | T-ALL cells depend on cap-dependent translation for their survival | - eIF4A inhibitors (ex. silvestrol)<br>- eIF4E inhibitors (ex. 4EGI-1) |

## Chapter 1: Introduction

## References

1. Carpenter AC, Bosselut R. Decision checkpoints in the thymus. Nature immunology. 2010;11:666-673.

2. Rothenberg EV. The chromatin landscape and transcription factors in T cell programming. Trends in immunology. 2014;35:195-204.

3. Rothenberg EV. Epigenetic mechanisms and developmental choice hierarchies in T- lymphocyte development. Briefings in functional genomics. 2013;12:512-524.

4. Barrett AJ, Horowitz MM, Pollock BH, et al. Bone marrow transplants from HLA-identical siblings as compared with chemotherapy for children with acute lymphoblastic leukemia in a second remission. The New England journal of medicine. 1994;331:1253-1258.

5. Goldberg JM, Silverman LB, Levy DE, et al. Childhood T-cell acute lymphoblastic leukemia: the Dana-Farber Cancer Institute acute lymphoblastic leukemia consortium experience. Journal of clinical oncology : official journal of the American Society of Clinical Oncology. 2003;21:3616- 3622.

6. Van Vlierberghe P, Ferrando A. The molecular basis of T cell acute lymphoblastic leukemia. The Journal of clinical investigation. 2012;122:3398-3406.

7. Ferrando AA, Neuberg DS, Staunton J, et al. Gene expression signatures define novel oncogenic pathways in T cell acute lymphoblastic leukemia. Cancer cell. 2002;1:75-87.

8. Homminga I, Pieters R, Langerak AW, et al. Integrated transcript and genome analyses reveal NKX2-1 and MEF2C as potential oncogenes in T cell acute lymphoblastic leukemia. Cancer cell. 2011;19:484-497.

9. Van Vlierberghe P, van Grotel M, Tchinda J, et al. The recurrent SET-NUP214 fusion as a new HOXA activation mechanism in pediatric T-cell acute lymphoblastic leukemia. Blood. 2008;111:4668-4680.

10. Soulier J, Clappier E, Cayuela JM, et al. HOXA genes are included in genetic and biologic networks defining human acute T-cell leukemia (T-ALL). Blood. 2005;106:274-286.

11. Ribeiro D, Melao A, Barata JT. IL-7R-mediated signaling in T-cell acute lymphoblastic leukemia. Advances in biological regulation. 2013;53:211-222.

12. Fragoso R, Barata JT. Kinases, tails and more: Regulation of PTEN function by phosphorylation. Methods. 2015;77-78:75-81.

13 Fragoso R, Barata JT. PTEN and leukemia stem cells. Advances in biological regulation. 2014;56:22-29.

14. Correia NC, Girio A, Antunes I, Martins LR, Barata JT. The multiple layers of non-genetic regulation of PTEN tumour suppressor activity. European journal of cancer. 2014;50:216-225.

15. Martelli AM, Tabellini G, Ricci F, et al. PI3K/AKT/mTORC1 and MEK/ERK signaling in T-cell acute lymphoblastic leukemia: new options for targeted therapy. Advances in biological regulation. 2012;52:214-227.

16. Cardoso BA, Girio A, Henriques C, et al. Aberrant signaling in T-cell acute lymphoblastic leukemia: biological and therapeutic implications. Brazilian journal of medical and biological research = Revista brasileira de pesquisas medicas e biologicas / Sociedade Brasileira de Biofisica [et al]. 2008;41:344-350.

17. Martelli AM, Lonetti A, Buontempo F, et al. Targeting signaling pathways in T-cell acute lymphoblastic leukemia initiating cells. Advances in biological regulation. 2014;56:6-21.

18. Hebert J, Cayuela JM, Berkeley J, Sigaux F. Candidate tumor-suppressor genes MTS1 (p16INK4A) and MTS2 (p15INK4B) display frequent homozygous deletions in primary cells from T- but not from B-cell lineage acute lymphoblastic leukemias. Blood. 1994;84:4038-4044.

19. Jacobs JJ, Kieboom K, Marino S, DePinho RA, van Lohuizen M. The oncogene and Polycomb- group gene bmi-1 regulates cell proliferation and senescence through the ink4a locus. Nature. 1999;397:164-168.

20. Bracken AP, Kleine-Kohlbrecher D, Dietrich N, et al. The Polycomb group proteins bind throughout the INK4A-ARF locus and are disassociated in senescent cells. Genes & development. 2007;21:525-530.

21. Volanakis EJ, Williams RT, Sherr CJ. Stage-specific Arf tumor suppression in Notch1-induced T-cell acute lymphoblastic leukemia. Blood. 2009;114:4451-4459.

22. Volanakis EJ, Boothby MR, Sherr CJ. Epigenetic regulation of the Ink4a-Arf (Cdkn2a) tumor suppressor locus in the initiation and progression of Notch1-driven T cell acute lymphoblastic leukemia. Experimental hematology. 2012.

23. Zuurbier L, Gutierrez A, Mullighan CG, et al. Immature MEF2C-dysregulated T-cell leukemia patients have an early T-cell precursor acute lymphoblastic leukemia gene signature and typically have non-rearranged T-cell receptors. Haematologica. 2014;99:94-102.

24. Van Vlierberghe P, Ambesi-Impiombato A, Perez-Garcia A, et al. ETV6 mutations

in early immature human T cell leukemias. The Journal of experimental medicine. 2011;208:2571-2579.

25. Zhang J, Ding L, Holmfeldt L, et al. The genetic basis of early T-cell precursor acute lymphoblastic leukaemia. Nature. 2012;481:157-163.

26. Van Vlierberghe P, Ambesi-Impiombato A, De Keersmaecker K, et al. Prognostic relevance of integrated genetic profiling in adult T-cell acute lymphoblastic leukemia. Blood. 2013;122:74-82.

27. Shlush LI, Zandi S, Mitchell A, et al. Identification of pre-leukaemic haematopoietic stem cells in acute leukaemia. Nature. 2014;506:328-333.

28. Tremblay CS, Curtis DJ. The clonal evolution of leukemic stem cells in T-cell acute lymphoblastic leukemia. Current opinion in hematology. 2014;21:320-325.

29. Neumann M, Heesch S, Schlee C, et al. Whole-exome sequencing in adult ETP-ALL reveals a high rate of DNMT3A mutations. Blood. 2013;121:4749-4752.

30. McCormack MP, Young LF, Vasudevan S, et al. The Lmo2 oncogene initiates leukemia in mice by inducing thymocyte self-renewal. Science. 2010;327:879-883.

31. McCormack MP, Shields BJ, Jackson JT, et al. Requirement for Lyl1 in a model of Lmo2- driven early T-cell precursor ALL. Blood. 2013;122:2093-2103.

32. Smith S, Tripathi R, Goodings C, et al. LIM domain only-2 (LMO2) induces T-cell leukemia by two distinct pathways. PloS one. 2014;9:e85883.

33. Gerby B, Tremblay CS, Tremblay M, et al. SCL, LMO1 and Notch1 reprogram thymocytes into self-renewing cells. PLoS genetics. 2014;10:e1004768.

34. Goossens S, Van Vlierberghe P. Controlling pre-leukemic thymocyte self-renewal. PLoS genetics. 2014;10:e1004881.

35. Shields BJ, Alserihi R, Nasa C, Bogue C, Alexander WS, McCormack MP. Hhex regulates Kit to promote radioresistance of self-renewing thymocytes in Lmo2-transgenic mice. Leukemia. 2015;29:927-938.

36. Baldus CD, Martus P, Burmeister T, et al. Low ERG and BAALC expression identifies a new subgroup of adult acute T-lymphoblastic leukemia with a highly favorable outcome. Journal of clinical oncology : official journal of the American Society of Clinical Oncology. 2007;25:3739- 3745.

37. Gutierrez A, Dahlberg SE, Neuberg DS, et al. Absence of biallelic TCRgamma deletion predicts early treatment failure in pediatric T-cell acute lymphoblastic leukemia. Journal of clinical oncology : official journal of the American Society of

Clinical Oncology. 2010;28:3816- 3823.

38. Grossmann V, Haferlach C, Weissmann S, et al. The molecular profile of adult T-cell acute lymphoblastic leukemia: mutations in RUNX1 and DNMT3A are associated with poor prognosis in T-ALL. Genes, chromosomes & cancer. 2013;52:410-422.

39. Ben Abdelali R, Roggy A, Leguay T, et al. SET-NUP214 is a recurrent gammadelta lineage- specific fusion transcript associated with corticosteroid/chemotherapy resistance in adult T-ALL. Blood. 2014;123:1860-1863.

40. Ben Abdelali R, Asnafi V, Petit A, et al. The prognosis of CALM-AF10-positive adult T-cell acute lymphoblastic leukemias depends on the stage of maturation arrest. Haematologica. 2013;98:1711-1717.

41. Trinquand A, Tanguy-Schmidt A, Ben Abdelali R, et al. Toward a NOTCH1/FBXW7/RAS/PTEN-based oncogenetic risk classification of adult T-cell acute lymphoblastic leukemia: a Group for Research in Adult Acute Lymphoblastic Leukemia study. Journal of clinical oncology : official journal of the American Society of Clinical Oncology. 2013;31:4333-4342.

42. Beldjord K, Chevret S, Asnafi V, et al. Oncogenetics and minimal residual disease are independent outcome predictors in adult patients with acute lymphoblastic leukemia. Blood. 2014;123:3739-3749.

43. Coustan-Smith E, Mullighan CG, Onciu M, et al. Early T-cell precursor leukaemia: a subtype of very high-risk acute lymphoblastic leukaemia. The lancet oncology. 2009;10:147-156.

44. Inuzuka H, Shaik S, Onoyama I, et al. SCF(FBW7) regulates cellular apoptosis by targeting MCL1 for ubiquitylation and destruction. Nature. 2011;471:104-109.

45. Homminga I, Pieters R, Langerak AW, et al. Integrated transcript and genome analyses reveal NKX2-1 and MEF2C as potential oncogenes in T cell acute lymphoblastic leukemia. Cancer cell;19:484-497.

46. Inukai T, Kiyokawa N, Campana D, et al. Clinical significance of early T-cell precursor acute lymphoblastic leukaemia: results of the Tokyo Children's Cancer Study Group Study L99-15. British journal of haematology. 2012;156:358-365.

47. Patrick K, Wade R, Goulden N, et al. Outcome for children and young people with Early T-cell precursor acute lymphoblastic leukaemia treated on a contemporary protocol, UKALL 2003. British journal of haematology. 2014;166:421-424.

48. Brent L. Wood SSW, Kimberly P. Dunsmore, Meenakshi Devidas, Barbara Asselin, Natia Esiashvili, Mignon L. Loh,Naomi J. Winick, William L. Carroll, Elizabeth A. Raetz and Stephen P. Hunger. T-Lymphoblastic Leukemia (T-ALL) Shows Excellent

Outcome, Lack of Significance of the Early Thymic Precursor (ETP) Immunophenotype, and Validation of the Prognostic Value of End- Induction Minimal Residual Disease (MRD) in Children's Oncology Group (COG) Study AALL0434. ASH 2014 Oral Presentation Plenary session December 7, 2014.

49. De Craene B, Berx G. Regulatory networks defining EMT during cancer initiation and progression. Nature reviews Cancer. 2013;13:97-110.

50. Denecker G, Vandamme N, Akay O, et al. Identification of a ZEB2-MITF-ZEB1 transcriptional network that controls melanogenesis and melanoma progression. Cell death and differentiation. 2014;21:1250-1261.

51. Brabletz S, Brabletz T. The ZEB/miR-200 feedback loop--a motor of cellular plasticity in development and cancer? EMBO reports. 2010;11:670-677.

52. Rosivatz E, Becker I, Specht K, et al. Differential expression of the epithelial-mesenchymal transition regulators snail, SIP1, and twist in gastric cancer. The American journal of pathology. 2002;161:1881-1891.

53. Goossens S, Janzen V, Bartunkova S, et al. The EMT regulator Zeb2/Sip1 is essential for murine embryonic hematopoietic stem/progenitor cell differentiation and mobilization. Blood. 2011;117:5620-5630.

54. Goossens S, Radaelli E, Blanchet O, et al. ZEB2 drives immature T-cell lymphoblastic leukaemia development via enhanced tumour-initiating potential and IL-7 receptor signalling. Nature communications. 2015;6:5794.

55. Bernard OA, Busson-LeConiat M, Ballerini P, et al. A new recurrent and specific cryptic translocation, t(5;14)(q35;q32), is associated with expression of the Hox11L2 gene in T acute lymphoblastic leukemia. Leukemia. 2001;15:1495-1504.

56. Nagel S, Kaufmann M, Drexler HG, MacLeod RA. The cardiac homeobox gene NKX2-5 is deregulated by juxtaposition with BCL11B in pediatric T-ALL cell lines via a novel t(5;14)(q35.1;q32.2). Cancer research. 2003;63:5329-5334.

57. De Keersmaecker K, Real PJ, Gatta GD, et al. The TLX1 oncogene drives aneuploidy in T cell transformation. Nature medicine. 2010;16:1321-1327.

58. Gutierrez A, Kentsis A, Sanda T, et al. The BCL11B tumor suppressor is mutated across the major molecular subtypes of T-cell acute lymphoblastic leukemia. Blood. 2011;118:4169-4173.

59. Hacein-Bey-Abina S, Garrigue A, Wang GP, et al. Insertional oncogenesis in 4 patients after retrovirus-mediated gene therapy of SCID-X1. The Journal of clinical investigation. 2008;118:3132-3142.

60. Comijn J, Berx G, Vermassen P, et al. The two-handed E box binding zinc finger protein SIP1 downregulates E-cadherin and induces invasion. Molecular cell. 2001;7:1267-1278.

61. Treanor LM, Zhou S, Janke L, et al. Interleukin-7 receptor mutants initiate early T cell precursor leukemia in murine thymocyte progenitors with multipotent potential. The Journal of experimental medicine. 2014;211:701-713.

62. Degryse S, de Bock CE, Cox L, et al. JAK3 mutants transform hematopoietic cells through JAK1 activation, causing T-cell acute lymphoblastic leukemia in a mouse model. Blood. 2014;124:3092-3100.

63. Mattick JS, Makunin IV. Small regulatory RNAs in mammals. Human molecular genetics. 2005;14 Spec No 1:R121-132.

64. Esquela-Kerscher A, Slack FJ. Oncomirs - microRNAs with a role in cancer. Nature reviews Cancer. 2006;6:259-269.

65. Lazare SS, Wojtowicz EE, Bystrykh LV, de Haan G. microRNAs in hematopoiesis. Experimental cell research. 2014;329:234-238.

66. Mavrakis KJ, Van Der Meulen J, Wolfe AL, et al. A cooperative microRNA-tumor suppressor gene network in acute T-cell lymphoblastic leukemia (T-ALL). Nature genetics. 2011;43:673-678.

67. Nagel S, Venturini L, Przybylski GK, et al. Activation of miR-17-92 by NK-like homeodomain proteins suppresses apoptosis via reduction of E2F1 in T-cell acute lymphoblastic leukemia. Leukemia & lymphoma. 2009;50:101-108.

68. Mavrakis KJ, Wolfe AL, Oricchio E, et al. Genome-wide RNA-mediated interference screen identifies miR-19 targets in Notch-induced T-cell acute lymphoblastic leukaemia. Nature cell biology. 2010;12:372-379.

69. Gusscott S, Kuchenbauer F, Humphries RK, Weng AP. Notch-mediated repression of miR- 223 contributes to IGF1R regulation in T-ALL. Leukemia research. 2012;36:905-911.

70. Kumar V, Palermo R, Talora C, et al. Notch and NF-kB signaling pathways regulate miR- 223/FBXW7 axis in T-cell acute lymphoblastic leukemia. Leukemia. 2014;28:2324-2335.

71. Mansour MR, Sanda T, Lawton LN, et al. The TAL1 complex targets the FBXW7 tumor suppressor by activating miR-223 in human T cell acute lymphoblastic leukemia. The Journal of experimental medicine. 2013;210:1545-1557.

72. Mets E, Van Peer G, Van der Meulen J, et al. MicroRNA-128-3p is a novel

oncomiR targeting PHF6 in T-cell acute lymphoblastic leukemia. Haematologica. 2014;99:1326-1333.

73. Sanghvi VR, Mavrakis KJ, Van der Meulen J, et al. Characterization of a set of tumor suppressor microRNAs in T cell acute lymphoblastic leukemia. Science signaling. 2014;7:ra111.

74. Mets E, Van der Meulen J, Van Peer G, et al. MicroRNA-193b-3p acts as a tumor suppressor by targeting the MYB oncogene in T-cell acute lymphoblastic leukemia. Leukemia. 2015;29:798- 806.

75. Guttman M, Rinn JL. Modular regulatory principles of large non-coding RNAs. Nature. 2012;482:339-346.

76. Mattick JS, Rinn JL. Discovery and annotation of long noncoding RNAs. Nature structural & molecular biology. 2015;22:5-7.

77. Wang KC, Chang HY. Molecular mechanisms of long noncoding RNAs. Molecular cell. 2011;43:904-914.

78. Trimarchi T, Bilal E, Ntziachristos P, et al. Genome-wide mapping and characterization of Notch-regulated long noncoding RNAs in acute leukemia. Cell. 2014;158:593-606.

79. Durinck K, Wallaert A, Van de Walle I, et al. The Notch driven long non-coding RNA repertoire in T-cell acute lymphoblastic leukemia. Haematologica. 2014;99:1808-1816.

80. Consortium EP. An integrated encyclopedia of DNA elements in the human genome. Nature. 2012;489:57-74.

81. Zhu Y, Sun L, Chen Z, Whitaker JW, Wang T, Wang W. Predicting enhancer transcription and activity from chromatin modifications. Nucleic acids research. 2013;41:10032-10043.

82. Arner E, Daub CO, Vitting-Seerup K, et al. Gene regulation. Transcribed enhancers lead waves of coordinated transcription in transitioning mammalian cells. Science. 2015;347:1010- 1014.

83. Rao SS, Huntley MH, Durand NC, et al. A 3D map of the human genome at kilobase resolution reveals principles of chromatin looping. Cell. 2014;159:1665-1680.

84. Loven J, Hoke HA, Lin CY, et al. Selective inhibition of tumor oncogenes by disruption of super-enhancers. Cell. 2013;153:320-334.

85. Whyte WA, Orlando DA, Hnisz D, et al. Master transcription factors and mediator establish super-enhancers at key cell identity genes. Cell. 2013;153:307-319.

86. Vahedi G, Kanno Y, Furumoto Y, et al. Super-enhancers delineate disease-associated regulatory nodes in T cells. Nature. 2015;520:558-562.

87. Mansour MR, Abraham BJ, Anders L, et al. Oncogene regulation. An oncogenic super- enhancer formed through somatic mutation of a noncoding intergenic element. Science. 2014;346:1373-1377.

88. Navarro JM, Touzart A, Pradel LC, et al. Site- and allele-specific polycomb dysregulation in T- cell leukaemia. Nature communications. 2015;6:6094.

89. Wang H, Zang C, Taing L, et al. NOTCH1-RBPJ complexes drive target gene expression through dynamic interactions with superenhancers. Proceedings of the National Academy of Sciences of the United States of America. 2014;111:705-710.

90. Herranz D, Ambesi-Impiombato A, Palomero T, et al. A NOTCH1-driven MYC enhancer promotes T cell development, transformation and acute lymphoblastic leukemia. Nature medicine. 2014;20:1130-1137.

91. Yashiro-Ohtani Y, Wang H, Zang C, et al. Long-range enhancer activity determines Myc sensitivity to Notch inhibitors in T cell leukemia. Proceedings of the National Academy of Sciences of the United States of America. 2014;111:E4946-4953.

92. Ntziachristos P, Tsirigos A, Van Vlierberghe P, et al. Genetic inactivation of the polycomb repressive complex 2 in T cell acute lymphoblastic leukemia. Nature medicine. 2012;18:298-301.

93. De Keersmaecker K, Atak ZK, Li N, et al. Exome sequencing identifies mutation in CNOT3 and ribosomal genes RPL5 and RPL10 in T-cell acute lymphoblastic leukemia. Nature genetics. 2013;45:186-190.

94. Ntziachristos P, Tsirigos A, Welstead GG, et al. Contrasting roles of histone 3 lysine 27 demethylases in acute lymphoblastic leukaemia. Nature. 2014;514:513-517.

95. Van der Meulen J, Sanghvi V, Mavrakis K, et al. The H3K27me3 demethylase UTX is a gender- specific tumor suppressor in T-cell acute lymphoblastic leukemia. Blood. 2015;125:13-21.

96. Pagliarini R, Shao W, Sellers WR. Oncogene addiction: pathways of therapeutic response, resistance, and road maps toward a cure. EMBO reports. 2015;16:280-296.

97. Real PJ, Tosello V, Palomero T, et al. Gamma-secretase inhibitors reverse

glucocorticoid resistance in T cell acute lymphoblastic leukemia. Nature medicine. 2009;15:50-58.

98. Yoon SO, Zapata MC, Singh A, Jo WS, Spencer N, Choi YS. Gamma secretase inhibitors enhance vincristine-induced apoptosis in T-ALL in a NOTCH-independent manner. Apoptosis : an international journal on programmed cell death. 2014;19:1616-1626.

99. Samon JB, Castillo-Martin M, Hadler M, et al. Preclinical analysis of the gamma-secretase inhibitor PF-03084014 in combination with glucocorticoids in T-cell acute lymphoblastic leukemia. Molecular cancer therapeutics. 2012;11:1565-1575.

100. Moellering RE, Cornejo M, Davis TN, et al. Direct inhibition of the NOTCH transcription factor complex. Nature. 2009;462:182-188.

101. Wu Y, Cain-Hom C, Choy L, et al. Therapeutic antibody targeting of individual Notch receptors. Nature. 2010;464:1052-1057.

102. Medyouf H, Gusscott S, Wang H, et al. High-level IGF1R expression is required for leukemia-initiating cell activity in T-ALL and is supported by Notch signaling. The Journal of experimental medicine. 2011;208:1809-1822.

103. Roti G, Carlton A, Ross KN, et al. Complementary Genomic Screens Identify SERCA as a Therapeutic Target in NOTCH1 Mutated Cancer. Cancer cell. 2013.

104. Mazzucchelli R, Durum SK. Interleukin-7 receptor expression: intelligent design. Nature reviews Immunology. 2007;7:144-154.

105. Jiang Q, Li WQ, Hofmeister RR, et al. Distinct regions of the interleukin-7 receptor regulate different Bcl2 family members. Molecular and cellular biology. 2004;24:6501-6513.

106. Zenatti PP, Ribeiro D, Li W, et al. Oncogenic IL7R gain-of-function mutations in childhood T-cell acute lymphoblastic leukemia. Nature genetics. 2011;43:932-939.

107. Shochat C, Tal N, Bandapalli OR, et al. Gain-of-function mutations in interleukin-7 receptor-alpha (IL7R) in childhood acute lymphoblastic leukemias. The Journal of experimental medicine. 2011;208:901-908.

108. Flex E, Petrangeli V, Stella L, et al. Somatically acquired JAK1 mutations in adult acute lymphoblastic leukemia. The Journal of experimental medicine. 2008;205:751-758.

109. Lacronique V, Boureux A, Valle VD, et al. A TEL-JAK2 fusion protein with constitutive kinase activity in human leukemia. Science. 1997;278:1309-1312.

110. Onnebo SM, Rasighaemi P, Kumar J, Liongue C, Ward AC. Alternative TEL-JAK2 fusions associated with T-cell acute lymphoblastic leukemia and atypical chronic myelogenous leukemia dissected in zebrafish. Haematologica. 2012;97:1895-1903.

111. Kleppe M, Lahortiga I, El Chaar T, et al. Deletion of the protein tyrosine phosphatase gene PTPN2 in T-cell acute lymphoblastic leukemia. Nature genetics. 2010;42:530-535.

112. Kleppe M, Soulier J, Asnafi V, et al. PTPN2 negatively regulates oncogenic JAK1 in T-cell acute lymphoblastic leukemia. Blood. 2011;117:7090-7098.

113. Gonzalez-Garcia S, Garcia-Peydro M, Martin-Gayo E, et al. CSL-MAML-dependent Notch1 signaling controls T lineage-specific IL-7R{alpha} gene expression in early human thymopoiesis and leukemia. The Journal of experimental medicine. 2009;206:779-791.

114. Meyer SC, Levine RL. Molecular pathways: molecular basis for sensitivity and resistance to JAK kinase inhibitors. Clinical cancer research : an official journal of the American Association for Cancer Research. 2014;20:2051-2059.

115. Passamonti F, Vannucchi AM, Cervantes F, et al. Ruxolitinib and survival improvement in patients with myelofibrosis. Leukemia. 2015;29:739-740.

116. Maude SL, Dolai S, Delgado-Martin C, et al. Efficacy of JAK/STAT pathway inhibition in murine xenograft models of early T-cell precursor (ETP) acute lymphoblastic leukemia. Blood. 2015;125:1759-1767.

117. Carrette F, Surh CD. IL-7 signaling and CD127 receptor regulation in the control of T cell homeostasis. Seminars in immunology. 2012;24:209-217.

118. Peirs S, Matthijssens F, Goossens S, et al. ABT-199 mediated inhibition of BCL-2 as a novel therapeutic strategy in T-cell acute lymphoblastic leukemia. Blood. 2014;124:3738-3747.

119. Chonghaile TN, Roderick JE, Glenfield C, et al. Maturation stage of T-cell acute lymphoblastic leukemia determines BCL-2 versus BCL-XL dependence and sensitivity to ABT- 199. Cancer discovery. 2014;4:1074-1087.

120. Anderson NM, Harrold I, Mansour MR, et al. BCL2-specific inhibitor ABT-199 synergizes strongly with cytarabine against the early immature LOUCY cell line but not more-differentiated T-ALL cell lines. Leukemia. 2014;28:1145-1148.

121. Souers AJ, Leverson JD, Boghaert ER, et al. ABT-199, a potent and selective BCL-2 inhibitor, achieves antitumor activity while sparing platelets. Nature medicine. 2013;19:202-208.

122. Cully M, You H, Levine AJ, Mak TW. Beyond PTEN mutations: the PI3K pathway as an integrator of multiple inputs during tumorigenesis. Nature reviews Cancer. 2006;6:184-192.

123. Palomero T, Sulis ML, Cortina M, et al. Mutational loss of PTEN induces resistance to NOTCH1 inhibition in T-cell leukemia. Nature medicine. 2007;13:1203-1210.

124. Zuurbier L, Petricoin EF, 3rd, Vuerhard MJ, et al. The significance of PTEN and AKT aberrations in pediatric T-cell acute lymphoblastic leukemia. Haematologica. 2012;97:1405- 1413.

125. Remke M, Pfister S, Kox C, et al. High-resolution genomic profiling of childhood T-ALL reveals frequent copy-number alterations affecting the TGF-beta and PI3K-AKT pathways and deletions at 6q15-16.1 as a genomic marker for unfavorable early treatment response. Blood. 2009;114:1053-1062.

126. Gutierrez A, Sanda T, Grebliunaite R, et al. High frequency of PTEN, PI3K, and AKT abnormalities in T-cell acute lymphoblastic leukemia. Blood. 2009;114:647-650.

127. Barata JT, Silva A, Brandao JG, Nadler LM, Cardoso AA, Boussiotis VA. Activation of PI3K is indispensable for interleukin 7-mediated viability, proliferation, glucose use, and growth of T cell acute lymphoblastic leukemia cells. The Journal of experimental medicine. 2004;200:659- 669.

128. Johnson SE, Shah N, Bajer AA, LeBien TW. IL-7 activates the phosphatidylinositol 3- kinase/AKT pathway in normal human thymocytes but not normal human B cell precursors. Journal of immunology. 2008;180:8109-8117.

129. Yilmaz OH, Valdez R, Theisen BK, et al. Pten dependence distinguishes haematopoietic stem cells from leukaemia-initiating cells. Nature. 2006;441:475-482.

130. Zhang J, Grindley JC, Yin T, et al. PTEN maintains haematopoietic stem cells and acts in lineage choice and leukaemia prevention. Nature. 2006;441:518-522.

131. Blackburn JS, Liu S, Wilder JL, et al. Clonal evolution enhances leukemia-propagating cell frequency in T cell acute lymphoblastic leukemia through Akt/mTORC1 pathway activation. Cancer cell. 2014;25:366-378.

132. Avellino R, Romano S, Parasole R, et al. Rapamycin stimulates apoptosis of childhood acute lymphoblastic leukemia cells. Blood. 2005;106:1400-1406.

133. Wei G, Twomey D, Lamb J, et al. Gene expression-based chemical genomics identifies rapamycin as a modulator of MCL1 and glucocorticoid resistance. Cancer cell. 2006;10:331-342.

134. Easton JB, Houghton PJ. mTOR and cancer therapy. Oncogene. 2006;25:6436-6446.

135. Fan QW, Knight ZA, Goldenberg DD, et al. A dual PI3 kinase/mTOR inhibitor reveals emergent efficacy in glioma. Cancer cell. 2006;9:341-349.

136. Chiarini F, Fala F, Tazzari PL, et al. Dual inhibition of class IA phosphatidylinositol 3- kinase and mammalian target of rapamycin as a new therapeutic option for T-cell acute lymphoblastic leukemia. Cancer research. 2009;69:3520-3528.

137. Fala F, Blalock WL, Tazzari PL, et al. Proapoptotic activity and chemosensitizing effect of the novel Akt inhibitor (2S)-1-(1H-Indol-3-yl)-3-[5-(3-methyl-2H-indazol-5-yl)pyridin-3- yl]oxypropan2-ami ne (A443654) in T-cell acute lymphoblastic leukemia. Molecular pharmacology. 2008;74:884-895.

138. Subramaniam PS, Whye DW, Efimenko E, et al. Targeting nonclassical oncogenes for therapy in T-ALL. Cancer cell. 2012;21:459-472.

139. Ali S, Heathcote DA, Kroll SH, et al. The development of a selective cyclin-dependent kinase inhibitor that shows antitumor activity. Cancer research. 2009;69:6208-6215.

140. Kwiatkowski N, Zhang T, Rahl PB, et al. Targeting transcription regulation in cancer with a covalent CDK7 inhibitor. Nature. 2014;511:616-620.

141. Chipumuro E, Marco E, Christensen CL, et al. CDK7 inhibition suppresses super-enhancer-linked oncogenic transcription in MYCN-driven cancer. Cell. 2014;159:1126-1139.

142. Christensen CL, Kwiatkowski N, Abraham BJ, et al. Targeting transcriptional addictions in small cell lung cancer with a covalent CDK7 inhibitor. Cancer cell. 2014;26:909-922.

143. Wolfe AL, Singh K, Zhong Y, et al. RNA G-quadruplexes cause eIF4A-dependent oncogene translation in cancer. Nature. 2014;513:65-70.

144. Schwarzer A, Holtmann H, Brugman M, et al. Hyperactivation of mTORC1 and mTORC2 by multiple oncogenic events causes addiction to eIF4E-dependent mRNA translation in T-cell leukemia. Oncogene. 2014;0.

145. Girardi T, De Keersmaecker K. T-ALL: ALL a matter of Translation? Haematologica. 2015;100:293-295.

146. Chiu PP, Jiang H, Dick JE. Leukemia-initiating cells in human T-lymphoblastic leukemia exhibit glucocorticoid resistance. Blood. 2010;116:5268-5279.

147. Diamanti P, Cox CV, Moppett JP, Blair A. Parthenolide eliminates leukemia-initiating cell populations and improves survival in xenografts of childhood acute lymphoblastic leukemia. Blood. 2013;121:1384-1393.

148. Cox CV, Martin HM, Kearns PR, Virgo P, Evely RS, Blair A. Characterization of a progenitor cell population in childhood T-cell acute lymphoblastic leukemia. Blood. 2007;109:674-682.

149. Gerby B, Clappier E, Armstrong F, et al. Expression of CD34 and CD7 on human T-cell acute lymphoblastic leukemia discriminates functionally heterogeneous cell populations. Leukemia. 2011;25:1249-1258.

150. Clappier E, Gerby B, Sigaux F, et al. Clonal selection in xenografted human T cell acute lymphoblastic leukemia recapitulates gain of malignancy at relapse. The Journal of experimental medicine. 2011;208:653-661.

151. Dumortier A, Jeannet R, Kirstetter P, et al. Notch activation is an early and critical event during T-Cell leukemogenesis in Ikaros-deficient mice. Molecular and cellular biology. 2006;26:209-220.

152. Tzoneva G, Perez-Garcia A, Carpenter Z, et al. Activating mutations in the NT5C2 nucleotidase gene drive chemotherapy resistance in relapsed ALL. Nature medicine. 2013.

153. Meyer JA, Wang J, Hogan LE, et al. Relapse-specific mutations in NT5C2 in childhood acute lymphoblastic leukemia. Nature genetics. 2013;45:290-294.

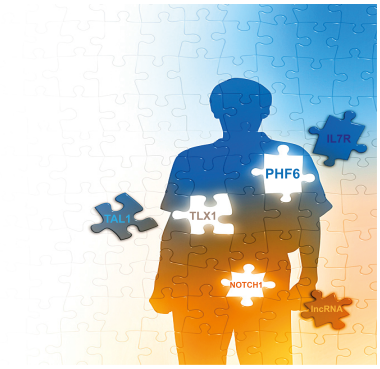


# CHAPTER 2

## Research objectives

# Research objectives

Over the last decade, technological advances in next-generation sequencing have revolutionized the discovery and functional characterization of the genomic, transcriptomic and epigenomic landscapes that drive cancer formation. Interestingly, epigenetic regulators now often emerge as hubs in the transcriptional networks that govern malignant transformation, being frequently mutated in many cancer types.

T-cell acute lymphoblastic leukemia (T-ALL) is an aggressive and genetically heterogeneous hematological disorder arising from uncontrolled clonal expansion and arrested differentiation of thymocytes. Although a plethora of genetic defects driving T-ALL formation and progression have been extensively studied over many years, the substantial contribution of epigenetic deregulation to acute T-cell leukemia has only recently been underscored with the identification of mutations affecting *EZH2*, *UTX* and *PHF6* and the elucidation of the putative oncogenic properties of *JMJD3*. A better understanding of how these chromatin modifiers act in concert with other master regulators in normal T-cell development and how their deregulated expression causes T-ALL blast formation and expansion will foster the development and implementation of novel targeted therapeutic strategies in T-ALL. Interestingly, to aim for full comprehension of transcriptional regulatory complexity, also the pool of non-coding RNAs, consisting mainly of microRNAs (miRNAs) and long non-coding RNAs (lncRNAs) should be taken into account. MiRNAs have been shown to be directly involved in cancer, including in T-ALL. Now, lncRNAs are emerging as a class of non-coding RNAs displaying a versatile functional repertoire, mainly in concert with chromatin remodeling complexes and substantially contributing to various malignancies. Furthermore, the observation that many lncRNAs exhibit a tissue-specific expression, makes them ideal targets for therapeutic intervention with reduced toxic effects.

In this PhD thesis, I aimed to perform an in depth comprehensive and integrative analysis of the functional cross-talk between the known T-ALL driver oncogenes NOTCH1 and TLX1, expand their respective transcriptional networks towards non-coding RNAs and unravel the role of PHF6 as a novel key epigenetic regulator in normal and malignant T-cell development.

## Chapter 2: Research Objectives

### Aim 1: Landscaping the functional consequences of the genome-wide TLX1 binding profile in T-ALL

The '*T-cell leukemia homeobox 1*' (*HOX11*, *TLX1*) gene encodes a homeobox transcription factor that is ectopically expressed in a subset of human T-ALL cases, as a consequence of chromosomal translocations and defines one of the major T-ALL subgroups. The current understanding of the oncogenic properties downstream of TLX1 includes aneuploidy resulting from mitotic checkpoint deregulation, T-cell differentiation arrest caused by repression of TCRα enhancer activity and simultaneous inhibition of a plethora of T-ALL tumor suppressor genes. These studies provided important insights in the mechanisms that mediate T-cell transformation downstream of TLX1, but were solely focused on TLX1 binding at the promoter of direct target genes.

Therefore, I studied in more depth the functional consequences of genome-wide TLX1 binding in the context of human T-ALL development (**paper 1, Leukemia, 2015**). To this end, an integrative genomic approach was applied to investigate the functional consequences of ectopic TLX1 binding in the context of normal T cell development as well as in the process of malignant T-cell transformation.

In addition, I aimed to expand this network under control of TLX1 towards long non-coding RNAs (lncRNAs) (**paper 6, in preparation**). To this end, we performed poly-A RNA-sequencing of an *in vitro* TLX1 knockdown model system in ALL-SIL lymphoblasts and from a primary T-ALL cohort of 64 patients. Next, we integrated H3K27ac ChIP-seq data to identify the set of TLX1 regulated, super-enhancer associated lncRNAs. The use of RNA-sequencing as a discovery tool, allowed us also to retrieve a set of previously unannotated lncRNAs implicated in the the TLX1 regulatory network.

## Chapter 2: Research Objectives

### Aim 2: Scrutinizing the role of PHF6 as a novel master regulator of normal hematopoiesis and its function as a tumor suppressor in T-ALL pathogenesis

In 2010, our research team was involved in the identification of a novel T-ALL tumor suppressor gene *PHF6*. In collaboration with the research group of Adolfo Ferrando (Columbia University Medical Center, New York, USA) a mutation screening was performed for X-linked protein coding genes in T-ALL patients. In 16% of pediatric and 38% of adult cases, *PHF6* mutations and deletions were identified. Interestingly, in the context of hematological malignancies, *PHF6* lesions were found later only to a minor extent also in acute myeloid leukemia patients and not in B-cell malignancies, underscoring the role of PHF6 as a T-ALL specific tumor suppressor. Notably, *PHF6* deficiency in B-ALL cells leads, in contrast to a T-ALL context, to impaired cell growth. These observations thus suggest a potential critical role for PHF6 as a regulator of hematopoietic lineage commitment. To this end, we studied the effects of PHF6 knockdown in $CD34^+$ thymocyte progenitors with respect to hematopoietic differentiation (**paper 2, in preparation**). In addition, I aimed to unravel the functional interaction between TLX1 and PHF6 in T-ALL formation and scrutinize its potential functional interaction with other chromatin remodeling complexes at the level of transcriptional networks. (**paper 3, in preparation**).

### Aim 3: Identification of TAL1 as a novel driver of miRNA expression in T-ALL oncogenesis

TAL1/SCL is a crucial regulator in normal hematopoietic development and is one of the most frequently altered T-ALL oncogenes as a consequence of a t(1;14) translocation (1-2% of all cases) or SIL-TAL fusion due to an interstitial deletion (15-20% of T-ALLs). The transcriptional network under control of TAL1 in normal and malignant T-cell development has already been extensively studied and requires amongst others interaction with the chromatin modifier enzyme '*lysine specific demethylase 1*' (LSD1). We hypothesized that TAL1 could also act as a crucial regulator of miRNA expression in T-ALL (**paper 4, Leukemia, 2013**) and therefore scrutinized the miRNAs that are under control of TAL1 in T-ALL lymphoblasts.

## Chapter 2: Research Objectives

### Aim 4: The role of long non-coding RNAs in the NOTCH1 signaling pathway in normal and malignant T-cell development

Besides the genetic alterations that discriminate the different T-ALL oncogenic subtypes, a set of mutations in T-ALL are prevalent in a subtype independent manner. The prototype example is the occurrence of activating *NOTCH1* mutations, present in over 60% of all T-ALL cases. The NOTCH1 receptor plays a crucial role in normal and malignant T-cell development. Although the signaling cascade downstream of NOTCH1 has been studied extensively in the past, the role of non-coding RNAs has thus far not been explored. Therefore, we aimed to identify the set of lncRNAs (**paper 5, Haematologica, 2014**) under control of NOTCH1 in both thymic $CD34^+$ and $CD4^+CD8^+$ progenitor cells as well as in T-ALL blasts.

### Statement on the bio-informatics analyses throughout this doctoral thesis

Throughout this PhD thesis, a plethora of bio-informatics analyses were executed to support or guide the experimental data that is described. I performed differential gene expression analyses of the micro-array expression datasets using R included in this PhD thesis, as well as GSEA and Gene Ontology analyses on these expression datasets. With respect to data-mining of the RNA-seq and ChIP-seq datasets throughout this thesis, I was assisted by a dedicated bio-informatician, Wouter van Loocke, who is therefore clearly stated as a prominent co-author on many of the publications (either published or in preparation) included in this doctoral thesis.

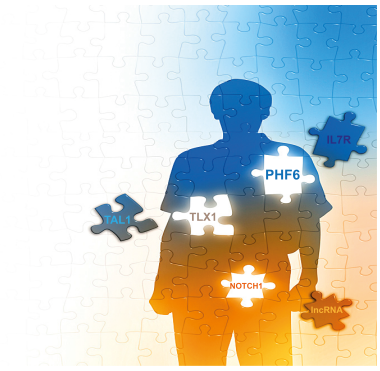


# CHAPTER 3

## Results

# Results

## Part 1. IL7R at the crossroads of the transcriptional circuitry of TLX1 and PHF6

**Paper 1:** Characterization of the genome-wide TLX1 binding profile in T-cell acute lymphoblastic leukemia (Leukemia, 2015) - *pg. 105*

**Paper 2:** PHF6 as a key regulator of normal hematopoiesis (in preparation) - *pg. 143*

**Paper 3:** Functional dissection of PHF6 as a key epigenetic regulator in TLX1-driven T-ALL (in preparation) - *pg. 167*

## Chapter 3: Results

## Chapter 3: Results

# Characterization of the genome-wide TLX1 binding profile in T-cell acute lymphoblastic leukemia

Kaat Durinck[1], Wouter Van Loocke[1], Joni Van der Meulen[1], Inge Van de Walle[2], Maté Ongenaert[1], Pieter Rondou[1], Annelynn Wallaert[1], Charles E. de Bock[3], Nadine Van Roy[1], Bruce Poppe[1], Jan Cools[3], Jean Soulier[4], Tom Taghon[2], Frank Speleman[1] and Pieter Van Vlierberghe[1]

*[1]Center for Medical Genetics, Ghent University, Ghent, Belgium*

*[2]Department of Clinical Chemistry, Microbiology and Immunology, Ghent University, Ghent, Belgium*

*[3]Laboratory for the Molecular Biology of Leukemia, Center for Human Genetics, KU Leuven and Center for the Biology of Disease, VIB, Leuven, Belgium*

*[4]Genome Rearrangements and Cancer Laboratory, U944 INSERM, University Paris Diderot and Hematology Laboratory, Saint-Louis Hospital, Paris, France*

**Leukemia. 2015 Dec;29(12):2317-27**

## Chapter 3: Results

**ABSTRACT**

The TLX1 transcription factor is critically involved in the multi-step pathogenesis of T-cell acute lymphoblastic leukemia (T-ALL) and often cooperates with *NOTCH1* activation during malignant T-cell transformation. However, the exact molecular mechanism by which these T-cell specific oncogenes cooperate during transformation remains to be established. Here, we used chromatin immunoprecipitation followed by sequencing to establish the genome-wide binding pattern of TLX1 in human T-ALL. This integrative genomics approach showed that ectopic TLX1 expression drives repression of T-cell specific enhancers and mediates an unexpected transcriptional antagonism with NOTCH1 at critical target genes, including *IL7R* and *NOTCH3*. These phenomena coordinately trigger a TLX1 driven pre-leukemic phenotype in human thymic precursor cells, reminiscent of the thymus regression observed in murine TLX1 tumor models, and create a strong genetic pressure for acquiring activating *NOTCH1* mutations as a prerequisite for full leukemic transformation. In conclusion, our results uncover a functional antagonism between cooperative oncogenes during the earliest phases of tumor development and provide novel insights in the multi-step pathogenesis of TLX1 driven human leukemia.

# Chapter 3: Results

## INTRODUCTION

*T-cell leukemia homeobox 1* (*TLX1*, *HOX11*) is a homeobox transcription factor oncogene that is ectopically expressed by chromosomal translocations in a subset of human T-cell acute lymphoblastic leukemia (T-ALL). *TLX1* activation is more prevalent in adult than in pediatric T-ALL and is generally associated with a favorable prognosis[1]. TLX1 driven T-ALLs show a unique gene expression signature related to early cortical thymocytes with corresponding expression of CD1a, CD4 and CD8 surface marker proteins. Initial studies showed that TLX1 could immortalize murine hematopoietic precursors[2,3], but its leukemic potential has only been fully established using TLX1 transgenic mouse models that develop clonal T-cell malignancies with a long latency[4,5]. These TLX1 induced murine T-cell tumors share common features with human TLX1 positive leukemia, including activation of Notch signaling, loss of the *Bcl11b* tumor suppressor gene and a transcriptional program that disrupts the mitotic checkpoint and induces aneuploidy during T-cell transformation[4]. Of note, *Lck-TLX1* transgenic mice present with a pre-leukemic phenotype, in which TLX1 positive T-cell precursors undergo a block in differentiation and show enhanced susceptibility towards apoptosis[4]. The decreased thymus size and reduced cellularity observed in *TLX1* transgenic mice, corresponds with earlier findings in the human context[6] and might be associated with transcriptional repression of the *TCRα* locus by the TLX1-ETS1-RUNX1 complex[7].

NOTCH1 is a critical regulator of T-cell development and serves as a prominent oncogene in the biology of T-ALL[8]. Critical NOTCH1 target genes are often co-regulated by a transcription factor complex that contains NOTCH1, ETS1 and RUNX1[9,10]. Notably, binding of this complex regularly occurs near super-enhancer regions[11,12,13] in the vicinity of genes that are critically involved in normal and malignant T-cell development[9,10]. Activating *NOTCH1* mutations occur in more than half of all T-ALLs[8], but are particularly prevalent in *TLX1* positive human T-ALLs[14]. Moreover, *Notch1* mutations are almost uniformly identified in murine T-cell tumors that developed from *TLX1* transgenic mice[4,5]. Therefore, *NOTCH1* activation and aberrant expression of *TLX1* are considered collaborative events in the multi-step pathogenesis of T-ALL. However, the exact molecular mechanisms by which these T-

cell specific oncogenes cooperate during malignant T-cell transformation and their functional relationship remains to be established.

Here, we used an integrative genomic approach to study the role of the TLX1 transcription factor oncogene in the multi-step pathogenesis of human T-ALL. Furthermore, we evaluated the functional relationship between the cooperative oncogenes *TLX1* and *NOTCH1* in T-ALL to understand their cooperative mechanism-of-action during T-cell transformation.

## METHODS

### Cell lines

ALL-SIL cells were obtained from the DSMZ cell line repository. Cells were maintained in RPMI-1640 medium (Life Technologies) supplemented with 20% fetal bovine serum, 1% of L-glutamine (Life Technologies) and 1% penicillin/streptomycin (Life Technologies).

### Clinical samples

Bone marrow lymphoblast samples from 64 T-ALL patients (15 immature, 25 *TAL/LMO*, 17 *TLX1/TLX3* and 7 *HOXA*) were collected with informed consent according to the declaration of Helsinki from Saint-Louis Hospital (Paris, France) and the study was approved by the Institut Universitaire d'Hématologie Institutional Review Board. This primary T-ALL cohort was previously investigated and the high-quality RNA samples from this cohort were used for gene expression profiling[15]. Gene expression data is accessible on ArrayExpress under accession no. E-MTAB-593[15].

### SiRNA-mediated knockdown, RNA-isolation, cDNA synthesis and RT-qPCR

ALL-SIL cells were electroporated (250 V, 1000 µF) using a Genepulser Xcell device (Biorad) with 400 nM of Silencer Select Negative Control 1 siRNA (Ambion, #) or siRNAs targeting *TLX1* (Silencer Select, Ambion). ALL-SIL cells were collected 24h post-electroporation. Total RNA was isolated using the miRNeasy mini kit (Qiagen) with DNA digestion on-column. By means of spectrophotometry, RNA concentrations were measured (Nanodrop 1000) and RNA integrity was evaluated (Experion, Bio-Rad). Next, cDNA synthesis was performed using the iScript cDNA synthesis Kit (Bio-Rad) followed by RT-qPCR using the LightCycler 480 (Roche). Finally, qPCR data was analyzed according to the ΔΔCt-method using the qBasePLUS software (Biogazelle).

### Western blotting

SDS-PAGE was performed according to standard protocols. For immunoblotting, following antibodies were used: rabbit polyclonal antibody to TLX1 (1:500, Santa Cruz Biotechnology), mouse monoclonal antibody to alpha-tubulin (1:2000, Sigma-Aldrich), mouse monoclonal antibody to beta-actin (1:2000, Sigma- Aldrich), rabbit polyclonal antibody to ICN1 (1:1000, Cell Signaling) and rabbit polyclonal antibody to c-MYC (1:500, Santa Cruz Biotechnology). Protein level quantification was performed using the ImageJ software.

### Micro-array based gene expression profiling

RNA samples from ALL-SIL cells as well as $CD34^+$ thymus precursor cells were profiled on a custom designed Agilent micro-array covering all protein coding genes (33,128 mRNA probes, Human Sureprint G3 8x60k micro-arrays (Agilent)) and 12,000 lncRNAs (23,042 unique lncRNA probes)[16]. Expression data were normalized using the VSN-package (Bioconductor release 2.12) in R. Differential expression analysis was performed in R using Limma. All gene expression profiling data has been deposited in the GEO database (GSE62144).

## Chapter 3: Results

### Compound treatment of T-ALL cell lines

ALL-SIL cells were seeded at a density of $1*10^6$ cells/ml and treated for 12h with either DMSO or 1 µM of JQ1 compound (BPS Bioscience). ALL-SIL cells were seeded at a density of $1*10^6$cells/ml and treated for 48h with either DMSO or 1 µM of compound E (Enzo Life Sciences). Cells were harvested at the indicated time-points and RNA-isolation was performed as described above.

### ChIP-seq and ChIP-qPCR

The ChIP-protocol has been adapted from previous studies[17]. In brief, $1*10^7$ cells were cross-linked with 1,1% formaldehyde (Sigma-Aldrich) at room temperature for 10 min and the cross-linking reaction was quenched with glycine (125 mM final concentration, Sigma-Aldrich). Nuclei were isolated and chromatin was purified by chemical lysis. Next, the purified chromatin was fragmented to 200-300 bp fragments by sonication (Covaris). Chromatin immunoprecipitation was performed by incubation of the chromatin fraction overnight with 100 µl of protein-A coated beads (Thermo- Scientific) and 10 µg of fibrillarin-specific (Abcam), H3K27ac-specific antibody (Abcam) or TLX1-specific antibody (Santa-Cruz Biotechnology). The next day, beads were washed to remove non-specific binding events and enriched chromatin fragments were eluted from the beads, followed by reverse cross-linking by incubation at 65°C overnight. DNA was subsequently purified by phenol/chloroform extraction, assisted by phase lock gel tubes (5Prime). DNA obtained from the ChIP-assays was adaptor-ligated, amplified and analyzed by Illumina Hiseq 2000. Raw sequencing data was mapped to the human reference genome (GRCh37/h19) using Bowtie[18]. Peak calling was performed using MACS 1.4[19]. ChIP seq data has been deposited in the GEO database (GSE62144).

Relative real-time PCR quantification of promoter sequences was normalized to *HPRT1* DNA levels (negative control region) in chromatin immunoprecipitates performed with TLX1-specific antibody (Santa Cruz Biotechnology) or fibrillarin-specific antibody (negative control antibody) (Abcam). Additionally, real-time PCR quantification was normalized in chromatin immunoprecipitates performed with a

RUNX1 (Abcam) and ETS1 (Cell signaling) specific antibodies to immunoprecipitation with a fibrillarin-specific antibody. ChIP-qPCR primers for *CHEK1*, *BUB1*, *BCL11B* and *BRCA2* were used as described previously[4]. Enrichment was calculated using the ΔΔCt method.

**Motif enrichment**

A TLX1 peak multi-fasta file (500 bp centered around the peak summits) was produced using BedTools[20] and was subsequently submitted to the MEME-ChIP[21] public server for motif enrichment analysis. This motif analysis was performed on the top quartile (25% of the highest scoring) of TLX1 ChIP-seq peaks. The 'fasta-get-markov' module, included in the MEME suite, was used to create a background model based on all TLX1 peaks as called by MACS1.4.

**ChIP-seq peak heatmaps**

Public ChIP-seq data for ETS1, RUNX1, ICN1 and BRD4 in CUTLL1[9] were downloaded from GEO series GSE51800. Fastq files were aligned to the reference genome (hg19) with Bowtie. HOMER[22] was used to produce tag directories and heatmap data matrices of public ChIP-seq data and TLX1 ChIP-seq data. Heatmaps were produced in R. TSS-centered heatmaps were ordered based on average linkage clustering of the rows in the TLX1 heatmap. TLX1 ChIP-seq peak heatmaps were ordered by descending TLX1 peak heights.

## Chapter 3: Results

### Thymocyte transduction and culturing on OP9-DLL1

Pediatric thymus samples were obtained and used according to the guidelines of the Medical Ethical Commission of the Ghent University Hospital (Belgium). $CD34^+$ thymocytes were purified using magnetic activated cell sorting (MACS, Miltenyi Biotec) and cultured for 24h in complete IMDM, supplemented with penicillin (100 U/ml), streptomycin (100 µg/ml), L-glutamine (2 mM) (all from Invitrogen) and 10% heat-inactivated FCS (Biochrom) in the presence of 10 ng/ml IL-7 and SCF. After 24h, cells were retrovirally transduced with either LZRS-IRES-EGFP (LIE) or LZRS- TLX1-IRES-EGFP (TLX1) as described previously[23]. For the double transfection experiments, retroviral transduction was performed using either MSCV-mCherry or MSCV-mCherry-TLX1 (TLX1) at 24h. Next, $mCherry^+$ cells were sorted and directly transduced with either MSCV-EGFP or MSCV-EGFP-ICN1 at 48h. Next, equal numbers of transduced cells were seeded onto confluent OP9-GFP or OP9-DLL1 plates in α-MEM media supplemented with 20% heat-inactivated FCS plus 100 U/ml penicillin, 100 µg/ml streptomycin, 2 mM L-glutamine and the T-lineage supporting cytokines SCF, Flt3-L and IL-7 at 5 ng/ml each. Following 72h of OP9 co-culture, cells were harvested by forceful pipetting and stained with CD45-PE (Miltenyi) to purify $CD45^+EGFP^+$, $CD45^+mCherry^+$ or $CD45^+mCherry^+EGFP^+$ human transduced leukocytes through sorting to remove contaminating OP9 stromal cells. After sorting, part of the cells were lysed in 700 µl QIAzol (Qiagen) and stored at -80°C prior to RNA isolation, while the other part was used to perform T-cell differentiation experiments as described previousy[24]. To evaluate T cell development, co-cultures were harvested at indicated time points by forceful pipetting, stained with monoclonal antibodies as described previously[26] and analyzed on a LSRII flow cytometer using FACSDiva software (BD Bioscience).

### Ectopic TLX1 expression in CUTLL1

CUTLL1 cells were seeded at a density of 1*10e6 cells/ml in RPMI-1640 medium supplemented with 20% fetal bovine serum and retrovirally transduced with either LZRS-IRES-EGFP (control vector) or LZRS-TLX1-IRES-EGFP (TLX1). After 72h,

transduced cells were sorted to purify EGFP$^+$ CUTLL1 cells. After sorting, cells were lysed in 700 µl QIAzol (Qiagen) and stored at -80°C prior to RNA isolation.

**RESULTS**

**Genome-wide binding profile of TLX1 in human T-ALL**

To identify the genome-wide binding pattern of TLX1 in the context of human T-ALL, we performed chromatin immunoprecipitation followed by sequencing (ChIP-seq) in ALL-SIL, a human T-ALL cell line with ectopic *TLX1* expression as a result of the t(10;14)(q24;q11) translocation. This analysis identified 18,187 unique TLX1 binding peaks (FDR<0.05) with a distribution of 19.8% in the proximity of transcriptional start sites (TSSs) of protein-coding genes, 43.5% in intronic and 36.7% in intergenic regions of the human genome (**Supplementary Figure 1a**). Notably, genes characterized by the strongest TLX1 binding events showed higher average expression levels as compared to genes with moderate or no TLX1 binding (**Supplementary Figure 1b**). The validity of our approach was confirmed by ChIP-qPCR analysis of TLX1 binding at promoter regions of previously reported TLX1 targets[4], including *BCL11B*, *BUB1*, *CHEK1* and *BRCA2* (**Supplementary Figure 1c**).

To unravel the transcriptional consequences of TLX1 binding, we performed micro-array gene expression analysis before and after TLX1 knockdown in ALL-SIL cells using 2 independent TLX1 targeting siRNAs (**Figure 1a, Supplementary Figure 2a and 2b**). Gene Set Enrichment Analysis (GSEA) confirmed that TLX1 binding peaks (top 500 and top 1000 scoring peaks) located near TSSs of protein-coding genes were significantly enriched in genes upregulated after TLX1 knockdown in ALL-SIL (**Figure 1b and Supplementary Figure 2c**), in line with the previously recognized role of TLX1 as a transcriptional repressor in T-ALL[4,25]. In addition, this notion was further confirmed by a significantly higher number of TLX1 bound genes that are upregulated as compared to downregulated after TLX1 knockdown (**Figure 1c**). Notably, the average gene expression levels of targets repressed by TLX1 were higher in comparison to TLX1 activated genes or those that were not significantly differentially expressed upon TLX1 knockdown in ALL-SIL (**Figure 1d**). Consistent with

previous reports, we also obtained a significant enrichment of the TLX1 binding peaks near TSSs in genes that are downregulated in both *TLX1* or *TLX3* driven primary T-ALLs, in keeping with previously noted overlap between TLX1 and TLX3 transcriptional programs[4,25] (**Figure 1e**).

Next, we evaluated the presence of co-factor binding sites at TLX1-bound regions by means of motif analysis (**Figure 1f**). A strong enrichment was found for RUNX family member (E-value: 2.9e-288) and ETS transcription factor motifs (E-value: 1.5e-227), consistent with previously published data[7,25]. Moreover, but to a lesser extent, we found enrichment for other co-factors previously linked to TLX1 functionality, including MEIS and PBX transcription factor family members[26,27].

The genome-wide binding profiles of RUNX1 and ETS1 were previously shown to be highly overlapping in the context of T-ALL[9]. Moreover, ETS1 cooperates with TLX1 at the *TCRα* locus and RUNX1 was shown to act as a central hub in the TLX1 regulatory network[25]. Given this, we integrated our TLX1 ChIP-seq profiles with publically available ETS1 and RUNX1 ChIP-seq data[9] and evaluated the extent of overlap between these transcription factors at the TSSs of genes that are upregulated after TLX1 knockdown in ALL-SIL (*bona fide* TLX1 repressed target genes). We generated a heatmap of the TLX1 ChIP-seq binding profile for the top-500 genes upregulated upon TLX1 knockdown by clustering of TLX1 ChIP-seq signals within a 10 kb window surrounding the TSS (**Figure 1g**). Next, ChIP-seq binding profiles for RUNX1 and ETS1 were visualized in the exact same gene order as defined by the TLX1 ChIP-seq data (**Figure 1g**). Similar and overlapping patterns observed in these ChIP-seq heatmaps support our motif analysis (**Figure 1f**) and confirm a high degree of overlap between TLX1, ETS1 and RUNX1 binding sites in the promoter of TLX1 repressed genes. To verify whether these overlapping binding patterns between TLX1, RUNX1 and ETS1 also result in a similar transcriptional read-out, we performed siRNA-mediated knockdown for *RUNX1* and *ETS1* in ALL-SIL. The resulting gene signatures were scored to the transcriptional profile associated with *TLX1* inactivation in ALL-SIL by GSEA. This analysis points towards a common transcriptional regulatory network between these three transcriptional regulators (**Supplementary Figure 3a and 3b**). Furthermore, ChIP-qPCR analysis in ALL-SIL confirmed direct binding of both RUNX1

and ETS1 at the exact same binding sites as observed for TLX1 at canonical target genes, including *BCL11B*, *CHEK1*, *BRCA2* and *BUB1* (**Supplementary Figure 3c and 3d**). Overlapping binding patterns between TLX1, RUNX1 and ETS1 could not be observed using the top-500 down-regulated genes upon TLX1 knockdown (**Supplementary Figure 4**).

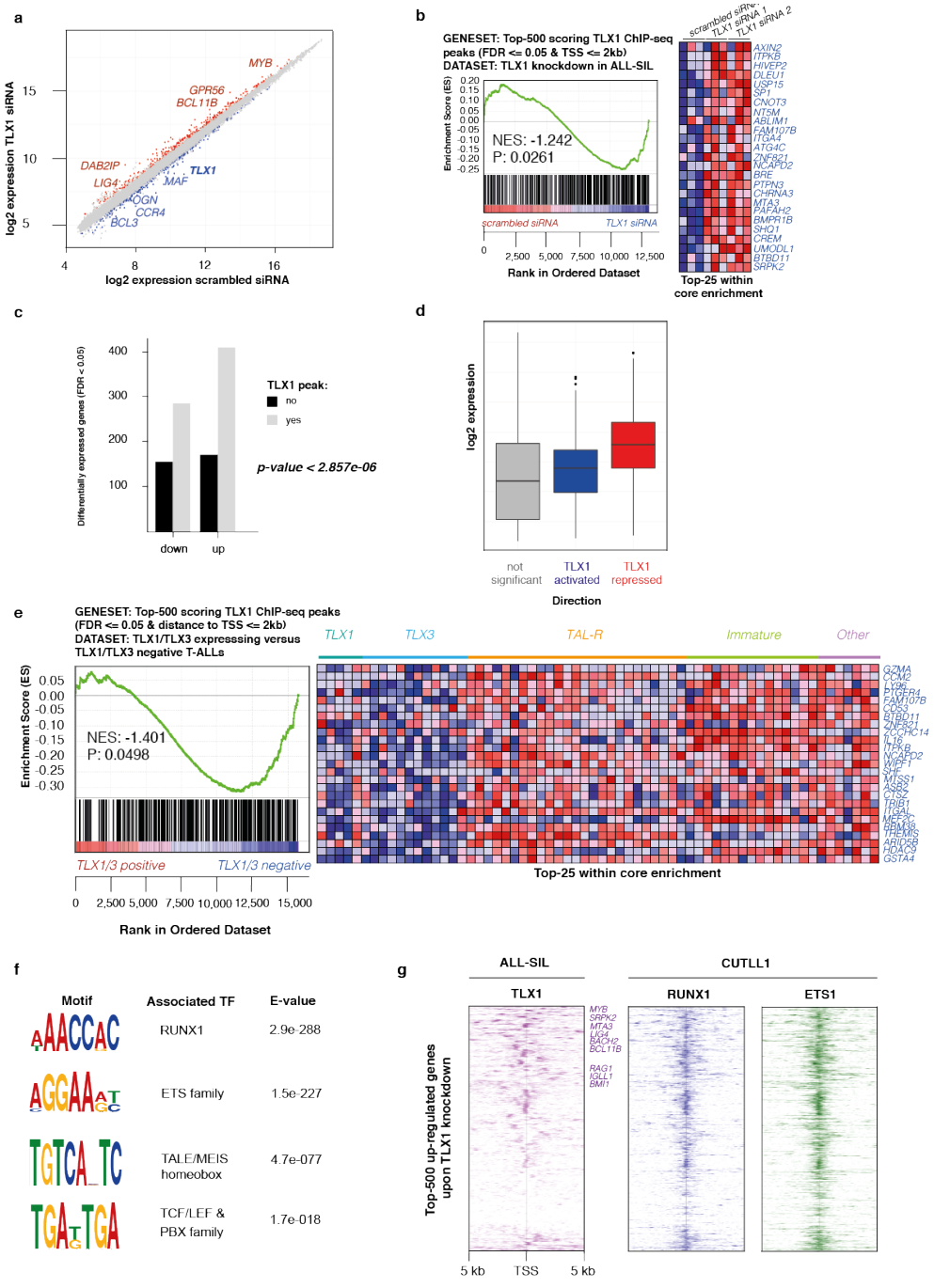


**Figure 1**: **Characterizing the genome-wide TLX1 binding pattern.** (**a**) Scatter plot showing significantly down- (blue) and upregulated (red) genes (p-adj. value < 0.05) upon TLX1 knockdown in ALL-SIL leukemic cells, (**b**) GSEA shows a significant enrichment of the top-500 scoring (FDR<0.05) TLX1 binding sites in proximity (<=2kb) of the TSS amongst the TLX1 repressed genes, (**c**) Barplot showing the distribution of TLX1 ChIP-seq peaks between genes up- or downregulated upon TLX1 knockdown in ALL-SIL, (**d**) Boxplot showing that TLX1 repressed genes have a higher average expression level in comparison to genes either activated by TLX1 or not differentially expressed upon TLX1 knockdown in ALL-SIL (**e**) Validation of the same geneset as defined in (**b**) in a primary cohort of 64 T-ALL patients (5 *TLX1+* cases and 12 *TLX3+* cases), (**f**) MEME-ChIP motif analysis identifies RUNX and ETS family member motifs amongst the strongest enriched DNA-motifs in TLX1 binding sites identified by ChIP-sequencing, (**g**) Heatmap representation of ChIP-profiles of TLX1 in ALL-SIL cells and ETS1-RUNX1 sites in CUTLL1 cells at the top-500 upregulated genes upon TLX1 knockdown, clustered according to average linkage.

## Chapter 3: Results

### TLX1 binding at super-enhancers in human T-ALL

Recently, enhancer sites with broad binding of traditional enhancer associated histone marks (H3K27ac and H3K4me1) and co-occupation of the transcriptional co-activators BRD4 and MED1 were identified[11,12]. These so-called super-enhancers mark the binding sites for transcription factor complexes that establish a unique cell identity program and drive expression of both lineage identity genes as well as prominent oncogenes in human cancer.

Given the role of TLX1 as oncogenic transcriptional repressor, we wondered whether TLX1 could interfere with super-enhancer activity[11,12] in the context of *TLX1*-driven human leukemia. For this, we performed H3K27ac ChIP-seq analysis in the T-ALL cell line ALL-SIL and used the normalized H3K27ac cluster signals in function of the normalized ranks to identify super-enhancers in this *TLX1* driven tumor line, as previously described[12] (**Supplementary Figure 5a**). Next, we performed a similar analysis based on TLX1 ChIP-seq data and clustered TLX1 peaks within 12.5 kb from each other. These TLX1 clusters were superimposed on the H3K27ac super-enhancer plot, which revealed a large overlap between super-enhancer sites and TLX1 binding clusters in the ALL-SIL genome (**Figure 2a**). Notably, these top-ranked super-enhancer sites were often located within the vicinity of crucial regulators involved in normal and malignant T-cell development, for example *ZFP36L2* and *HIVEP3* (**Figure 2b**).

To further confirm true super-enhancer identity of TLX1 bound super-enhancer sites, we interrogated their responsiveness to treatment with the small-molecule BET-inhibitor JQ1[28]. Response to treatment was verified by downregulation of *c-MYC* RNA levels (**Supplementary Figure 5b**) and protein levels (**Supplementary Figure 5c**). For this, we used micro-array analysis to evaluate the transcriptional response of ALL-SIL cells upon JQ1 treatment (**Supplementary Figure 5d**). Notably, GSEA analysis showed that H3K27ac defined super-enhancers characterized by co-binding of TLX1 were significantly enriched in genes downregulated upon JQ1 treatment in ALL-SIL (**Figure 2c**). In addition, the same TLX1 bound super-enhancer sites were significantly enriched for genes that are upregulated upon TLX1 knockdown (suppressed by TLX1;

**Figure 2d**), suggesting that TLX1 interferes with enhancer function at these loci. Notably, the core enrichment for these GSEA analyses included several genes with an established role in either T-cell development (*PTPN3*, *RAG2*, *BACH2*, *HIVEP3*, *CD2*) or T-ALL pathogenesis (*ETV6*, *MYB*) (**Figure 2e**). The response of these genes to JQ1 treatment or TLX1 knockdown, respectively, was confirmed by RT-qPCR (**Figure 2f**).

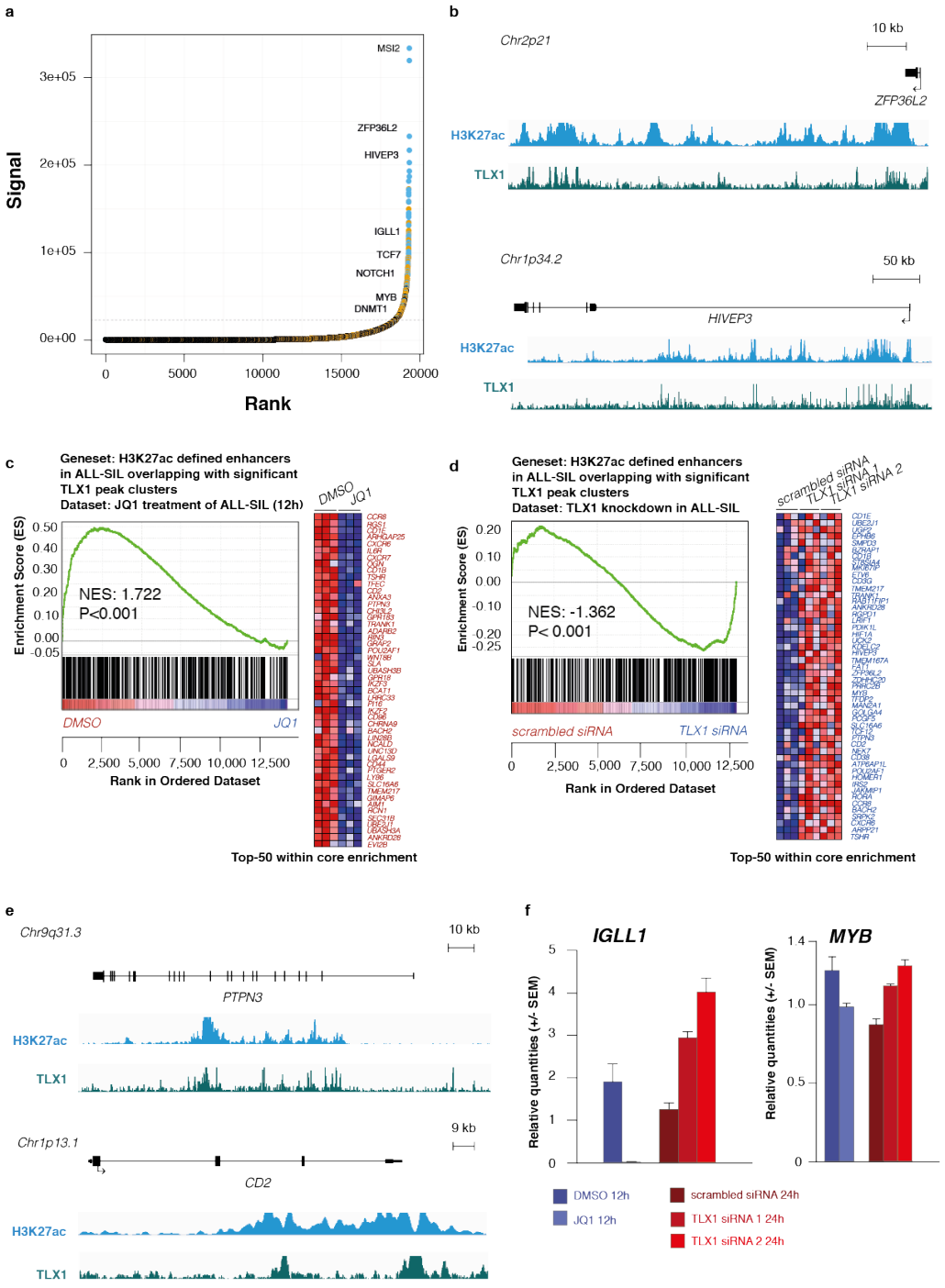


**Figure 2: The role of TLX1 at (super)-enhancer sites.** (**a**) Hockey-stick plot representing the normalized rank and cluster signal of clusters of H3K27ac peaks (super-enhancers) overlapping with significant TLX1 ChIP-seq peak clusters (blue dots), overlapping with TLX1 binding events that are not organized in significant clusters (orange dots) or not overlapping with TLX1 binding events (black dots), (**b**) Examples of H3K27ac defined super-enhancer sites characterized by large TLX1 ChIP-seq peak clusters within the proximity of *ZFP36L2* and *HIVEP3*, (**c**) GSEA of the top-500 scoring H3K27ac defined super-enhancer sites with significant TLX1 clusters (orange and blue dots from **a**) within the set of genes downregulated by JQ1 in ALL-SIL, (**d**) GSEA of the same geneset as in (**c**) within the set of genes upregulated upon TLX1 knockdown in ALL-SIL, (**e**) Examples of H3K27ac and TLX1 ChIP-seq signals at the *PTPN3* and *CD2* loci, both significantly enriched in the GSEA analyses shown in (**c**) and (**d**), (**f**) Confirmation of *IGLL1* and *MYB* responsiveness to JQ1 treatment and TLX1 knockdown in ALL-SIL by RT-qPCR.

## Chapter 3: Results

### Transcriptional antagonism between the cooperative oncogenes TLX1 and NOTCH1

Previous studies have shown that NOTCH1, ETS1 and RUNX1 define a transcription factor complex that co-regulates important NOTCH1 target genes[9,10]. Moreover, binding of this complex can also occur near super-enhancer regions in the vicinity of genes critically involved in normal and malignant T-cell development[9]. Given that RUNX1 and ETS1 often co-occupy TLX1 binding sites and that TLX1 can also associate with regions of super-enhancer activity, we wondered whether TLX1 could interfere with the transcriptional program mediated by NOTCH1.

To address this issue, we evaluated the relationship between the NOTCH1 transcriptional program and the gene expression signature associated with TLX1 knockdown in ALL-SIL. Surprisingly, GSEA analysis showed that NOTCH1 positively regulated genes (down-regulated upon GSI treatment of ALL-SIL cells[29]; **Supplementary Figures 6a-c**) were significantly enriched for genes repressed by TLX1 (**Figure 3a**). TLX1 and ICN1 binding near the *NOTCH3* and *IL7R* loci are shown as representative examples for overlapping binding events of these factors at canonical NOTCH1 target genes (**Figure 3b**). Notably, next to some of the canonical NOTCH1 targets also *NOTCH1* itself is upregulated upon TLX1 knockdown in ALL-SIL, at both the mRNA and protein level (**Figure 3c**). The TLX1-driven repression of some of these NOTCH1 target genes was confirmed upon ectopic TLX1 expression in the CUTLL1 cell line (as shown for *NOTCH3*; **Figure 3d**). Interestingly, strong and overlapping binding of TLX1 with NOTCH1 was also observed at the recently identified long-range acting *MYC*-enhancer[30] (**Figure 3e**). Finally, alignment of the genome-wide ICN1, ETS1 and RUNX1 ChIP-seq peaks in CUTLL1 T-ALL cells with those of TLX1 in ALL-SIL cells showed a striking binding overlap for these transcription factors as visualized by ChIP-seq heatmaps (3 kb centered around the TLX1 summits; **Figure 3f and Supplementary Figure 6d**).

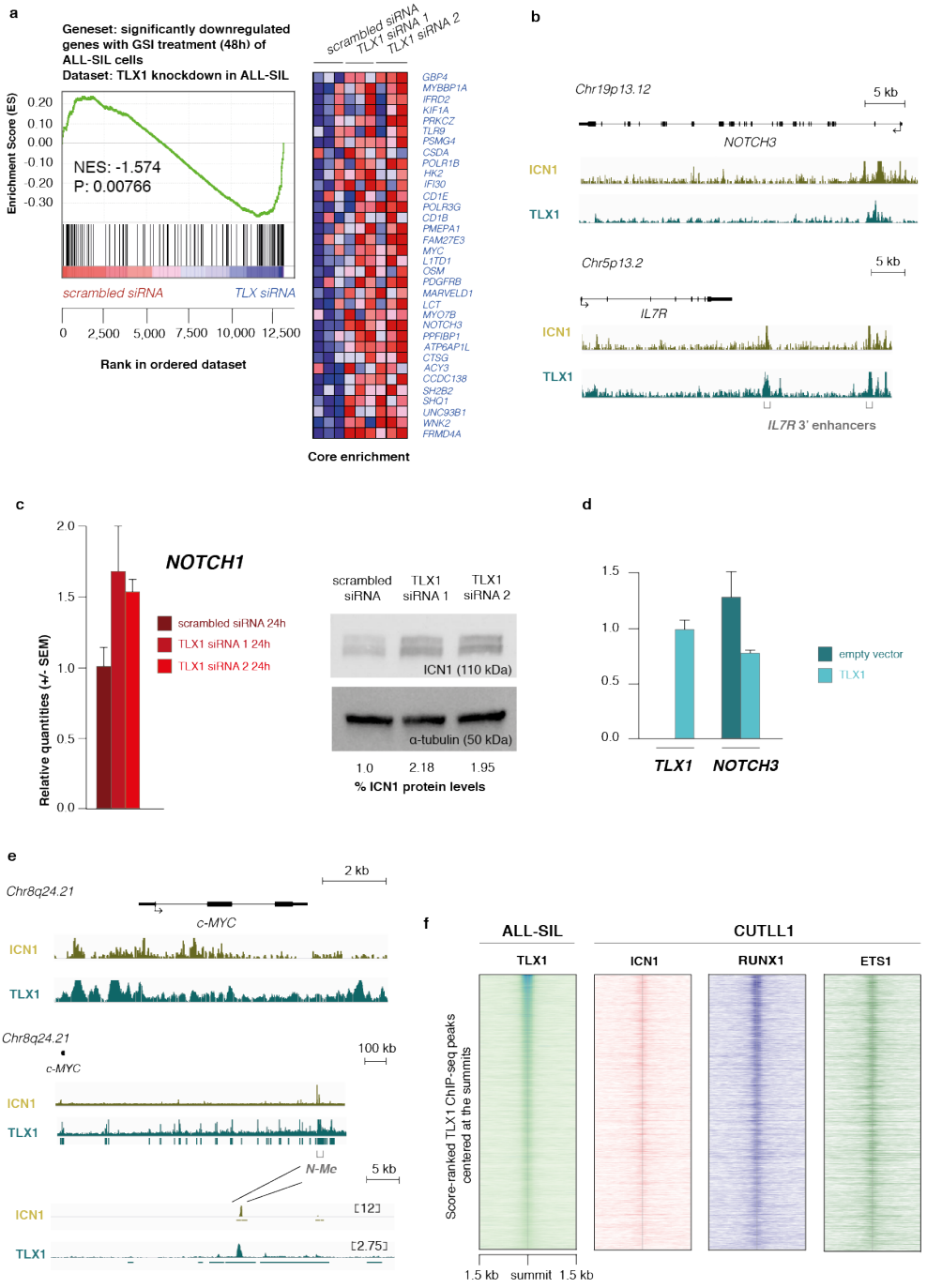


**Figure 3**: **Transcriptional antagonism between cooperative oncogenes NOTCH1 and TLX1 in T-ALL.** (**a**) GSEA shows that the top-500 downregulated genes upon GSI treatment of ALL-SIL T-ALL cells are significantly enriched within the set of genes that are upregulated upon TLX1 knockdown in ALL-SIL, (**b**) ChIP-seq profiles of ICN1 and TLX1 showing overlapping binding patterns at the canonical NOTCH1 target genes *NOTCH3* and *IL7R*, (**c**) confirming upregulation of NOTCH1 upon TLX1 knockdown in ALL-SIL cells, (**d**) Ectopic expression of TLX1 in CUTLL1 leads to reduced expression of the canonical NOTCH1 target gene *NOTCH3* as shown by RT-qPCR, (e) ChIP-seq profiles of ICN1 and TLX1 at the *NOTCH3* and *IL7R* loci, (**e**) ChIP-seq profiles of ICN1 and TLX1 at the genomic region spanning from *c-MYC* towards its recently described long-range enhancer site[30] and visualization of the high-scoring and overlapping ICN1 and TLX1 peak at this specific enhancer site[30] (**f**) Heatmap representation of the ChIP-seq overlap of TLX1-ICN1-ETS1-RUNX1 sites across a genome-wide score-based ranking of TLX1 ChIP-seq signals.

## Chapter 3: Results

### TLX1 broadly interferes with normal T-cell development

Previously, it has been shown that *Lck-TLX1* transgenic mice are characterized by reduced thymus size and cellularity as a pre-leukemic phenotype that precedes full leukemic transformation[4]. In addition, enforced TLX1 expression in human cord blood $CD34^+$ progenitor cells disrupted primary T-cell differentiation and triggered enhanced thymocyte apoptosis[6]. These data suggest that ectopic induction of the TLX1 oncogene in T-cell precursors negatively affects T-cell differentiation, proliferation and survival.

To further study the role of TLX1 during the initial phases of tumor development, human thymus-derived $CD34^+$ precursor T-cells were infected with a retroviral construct that drives ectopic TLX1 expression and cultured on a feeder layer of OP9 stromal cells expressing the NOTCH1 ligand DLL1 (**Figure 4a**). In line with previous results[6], ectopic TLX1 expression strongly perturbed normal T-cell development, with a drastic reduction in absolute number of thymocytes as compared to control cells (**Figure 4b**). Moreover, at day 12 of co-culture, we observed a drastic reduction in $CD4^+CD8^+$ double positive (17.1% vs. 63,2%) (**Figure 4c**) as well as $CD7^+CD1a^+$ and $CD3^+$ TCRγδ positive (0.7% vs. 3.4%) T-cells overexpressing TLX1 (**Supplementary Figure 7**). In line with the transcriptional antagonism between TLX1 and NOTCH1 described above, thymocytes that ectopically express TLX1 also showed a reduction in IL7Rα (CD127) surface expression compared with controls (**Figure 4d**). Moreover, the previously established enhancer sites downstream of the *IL7R* locus showed overlapping binding of ETS1, RUNX1, ICN1, BRD4 and TLX1 (**Figure 4e**).

Cortical thymocyte maturation arrest in TLX1 positive human T-ALL has been linked to TLX1-mediated repression of TCRα enhancer activity and a subsequent block in *TCR-Jα* rearrangement[7]. Notably, our TLX1 ChIP-seq data confirmed these findings with TLX1 binding at the *TCRα* enhancer site in the *TCRα* locus (**Figure 4e**). However, our data also suggest that TLX1 may be implicated in a more global repression of the T-cell recombination machinery including a broad pattern of TLX1 binding at the *TCRα* and *TCRβ* locus (**Figure 4e**) as well as simultaneous binding near critical regulators of V(D)J-recombination including *RAG1* (**Figure 4e**).

Furthermore, gene expression profiling analysis of TLX1 overexpressing versus control human $CD34^+$ thymocytes derived from two representative $CD34^+$ donors at 72 hours post transduction, confirmed genome-wide antagonistic effects between TLX1 and NOTCH1 in this independent *in vitro* model system. TLX1 driven transcriptional repression of *NOTCH1*, *NOTCH3*, *IL7R*, *IGLL1*, *SHQ1*, *RAG1* and *RAG2* are shown as representative examples (**Figure 4f**). Moreover, upregulation of some of these genes was also confirmed by RT-qPCR upon TLX1 knockdown in ALL-SIL (**Figure 4g**).

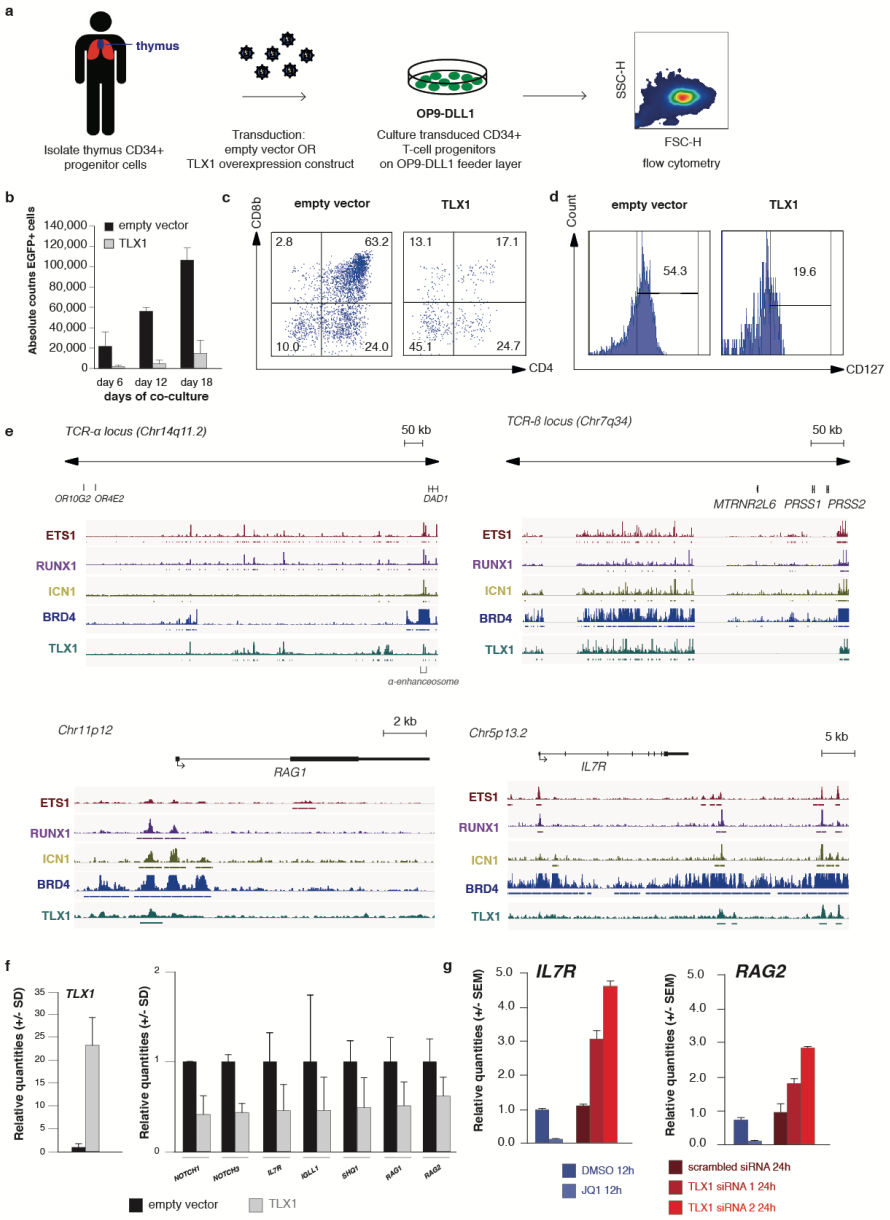


**Figure 4**: **Ectopic TLX1 expression broadly interferes with the normal T-cell differentiation program.** (**a**) Schematic overview of the workflow used for retroviral infection of human thymic CD34$^+$ progenitor T-cells with a TLX1 overexpression construct followed by immunophenotypic and transcriptional characterization upon *in vitro* culturing on a feeder layer of OP9 stromal cells expressing the NOTCH1 ligand DLL1, (**b**) Bar plot showing the averaged absolute counts of EGFP-positive CD34$^+$ T- cell progenitors of three independent donors 6, 12 and 18 days post infection on the *in vitro* OP9-DLL1 co-culture system. (**c**) Flow cytometry profiles of CD34$^+$ progenitor T-cells 12 days post-transduction (representative example shown for three replicates) showing a CD4$^+$CD8$^+$ stage arrest of T-cell progenitors ectopically expressing TLX1, (**d**) Flow cytometry profile showing a drastic reduction in of the percentage of IL7Rα surface positive (CD127$^+$) T-cell progenitors ectopically expressing TLX1, (**e**) TLX1 binding profile to loci critically involved in T-cell development including *TCR* loci, *RAG1* and *IL7R*, (**f**) CD34$^+$ T-cell progenitors (2 independent donors) transduced either with empty vector or with the TLX1 overexpression construct were profiled on a custom Agilent micro-array platform (see also Materials and methods). The average relative expression percentages in CD34$^+$ thymocytes transduced with empty vector versus CD34$^+$ T-cell progenitors ectopically expressing TLX1 from both independent experiments are shown for *NOTCH1*, *NOTCH3*, *IL7R*, *IGLL1*, *SHQ1* and *RAG1*, (**g**) RT-qPCR profiles of *IL7R* and *RAG2* confirming upregulated expression of these genes upon TLX1 knockdown in ALL-SIL.

To further study the functional antagonism between TLX1 and NOTCH1, we verified whether ICN1 would be able to rescue the reduction in cell counts induced by TLX1 ectopic expression in T-cell progenitor cells. To this end, human CD34$^{+}$ progenitor T-cells from three independent donors were sequentially transduced with a TLX1 and/or ICN1 overexpression constructs. Absolute total cell counts were measured 18 and 24 days post-transduction (**Figure 5**). As previously documented, TLX1 overexpression induced a reduction in cell numbers. However and most notably, ICN1 expression rescued this TLX1-driven phenotype and partially restored cell numbers in these co-culture experiments (**Figure 5**).

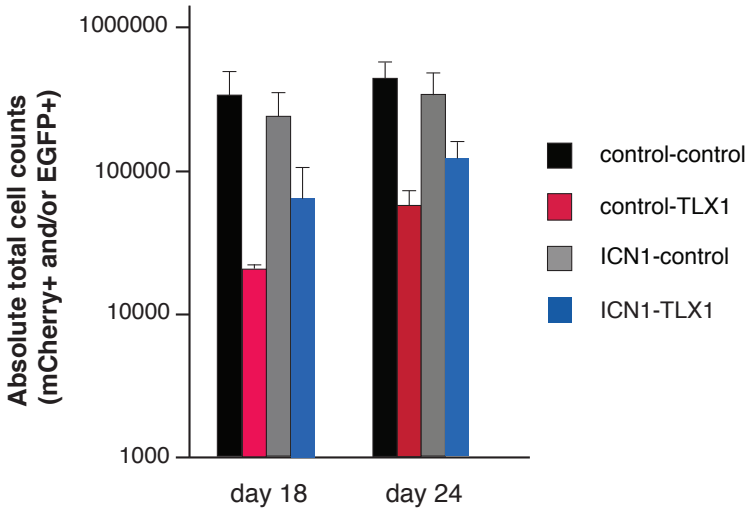


**Figure 5**: ***Ex vivo*** **TLX1-ICN1 co-expression in human and mouse T-cell progenitor cells**. Averaged absolute total cell counts of CD34$^{+}$ progenitor T-cells cultured from three independent donors on OP9-DLL1 for 18 or 24 days and transduced with either control vectors, a TLX1 overexpression, an ICN1 overexpression construct or TLX1 and ICN1 together.

### A tumor suppressor network within the TLX1 regulome in T-ALL

Previous studies have shown direct binding of TLX1 in the promoter region of well-established T-ALL tumor suppressor genes[4,25], including *BCL11B*, *RUNX1* and *WT1*[4,25]. From this, a model emerged in which TLX1-mediated suppression of tumor suppressors would eventually provide genetic pressure towards genomic deletion or mutation of these factors during TLX1-driven transformation[4,25].

To further expand the tumor suppressor network regulated by TLX1, we evaluated the TLX1 binding pattern near currently known T-ALL tumor suppressor genes. This analysis revealed a broad network of tumor suppressors bound by TLX1 including *TET1*, *EZH2*, *FBXW7*, *PTEN*, *BCL11B*, *FAT1*, *RUNX1*, *LEF1*, *GATA3*, *ETV6*, *WT1*, *PTPN2*, *CDKN1B*, *RB1*, *DNM2*, *CNOT3*, *RPL5*, *RPL10* and *SH2B3* (**Figure 6a, Supplementary Figure 8 and 9**). In line with other results obtained from the genome- wide TLX1 binding profile, ChIP-seq peaks for ETS1, RUNX1 and ICN1 showed high positional overlap with TLX1 binding sites in the vicinity of these T-ALL tumor suppressor genes as shown for *BCL11B*, *CNOT3*, *ETV6* and *FAT1* (**Figure 6a**).

Gene expression profiling confirmed upregulation for the majority of these factors upon TLX1 knockdown in ALL-SIL (**Figure 6b and 6c**) and was confirmed for *BCL11B* by RT-qPCR analysis (**Figure 6c**). Although the majority of these tumor suppressors were downregulated upon JQ1 treatment in ALL-SIL (**Figure 6d**), the strongest and most significant effects were observed for *FAT1*, *WT1* and *ETV6* (**Figure 6e**), as confirmed by RT-qPCR for *ETV6* **(Figure 6e**).

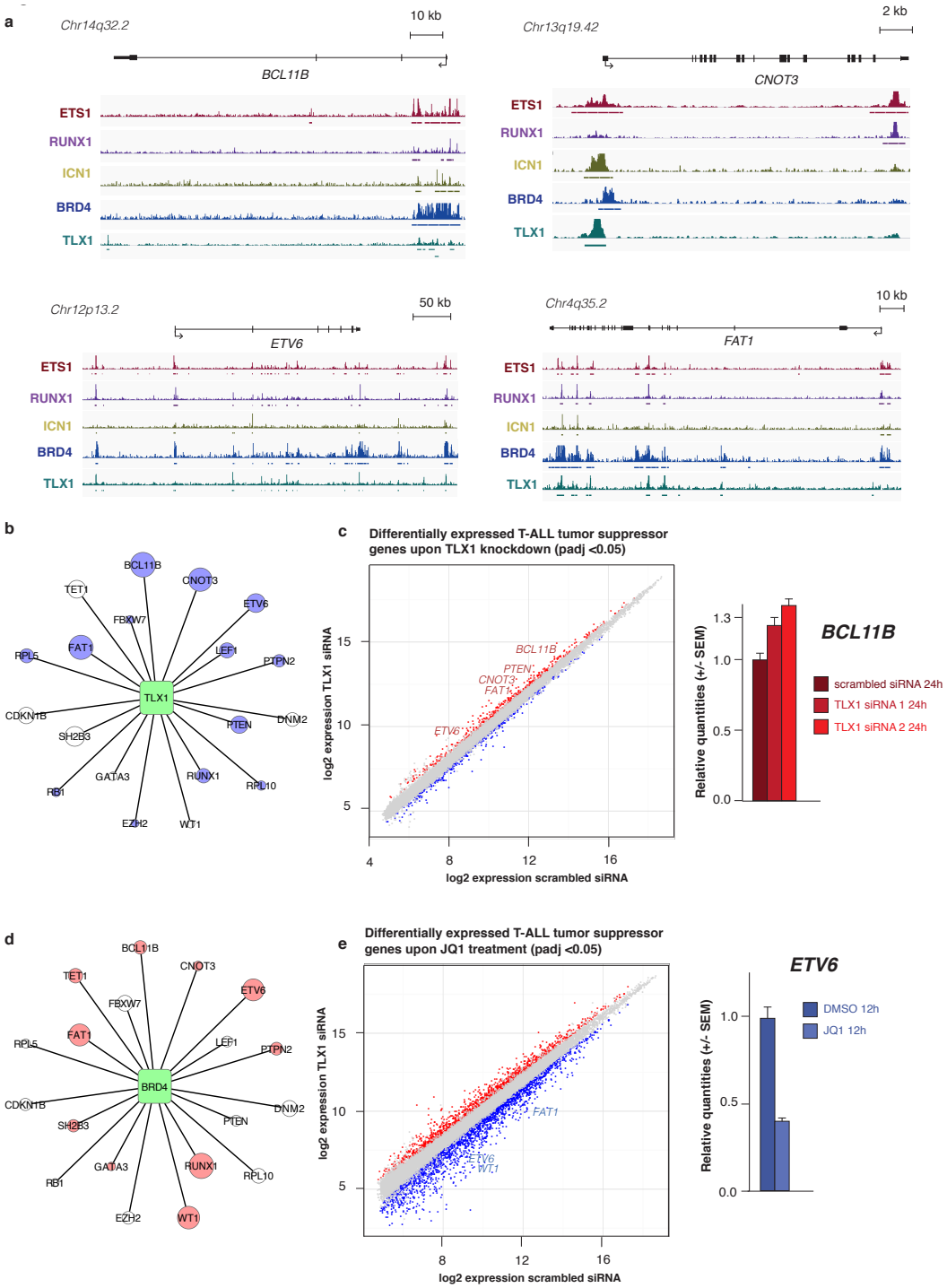


**Figure 6**: **T-ALL tumor suppressor genes in the TLX1 regulatory network.** (**a**) TLX1 ChIP-seq binding profiles at the known T-ALL tumor suppressor genes *BCL11B*, *CNOT3*, *ETV6* and *FAT1*, (**b**) Schematic overview with nodes of TLX1-bound tumor suppressor genes. Tumor suppressors that are upregulated upon TLX1 knockdown in ALL-SIL are shown in blue and the size of the node corresponds to the respective fold change, (**c**) Scatter plot indicating the tumor suppressor genes significantly upregulated upon TLX1 knockdown and confirmation of *BCL11B* upregulation by RT-qPCR, (**d**) Similar overview as (**b**). Tumor suppressors that are downregulated upon JQ1 treatment in ALL-SIL are shown in red and the size of the node corresponds to the respective fold change, (**e**) Scatter plot indicating significantly differentially expressed tumor suppressor genes in ALL-SIL upon JQ1 exposure.

## DISCUSSION

TLX1 is a driver oncogene in the pathogenesis of T-ALL that mediates T-cell transformation through transcriptional repression of its target genes. Our current understanding of the oncogenic properties downstream of TLX1 includes aneuploidy as a result of a deregulated mitotic checkpoint machinery[4], T-cell differentiation arrest caused by repression of *TCRα* enhancer activity[25] and simultaneous inhibition of T- ALL tumor suppressor genes[4,25]. These studies provided important insights in the mechanisms that mediate T-cell transformation downstream of TLX1, but were solely focused on TLX1 binding at the promoter of direct target genes. Therefore, the functional consequences of genome-wide TLX1 binding in the context of human T-ALL development remained to be established.

Here, we report the genome-wide binding profile of TLX1 in human T-ALL and confirm ETS1 and RUNX1[7,25] as critical co-factors in TLX1 mediated transcriptional repression. Moreover, we identified clusters of high intensity TLX1 binding peaks at H3K27ac defined super-enhancers with broad binding of BRD4[9], which were localized in the vicinity of genes that define the T-cell lineage identity. The concept of TLX1 driven repression of super-enhancers provides additional insights in the mechanisms that drive T-cell transformation downstream of TLX1, including global interference with T-cell differentiation and the V(D)J-recombination machinery by targeting enhancers near the *TCR* loci, *RAG1*, *RAG2* and *BCL11B*.

ETS1 and RUNX1 interact with NOTCH1 to regulate gene expression in both normal T-cell development as well as non-TLX1 driven T-ALL and key components of the NOTCH1 transcriptional program are driven by super-enhancer sequences[9,10]. Therefore, we subsequently explored the presumed cooperative relationship between TLX1 and NOTCH1. Integration of TLX1, ICN1, ETS1 and RUNX1 binding patterns with transcriptional read-out in T-ALL revealed an unprecedented transcriptional antagonism between TLX1 and NOTCH1, including TLX1 driven repression of the canonical NOTCH1 targets *NOTCH3*, *IGLL1*, *WNK2*, *SHQ1*, *c-MYC* and *IL7R*. Interestingly, TLX1 mediated repression of the *IL7R* gene occurred at the recently described distal super-enhancer[9] that is co-occupied by ICN1, RUNX1, ETS1

and BRD4. In line with this notion, ectopic *TLX1* expression in $CD34^+$ human thymic precursor T-cells caused significant down-regulation of NOTCH1 target genes including reduced IL7R-alpha (CD127) surface expression.

Although transcriptional antagonism between cooperative T-ALL oncogenes seems counterintuitive, it provides intriguing new insights in the multi-step pathogenesis of TLX1 driven human leukemia. The model that emerges from our results is that ectopic expression of TLX1 would hijack ETS1 and RUNX1 functionality in the context of T-cell development. At a genome-wide level, this would trigger inhibition of enhancer activity, repression of key components of the NOTCH1 transcriptional program and global interference with normal T-cell differentiation and the V(D)J-recombination machinery. These oncogenic properties would eventually result in a pre-leukemic phenotype reminiscent of the thymic regression observed in murine TLX1 tumor models and drive T-cell maturation arrest. At the level of secondary genetic lesions required for full malignant transformation, this model implies a strong genetic pressure for acquiring activating *NOTCH1* mutations to overcome the initial TLX1 mediated suppression of NOTCH1 signaling, which is in line with the high frequency of gain-of-function NOTCH1 mutations in human[14] and murine[4,5] *TLX1* driven T-ALL. Moreover, broad TLX1 mediated downregulation of an extensive network of T-ALL tumor suppressor genes provides additional genetic pressure to reinforce tumor suppressor gene inactivation by genomic deletions or mutations during tumor progression in *TLX1* positive leukemias. Notably, this model differs from the classical concept of the multistep pathogenesis of T-ALL in which cooperative oncogenes and tumor suppressors alter proliferation, differentiation and survival of thymic precursor cell and expand the oncogenic phenotype of the developing tumor cell in a stepwise fashion. Nevertheless, this particular model should be further confirmed beyond the use of T-ALL cell lines by analyzing the genome-wide TLX1 binding pattern in patient derived T-ALL xenografts.

All together, our results uncover novel mechanistic insights in the role of TLX1 during the earliest stages of T-cell transformation and illustrate the power of integrative genomic analyses to understand the multistep pathogenesis of *TLX1* driven human leukemia.

**ACKNOWLEDGEMENTS**

The authors would like to thank following funding agencies: the Fund for Scientific Research Flanders ('FWO Vlaanderen' research projects G.0202.09, G.0869.10N, 3G055013N, 3G056413N to FS; 3GA00113N, 3G065614, G.0C47.13N to PVV and G0B2913N, G037514N, 3G002711 to TT; doctoral grant to AW, postdoctoral grants to IvdW, TT, PVV, and PR; BP is a senior clinical investigator), IWT Vlaanderen (PhD grant to KD); Ghent University (GOA grant 01G01910 to FS), the Cancer Plan from the Federal Public Service of Health (FS), the Children Cancer Fund Ghent (FS) and the Belgian Program of Interuniversity Poles of Attraction (IUAP P7/03 and P7/07). Additional funding was provided by the Cancéropole IDF, the CIT program from the Ligue Contre le Cancer, ERC St Grant Consolidator 311660, and the ANR-10-IBHU-0002 Saint-Louis Institute program (J.S). We also would like to thank Aline Eggermont for excellent technical assistance.

**AUTHORSHIP**

K.D. performed and analyzed experiments and wrote the paper. W.V.L. and M.O. performed bioinformatics on large-scale data sets. J.V.d.M., I.V.d.W., P.R., A.W. and C.E.d.B., performed experiments. J.C., J.S., B.P., N.V.R., T.T. F.S. and P.V.V. designed the experiments, directed research, analyzed data and wrote the paper. All the authors read and edited the manuscript.

**REFERENCES**

1. Ferrando AA, Neuberg DS, Dodge RK, Paietta E, Larson RA, Wiernik PH, et al. Prognostic importance of TLX1 (HOX11) oncogene expression in adults with T-cell acute lymphoblastic leukaemia. Lancet 2004 Feb 14; 363(9408): 535-536.

2. Hawley RG, Fong AZ, Reis MD, Zhang N, Lu M, Hawley TS. Transforming function of the HOX11/TCL3 homeobox gene. Cancer research 1997 Jan 15; 57(2): 337-345.

3. Hawley RG, Fong AZ, Lu M, Hawley TS. The HOX11 homeobox-containing gene of human leukemia immortalizes murine hematopoietic precursors. Oncogene 1994 Jan; 9(1): 1-12.

4. De Keersmaecker K, Real PJ, Gatta GD, Palomero T, Sulis ML, Tosello V, et al. The TLX1 oncogene drives aneuploidy in T cell transformation. Nature medicine 2010 Nov; 16(11): 1321-1327.

5. Rakowski LA, Lehotzky EA, Chiang MY. Transient responses to NOTCH and TLX1/HOX11 inhibition in T-cell acute lymphoblastic leukemia/lymphoma. PloS one 2011; 6(2): e16761.

6. Owens BM, Hawley TS, Spain LM, Kerkel KA, Hawley RG. TLX1/HOX11-mediated disruption of primary thymocyte differentiation prior to the CD4+CD8+ double-positive stage. British journal of haematology 2006 Jan; 132(2): 216-229.

7. Dadi S, Le Noir S, Payet-Bornet D, Lhermitte L, Zacarias-Cabeza J, Bergeron J, et al. TLX homeodomain oncogenes mediate T cell maturation arrest in T-ALL via interaction with ETS1 and suppression of TCRalpha gene expression. Cancer cell 2012 Apr 17; 21(4): 563-576.

8. Weng AP, Ferrando AA, Lee W, Morris JPt, Silverman LB, Sanchez-Irizarry C, et al. Activating mutations of NOTCH1 in human T cell acute lymphoblastic leukemia. Science 2004 Oct 8; 306(5694): 269-271.

9. Wang H, Zang C, Taing L, Arnett KL, Wong YJ, Pear WS, et al. NOTCH1-RBPJ complexes drive target gene expression through dynamic interactions with superenhancers. Proceedings of the National Academy of Sciences of the United States of America 2014 Jan 14; 111(2): 705-710.

10. Wang H, Zou J, Zhao B, Johannsen E, Ashworth T, Wong H, et al. Genome-wide analysis reveals conserved and divergent features of Notch1/RBPJ binding in human and murine T-lymphoblastic leukemia cells. Proceedings of the National Academy of Sciences of the United States of America 2011 Sep 6; 108(36): 14908-14913.

11. Hnisz D, Abraham BJ, Lee TI, Lau A, Saint-Andre V, Sigova AA, et al. Super-enhancers in the control of cell identity and disease. Cell 2013 Nov 7; 155(4): 934-947.

12. Whyte WA, Orlando DA, Hnisz D, Abraham BJ, Lin CY, Kagey MH, et al. Master transcription factors and mediator establish super-enhancers at key cell identity genes. Cell 2013 Apr 11; 153(2): 307-319.

13. Loven J, Hoke HA, Lin CY, Lau A, Orlando DA, Vakoc CR, et al. Selective inhibition of tumor oncogenes by disruption of super-enhancers. Cell 2013 Apr 11; 153(2): 320-334.

14. Asnafi V, Buzyn A, Le Noir S, Baleydier F, Simon A, Beldjord K, et al. NOTCH1/FBXW7 mutation identifies a large subgroup with favorable outcome in adult T-cell acute lymphoblastic leukemia (T-ALL): a Group for Research on Adult Acute Lymphoblastic Leukemia (GRAALL) study. Blood 2009 Apr 23; 113(17): 3918-3924.

15. Clappier E, Gerby B, Sigaux F, Delord M, Touzri F, Hernandez L, et al. Clonal selection in xenografted human T cell acute lymphoblastic leukemia recapitulates gain of malignancy at relapse. The Journal of experimental medicine 2011 Apr 11; 208(4): 653-661.

16. Volders PJ, Helsens K, Wang X, Menten B, Martens L, Gevaert K, et al. LNCipedia: a database for annotated human lncRNA transcript sequences and structures. Nucleic acids research 2013 Jan; 41(Database issue): D246-251.

17. Lee TI, Johnstone SE, Young RA. Chromatin immunoprecipitation and microarray-based analysis of protein location. Nature protocols 2006; 1(2): 729-748.

18. Langmead B, Trapnell C, Pop M, Salzberg SL. Ultrafast and memory-efficient alignment of short DNA sequences to the human genome. Genome biology 2009; 10(3): R25.

19. Feng J, Liu T, Zhang Y. Using MACS to identify peaks from ChIP-Seq data. Current protocols in bioinformatics / editoral board, Andreas D Baxevanis [et al] 2011 Jun; Chapter 2: Unit 2 14.

20. Quinlan AR, Hall IM. BEDTools: a flexible suite of utilities for comparing genomic features. Bioinformatics 2010 Mar 15; 26(6): 841-842.

21. Machanick P, Bailey TL. MEME-ChIP: motif analysis of large DNA datasets. Bioinformatics 2011 Jun 15; 27(12): 1696-1697.

22. Heinz S, Benner C, Spann N, Bertolino E, Lin YC, Laslo P, et al. Simple combinations of lineage-determining transcription factors prime cis-regulatory elements required for macrophage and B cell identities. Molecular cell 2010 May 28; 38(4): 576-589.

23. Van de Walle I, Waegemans E, De Medts J, De Smet G, De Smedt M, Snauwaert S, et al. Specific Notch receptor-ligand interactions control human TCR-alphabeta/gammadelta development by inducing differential Notch signal strength. The Journal of experimental medicine 2013 Apr 8; 210(4): 683-697.

24. Van de Walle I, De Smet G, Gartner M, De Smedt M, Waegemans E, Vandekerckhove B, et al. Jagged2 acts as a Delta-like Notch ligand during early hematopoietic cell fate decisions. Blood 2011 Apr 28; 117(17): 4449-4459.

25. Della Gatta G, Palomero T, Perez-Garcia A, Ambesi-Impiombato A, Bansal M, Carpenter ZW, et al. Reverse engineering of TLX oncogenic transcriptional networks identifies RUNX1 as tumor suppressor in T-ALL. Nature medicine 2012 Mar; 18(3): 436-440.

26. Allen TD, Zhu YX, Hawley TS, Hawley RG. TALE homeoproteins as HOX11-interacting partners in T-cell leukemia. Leukemia & lymphoma 2000 Oct; 39(3-4): 241-256.

27. Milech N, Gottardo NG, Ford J, D'Souza D, Greene WK, Kees UR, et al. MEIS proteins as partners of the TLX1/HOX11 oncoprotein. Leukemia research 2010 Mar; 34(3): 358-363.

28. Filippakopoulos P, Qi J, Picaud S, Shen Y, Smith WB, Fedorov O, et al. Selective inhibition of BET bromodomains. Nature 2010 Dec 23; 468(7327): 1067-1073.

29. Durinck K, Wallaert A, Van de Walle I, Van Loocke W, Volders PJ, Vanhauwaert S, et al. The Notch driven long non-coding RNA repertoire in T-cell acute lymphoblastic leukemia. Haematologica 2014 Oct 24.

30. Herranz D, Ambesi-Impiombato A, Palomero T, Schnell SA, Belver L, Wendorff AA, et al. A NOTCH1-driven MYC enhancer promotes T cell development, transformation and acute lymphoblastic leukemia. Nature medicine 2014 Sep 7.

# Chapter 3: Results

## SUPPLEMENTARY FIGURES

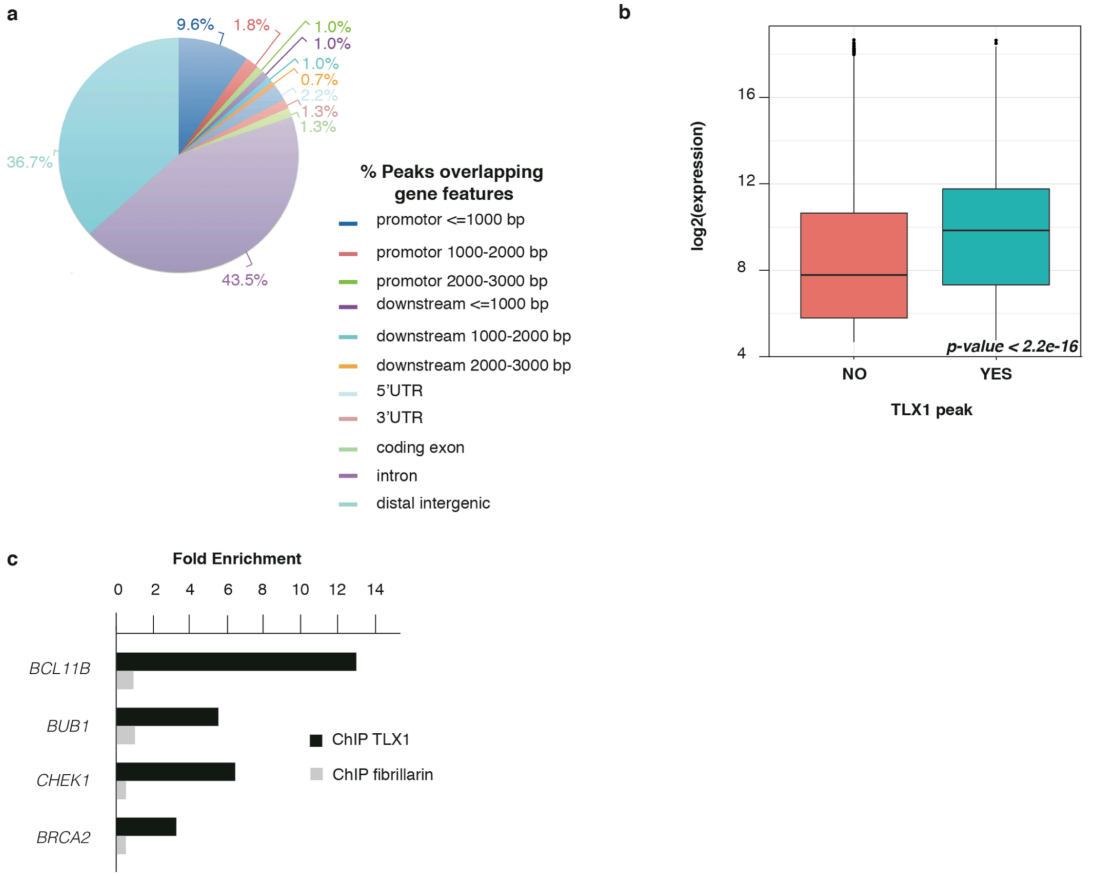


**Supplementary Figure 1**: (**a**) Pie chart representation of the TLX1 ChIP-seq peak distribution overlapping with specific gene features, (**b**) Boxplot showing that binding of TLX1 correlates to higher average gene expression of the target gene, (**c**) ChIP-qPCR assays for *BCL11B*, *BUB1*, *CHEK1* and *BRCA2* validating TLX1 binding as shown by TLX1 ChIP-seq and previously reported by ChIP-chip data[4].

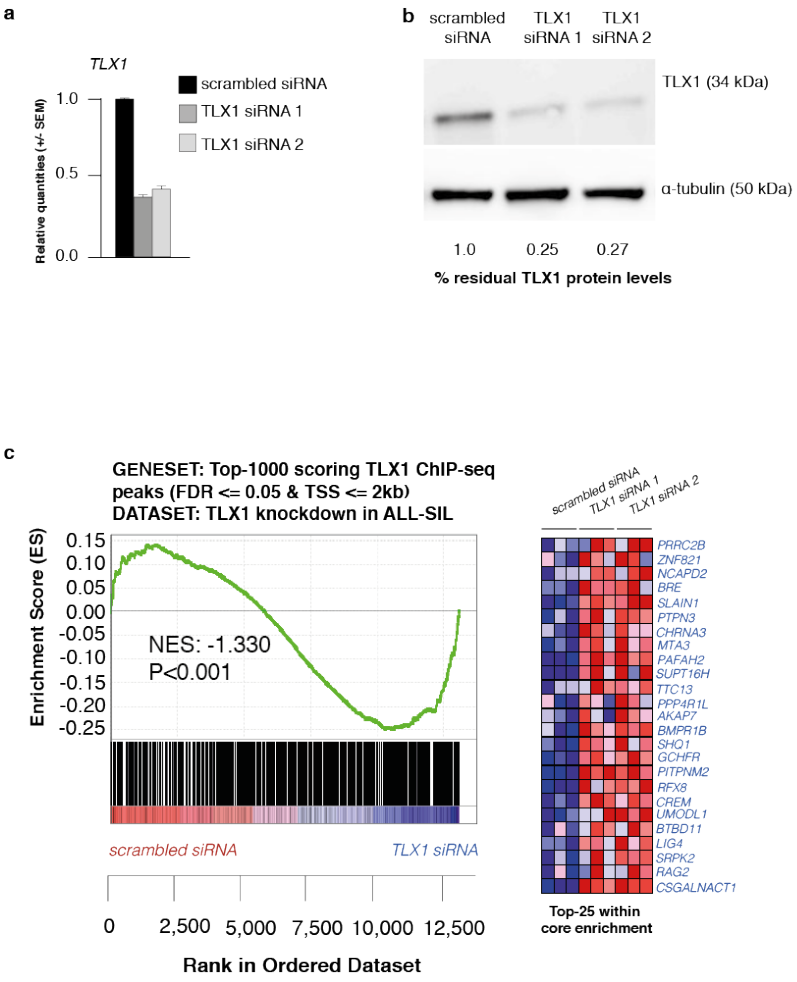


**Supplementary Figure 2**: (**a-b**) Validation of TLX1 knockdown 24h post- electroporation in ALL-SIL cells using 2 different siRNAs over 3 independent replicates (**a**) by RT-qPCR and (**b**) western blot analysis, (**c**) GSEA analysis (using the public gene set database MSigdb c2v3.1) shows significant enrichment of BCL11B target genes within the set of genes up-regulated upon TLX1 knockdown. (**c**) GSEA analysis shows a significant enrichment of the top-1000 scoring (FDR<0.05) TLX1 binding sites in proximity (<=2kb) of the TSS amongst the TLX1 repressed genes in ALL-SIL.

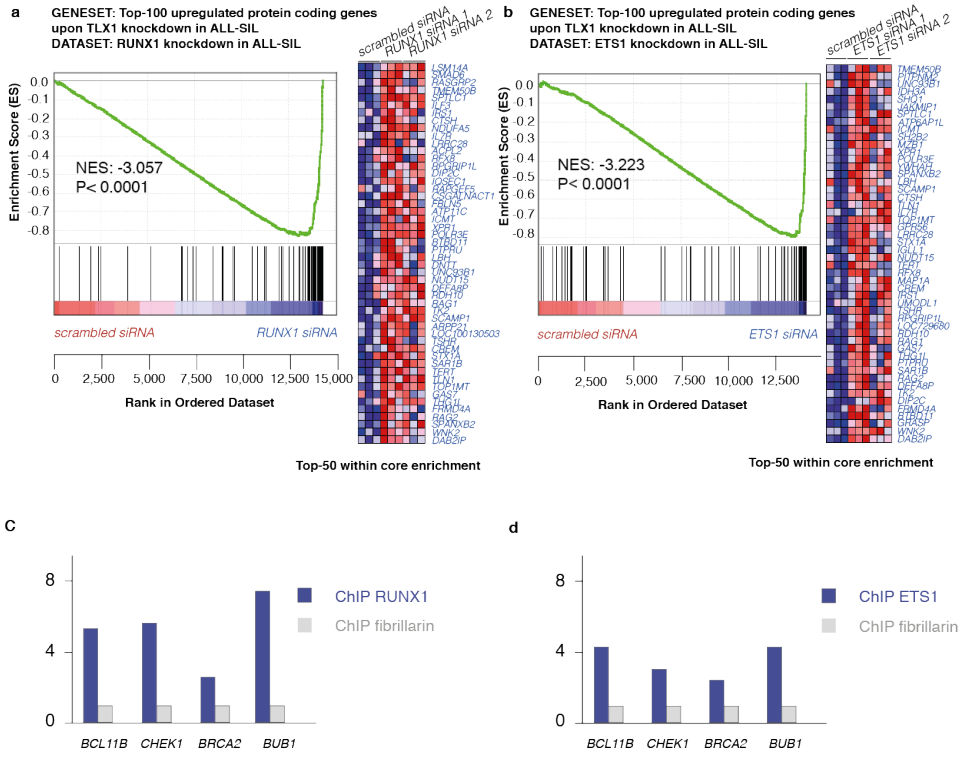


**Supplementary Figure 3**: GSEA analysis shows a significant enrichment of genes repressed by TLX1 in the set of genes up-regulated upon knockdown of RUNX1 (**a**) or ETS1 (**b**) in ALL-SIL cells, (**c**) ChIP-qPCR assay showing significant binding of RUNX1 to validated TLX1 target genes *BCL11B*, *CHEK1*, *BRCA2* and *BUB1*, (**d**) ChIP-qPCR assay showing significant binding of RUNX1 to validated TLX1 target genes *BCL11B*, *CHEK1*, *BRCA2* and *BUB1*.

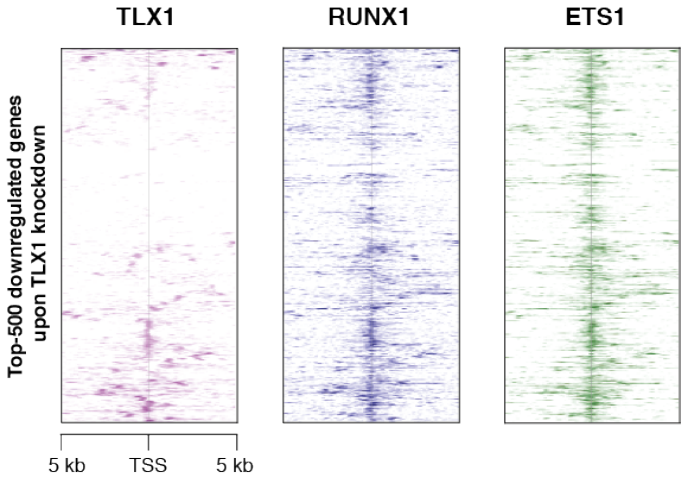


**Supplementary Figure 4:** ChIP-seq heatmap representation is shown for TLX1, RUNX1 and ETS1 ChIP-seq binding profiles within 10 kb from the TSS of the top-500 down-regulated genes upon TLX1 knockdown in ALL-SIL with clustering according to average linkage.

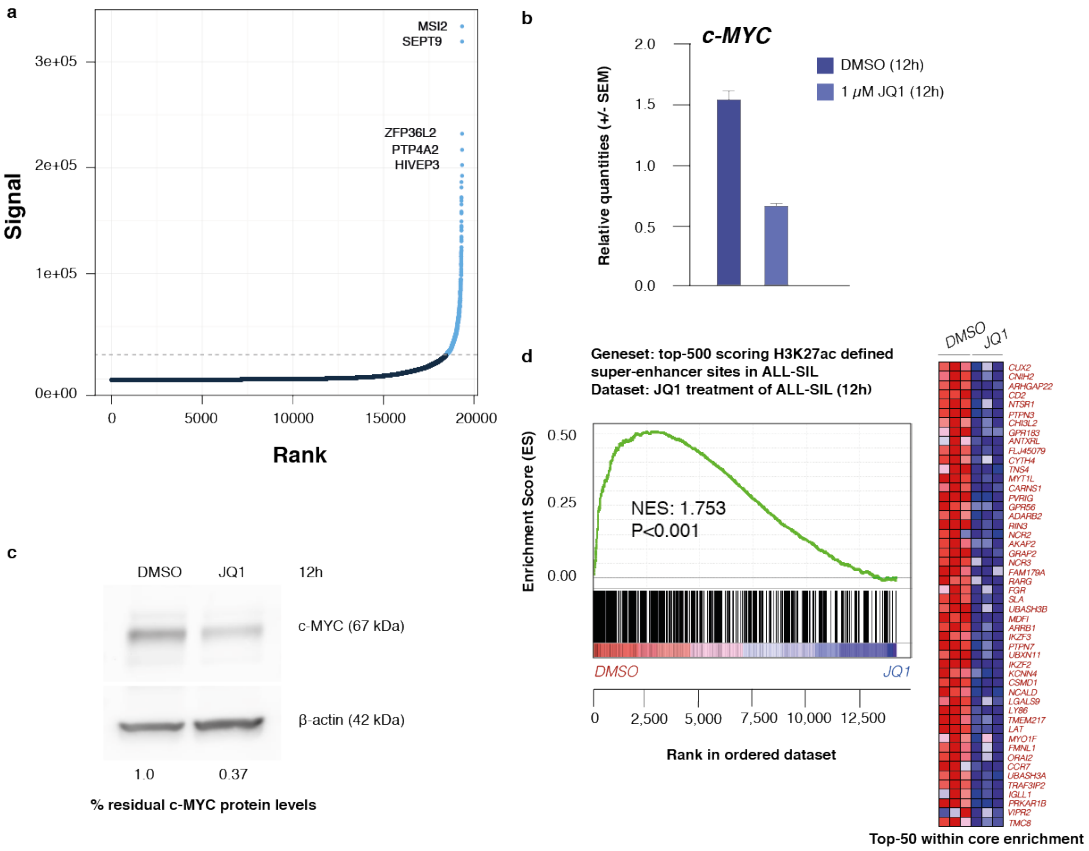


**Supplementary Figure 5**: (**a**) Hockey-stick plot representing the normalized rank and cluster signal of clusters of H3K27ac peaks in ALL-SIL, (**b-c**) Validation of c- MYC down-regulation 12h post-treatment with JQ1 of ALL-SIL cells by (**b**) RT-qPCR and (**c**) western blot analysis, (**d**) GSEA shows significant enrichment of the top-500 scoring H3K27ac defined super-enhancers (shown in in panel (**a**)) within the set of JQ1 downregulated genes.

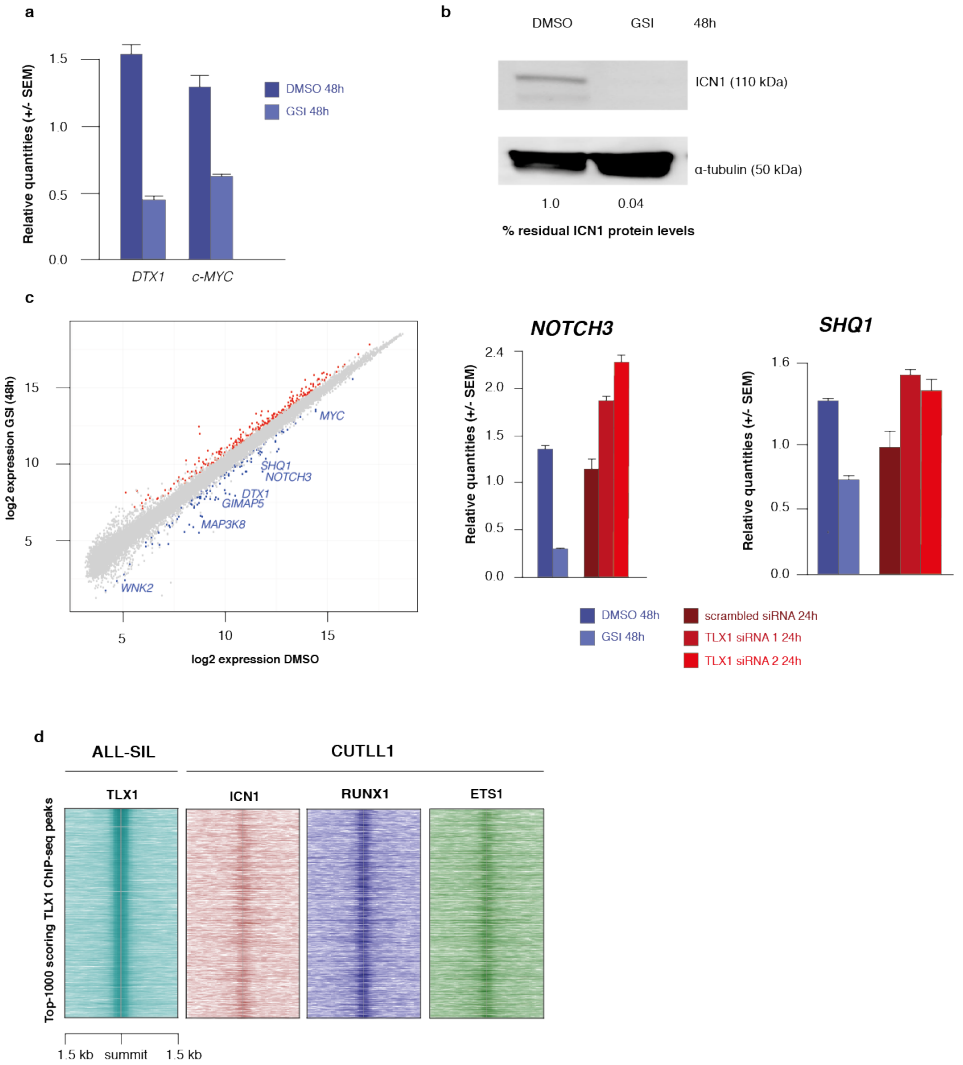


**Supplementary Figure 6**: (**a**) Downregulation of *DTX1* and *c-MYC* expression upon GSI-treatment (48h) of ALL-SIL leukemic cells was validated by RT-qPCR, (**b**) western blot analysis shows down-regulation of ICN1 levels upon GSI treatment of ALL-SIL cells, (**c**) Scatterplot of significantly downregulated genes upon GSI treatment of ALL-SIL cells, (**d**) Heatmap representation of the ChIP-seq overlap of TLX1-ICN1-ETS1-RUNX1 sites across a score-based ranking of TLX1 ChIP-seq signals (shown for top-1000 scoring peaks).

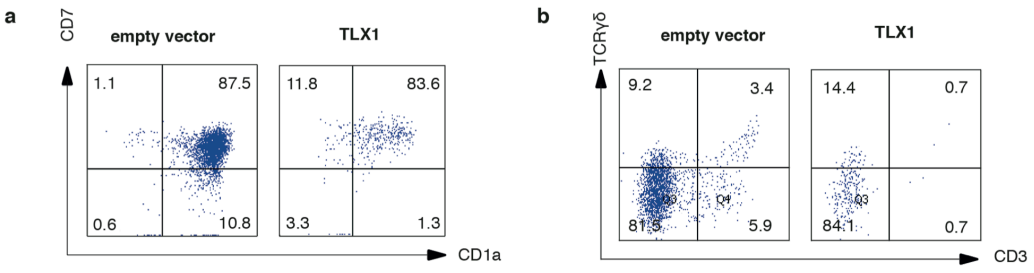


**Supplementary Figure 7**: Flow cytometry profiles of $CD34^+$ progenitor T-cells 12 days post-transduction (representative example shown for three replicates) showing a strong reduction in $CD7^+CD1a^+$ and $CD3^+$ TCRγδ-cells of thymocytes ectopically expressing TLX1.

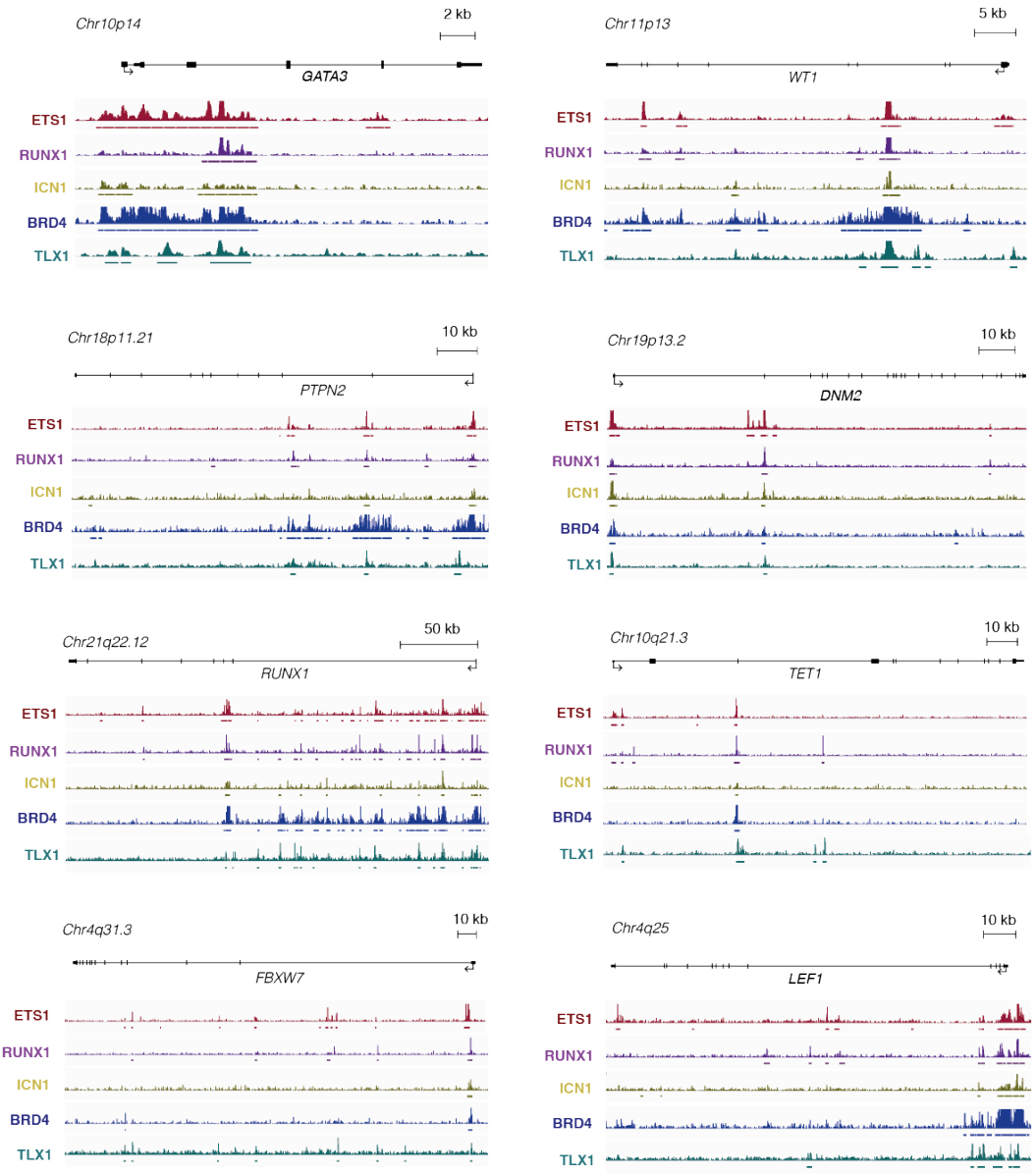


**Supplementary Figure 8**: ChIP-seq profiles of ETS1, RUNX1, ICN1, BRD4 and TLX1 show high positional overlap at tumor suppressor genes mutated and/or deleted in T-ALL (*GATA3*, *WT1*, *PTPN2*, *DNM2*, *RUNX1*, *TET1*, *FBXW7*, *LEF1*)

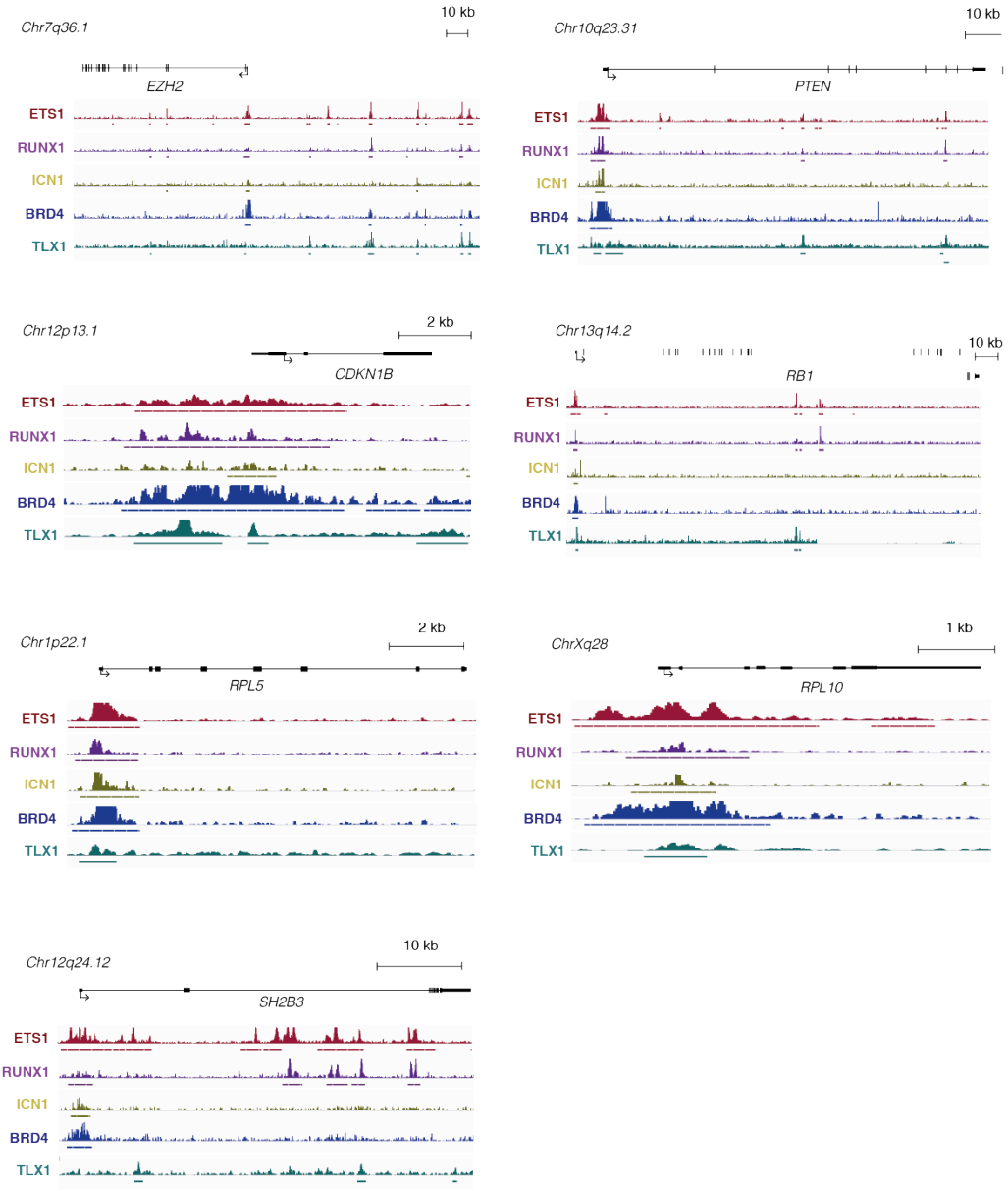


**Supplementary Figure 9**: ChIP-seq profiles of ETS1, RUNX1, ICN1, BRD4 and TLX1 show high positional overlap at tumor suppressor genes mutated and/or deleted in T-ALL (*EZH2*, *PTEN*, *CDKN1B*, *RB1*, *RPL5*, *RPL10*, *SH2B3*).

## Chapter 3: Results

## Chapter 3: Results

## Chapter 3: Results

# PHF6 is a key regulator of normal hematopoiesis

Kaat Durinck*[1], Inge Van de Walle.*[2], Pieter van Vlierberghe[1], Frank Speleman**[1], Tom Taghon**[2]

[1]*Center for Medical Genetics, Ghent University, Ghent, Belgium*

[2]*Department of Clinical Chemistry, Microbiology and Immunology, Ghent University, Ghent, Belgium*

**shared first author, equally contributed to this work*

***shared last author*

**In preparation**

# Chapter 3: Results


## Abstract

Transcriptional control within the mammalian hematopoietic system involves a complex wiring of genetic and epigenetic regulatory networks. In the past decade, studies have shown that an intricate crosstalk between lineage-specific factors and proteins controlling the chromatin architecture is essential in maintaining hematological homeostasis. Analysis of the mutational landscape of various hematological malignancies has shown that key regulators implicated in lineage commitment and differentiation are frequently implicated in leukemic transformation. In T-cell acute lymphoblastic leukemia, the role of various oncogenic and tumor suppressing transcription factors has been extensively investigated. More recently, an exceptional high prevalence of mutations affecting epigenetic modifiers in T-ALL has also been reported. In order to understand the exact contribution of such lesions on normal differentiation and oncogenic transformation, further functional characterization of this subclass of proteins is warranted. *PHF6* is one of these putative epigenetic players for which a high frequency of loss-of-function mutations has been described in T-ALL. Here, we demonstrate a key regulatory role for PHF6 in early hematopoietic differentiation along the T-cell, B-cell, myeloid and NK-cell lineages. In addition, we show that PHF6 is involved in the maintenance of a NOTCH1 gene signature during T-lineage differentiation. In conclusion, this study provides novel insights into the complex (epi-)genetic control of haematopoiesis and provides a basis for further research towards understanding the specific impact of *PHF6* loss-of-function in T-cell leukemogenesis.

# Chapter 3: Results

## Introduction

Hematopoietic cell development is a dynamic and hierarchically structured process, with a functionally diverse set of blood cell types arising from hematopoietic stem cells (HSC) residing within the bone marrow niche. Two major lineages arise from this HSC pool, i.e. the lymphoid lineage differentiating towards T-cells, B-cells and NK-cells and the myeloid lineage comprising macrophages, monocytes and platelets amongst others. The transcriptional programs required for establishment and maintenance of this complex biological system requires an interrelation between lineage-specific transcriptional regulators and more generally acting epigenetic modifiers in a time- and context-dependent fashion. For example, establishment of the T-cell lineage is primarily supported by the action of BCL11B, TCF7 and GATA3, providing guidance for T-cell commitment and differentiation respectively[1]. At the epigenetic level, promoter methylation has an established role in cellular differentiation, including in the hematopoietic compartments. The presence and distribution of this epigenetic modification is regulated by a balanced interplay between DNA methyltransferases (DNMT) such as DNMT3 and the 'ten-eleven' translocation (TET) protein family of demethylases. It has already been shown that amongst others, TET2 is a crucial enzyme in the hematopoietic system[2-4] and the finding of recurrent mutations of *TET2* in various hematological cancers further underscores its importance. Furthermore, enzymes involved in post-translational modification of histone proteins are also frequently deregulated by genomic alterations. Aberrant activity of these epigenetic modifiers leads to alterations in chromatin domain organization and function, contributing to a large extent to malignant transformation of hematopoietic progenitor cells[5-7]. Therefore, strict

regulation of the epigenetic states that govern critical checkpoints and lineage commitment is crucial to ensure normal hematopoiesis and avoid malignant transformation.

Recent studies indeed illustrated, amongst others, the high mutational frequencies in chromatin regulator encoding genes in T-ALL, an aggressive malignant blood disorder that arises from oncogenic transformation of precursor T-cells[8]. In addition to the plethora of activating mutations in well-known driver genes such as *NOTCH1*[9], an important role for epigenetic regulators has now also been established. This includes amongst others '*Enhancer of Zeste Homolog 2*' (*EZH2*), catalytic component of the 'Polycomb Repressor Complex 2' (PRC2) and frequently affected core histone methyltransferase in many cancer types. EZH2 serves as an important switch, balancing self-renewal capacity of hematopoietic stem cells (HSC) with their progression to specific blood cell types[10,11]. Loss-of-function mutations and deletions affecting the genes encoding EZH2 and its interaction partner 'Suppressor of Zeste Homolog 12' (SUZ12) occur in about 25% of T-ALL patients. Furthermore, it has been shown that *PRC2* mutations could further potentiate NOTCH1 driven T-ALL[6].

Like *EZH2*, *PHF6* belongs to one of the top-15 mutated epigenetic modifiers in pediatric cancers, albeit exclusively associated with leukemia. *PHF6* mutations occur in 16% of pediatric and 38% of adult T-ALLs, thus representing one of the most prominent tumor suppressors in this malignancy[12]. Interestingly, in a recent study, PHF6 was also shown to act as an oncogene in B-cell malignancies[13]. Based on these findings, we hypothesized that like EZH2, PHF6 could also act as a key regulator of normal hematopoietic differentiation and lineage commitment. The protein structure of PHF6 is composed of four nuclear localization signals (NLS) that target

the protein to the nucleoplasm and nucleolar compartments[12,14] and two imperfect 'plant homeodomain' (PHD) zinc fingers. The latter are known as methyl lysine binding pockets[15] and thus suggest a role for PHF6 in epigenetic regulation of gene expression. Since no catalytic domains are present in the molecular architecture of PHF6, the protein has a presumed function as an epigenetic reader recruiting other chromatin remodelers and modifier enzymes to its target sites to mediate epigenetic control of gene transcription. Recently, this hypothesis has been supported through the identification of protein-protein interactions between PHF6 and the CHD4, RBBP4 and HDAC1 components of the 'Nucleosome Remodeling and Deacetylase' complex (NurD)[16,17]. Interestingly, the NurD complex has an established role in maintenance of the HSC population and T-lymphopoiesis[18]. Of further interest, *PHF6* mutations were recently also identified in Coffin-Siris syndrome[19], a mental retardation syndrome primarily caused by *de novo* mutations in multiple members of the SWI-SNF complex. This SWI-SNF complex has, like the NurD complex, an established function in hematopoiesis thus suggesting that PHF6 may act in concert with or be part of the SWI-SNF and/or NurD complexes during blood formation.

Here, we provide compelling evidence for a master regulator role for PHF6 during early hematopoietic differentiation along the T-cell, B-cell, myeloid and NK-cell lineages. In the context of T-cell differentiation we provide evidence for a positive regulation of PHF6 on NOTCH1 driven gene expression with additive effects on T-lineage differentiation.

# Chapter 3: Results

## Materials and methods

### Isolation of HPCs

Cord blood (CB), peripheral blood (PBL) and pediatric thymus samples were obtained and used according to the guidelines of the Medical Ethical Commission of Ghent University Hospital (Belgium). After lymphoprep density gradient of CB and PBL, mononuclear cells were isolated and used for further purifications. PBL-derived mononuclear cells were labelled with CD3-FITC and sorted on CD3+ to isolate T-cells. To isolate monocytes, PBL cell populations were depleted in a first round with CD3/CD19/glycophorin (unlabeled antibodies) and in a second round with Dynal beads, followed by staining of the depleted fraction with CD3/CD56/CD19 (FITC) and CD14-PE to sort CD3-CD19-CD56-CD14+ monocytes. For isolation of B- and NK-cells, PBL cells were first depleted for CD3/CD14/glycophorin and after depletion labeled with CD/CD14-FITC, CD19-APC and CD56-PE to sort for CD3-CD14-CD19+ B-cells and CD3-CD14-CD56+ NK-cells. CB-derived $CD34^+$ cells were purified using magnetic activated cell sorting beads (MACS, Miltenyi Biotec). Subsequently, enriched cord blood $CD34^+$ cells were labeled with CD34-PE, CD3-APC, CD14-APC, CD19-APC and CD56-APC to sort $CD34^+Lin^-$ cells with a FACSAriaII (BDIS). Thymocyte subsets were purified as described[22,23,25] and purity of the sorted cells was checked on a FACSCalibur or LSRII (BDIS) and was always >98%.

### Viral constructs and transduction of HPCs

pLKO.1-puroR (SHC002, control shRNA) and TRCN0000020122 (SHC20122, *PHF6* shRNA) lentiviral vectors were purchased from Sigma in which the puromycin resistance gene was replaced with a PCR-amplified EGFP cDNA using BamHI and KpnI

restriction sites. Infectious lentivirus was produced by jetPEI (polyplus transfection™) mediated transfection of the 293FT cell line with either pLKO.1-SHC002-EGFP or pLK0.1-SHC20122-EGFP, in conjuction of the pCMV-VSV-G (envelope) and p8.91 (packaging) constructs. The virus supernatant was harvested 2 and 3 days after transfection. Lentiviral transduction of HPCs was performed on sorted $CD34^+lin^-$ CB cells or $CD34^+$ thymocytes previously cultured in complete IMDM medium containing 10% FCS and supplemented with TPO (20ng/ml), SCF (100ng/ml) and FLT3-L (100ng/ml) or SCF (10ng/ml) and IL-7 (10ng/ml), respectively, for two days (cord blood) or one day (thymocytes). 48 hours after transduction, cells were harvested and sorted for $EGFP^+$ transduced cells.

**OP9 co-cultures and flow cytometry**

Transduced and sorted $CD34^+lin^-EGFP^+$ CB cells or $CD34^+EGFP^+$ thymocytes were seeded in a 24-well plate containing a confluent layer of either control OP9 stromal cells (OP9-GFP) or Delta-like ligand-1 expressing OP9 stromal cells (OP9-DLL1). All co-cultures were performed in α-MEM media (Invitrogen) supplemented with 20% heat-inactivated FCS plus 100 U/ml penicillin, 100 µg/ml streptomycin and 2mM L-glutamin (all from Invitrogen). To induce and support T- and B-cell differentiation, cultures were performed in the presence of SCF, IL-7 and FLT3-L (all 5 ng/ml) on OP9-DLL1 and OP9-GFP, respectively. For the generation of NK cells, co-cultures were supplemented with 10 ng/ml IL-15. For myeloid differentiation, co-cultures were executed with SCF, TPO, FLT3-L (all 20 ng/ml) and G-CSF and GMCSF both 10 ng/ml. Co-cultures were harvested by forceful pipetting at indicated time points. Obtained cell suspensions were blocked with anti-mouse FcRγII/III (clone 2.4.G2) and human

IgG (Fcblock, Miltenyi) to avoid non-specific binding and subsequently stained with combinations of anti-human monoclonal antibodies (BDIS, eBioscience, Biolegend and Miltenyi). Cells were examined for the expression of cell surface markers on a LSRII (BDIS).

**Gene expression profiling**

RNA samples from control and PHF6 shRNA transduced $CD34^+$ thymocytes of OP9-GFP and OP9-DLL1 co-cultures were harvested 72h post-transduction and profiled on a custom designed Agilent micro-array covering all protein coding genes (33,128 mRNA probes, Human Sureprint G3 8x60k micro-arrays (Agilent)) and 12,000 lncRNAs (23,042 unique lncRNA probes). For transduction on OP9-GFP co-cultures, 3 independent samples were profiled and for OP9-DLL1 co-cultures 4 independent samples. Expression data were normalized using the VSN-package (Bioconductor release 2.12) in R. Differential expression analysis was performed in R using limma. Public datasets (GSE24759) were normalized using the Affy-package (Bioconductor release 2.12) in R.

**Gene Set Enrichment Analysis**

Gene Set Enrichment Analysis (GSEA)[20] was used to score our genesets compiled from the publically available gene expression data[21]. To compile the genesets used in this study, the p-value (<0.05) was consistently used as the major cut-off to define a gene signature.

## Results

**PHF6 is an essential regulator of normal thymopoiesis through reduction of Notch activity during human T cell development.**

Given the high incidence of *PHF6* inactivating mutations in T-ALL, we first focused on the role of PHF6 during normal human T-cell development. To this end, PHF6 shRNA mediated knockdown in Jurkat T-ALL cells was first optimized prior to subsequent further testing on the *in vitro* OP9-DLL1 co-culture system. A knockdown level for PHF6 of >90% at the protein level could be obtained (**Fig. 1A**). Next, we initiated OP9-DLL1 co-cultures with control shRNA or PHF6 shRNA transduced human $CD34^+$ thymocytes as these are the direct precursors of human T-cells. Remarkably, knockdown of PHF6 significantly accelerated differentiation towards the $CD4^+/CD8^+$ double positive (DP) stage (**Fig. 1B and 1C**). Most notably, a similar phenotypic effect was previously observed upon reduction of Notch activation in the same cellular model system, suggesting that PHF6 and NOTCH1 might be functionally interconnected in the context of early T-cell differentiation[22,23]. To further elucidate this functional interplay, we used 'Gene Set Enrichment Analysis' (GSEA) to compare a gene signature related to active NOTCH1 signaling in CUTLL1 cells[24] with the gene expression dataset obtained upon PHF6 knockdown in Jurkat T-ALL cells. This analysis revealed a significant overlap (NES: 1.533, p-value<0.001) between NOTCH1-induced transcripts and genes positively regulated by PHF6 (**Fig. 1D**), supporting our phenotypic readout on OP9-DLL1 co-cultures and in line with recent work that also described a putative link between PHF6 and transcriptional regulation of *NOTCH1*[13].

To further explore the putative interaction between PHF6 and NOTCH1, we modulated both factors in human $CD34^+$ thymic precursors using stable PHF6 knockdown and pharmacological inhibition of NOTCH1 using a gamma-secretase inhibitor (GSI, DAPT) compound and followed T-cell differentiation using OP9-DLL4 co-cultures (closely resembles DLL1 function)[25]. In line with our initial results using OP9-DLL1 co-cultures, thymocytes with PHF6 deficiency progressed significantly faster towards the DP stage cells as compared to control cells, similar to what we observed for control transduced cells that are exposed to GSI (**Fig. 1E** (6 days of co-culture) and **Fig. 1G** (18 days of co-culture)). Interestingly, combined reduction of PHF6 expression (shRNA) and Notch pathway activity (GSI) further increased this accelerated differentiation and resulted in the highest frequency of DP cells as well as increased absolute numbers of DP thymocytes at the earliest time point (**Fig. 1F**). At later timepoints, the absolute DP cell counts between the GSI fractions with or without loss of PHF6 were comparable (**Fig. 1H**), consistent with the absolute requirement for Notch in thymocyte proliferation[26,27].

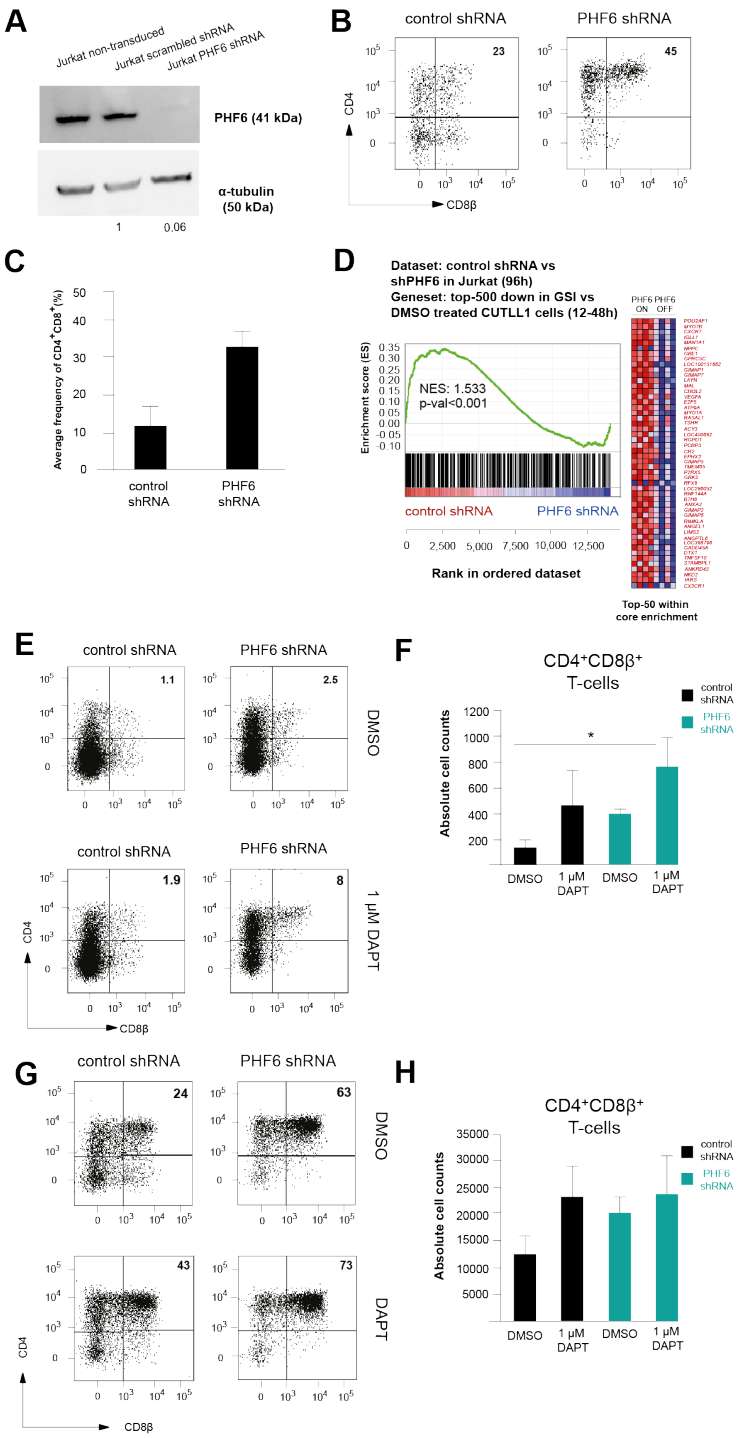


**Figure 1: PHF6 knockdown in cord blood CD34$^+$ progenitors leads to accelerated CD4$^+$CD8$^+$ development in concert with NOTCH1.** (**A**) Validation of stable shRNA-mediated knockdown in Jurkat T-ALL cells by western blot analysis, (**B**) PHF6 deficiency leads to accelerated (increased frequency) CD4$^+$CD8$^+$ (DP) stage development of CD34$^+$ thymocyte progenitor cells (also in absolute counts (**C**)), (**D**) Gene Set Enrichment Analysis reveals significant overlap between genes downregulated upon PHF6 knockdown in Jurkat cells and genes downregulated upon pharmacological inhibition of NOTCH1 signaling by gamma-secretase inhibitor (GSI, DAPT) treatment in CUTLL1 T-ALL cells, (**E-H**) PHF6 knockdown or GSI-treatment of cord blood CD34$^+$ progenitors induces a similar increased progression of CD34$^+$ precursor cells towards the DP (CD4$^+$CD8$^+$) T-cell stage, with combination of both showing an additive effect in absolute counts at an early timepoint (6 days) during co-culture analysis (**E,F**) but no longer at a later timepoint of co-culture (18 days) (**G,H**).

Consistent with the DP phenotype, loss of PHF6 skewed differentiation of human T-cell precursors towards TCR-αβ T cells (**Fig. 2A and 2B**) at the expense of TCR-γδ T-cell lineage development (**Fig. 2C and 2D**). This differential PHF6 dependency between both T-cell lineages is consistent with their Notch dependent development[22,23], further supporting a functional cooperation between NOTCH1 and PHF6 during normal T-cell development.

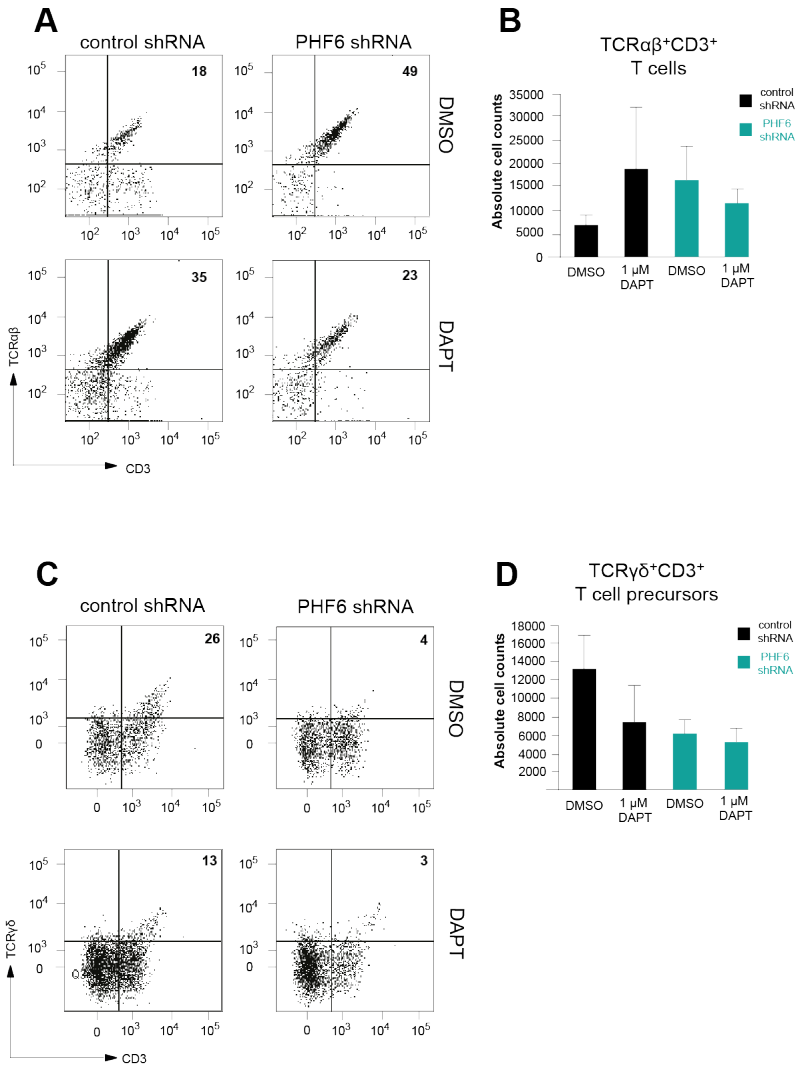


**Figure 2: PHF6 knockdown in cord blood CD34$^+$ progenitors leads to skewed T-cell lineage development towards the TCR-αβ lineage at expense of TCR-γδ lineage development.** (**A-B**) PHF6 knockdown in cord blood CD34$^+$ progenitor cells leads to increased/skewed TCR-αβ lineage commitment, (**C-D**) at the expense of γδ T-cell lineage commitment with a functional cooperative effect with NOTCH1 inhibition.

To further explore the transcriptional changes that are mediated by PHF6 in both normal and malignant T-cell development we compared gene expression profiles associated with shRNA mediated knockdown of PHF6 in Jurkat T-ALL cells and $CD34^+$ cultured on OP9-DLL1. For the assembly of the geneset of this GSEA analysis, the p-value (<0.05) was used as a cut-off to identify the signature. The gene profiles induced upon PHF6 depletion in both *in vitro* model systems appeared very robust and showed a significant overlap as visualized by GSEA, further confirming that PHF6 controls overlapping gene regulatory programs in both T-ALL lymphoblasts and normal immature T-cells (**Fig. 3A and 3B**). Consistent with its role in TCR-γδ T-cell development, *ETV5* was identified as one of the common top-candidate genes that was downregulated upon PHF6 knockdown (**Fig. 3A**). In contrast, the αβ-lineage essential transcription factor *RORC* is upregulated upon PHF6 knockdown (**Fig. 3B**), indicating that PHF6 affects the expression of key regulators of TCR-αβ and – γδ T cell development.

Unexpectedly, PHF6 knockdown also resulted in upregulation of *NOTCH3* and *IL7R*, two Notch target genes that are implicated in preferentially driving TCR-γδ T cell development[23,28,29], in keeping with anti-correlation between *PHF6* and *IL7R* expression during discrete stages of T-cell development and thus revealing Notch-independent regulatory roles for PHF6 (**Fig. 3C**). Further experiments to unravel the broader gene regulatory control of PHF6 during normal hematopoiesis and in particular the role of PHF6 regulation of *IL7R* expression are currently ongoing.

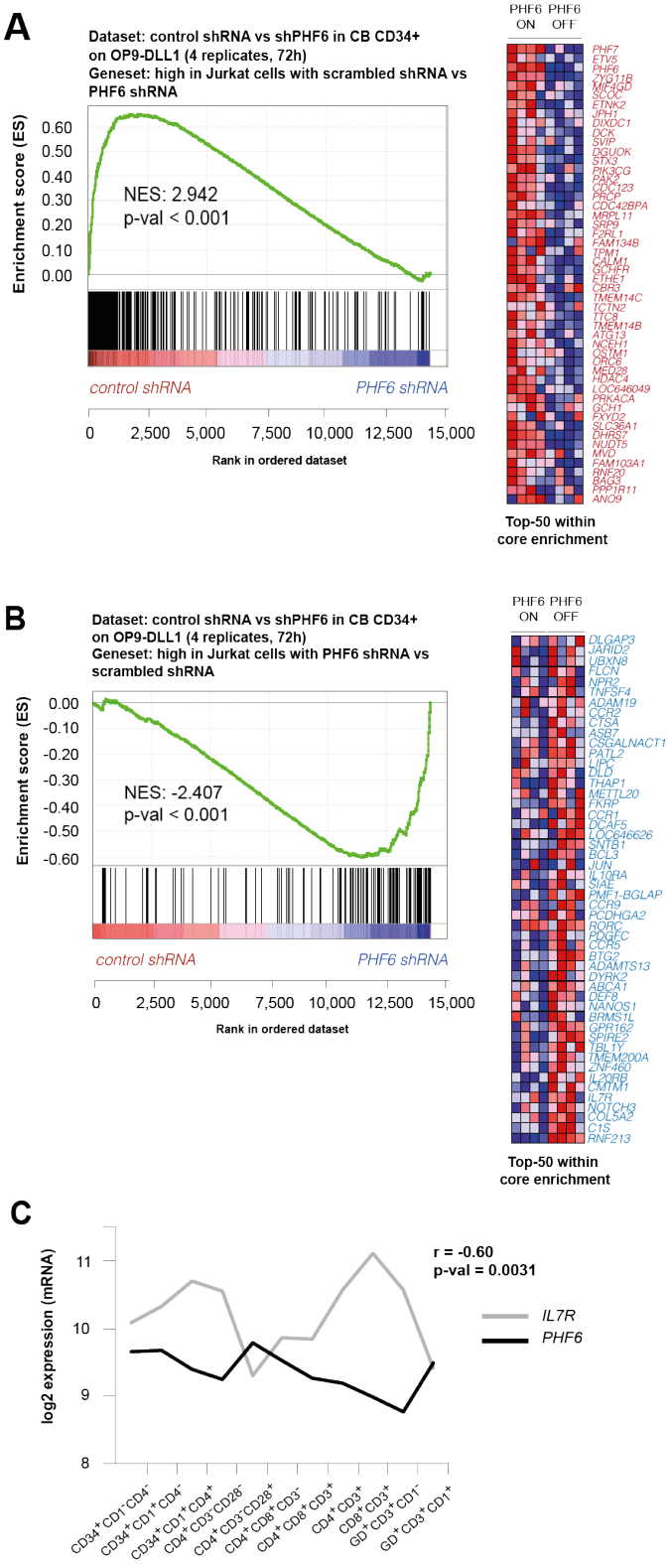


**Figure 3: Identification of key PHF6 downstream target genes in thymocyte progenitor cells**. Gene Set Enrichment Analysis reveals a significant overlap between genes down- (**A**) and upregulated (**B**) upon PHF6 knockdown in Jurkat and $CD34^+$ cord blood progenitor cells, **(C)** *PHF6* and *IL7R* mRNA expression dynamics are anti-correlated across the different T-cell subsets that can be discriminated during normal human T-cell development.

## Chapter 3: Results

### PHF6 is implicated in control of multiple hematopoietic cell lineage gene regulatory programs

In view of the literature data pointing at a role of PHF6 in B-cell oncogenesis[13], we hypothesized that PHF6 could play a broader role in hematopoietic lineage decisions. To investigate this, we measured *PHF6* gene expression levels in subsets of various human blood cell types (**Fig. 4**). Expression was observed in all tested samples with prominently high expression levels in $CD34^+$ HPCs and $CD19^+$ B cells and lower expression in $CD3^+$ T cells. $CD56^+$ NK cells and $CD14^+$ monocyte cells displayed the lowest *PHF6* expression levels.

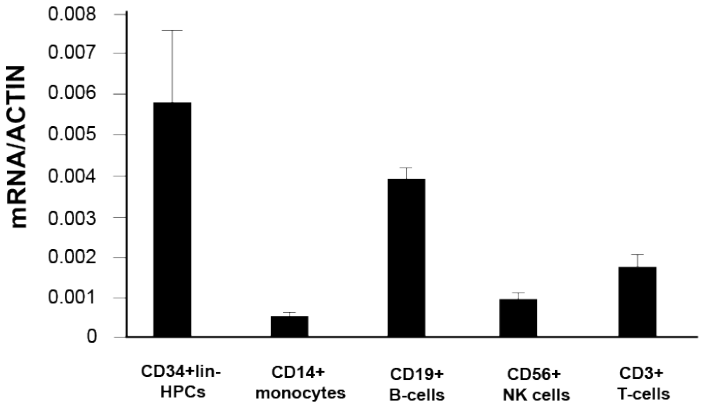


**Figure 4: *PHF6* expression levels across different types of hematopoietic cell lineages.** *PHF6* expression levels are depicted in hematopoietic progenitor cells (HPCs), $CD14^+$ monocytes, $CD19^+$ B-cells, $CD56^+$ NK-cells and $CD3^+$ T-cells.

In a next step, PHF6 knockdown was executed in $CD34^+lin^-$ cord blood (CB) hematopoietic progenitor cells (HPCs) and the impact of PHF6 modulation on human B-cell, NK-cell and myeloid lineage development was evaluated using the well-established OP9 co-cultures[25].

In OP9-GFP cultures conditions that permit B-cell development, we observed a significant increase in both the frequency and absolute number of $CD19^{+}HLA\text{-}DR^{+}$ B-cells upon PHF6 knockdown compared to the control condition (**Fig. 5A and 5B**).

To study the role of PHF6 in human NK-cell differentiation, we performed OP9-GFP co-cultures to which the critical NK-lineage cytokine IL-15 was added, in addition to SCF and FLT3-L. Knockdown of PHF6 significantly decreased the generation of $CD56^{+}CD5^{-}$ NK-cells from $CD34^{+}$ CB HPCs compared to control transduced cells (**Fig. 5C and 5D**), indicating that PHF6 expression is required for human NK-cell development.

Finally, to study the requirement for PHF6 during myeloid lineage differentiation, we performed OP9-GFP stromal co-cultures with control or PHF6 shRNA transduced $CD34^{+}$ HPCs in the presence of myeloid growth factors[25,30]. Under these conditions, downregulation of PHF6 induced a consistent increase in the frequency of $CD14^{+}CD4^{+}$ monocytes (**Fig. 5E**), but without increase in absolute monocyte cell numbers (**Fig. 5F**). Rather, a small, but not significant reduction in the absolute number of monocytes was observed after two weeks of co-culture upon PHF6 knockdown compared to the control co-cultures. Thus, in line with the rare occurrence of *PHF6* mutations in myeloid malignancies, only minor changes in myeloid lineage differentiation were observed upon PHF6 knockdown.

To better understand these alterations in hematopoietic lineage differentiation, gene expression profiling was performed after short-term shRNA-mediated knockdown (72h) of PHF6 in $CD34^{+}$ progenitor cells cultured on OP9-GFP. These expression signatures were subsequently compared to publically available transcriptional profiles of sorted populations of different human hematopoietic cell

types[21] (GSE24759). Consistent with the preferential differentiation towards B-lymphocytes, B-cell lineage genes were significant enriched upon PHF6 knockdown when compared to myeloid (**Fig. 5G**) or NK-cell signatures (**Fig. 5H**). Thus, loss of PHF6 in human HPCs alters downstream gene expression and consequently, hematopoietic lineage differentiation.

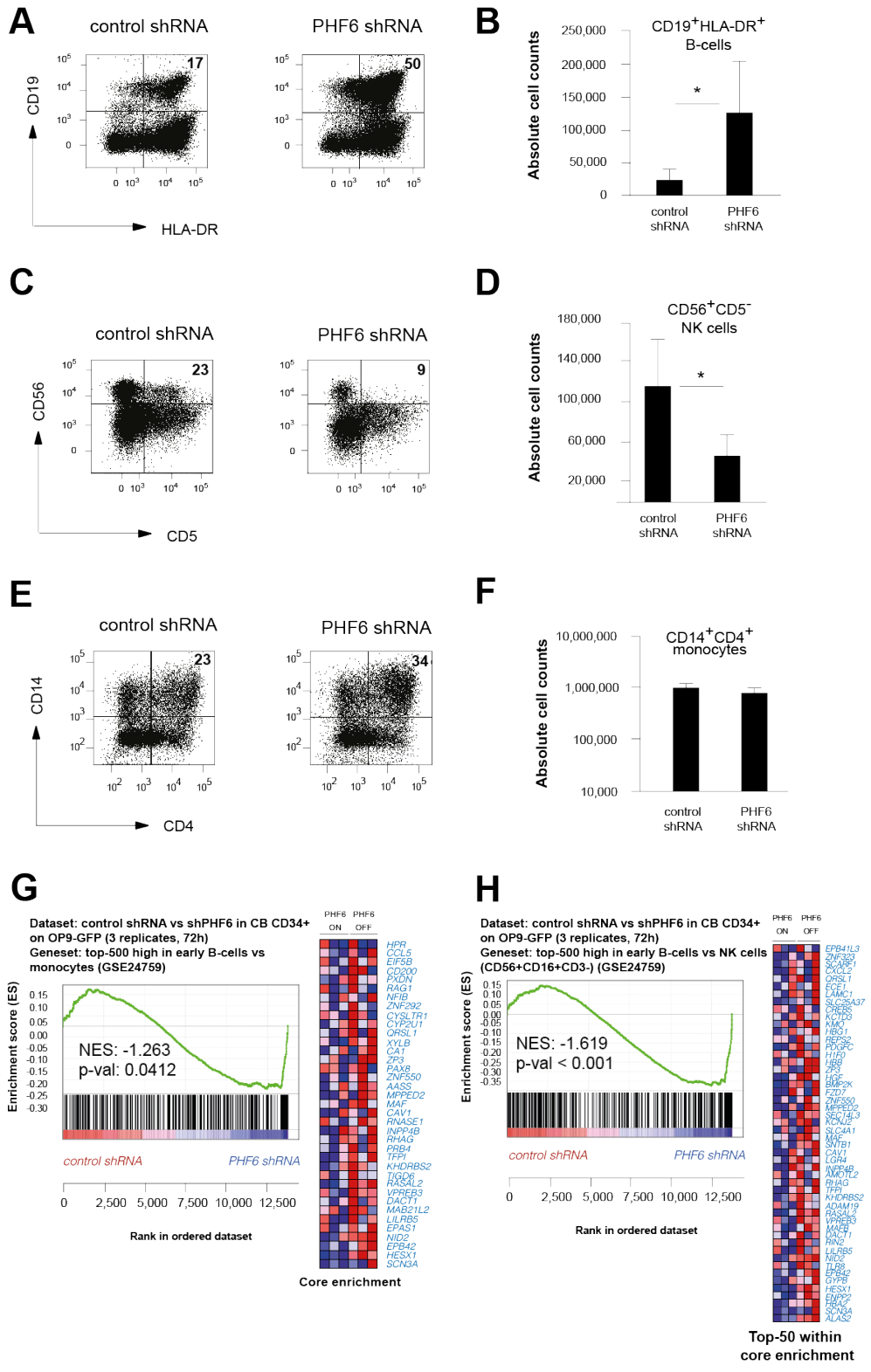


**Figure 5: PHF6 deficiency strongly impacts on the development of different hematopoietic lineage types.** PHF6 knockdown in CD34$^{+}$ cord blood progenitor cells cultured on an OP9-GFP stromal feeder layer significantly enhances in comparison to control cells the development of B-cells (**A-B**), reduces the number of developing NK-cells (**C-D**), without significantly altering monocyte development (**E-F**), (**G-H**) Gene Set Enrichment Analysis (GSEA) shows significant enrichment of a B-cell signature in PHF6 knockdown cells compared to controls at the expense of a monocyte (**G**) or NK-cell (**H**) gene signature.

## Discussion

This study for the first time provides a comprehensive view on the role of PHF6 in control of multiple hematopoietic cell lineage decisions. While our data illustrate a broad involvement across various hematopoietic cell types, we were able to dissect in more detail the regulated transcriptional profile and underlying mechanistic basis of PHF6 driven lineage control during thymopoiesis. Importantly, robust regulation of two key transcription factors *ETV5* and *RORC* was demonstrated in addition to a crosstalk with Notch pathway activity, providing an explanation for the observed effects on perturbed T-cell maturation upon PHF6 knockdown. Interestingly, gene expression profiling also revealed PHF6 controlled down regulation of *NOTCH3* and *IL7R*, both essential factors in T-cell development that are associated with TCR-γδ T-cell development. The exact importance of this observation in the context of thymopoiesis remains to be determined and is currently under investigation. Since the increased expression of both genes upon PHF6 knockdown is inconsistent with the observed loss of TCR-γδ T cell development and accelerated differentiation into DP αβ-lineage cells, we are currently testing the hypothesis that signaling incompetent IL7Rα homodimers are formed that limit IL7 levels within the cultures[31], thereby causing these differentiation effects that effectively resemble loss of IL7R signaling[22]. In addition, ChIP-sequencing to determine the genome-wide PHF6 binding profile and chromatin mark distribution at PHF6 binding sites (as well as ATAC-sequencing) should shed a more detailed light onto the mode-of-action of PHF6 as an epigenetic modulator of gene expression. Also, the role of PHF6 in T-ALL formation is largely unexplained. Interestingly, both *ETV5* and *IL7R* are known oncogenes in cancer and the impact of altered expression levels for both genes upon

PHF6 knockdown remains to be investigated. Of particular interest, *IL7R* has been described as a *bona fide* oncogene in T-ALL and activating mutations driving JAK/STAT signaling have been recurrently described. Moreover, the particular enrichment of *PHF6* mutations in TLX1 driven T-ALLs is intriguing. The observation of repression of *IL7R* expression by both TLX1[32] and PHF6 (this study) possibly provides a strong selective pressure towards *PHF6* loss-of-function mutations in TLX1-driven leukemia (see also **paper 3**, **Chapter 3, Part 1**).

## Author contributions

KD and IvdW equally contributed to this work, both for the execution of the experiments and writing of the manuscript. FS, PV and TT wrote the manuscript and supervised the experiments performed.

**References**

1. Rothenberg, E.V. Transcriptional drivers of the T-cell lineage program. *Curr Opin Immunol* **24**, 132-138 (2012).

2. Solary, E., Bernard, O.A., Tefferi, A., Fuks, F. & Vainchenker, W. The Ten-Eleven Translocation-2 (TET2) gene in hematopoiesis and hematopoietic diseases. *Leukemia* **28**, 485-496 (2014).

3. Haladyna, J.N., Yamauchi, T., Neff, T. & Bernt, K.M. Epigenetic modifiers in normal and malignant hematopoiesis. *Epigenomics* **7**, 301-320 (2015).

4. Nakajima, H. & Kunimoto, H. TET2 as an epigenetic master regulator for normal and malignant hematopoiesis. *Cancer Sci* **105**, 1093-1099 (2014).

5. Lafave, L.M. & Levine, R.L. Mining the epigenetic landscape in ALL. *Nat Genet* **45**, 1269-1270 (2013).

6. Ntziachristos, P*., et al.* Genetic inactivation of the polycomb repressive complex 2 in T cell acute lymphoblastic leukemia. *Nat Med* **18**, 298-301 (2012).

7. Van der Meulen, J*., et al.* The H3K27me3 demethylase UTX is a gender-specific tumor suppressor in T-cell acute lymphoblastic leukemia. *Blood* **125**, 13-21 (2015).

8. Huether, R*., et al.* The landscape of somatic mutations in epigenetic regulators across 1,000 paediatric cancer genomes. *Nat Commun* **5**, 3630 (2014).

9. Weng, A.P*., et al.* Activating mutations of NOTCH1 in human T cell acute lymphoblastic leukemia. *Science* **306**, 269-271 (2004).

10. Lund, K., Adams, P.D. & Copland, M. EZH2 in normal and malignant hematopoiesis. *Leukemia* **28**, 44-49 (2014).

11. Lee, S.C*., et al.* Polycomb repressive complex 2 component Suz12 is required for hematopoietic stem cell function and lymphopoiesis. *Blood* **126**, 167-175 (2015).

12. Van Vlierberghe, P*., et al.* PHF6 mutations in T-cell acute lymphoblastic leukemia. *Nat Genet* **42**, 338-342 (2010).

13. Meacham, C.E*., et al.* A genome-scale in vivo loss-of-function screen identifies Phf6 as a lineage-specific regulator of leukemia cell growth. *Genes Dev* **29**, 483-488 (2015).

14. Lower, K.M*., et al.* Mutations in PHF6 are associated with Borjeson-Forssman-Lehmann syndrome. *Nat Genet* **32**, 661-665 (2002).

15. Mellor, J. It takes a PHD to read the histone code. *Cell* **126**, 22-24 (2006).

16. Todd, M.A. & Picketts, D.J. PHF6 interacts with the nucleosome remodeling and deacetylation (NuRD) complex. *J Proteome Res* **11**, 4326-4337 (2012).

17. Liu, Z*., et al.* Structural basis of plant homeodomain finger 6 (PHF6) recognition by the retinoblastoma binding protein 4 (RBBP4) component of the nucleosome remodeling and deacetylase (NuRD) complex. *J Biol Chem* **290**, 6630-6638 (2015).

18. Ramirez, J. & Hagman, J. The Mi-2/NuRD complex: a critical epigenetic regulator of hematopoietic development, differentiation and cancer. *Epigenetics* **4**, 532-536 (2009).

19. Wieczorek, D*., et al.* A comprehensive molecular study on Coffin-Siris and Nicolaides-Baraitser syndromes identifies a broad molecular and clinical spectrum converging on altered chromatin remodeling. *Hum Mol Genet* **22**, 5121-5135 (2013).

20. Subramanian, A*., et al.* Gene set enrichment analysis: a knowledge-based approach for interpreting genome-wide expression profiles. *Proc Natl Acad Sci U S A* **102**, 15545-15550 (2005).

21. Novershtern, N*., et al.* Densely interconnected transcriptional circuits control cell states in human hematopoiesis. *Cell* **144**, 296-309 (2011).

22. Van de Walle, I*., et al.* An early decrease in Notch activation is required for human TCR-alphabeta lineage differentiation at the expense of TCR-gammadelta T cells. *Blood* **113**, 2988-2998 (2009).

23. Van de Walle, I*., et al.* Specific Notch receptor-ligand interactions control human TCR-alphabeta/gammadelta development by inducing differential Notch signal strength. *J Exp Med* **210**, 683-697 (2013).

24. Durinck, K*., et al.* The Notch driven long non-coding RNA repertoire in T-cell acute lymphoblastic leukemia. *Haematologica* **99**, 1808-1816 (2014).

25. Van de Walle, I*., et al.* Jagged2 acts as a Delta-like Notch ligand during early hematopoietic cell fate decisions. *Blood* **117**, 4449-4459 (2011).

26. Garcia-Peydro, M., de Yebenes, V.G. & Toribio, M.L. Notch1 and IL-7 receptor interplay maintains proliferation of human thymic progenitors while suppressing non-T cell fates. *J Immunol* **177**, 3711-3720 (2006).

27. Taghon, T*., et al.* Notch signaling is required for proliferation but not for differentiation at a well-defined beta-selection checkpoint during human T-cell development. *Blood* **113**, 3254-3263 (2009).

28. Ye, S.K.*, et al.* Induction of germline transcription in the TCRgamma locus by Stat5: implications for accessibility control by the IL-7 receptor. *Immunity* **11**, 213-223 (1999).

29. Huang, J., Durum, S.K. & Muegge, K. Cutting edge: histone acetylation and recombination at the TCR gamma locus follows IL-7 induction. *J Immunol* **167**, 6073-6077 (2001).

30. Klinakis, A.*, et al.* A novel tumour-suppressor function for the Notch pathway in myeloid leukaemia. *Nature* **473**, 230-233 (2011).

31. McElroy, C.A.*, et al.* Structural reorganization of the interleukin-7 signaling complex. *Proc Natl Acad Sci U S A* **109**, 2503-2508 (2012).

32. Durinck, K.*, et al.* Characterization of the genome-wide TLX1 binding profile in T-cell acute lymphoblastic leukemia. *Leukemia* **29**, 2317-2327 (2015).

## Chapter 3: Results

# Functional dissection of PHF6 as a key epigenetic regulator in TLX1-driven T-ALL

Durinck K[1], Van de Walle I[2], Van Loocke W[1], Van der Meulen J[1], Matthijssens F[1], Eggermont E[1], Loontiens S[1], Poppe B[1], Van Roy N[1], Rondou P[1], De Bock C[3], Cools J[3], Taghon T[2], Van Vlierberghe P[1], Speleman F[1].

*[1]Center for Medical Genetics, Ghent University, Ghent, Belgium*

*[2]Department of Clinical Chemistry, Microbiology and Immunology, Ghent University, Ghent, Belgium*

*[3]Laboratory for the Molecular Biology of Leukemia, Center for Human Genetics, KU Leuven and Center for the Biology of Disease, VIB, Leuven, Belgium*

**In preparation**

# Chapter 3: Results


**ABSTRACT**

T-cell acute lymphoblastic leukemia (T-ALL) is a genetically heterogeneous disease with genetic subgroups being marked by particular driver oncogenes. In addition, mutations are present in various classes of genes, many of which occur across the defined genetic subsets such as *NOTCH1*. More recently, a remarkable high frequency of somatic mutations affecting epigenetic regulators was observed including *EZH2*, *UTX*, *JMJD3* and *PHF6*. The latter, a presumed epigenetic reader, was found mutated in 16% of pediatric and 38% of adult T-ALL patients with highest frequencies observed in the *TLX1/3* genetic subgroup. So far, the functional role of PHF6 in malignant T-cell transformation has not been resolved. To this end, we performed a functional landscaping of the transcriptional regulatory networks under control of PHF6 in T-ALL lymphoblasts. First, we provide evidence for loss of *PHF6* as a crucial cooperative event in TLX1-driven leukemia with opposing roles in regulation of expression of the IL7R receptor, playing an essential role in T-cell maturation and acting as a *bona fide* oncogene in T-ALL. Second, we provide data supporting a putative functional connection between PHF6 and the NurD and SWI-SNF chromatin modifying protein complexes. Our study paves the way for further novel therapeutic strategies targeting JAK-STAT signaling in *PHF6* mutated T-ALL and investigations unraveling the functional interactions with NurD and SWI-SNF protein complexes in epigenetic control of gene regulatory networks controlling thymocyte differentiation and malignant transformation.

# Chapter 3: Results

## INTRODUCTION

T-cell acute lymphoblastic leukemia (T-ALL) results from malignant transformation of immature thymocytes. T-ALL formation is characterized by the progressive accumulation of various genetic and epigenetic defects, therefore representing a paradigm for multistep cancer formation. Recent next-generation sequencing efforts have shown that genes encoding epigenetic regulatory proteins constitute a significant portion of the genes mutated in various cancer types[1]. Also in T-ALL, there is an emerging prominent role for the epigenome and its regulators to participate in malignant transformation[2], as recently illustrated by the discovery of the PCR2 complex component *EZH2* as a novel tumor suppressor[3].

We previously identified inactivating mutations and deletions in the *PHF6* gene in 16% of pediatric and 38% of adult T-ALL cases[4]. Notably, *PHF6* mutations were enriched in *TLX1* and *TLX3*-driven T-ALL. In addition, *PHF6* mutations were also found, although at low frequency, in acute myeloid leukemia[5] and hepatocellular carcinoma[6], marking the broader role of PHF6 in tumorigenesis. Constitutional mutations in *PHF6* were previously described in patients with Börjeson-Forssman-Lehmann syndrome (BFLS), an X-linked mental retardation disorder[7]. Interestingly, a case study by Chao and co-workers[8] reported the diagnosis of a BFLS patient with T-ALL, supporting the role of PHF6 as T-ALL specific tumor suppressor. Moreover, *PHF6* germline mutations were recently described in the Coffin-Siris and Nicolaides-Baraitser syndromes, congenital disorders previously characterized by mutations in various members of the SWI-SNF protein complex[9].

The protein structure of PHF6 is characterized by the presence of four nuclear localization signals (NLS) and two imperfect plant homeodomain (PHD) zinc fingers. The PHF6 protein is expressed in the nucleus with specific enriched expression in the nucleoli[7]. These nuclear compartments are known to harbor tandemly repeated ribosomal RNA (rRNA) gene clusters and it has recently been put forward that PHF6 suppresses rRNA synthesis through its interaction with the Upstream Binding Factor (UBF) protein[10]. The family of PHD-finger proteins has already been extensively

described in literature to constitute one of the largest protein families involved in modifying or reading the epigenetic code and this domain structure thus suggests a role for PHF6 as an epigenetic regulator of gene expression. This hypothesis is further supported by the observation of Todd and co-workers[11] that PHF6 interacts with the Nucleosome Remodeling and Deacetylation complex (NurD-complex).

In this study, we performed for the first time a dissection of the transcriptional landscape under control of PHF6 in T-ALL, revealing the potential mechanisms of a functional crosstalk with other known players in T-ALL oncogenesis and epigenetic modifiers such as the NurD and SWI-SNF chromatin remodeling complexes.

# Chapter 3: Results

## MATERIALS AND METHODS

### Cell lines

ALL-SIL cells were obtained from the DSMZ cell line repository. Cells were maintained in RPMI-1640 medium (Life Technologies) supplemented with 20% fetal bovine serum, 1% of L-glutamine (Life Technologies) and 1% penicillin/streptomycin (Life Technologies, 15160-047). MOHITO murine T-ALL cells were a kind gift from the lab of prof. Jan Cools[12] (Center for the Biology of Disease, VIB, Leuven, Belgium). Cells were maintained in RPMI-1640 medium (Life Technologies, catalog number 52400-025) supplemented with 20% fetal bovine serum, 1% of L-glutamine (Life Technologies, 15140-148), 1% penicillin/streptomycin (Life Technologies), 5 ng/ml murine IL-2 (PeproTech) and 10 ng/ml murine IL-7 (PeproTech).

### siRNA mediated knockdown, RNA-isolation, cDNA synthesis and RT-qPCR

ALL-SIL cells were electroporated (250 V, 1000 µF) using a Genepulser Xcell device (Biorad) with 400 nM of Silencer Select Negative Control 1 siRNA (Ambion) or siRNAs targeting PHF6 (ON-TARGETplus SMARTpool; Dharmacon, Lafayette, CO, USA and Silencer Select, Ambion), SMARCA4 (Silencer Select, Ambion) or CHD4 (Silencer Select, Ambion). ALL-SIL cells were collected 24h post-electroporation. Total RNA was isolated using the miRNeasy mini kit (Qiagen) with DNA digestion on-column. By means of spectrophotometry, RNA concentrations were measured (Nanodrop 1000) and RNA integrity was evaluated (Experion, Bio-Rad). Next, cDNA synthesis was performed using the iScript cDNA synthesis Kit (Bio-Rad) followed by RT-qPCR using the LightCycler 480 (Roche). Finally, qPCR data was analyzed according to the ΔΔCt-method using the qBasePLUS software (Biogazelle).

### CRISPR mediated knockout of Phf6 in MOHITO T-ALL cells

MSCV-Cas9-IRES-mCHERRY and pMX-U6_Phf6 guide viral vectors were produced in HEK293T cells using an EcoPack packaging plasmid and TurboFect transfection reagent (Fermentas). Supernatant containing virus was harvested 48 h after

transfection. MOHITO cells[12] were cultured in RPMI 1640 with 20% FCS and IL-2 (25 ng/mL; Peprotech), and IL7 (50 ng/mL; Peprotech). For retroviral transduction of MOHITO cels, 6-well plates were coated with RetroNectin solution overnight (final concentration 5 mg/cm$^2$, Takara Bio Inc.) and blocked with 2% FBS in PBS for 30 min before use. Viral supernatant was pre-loaded onto RetroNectin coated plates by centrifugation (2000 g, 30 min, 30°C). After centrifugation, viral supernatant was discarded, plates were washed with PBS and cells were added at a density of 0.5x106 cells/mL. Retroviral transduction was achieved using standard spin-infection procedure (2000 xg, 90 min, 30°C). Cells were placed in an incubator for 24-48 h to recover prior to FACS sorting of the mCHERRY and GFP double positive cells (Bio-Rad S3 sorter).

**Viral constructs and transduction of HPCs**

pLKO.1-puroR (control shRNA), TRCN0000015551 (*BRG1* shRNA1) and TRCN0000015552 (*BRG1* shRNA2) lentiviral vectors were purchased from Sigma in which the puromycin resistance gene was replaced with a PCR-amplified EGFP cDNA using BamHI and KpnI restriction sites. Infectious lentivirus was produced by jetPEI (polyplus transfection™) mediated transfection of the 293FT cell line with either pLKO.1-SHC002-EGFP or pLK0.1-SHC20122-EGFP, in conjuction of the pCMV-VSV-G (envelope) and p8.91 (packaging) constructs. The virus supernatant was harvested 2 and 3 days after transfection. Lentiviral transduction of HPCs was performed on sorted CD34$^+$lin$^-$ CB cells or CD34$^+$ thymocytes previously cultured in complete IMDM medium containing 10% FCS and supplemented with TPO (20ng/ml), SCF (100ng/ml) and FLT3-L (100ng/ml) or SCF (10ng/ml) and IL-7 (10ng/ml), respectively, for two days (cord blood) or one day (thymocytes). 48 hours after transduction, cells were harvested and sorted for EGFP$^+$ transduced cells.

**OP9 co-cultures and flow cytometry**

Transduced and sorted CD34$^+$lin$^-$EGFP$^+$ CB cells or CD34$^+$EGFP$^+$ thymocytes were seeded in a 24-well plate containing a confluent layer of either control OP9 stromal

cells (OP9-GFP) or Delta-like-ligand1 expressing OP9 stromal cells (OP9-DLL1). All co-cultures were performed in α-MEM media (Invitrogen) supplemented with 20% heat-inactivated FCS plus 100U/ml penicillin, 100 µg/ml streptomycin and 2mM L-glutamin (all from Invitrogen). To induce and support T and B cell differentiation, cultures were performed in the presence of SCF, IL-7 and FLT3-L (all 5 ng/ml) on OP9-DLL1 and OP9-GFP, respectively. Co-cultures were harvested by forceful pipetting at indicated time points. Obtained cell suspensions were blocked with anti-mouse FcRγII/III (clone 2.4.G2) and human IgG (Fcblock, Miltenyi) to avoid non-specific binding and subsequently stained with combinations of anti-human monoclonal antibodies (BDIS, eBioscience, Biolegend and Miltenyi). Cells were examined for the expression of cell surface markers on a LSRII (BDIS).

**RNA-sequencing**

In this study, RNA-sequencing by poly-A capture (unstranded, paired-end) was performed using 100 ng of RNA as input material (Biogazelle, Belgium). The sequencing read depth comprised for all samples +/-50 million reads, which were aligned to the reference genome hg38 with STAR-2.4.2a and default settings. Differential expression analysis was performed with DESeq2. Scrambled siRNA was used as control and compared with 2 independent PHF6 targeting siRNAs (3 replicates). A multifactorial design was used to control for batch effects.

**Gene expression profiling**

RNA samples from ALL-SIL cells were profiled on a custom designed Agilent micro-array covering all protein coding genes (33,128 mRNA probes, Human Sureprint G3 8x60k micro-arrays (Agilent)) and 12,000 lncRNAs (23,042 unique lncRNA probes). Expression data were normalized using the VSN-package (Bioconductor release 2.12) in R. Differential expression analysis was performed in R using Limma.

### Gene ontology analysis using the GREAT algorithm

The 'Genomic Regions Enrichment of Annotations' (GREAT) tool (http://bejerano.stanford.edu/great) was used to perform gene ontology on the set of up- or downregulated set of genes upon PHF6 knockdown. The 'mouse phenotype' ontology comprises mouse genotype-phenotype associations, mainly obtained by curation from literature., that are mapped to human genes.

## Chapter 3: Results

### RESULTS

### PHF6 modulation affects a broad gene regulatory landscape including multiple genes implicated in thymocyte maturation and T-ALL oncogenesis

We previously scrutinized the role of PHF6 in normal human hematopoiesis using the *in vitro* model system OP9-DLL1 (**paper 2** in this PhD thesis). In brief, we showed that PHF6 acts as a novel master regulator in hematopoietic lineage development, with PHF6 knockdown profoundly impacting on B-cell, T-cell and NK-cell lineages. A recent study by Meacham and colleagues suggested that PHF6 could act as an oncogene in B-cell malignancies[13], while we previously identified *PHF6* as a tumor suppressor in T-ALL[4] and observed a significant enrichment of *PHF6* loss-of function mutations in *TLX1*/*TLX3* positive T-ALL. In order to better understand the tumor suppressor role of PHF6 in T-ALL lymphoblasts and its functional connection to TLX1 in T-ALL blast formation, we evaluated the transcriptional effects of transient PHF6 knockdown in the TLX1 positive ALL-SIL T-ALL cell line. First, significant knockdown of PHF6 levels in ALL-SIL cells using two independent siRNAs was validated by RT-qPCR and western blot analysis, reaching up to 80% knockdown at the PHF6 protein level (**Fig. 1a and 1b**). Subsequent RNA-sequencing of these samples revealed 734 significantly downregulated and 216 upregulated protein-coding genes upon PHF6 knockdown. Within the set of downregulated genes, we found by 'Gene Ontology' (GO)-analysis using the GREAT algorithm[14] amongst others enrichment for genes with a key role in normal T-cell and B-cell differentiation (*CD7*, *NOTCH1*) (**Fig. 1c and 1d**), whereas the set of upregulated genes upon PHF6 knockdown was enriched not only in important T-cell marker genes (*RAG1*, *IL7R*, *MYB*), but also a gene signature related to epigenetic gene expression regulation (**Fig 1c and 1e**). Next, in order to further identify potential co-regulators of the gene sets that we identified under control of PHF6, we performed iRegulon analysis[15] on the set of significantly (p-value<0.05) down- and upregulated genes upon PHF6 knockdown. For the set of PHF6 activated genes we identified the transcriptional regulators TFAP2C (NES: 5.348), JAZF1 (NES: 4.657) and ZBTB7/MAZ (NES: 4.584) as top-scoring putative PHF6 co-factors. Interestingly, previously published work from Meacham and colleagues[13]

included PHF6 ChIP-sequencing in Jurkat T-ALL cells. We performed, by means of the MEME ChIP tool[16] motif discovery on this dataset (data not shown) and one of the top-scoring motifs (E-value: 3.2e-009) is the binding motif of the TFAP2C transcription factor. Notably, also TAL1 (NES: 4.099), ETS1 (NES: 4.038) and IKZF1 (NES: 3.990) were amongst the top-enriched co-factors. In a similar manner, we used iRegulon to identify putative PHF6 co-regulators for the set of PHF6 repressed genes. For this set of genes, we found enrichment for the TBX protein family (NES: 4.078), the HOX protein family (NES: 4.035) and PAX3/7 (NES: 4.00).

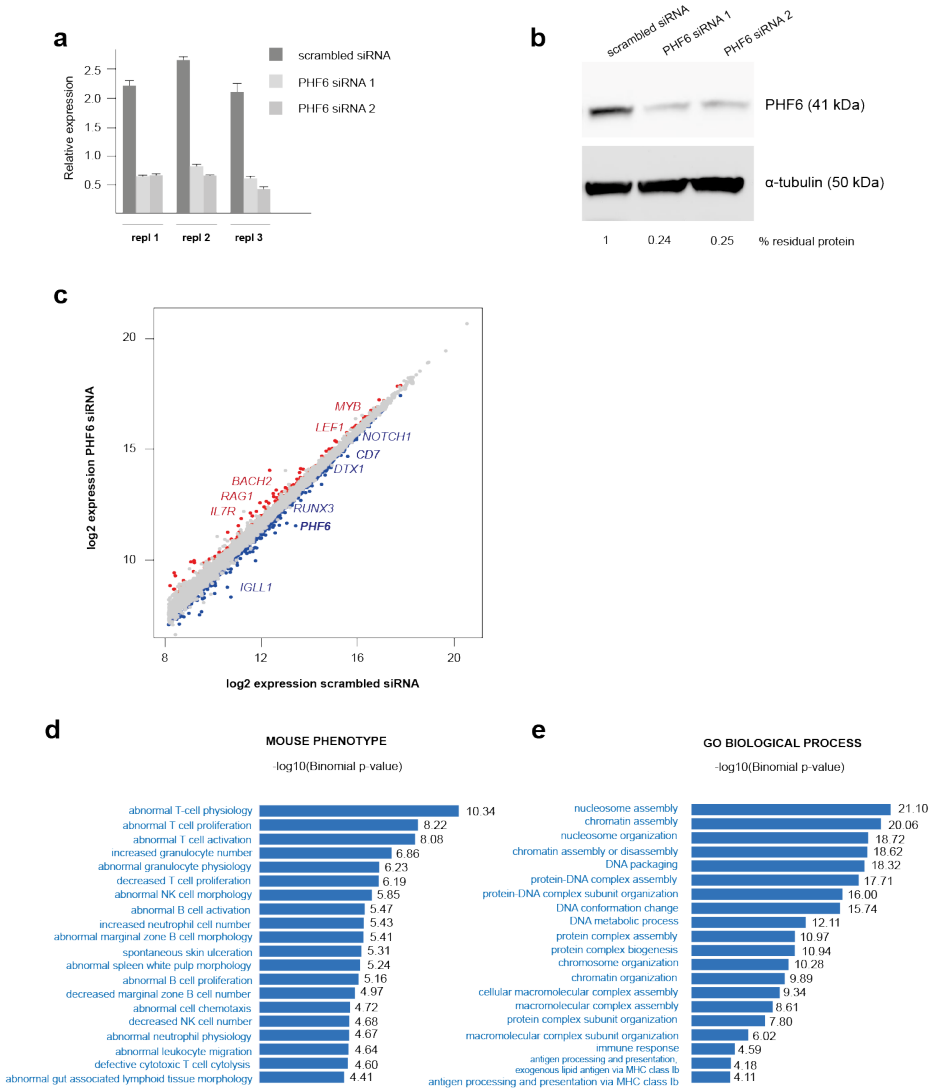


**Figure 1: Scrutinizing the PHF6 downstream regulatory network in T-ALL lymphoblasts.** Validation of PHF6 knockdown in ALL-SIL T-ALL cells by RT-qPCR (mRNA) (**a**) and western blot analysis (protein level) (**b**), diagonal plot showing some of the key targets that are downregulated (blue) or upregulated (red) upon PHF6 knockdown in ALL-SIL (**c**), Gene Ontology analysis (GREAT algorithm) on the set of downregulated (**d**) and upregulated (**e**) genes upon PHF6 knockdown in ALL-SIL.

## Chapter 3: Results

**PHF6 loss-of-function is an essential functional genetic event in TLX1-positive T-ALL**

To further elaborate on the potential functional interrelation with the ectopically expressed oncogenic factor TLX1, we scored the gene signatures obtained from PHF6 knockdown in ALL-SIL cells to the transcriptome profile obtained upon knockdown of TLX1 in the ALL-SIL cell line (**Fig. 2a and b**) using 'Gene Set Enrichment Analysis' (GSEA). We could show that TLX1 knockdown induces a largely overlapping gene signature to PHF6 knockdown. Interestingly, as we have previously shown in our study on the role of PHF6 in thymocyte progenitors (**paper 2**), one of the predominant upregulated genes upon PHF6 knockdown in T-ALL lymphoblasts is *IL7R* (**Fig. 1d**), a key NOTCH1 target gene that we have previously found to be repressed by TLX1[17] (**Fig. 2b**). We hypothesize that the PHF6-IL7R-TLX1 regulatory axis is crucial to explain the dependency of TLX1-positive T-ALL to cooperative *PHF6* loss, given the essential role of IL7R for survival of immature T-cells during maturation.

The upregulated expression of *IL7R* in ALL-SIL cells upon PHF6 was confirmed by RT-qPCR (**Fig. 2c**). Notably, comparing the *IL7R* mRNA expression levels between a panel of *PHF6* wild-type and mutant T-ALL cell lines, significantly higher expression of *IL7R* mRNA levels could be detected in *PHF6* mutant cells (DND-41, HPB-ALL and T-ALL1) in contrast to *PHF6* wild-type cells (Jurkat, ALL-SIL, LOUCY, KE-37, MOLT-16, PEER, CCRF-CEM, PF-382) (**Fig. 2d**).

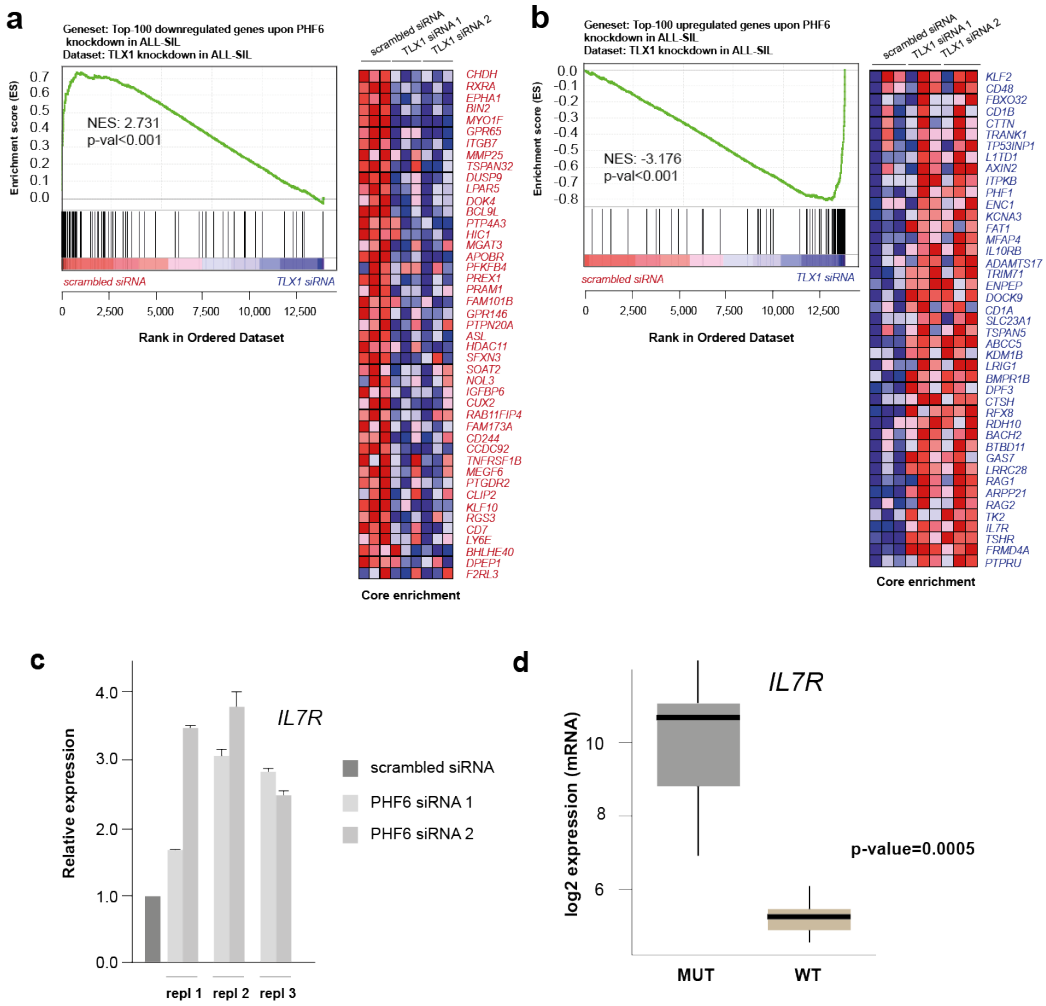


**Figure 2: Identification of a TLX1-IL7R-PHF6 regulatory axis in T-ALL lymphoblasts.** Gene Set Enrichment Analysis (GSEA) reveals a significant overlap between the downregulated (**a**) and upregulated (**b**) gene signatures associated with TLX1 and PHF6 knockdown in ALL-SIL cells, (**c**) Validation of *IL7R* upregulation upon PHF6 knockdown in ALL-SIL lymphoblasts by RT-qPCR, (**d**) Gene expression profiling from a T-ALL cell line panel indicates that *IL7R* mRNA levels are significantly higher in *PHF6* mutant T-ALL cell lines compared to *PHF6* wild-type cell lines.

In order to further functionally evaluate the effects of PHF6 knockdown on IL7R expression and the downstream JAK-STAT signaling cascade, we generated a stable *Phf6* CRISPR knock-out model in the murine T-ALL cell line MOHITO[12], given that this cell line is IL7-sensitive. Phf6 knockout was validated on protein level by western blot analysis (**Fig. 3a**). Next, we compared IL7R (CD127) surface expression and intracellular pSTAT5 levels by flow cytometry. The MOHITO cells transduced only with the construct encoding the Cas9 protein were used as a negative control. As a positive control for IL7R downstream JAK-STAT signaling induction by IL-7

administration, we used MOHITO cells transduced with both Cas9 and JAK3 encoding vectors. Using this approach, robust induction of IL7R-downstream pSTAT5 protein in JAK3 overexpressing cells was observed. Upon co-transduction of MOHITO T-ALL cells with a Cas9 and Phf6 gRNA encoding constructs, we observed that IL7R (CD127) surface expression was strongly induced with a concomitant modest induction of downstream pSTAT5 (**Fig. 3b**).This is in line with our previous findings (**paper 2**).

In conclusion, our results show for the first time a key regulatory effect of PHF6 on the IL7R-JAK-STAT pathway, indicating that *PHF6* mutated T-ALL patients could benefit from JAK-STAT cascade based molecular therapies, like ruxolitinib and tofacitinib treatment.

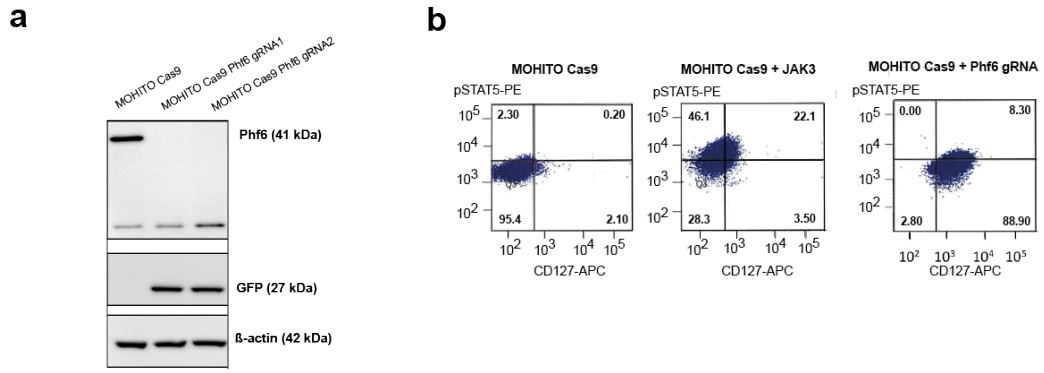


**Figure 3: MOHITO cells with Phf6 CRISPR knockout show increased levels of IL7R (CD127) surface expression and downstream pSTAT5 levels as compared to control cells**. (**a**) western blot analysis of MOHITO murine T-ALL lymphoblasts confirms complete loss of Phf6 protein expression using 2 independent PHF6 targeting gRNAs, (**b**) Flow cytometry analysis shows predominant upregulation of pSTAT5 levels upon overexpression of JAK3 (= positive control) in MOHITO cells, whereas Phf6 knockout mainly leads to upregulation of IL7R with a modest increase in intracellular pSTAT5 levels.

### PHF6 controls super-enhancer activity in T-ALL lymphoblasts

Given the known action of the SWI-SNF complex at enhancer regions[18], we compared the gene signature obtained upon PHF6 knockdown in ALL-SIL lymphoblasts to the transcriptional profile of ALL-SIL cells treated with the BET-inhibitor JQ1, a compound that is known to selectively bind and inhibit the bromodomain protein BRD4, thereby broadly affecting genes in the vicinity of (super)-enhancer sites[19]. This analysis revealed a significant downregulation of enhancer-associated protein coding genes upon PHF6 loss (**Fig. 4a**). To further

specify this analysis towards super-enhancer loci in ALL-SIL, we scored the top-500 scoring super-enhancers in the vicinity of protein-coding genes and evaluated how these were affected by PHF6 knockdown using GSEA (**Fig. 4b**). By means of a super-enhancer plot analysis, we identified that amongst others *IGLL1*, *RUNX3* and *NOTCH1* are significantly associated with super-enhancer sites in ALL-SIL that are under control of PHF6 (**Fig. 4c**).

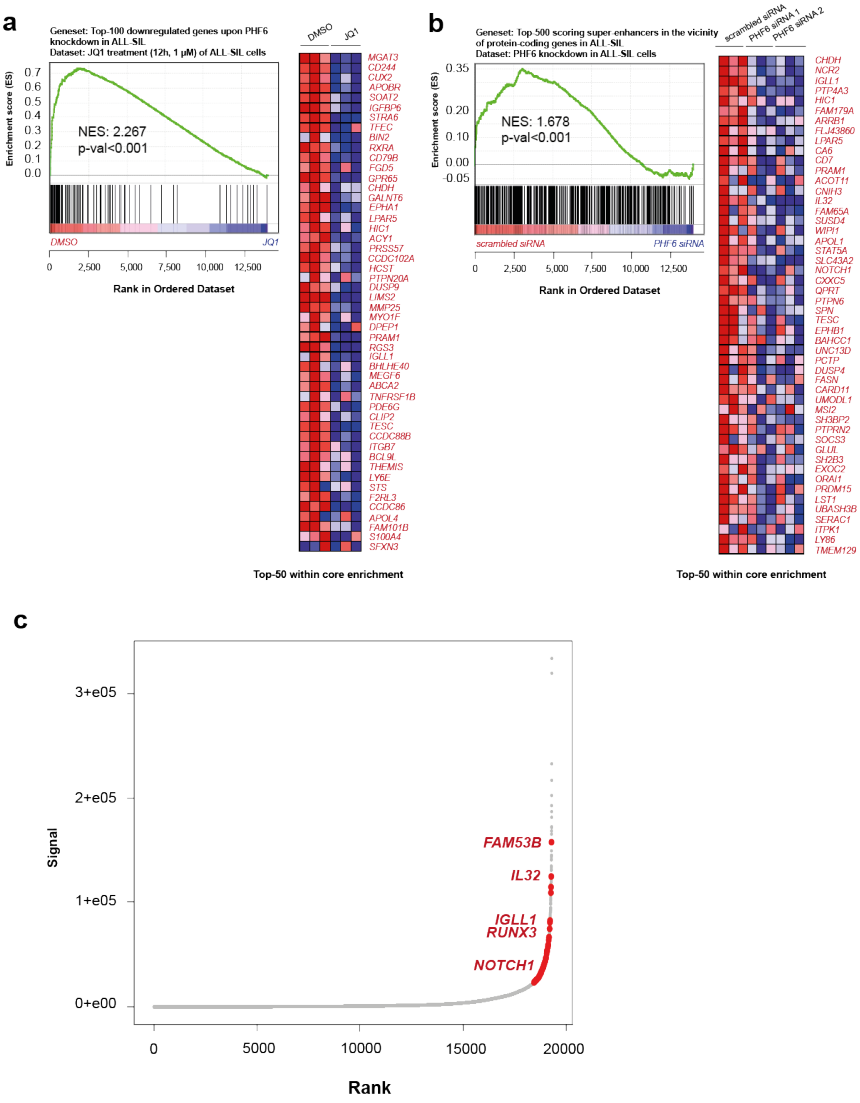


**Figure 4: The putative epigenetic regulator PHF6 controls (super)-enhancer activity in ALL-SIL lymphoblasts.** (**a**) Gene Set Enrichment Analysis shows a significant enrichment of the top-500 downregulated genes upon PHF6 knockdown in ALL-SIL within th set of genes that are downregulated upon JQ1 treatment in the same cellular context, (**b**) Gene Set Enrichment Analysis shows a significant enrichment of the top-500 scoring super-enhancer sites in the ALL-SIL genome near protein-coding genes within the gene signature downmodulated upon PHF6 knockdown, (**c**) Hockey-stick plot representing the normalized rank and cluster signals of H3K27Ac ChIP-seq peaks in ALL-SIL, with red dots representing those super-enhancer associated protein coding genes that are significantly differentially expressed upon PHF6 knockdown in ALL-SIL as determined by polyA RNA-sequencing.

## Chapter 3: Results

### Functional crosstalk of PHF6 as an epigenetic modifier with NurD and SWI-SNF chromatin remodeler complexes

Recently, Todd and co-workers[11] described the identification of a physical interaction between PHF6 and the core components of the NurD protein complex CHD4, RBBP4 and HDAC1. So far, no further functional evaluation of this interaction has been done in the context of T-ALL. Therefore, we performed transient knockdown of CHD4, a core catalytic component of NurD, in ALL-SIL cells. In total, we obtained 403 significantly downregulated and 526 upregulated protein-coding genes upon CHD4 knockdown. Notably, a comparative analysis by GSEA between the gene signatures obtained upon PHF6 and CHD4 knockdown in ALL-SIL cells revealed that the set of PHF6 activated genes is significantly repressed by CHD4 (**Fig. 5a**) while a small, but significant overlap could be identified between genes repressed by CHD4 and PHF6 (**Fig. 5b**). This potential functional antagonism between PHF6 and CHD4 will be further investigated in follow-up of this PhD mandate.

Given the recent identification of *PHF6* mutations in Coffin-Siris syndrome cases, we also evaluated the potential functional relation of PHF6 to the SWI-SNF complex. To this end, we performed transient knockdown of the catalytic SWI-SNF component, SMARCA4/BRG1, in ALL-SIL cells. In total, 331 protein-coding genes were downregulated and 263 protein-coding genes were upregulated upon transient SMARCA4/BRG1 knockdown. The gene signature induced upon SMARCA4/BRG1 knockdown significantly mimics the signature retrieved upon PHF6 knockdown in ALL-SIL cells as shown by GSEA (**Fig. 5c and 5d**). The role of SMARCA4/BRG1 in T-ALL is currently unknown. Further studies will be required to understand the role of the SWI-SNF chromatin remodeler complex in T-ALL pathogenesis.

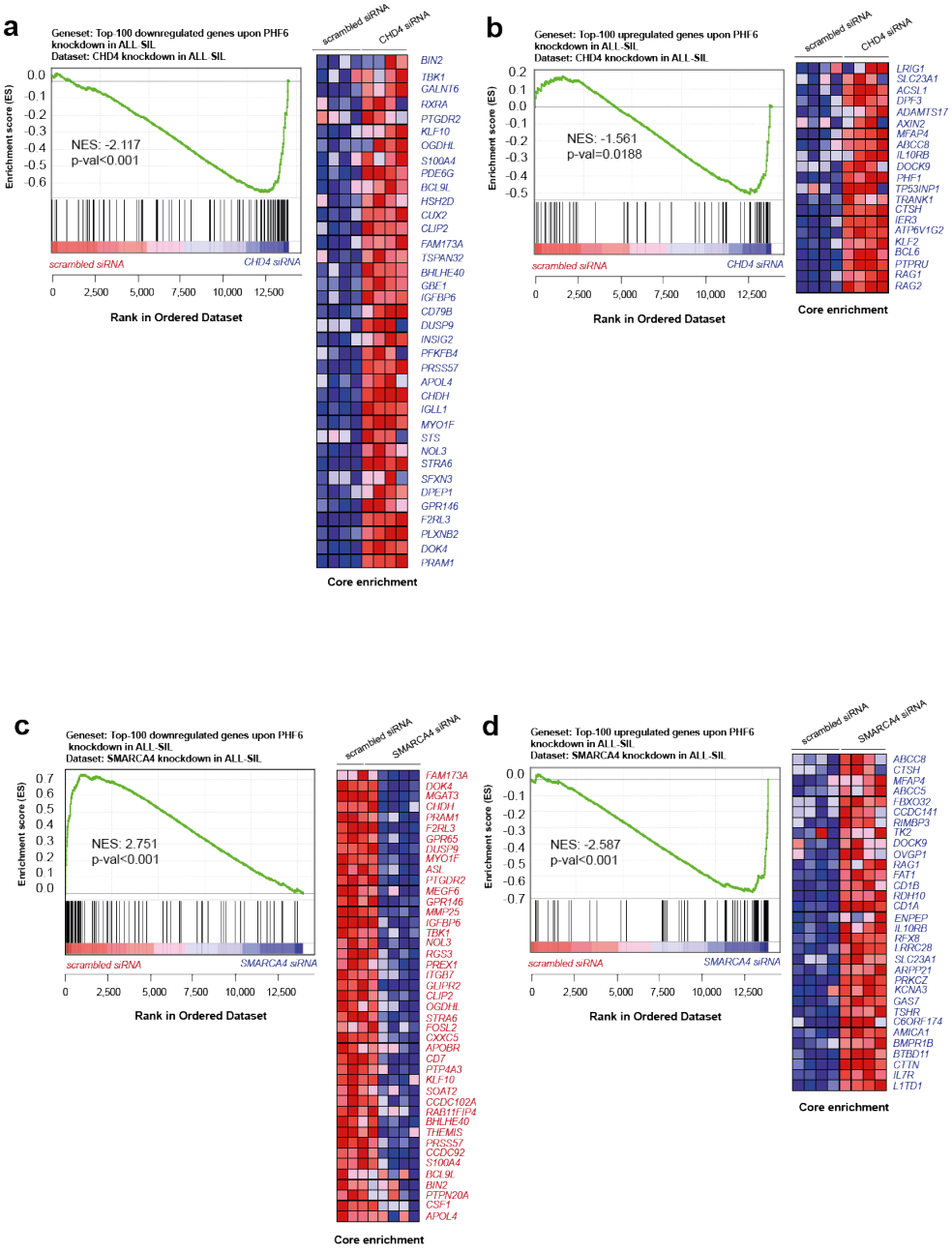


**Figure 5: The putative epigenetic regulator PHF6 controls overlapping gene signatures with the NurD and SWI-SNF chromatin remodeling complexes.** (**a**) Gene Set Enrichment Analysis shows a significant enrichment of PHF6 positively regulated genes in the set of CHD4 repressed genes, (**b**) a core set of genes significantly upregulated by PHF6 overlaps with genes upregulated upon CHD4 knockdown in ALL-SIL as shown by GSEA analysis, (**c-d**) Gene set Enrichment Analysis shows a significant overlap between PHF6 and SMARCA4 controlled gene signatures in ALL-SIL lymphoblasts.

## Chapter 3: Results

### The SWI-SNF complex core component SMARCA4/BRG1 plays a key role in normal hematopoiesis

A key role for SMARCA4/BRG1 in murine thymocyte development has been previously described[20]. In order to better understand the potential functional interaction between SMARCA4/BRG1 and PHF6 in T-ALL lymphoblasts, we evaluated potential converging effects on human hematopoiesis. In a first analysis, we performed stable knockdown of SMARCA4/BRG1 in cord blood $CD34^+$ progenitor cells and plated them either on an OP9-GFP stromal feeder layer to evaluate phenotypic effects on B-cell development or on an OP9-DLL1 stromal feeder layer to be able to monitor effects on T-cell lineage differentiation. We observed significant impact of SMARCA4/BRG1 knockdown on the precursor T-cell populations $CD34^+7^+$ (**Fig. 6a**), $CD7^+CD5^+$ (**Fig. 6b**) and γδ T-cell lineage development (**Fig. 6c**), with both SMARCA4/BRG1 shRNAs applied inducing a major reduction in the aforementioned populations both in frequencies and absolute counts.

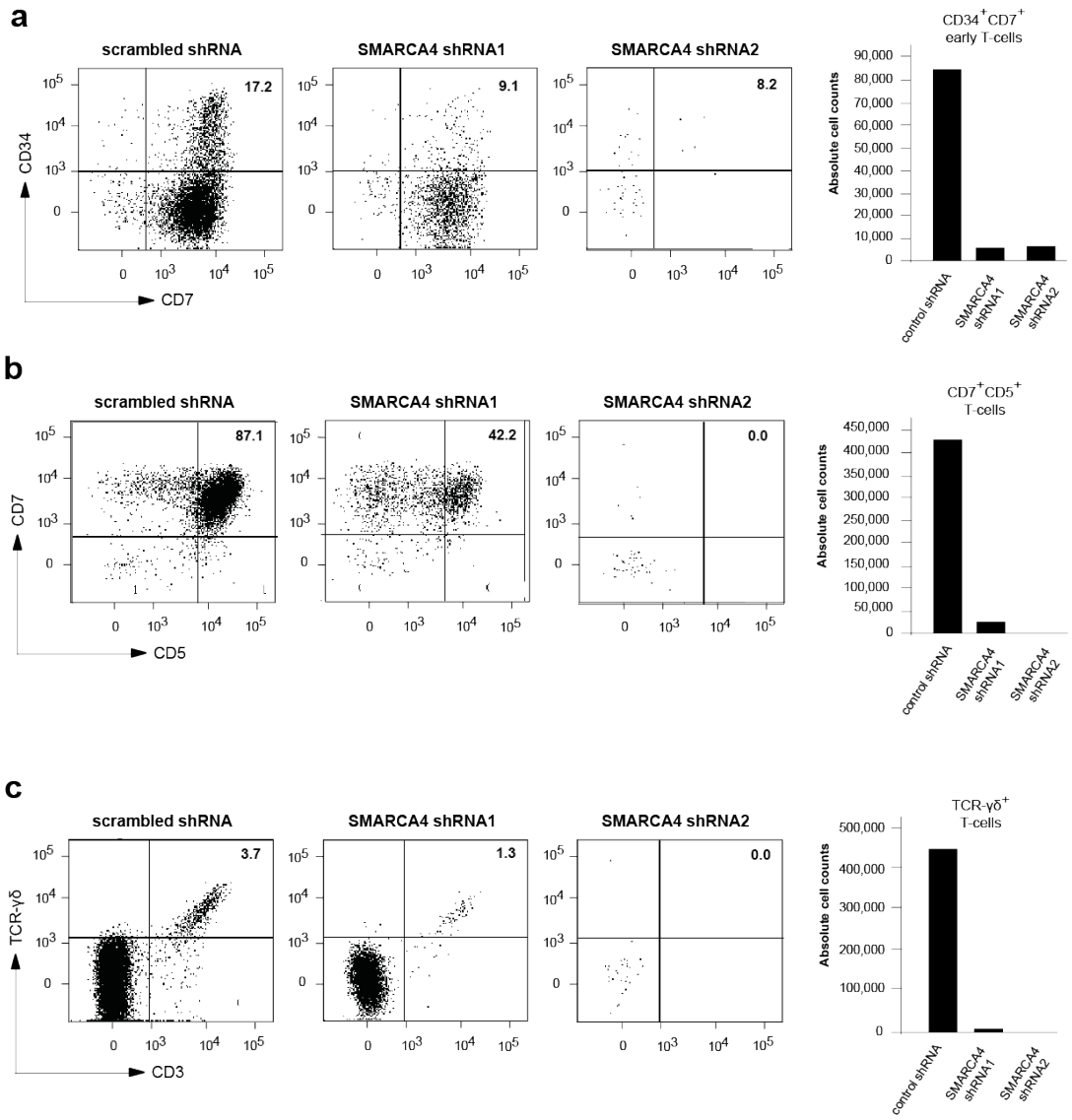


**Figure 6: BRG1 deficiency leads to abberant T-cell lineage development**. Stable knockdown of BRG1/SMARCA4 (2 independent shRNAs) in $CD34^+$ cord blood progenitor cells cultured on an OP9-DLL1 stromal feeder layer leads to (**a**) significant reduction in frequency (left) and absolute numbers of $CD34^+CD7^+$ early T-cell populations as well as (**b**) reduced $CD7^+CD5^+$ mature T-cell formation and (**c**) significant reduction in TCR-γδ lineage committed cells.

With respect to B-cell development, a similar drastic reducing effect on development of precursor B-cells could be observed upon SMARCA4/BRG1 knockdown (**Fig. 7**).

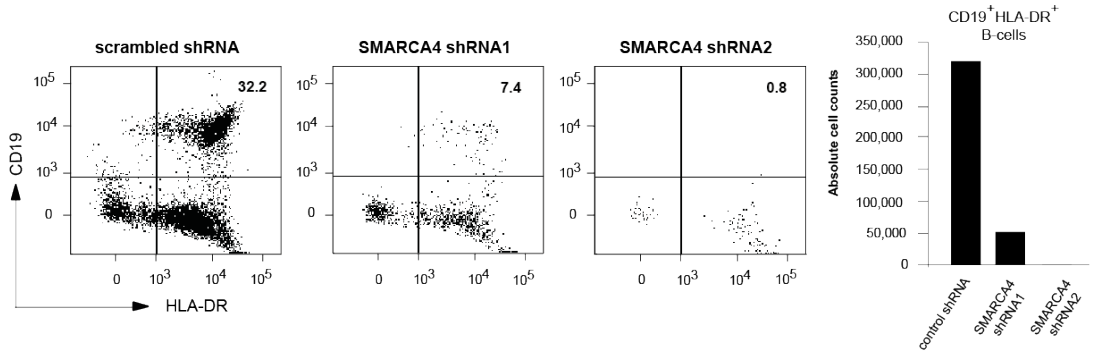


**Figure 7: BRG1/SMARCA4 knockdown in CD34$^+$ cord blood progenitors leads to a significant reduction in development towards CD19$^+$HLA-DR$^+$ B-cells.**

**DISCUSSION**

In this study, we performed a first landscaping of the transcriptional networks in T-ALL lymphoblasts, complementing our study focusing on the role of PHF6 in normal hematopoiesis (**paper 2**). Our results indicate a functional cooperative interaction between PHF6 loss and TLX1 ectopic expression for malignant T-cell transformation through a converging regulatory role on IL7R expression, a key signaling receptor for survival and differentiation of thymocyte progenitor cells and a crucial T-ALL oncogene. In addition, we show for the first time a significant overlap between the signature genes of the PHF6 downstream transcriptional network and the genes under control of the NurD and SWI-SNF chromatin remodeler complexes. This observation further strengthens the potential implication of PHF6 as an epigenetic regulator of gene expression. In order to further approach the PHF6 transcriptional network from an epigenetic perspective, we will perform ChIP-sequencing for PHF6 and a series of key histone modifications (H3K27ac, H3K4me1, H3K4me3, H3K27me3) under default conditions and upon PHF6 perturbation to evaluate how certain histone modification profiles are affected by PHF6 knockdown. Furthermore, we are currently optimizing the protocol for ATAC-sequencing in the lab, which will allow us to scrutinize the PHF6 controlled epigenetic landscape (default and in combination with perturbation) in precursor T-cells. So far, the role of the SWI-SNF

complex has not been studied in the context of T-ALL development. Interestingly, a recent study by Mullighan and colleagues (online communication ASH meeting, 2015) reported *SMARCA4/BRG1* mutations in pediatric T-ALL patients. Interestingly, our research team identified by arrayCGH analysis one T-ALL patient with a *SMARCA4/BRG1* deletion and one with an *ARID1A* deletion (unpublished data), suggestive that components of the SWI-SNF complex are involved in T-ALL pathogenesis. In order to better understand the underlying molecular mechanisms that mediate the observed significant effects of SMARCA4/BRG1 knockdown on T-cell and B-cell differentiation, we anticipate to perform gene expression profiles of the respective co-cultures.

The results of this study give a prelude to the use of IL7R-pathway directed drugs such as tofacitinib and ruxolitinib. We will test the sensitivity of *PHF6* deficient cells to these drugs compared to wild-type cells. To this end, the MOHITO cell model system with stable PHF6 CRISPR knockout is of great value. One would predict no selective pressure for activating mutations within the IL7R signaling pathway if *PHF6* inactivation already results in increased expression of IL7R, unless this is associated with reduced downstream signaling. Such a reduction in IL7R signaling would also be consistent with inhibition of TCR-γδ T cell development and accelerated differentiation towards αβ-lineage DP cells previously observed (**paper 2**). Using iRegulon, we identified that the PHF6 repressed genes are significantly enriched within the set of known downstream target genes of the STAT family members (STAT3 and STAT5A), indicating that downstream target genes of the IL7R signaling pathway are not activated upon PHF6 inactivation and thus suggesting that IL7R signaling is defective, despite increased IL7R expression (data not shown). This is currently further investigated by overexpression studies of the γc-chain (*IL2RG*) of the IL7R complex in Phf6 MOHITO knockout cells, to see whether we then can significantly induce/restore IL7R downstream JAK-STAT signaling.

Given the frequent co-occurrence of mutations in T-ALL in both *PHF6* and components of the IL7R pathway[21], we propose that PHF6 functions as a tumor suppressor during human T cell development by limiting the amount of IL7R expression, thereby preventing selective pressure to induce activation mutations within this signaling pathway as a result of the decrease in signaling.

**REFERENCES**

1. Watson, I.R., Takahashi, K., Futreal, P.A. & Chin, L. Emerging patterns of somatic mutations in cancer. *Nat Rev Genet* **14**, 703-718 (2013).

2. Huether, R.*, et al.* The landscape of somatic mutations in epigenetic regulators across 1,000 paediatric cancer genomes. *Nat Commun* **5**, 3630 (2014).

3. Ntziachristos, P.*, et al.* Genetic inactivation of the polycomb repressive complex 2 in T cell acute lymphoblastic leukemia. *Nat Med* **18**, 298-301 (2012).

4. Van Vlierberghe, P.*, et al.* PHF6 mutations in T-cell acute lymphoblastic leukemia. *Nat Genet* **42**, 338-342 (2010).

5. Van Vlierberghe, P.*, et al.* PHF6 mutations in adult acute myeloid leukemia. *Leukemia* **25**, 130-134 (2011).

6. Yoo, N.J., Kim, Y.R. & Lee, S.H. Somatic mutation of PHF6 gene in T-cell acute lymphoblatic leukemia, acute myelogenous leukemia and hepatocellular carcinoma. *Acta Oncol* **51**, 107-111 (2012).

7. Lower, K.M.*, et al.* Mutations in PHF6 are associated with Borjeson-Forssman-Lehmann syndrome. *Nat Genet* **32**, 661-665 (2002).

8. Chao, M.M.*, et al.* T-cell acute lymphoblastic leukemia in association with Borjeson-Forssman-Lehmann syndrome due to a mutation in PHF6. *Pediatr Blood Cancer* **55**, 722-724 (2010).

9. Wieczorek, D.*, et al.* A comprehensive molecular study on Coffin-Siris and Nicolaides-Baraitser syndromes identifies a broad molecular and clinical spectrum converging on altered chromatin remodeling. *Hum Mol Genet* **22**, 5121-5135 (2013).

10. Wang, J.*, et al.* PHF6 regulates cell cycle progression by suppressing ribosomal RNA synthesis. *J Biol Chem* **288**, 3174-3183 (2013).

11. Todd, M.A. & Picketts, D.J. PHF6 interacts with the nucleosome remodeling and deacetylation (NuRD) complex. *J Proteome Res* **11**, 4326-4337 (2012).

12. Kleppe, M., Mentens, N., Tousseyn, T., Wlodarska, I. & Cools, J. MOHITO, a novel mouse cytokine-dependent T-cell line, enables studies of oncogenic signaling in the T-cell context. *Haematologica* **96**, 779-783 (2011).

13. Meacham, C.E.*, et al.* A genome-scale in vivo loss-of-function screen identifies Phf6 as a lineage-specific regulator of leukemia cell growth. *Genes Dev* **29**, 483-488 (2015).

14. McLean, C.Y., *et al.* GREAT improves functional interpretation of cis-regulatory regions. *Nat Biotechnol* **28**, 495-501 (2010).

15. Janky, R., *et al.* iRegulon: from a gene list to a gene regulatory network using large motif and track collections. *PLoS Comput Biol* **10**, e1003731 (2014).

16. Bailey, T.L., *et al.* MEME SUITE: tools for motif discovery and searching. *Nucleic Acids Res* **37**, W202-208 (2009).

17. Durinck, K., *et al.* Characterization of the genome-wide TLX1 binding profile in T-cell acute lymphoblastic leukemia. *Leukemia* **29**, 2317-2327 (2015).

18. Shi, J., *et al.* Role of SWI/SNF in acute leukemia maintenance and enhancer-mediated Myc regulation. *Genes Dev* **27**, 2648-2662 (2013).

19. Loven, J., *et al.* Selective inhibition of tumor oncogenes by disruption of super-enhancers. *Cell* **153**, 320-334 (2013).

20. Gebuhr, T.C., *et al.* The role of Brg1, a catalytic subunit of mammalian chromatin-remodeling complexes, in T cell development. *J Exp Med* **198**, 1937-1949 (2003).

21. Vicente, C., *et al.* Targeted sequencing identifies associations between IL7R-JAK mutations and epigenetic modulators in T-cell acute lymphoblastic leukemia. *Haematologica* **100**, 1301-1310 (2015).

## Author contributions

KD and IvdW performed the experiments and wrote the manuscript, JvdM and FM assisted in performance of PHF6 knockdown experiments, WL performed the bio-informatics analyses and JC, TT, PVV and FS supervised the experiments and writing of the manuscript.

# Results

## Part 2. Landscaping transcriptional control of non-coding RNAs in T-cell acute lymphoblastic leukemia

## Chapter 3: Results

# Novel TAL1 targets beyond protein-coding genes: identification of TAL1-regulated microRNAs in T-cell acute lymphoblastic leukemia

NC Correia[1], K Durinck[2], AP Leite[1], M Ongenaert[2], P Rondou[2], F Speleman[2], FJ Enguita[1] and JT Barata[1]

[1]*Instituto de Medicina Molecular, Faculdade de Medicina da Universidade de Lisboa, Lisbon, Portugal*

[2]*Center for Medical Genetics, Department of Pediatrics and Genetics, Ghent University, Ghent, Belgium*

**Letter to the Editor**

**Leukemia. 2013 Jul;27(7):1603-6**

## Chapter 3: Results

The basic helix-loop-helix transcription factor TAL1 is aberrantly expressed in a majority of T-cell acute lymphoblastic leukemia (T-ALL) cases characterized by arrested development in the thymic late cortical stage.[1,2] Although TAL1 is a *bona fide* T-cell oncogene,[3] with known direct targets in T-ALL,[4] the aberrant transcriptional circuitry responsible for thymocyte transformation is not yet fully understood. MicroRNAs are small, non-coding RNAs that function as endogenous post-transcriptional repressors of protein-coding genes by binding to target sites in the 3′-UTR of messenger RNAs.[5] Aberrant expression of these molecules has been reported in several hematological malignancies, and microRNA expression signatures delineate ALL subgroups[6] and can be interpreted in light of their variation during hematopoiesis.[7] Individual microRNAs and networks have been implicated in T-ALL,[8] but the mechanisms responsible for altered microRNA expression in this malignancy remain poorly explored. Here, we report the identification of novel, non-protein-coding TAL1 target genes, implicating microRNA genes as part of the transcriptional network downstream of TAL1 that may be putatively involved in its oncogenic properties.

To identify a TAL1-dependent microRNA gene expression profile, we ectopically expressed TAL1 in the TAL1-negative T-ALL cell line P12 and performed low-density array analysis (see Supplementary Data online for materials and methods). From 204 detected microRNAs (out of 372 analyzed), we identified eight whose expression changed significantly upon TAL1 overexpression (**Figure 1a and Supplementary Tables 1 and 2**). Subsequent validation was performed by quantitative PCR analysis of each microRNA after enforcing or silencing the expression of TAL1. This allowed us to confirm the expected TAL1-mediated regulation for five microRNAs: namely, *miR-135a*, *miR-223* and *miR-330-3p* as being upregulated by TAL1; and *miR-146b-5p* and *miR-545* as being downregulated (**Figures 1b–f**). The three remaining microRNAs were excluded from subsequent analyses, as we stringently considered only those genes to be validated whose expression was regulated in the predicted manner upon both TAL1 overexpression and silencing (data not shown).

Next, we evaluated whether the validated microRNAs were direct targets of TAL1 in T-ALL cells. For this purpose, we scrutinized publicly available TAL1 ChIP-seq data (GEO accession number GSE29181) for two T-ALL cell lines (JURKAT and CCRF-CEM) and two primary T-ALL samples[4] for the presence of TAL1-binding peaks up to 10 kb upstream of the transcription start site of each microRNA gene. We identified one peak in a putative promoter region for *miR-146b* (**Supplementary Figure 1a**), suggesting that this gene may be a transcriptional target of TAL1. Furthermore, two peaks were observed upstream of the *miR-223* transcription start site (**Supplementary Figure 1b).** To confirm these findings, we performed TAL1 ChIP-quantitative PCR in JURKAT and CCRF-CEM cells using primers designed for the genomic areas covered by the two peaks in the *miR-223* locus. We confirmed that there is more than two-fold enrichment, as compared with a mock ChIP performed against fibrillarin, in the amplified area within 3.5 kb upstream of the *miR-223* transcription start site (**Figure 1g**). These results indicate that *miR-223* is a direct target of TAL1 in T-ALL. Interestingly, TAL1 appears to bind to a previously described region containing a conserved proximal genomic element with possible binding sites for the transcription factor C/EBP.[9] We did not find evidence from the available TAL1 ChIP-seq data for direct binding of TAL1 to the remaining microRNA genes, suggesting that *miR-135a*, *miR-330-3p* and *miR-545* are indirectly regulated by TAL1, at least in the T-ALL cells analyzed.

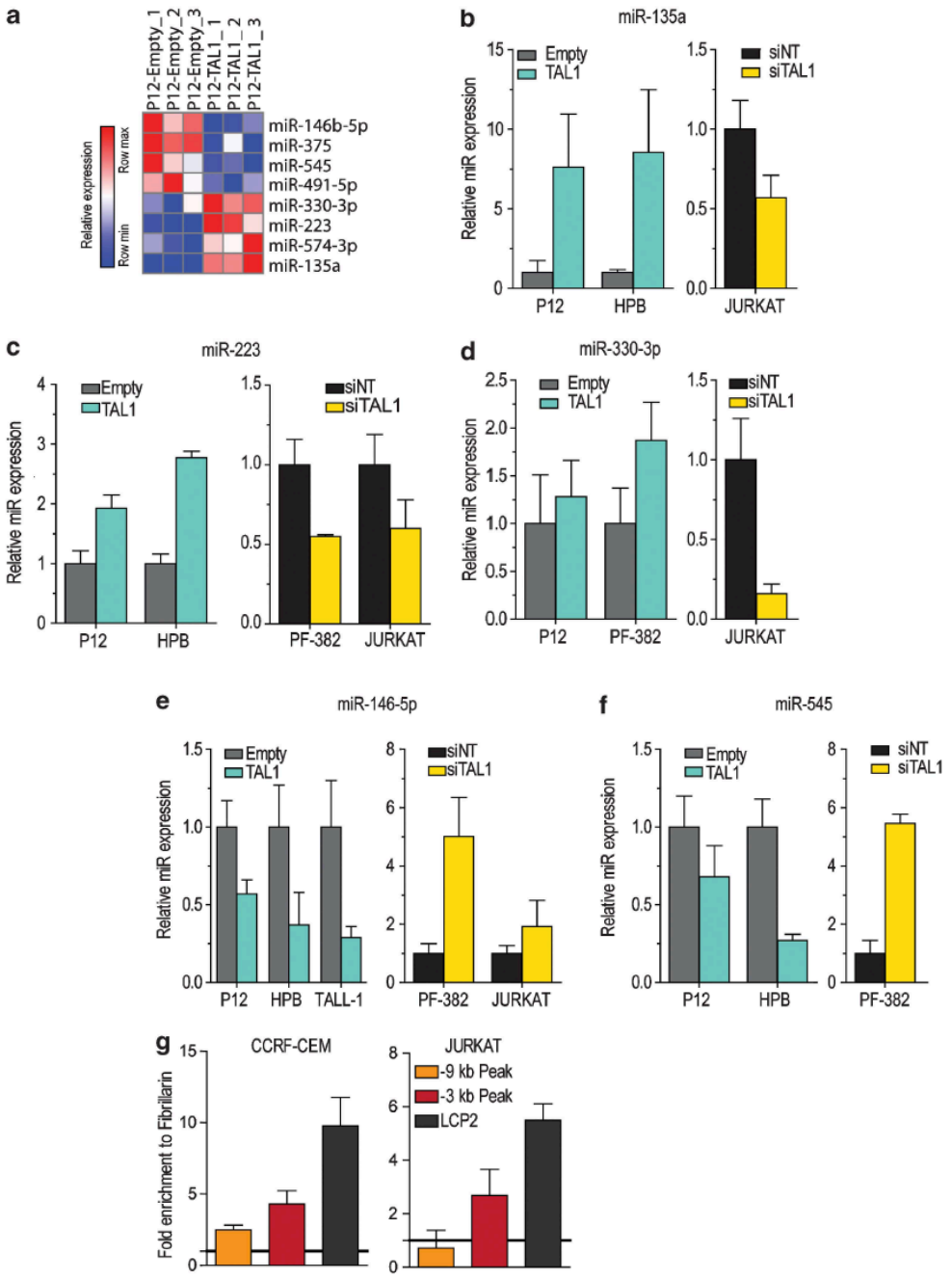


**Figure 1: Identification of TAL1-regulated microRNA genes.** (**a**) Heatmap of differentially expressed microRNAs upon TAL1 overexpression. MicroRNAs were hierarchically clustered (rows, microRNAs; columns, experiments). See Supplementary Table 2 for fold-difference values. Levels greater than or less than the mean are shown in shades of red or blue, respectively. (**b–f**) Quantitative PCR (qPCR) validation of microRNA expression modulation by TAL1. Relative expression of *hsa-miR-135a* (**b**), *hsa-miR-223* (**c**), *hsa-miR-330-3p* (**d**), *hsa-miR-146b-5p* (**e**), and *hsa-miR-545* (**f**) normalized to *SNORD38B* in T-ALL cell lines with overexpression (left) or knockdown of TAL1 (right). The bars represent the mean±s.d. of three independent replicates. siNT—non-targeting siRNA (**g**) TAL1 ChIP-qPCR in T-ALL cell lines. The occupancy by TAL1 of the genomic regions 9.2 and 3.5 kb upstream of the m*iR-223* transcription start site was analyzed by ChIP-qPCR in JURKAT and CCRF-CEM cells. The promoter region of *LCP2* was used as positive control for TAL1 binding, and a random intergenic region was used as negative control. TAL1 binding is expressed as the fold enrichment relative to a mock ChIP performed against fibrillarin. The error bars represent the 95% CI of the fold enrichment. The horizontal line denotes the fold enrichment detection for the negative control.

Interestingly, analysis of microRNA gene expression profiles in different T-ALL subsets[8] revealed that *TAL/LMO* primary samples (integrating *Sil-Tal1+* and *LMO+* cases, which frequently express high *TAL1* levels) display higher levels of *miR-223* (P =0.035) and tend to express lower levels of *miR-146b-5p* (P=0.092) than other T-ALL cases (**Supplementary Figure 2**). In line with these observations, *miR-223* appears to follow the same pattern of expression along normal human thymocyte development as TAL1,[10] with high levels in $CD34^+$ T-cell precursors and sharp downregulation in more differentiated subsets (**Supplementary Figure 3a**). A similar pattern was observed for *miR-135a* (**Supplementary Figure 3b**), in agreement with the notion that TAL1 positively regulates both genes. In contrast, *miR-146b-5p* is clearly upregulated in the double-positive to single-positive transition and is amongst the most upregulated microRNAs in mature, single-positive thymocytes.[11] The fact that *miR-146b-5p* levels associate with thymocyte maturation (**Supplementary Figure 4**) is in agreement with a model whereby TAL1 overexpression during leukemogenesis inhibits *miR-146b-5p* and promotes T-cell developmental arrest.

Data from the analysis of congruent putative interactions between known TAL1-regulated protein-coding genes and the validated microRNA genes are in line with the notion that the latter could be part of downstream networks collaborating in TAL1-mediated leukemogenesis (**Figure 2**). Indeed, most TAL1 upregulated genes that have 3'-UTRs predicted as targets for the TAL1-downregulated *miR-146b-5p* and *miR-545* have a known or putative oncogenic function (**Figure 2a**). For example, CD53 was shown to protect JURKAT cells from apoptosis, PDE3B appears to be involved in glucocorticoid resistance in CEM cells and ETS-1 participates in the T-cell maturation arrest mediated by *TLX* genes in T-ALL (see **Supplementary Table 3** for details and references). Interestingly, the T-ALL associated oncogene *MYB* was recently shown to be a direct TAL1 target forming a feed-forward loop involved in the TAL1-dependent leukemogenic program.[4] Our bioinformatics analyses now raise the possibility that TAL1 may reinforce *MYB* upregulation by inhibiting the expression of *miR- 545*. Also of note, three of the four genes (*KRT1*, *Rapgef5*, *JAZF1*) with predicted 3'-UTR seed sequences for both *miR-146b-5p* and *miR-545* are associated with protumoral functions (**Supplementary Table 3**). In sharp contrast,

the TAL1-downregulated genes that are predicted targets for *miR-135a*, *miR-223* and *miR-330-3p* display a clear abundance in (putative) tumor suppressors or in genes whose functions are compatible with anti-tumoral effects (**Figure 2b and Supplementary Table 4**). This is evident, for instance, in the case of the four genes potentially regulated by two microRNAs, in which only one has an oncogenic role (*IGF1R*) and three likely have tumor-suppressive functions (*SRGAP3*, *TOX*, *LRP12*).

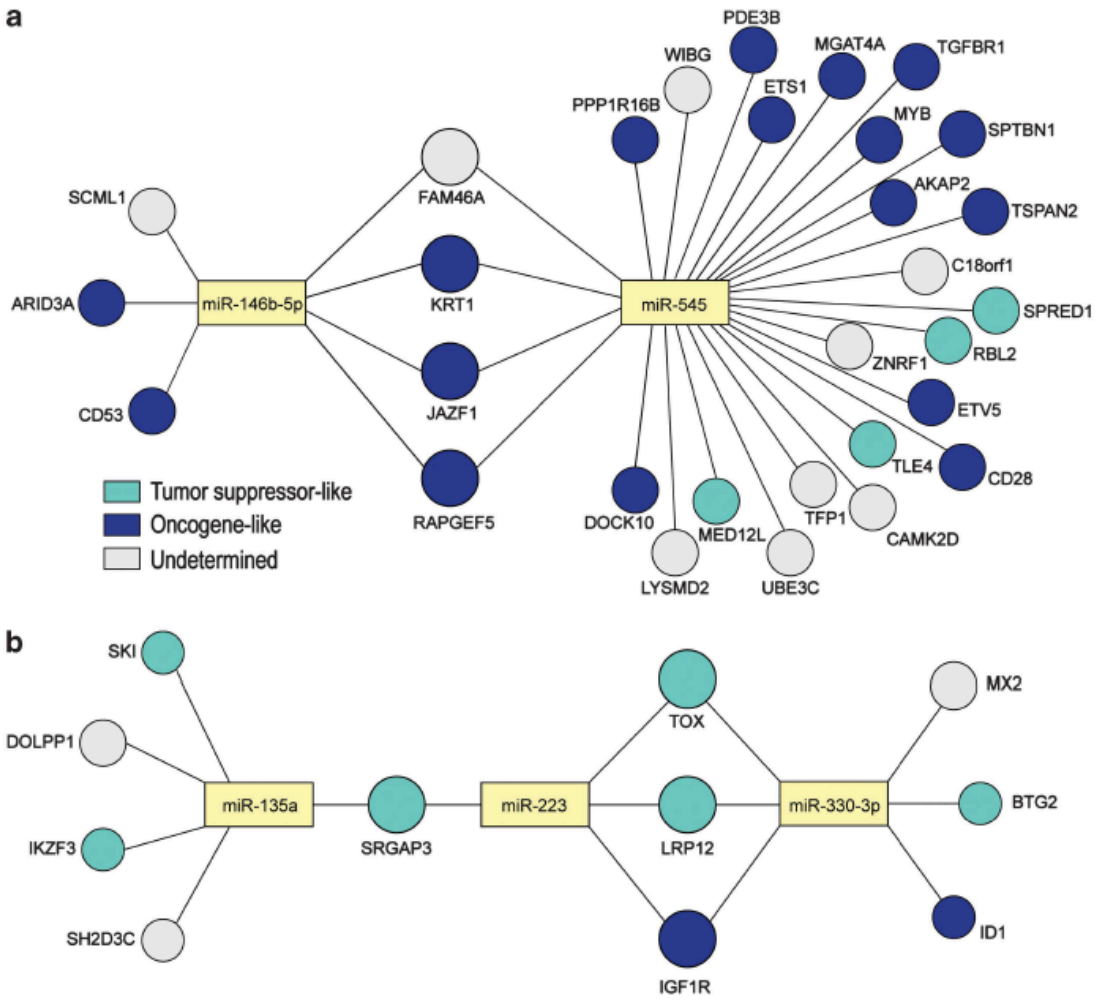


**Figure 2. Potential participation of the newly identified TAL1 microRNA target genes in TAL1-mediated leukemogenic pathways.** Cross-examination of congruent TAL1-regulated protein-coding and miRNA genes was performed as described in Supplementary Methods. (**a**) Downregulated miRNAs and their predicted target genes previously shown to be upregulated by TAL1. (**b**) Upregulated miRNAs and their predicted target genes previously shown to be downregulated by TAL1. Genes are color-coded according to their reported function in the context of cancer, as detailed in *Supplementary Tables 3 and 4*. '*Tumor suppressor-like*': *bona fide* or putative tumor suppressors or genes that have pro-apoptotic, anti-proliferative or pro-differentiating roles; '*Oncogene-like*': *bona fide* or putative oncogenes or genes that have anti-apoptotic or proliferative roles. '*Undetermined*': genes with undetermined function or whose role in cancer remains unknown.

Circumscription of our analysis to validate target genes of each microRNA, followed by gene set enrichment analysis showed an enrichment in biological processes related to inflammation (e.g. NF-kB signaling pathway and IL1/IL1R signaling pathway) and cancer (e.g. pathways in cancer), as detailed in **Supplementary Table 5 and Supplementary Table 6**. Interestingly, the validated targets for the TAL1-downregulated gene of *miR- 146-5p* include *IRAK1*, *TRAF6* and *NFKB1* (all of which are involved in chronic inflammation), as well as the oncogene *KIT* (**Supplementary Table 5 and Supplementary Figure 5**). In contrast, *miR-330-3p*, upregulated by TAL1, reportedly targets *E2F1* and *CDC42*, both of which are described to promote apoptosis in different cell types including Jurkat cells. *MiR-223* is a myeloid- specific microRNA essential for normal neutrophil maturation, and responsible for granulocyte differentiation and negative regulation of progenitor proliferation via *MEF2C* downregulation.[12] In agreement, *miR-223* functions as a tumor suppressor in acute myeloid leukemia,[13] and appears to be repressed in chronic myeloid leukemia, allowing for the expression of MEF2C.[14] In contrast, *miR-223* is frequently overexpressed in T-ALL, cooperating with NOTCH1 to accelerate the onset of disease in a Notch-induced leukemia mouse model. This effect was proposed to be due, at least in part, to inhibition of FBXW7, a negative regulator of Notch signaling.[8] However, FBXW7 targets the degradation of other oncogenic proteins, such as c-Myc and mTOR, and the expression of *miR-223* is significantly elevated in TAL1-positive T-ALL cases (**Supplementary Figure 2**), suggesting that the oncogenic function of this microRNA may extend beyond mere collaboration in Notch-induced leukemia. Moreover, the pro-leukemic role of mir-223 may be also achieved by downregulating targets such as *E2F1*, *FOXO1*, *RHOB* or *EPB41L3*, which have been associated with induction of apoptosis and/or have tumor-suppressive roles (**Supplementary Table 5**). Interestingly, the intriguing possibility that *miR-223* may potentially act downstream of TAL1 to negatively regulate *MEF2C*, recently identified as an oncogene in T-ALL,[15] would be in line with the observations that TAL1 and MEF2C tend to segregate, defining two discrete T-ALL subsets.[15] In summary, our studies identify and validate for the first time a small set of TAL1-regulated microRNA genes whose role may be important in the context of hematopoiesis and T-cell leukemogenesis.

**ACKNOWLEDGEMENTS**

This study was supported by grants from Fundacao para a Ciência e a Tecnologia (FCT; PTDC/BIM-ONC/1548/2012) and Liga Portuguesa Contra o Cancro (Terry Fox Award) to JTB; and FWO Vlaanderen (G056413N) and UGent (GOA 01G01910W) to FS. NCC and KD have PhD fellowships from FCT and IWT Vlaanderen, respectively. PR has a post-doctoral grant from FWO Vlaanderen. We would like to thank Steve Lefever for primer design.

**REFERENCES**

1. Ferrando AA, Neuberg DS, Staunton J, Loh ML, Huard C, Raimondi SC et al. Gene expression signatures define novel oncogenic pathways in T cell acute lympho-blastic leukemia. Cancer Cell 2002; 1: 75–87.

2. Cardoso BA, de Almeida SF, Laranjeira AB, Carmo-Fonseca M, Yunes JA, Coffer PJ et al. TAL1/SCL is downregulated upon histone deacetylase inhibition in T-cell acute lymphoblastic leukemia cells. Leukemia 2011; 25: 1578–1586.

3. O'Neil J, Shank J, Cusson N, Murre C, Kelliher M. TAL1/SCL induces leukemia by inhibiting the transcriptional activity of E47/HEB. Cancer Cell 2004; 5: 587–596.

4. Sanda T, Lawton LN, Barrasa MI, Fan ZP, Kohlhammer H, Gutierrez A et al. Core transcriptional regulatory circuit controlled by the TAL1 complex in human T cell acute lymphoblastic leukemia. Cancer Cell 2012; 22: 209–221.

5. Bartel DP. MicroRNAs: genomics, biogenesis, mechanism, and function. Cell 2004; 116: 281–297.

6. Schotte D, Pieters R, Den Boer ML. MicroRNAs in acute leukemia: from biological players to clinical contributors. Leukemia 2012; 26: 1–12.

7. Fabbri M, Croce CM, Calin GA. MicroRNAs in the ontogeny of leukemias and lymphomas. Leuk Lymphoma 2009; 50: 160–170.

8. Mavrakis KJ, Van Der Meulen J, Wolfe AL, Liu X, Mets E, Taghon T et al. A cooperative microRNA-tumor suppressor gene network in acute T-cell lymphoblastic leukemia (T-ALL). Nat Genet 2011; 43: 673–678.

9. Fukao, T., *et al.* An evolutionarily conserved mechanism for microRNA-223 expression revealed by microRNA gene profiling. *Cell* **129**, 617-631 (2007).

10. Pike-Overzet, K., *et al.* Ectopic retroviral expression of LMO2, but not IL2Rgamma, blocks human T-cell development from CD34+ cells: implications for leukemogenesis in gene therapy. *Leukemia* **21**, 754-763 (2007).

11. Ghisi, M., *et al.* Modulation of microRNA expression in human T-cell development: targeting of NOTCH3 by miR-150. *Blood* **117**, 7053-7062 (2011).

12. Johnnidis, J.B., *et al.* Regulation of progenitor cell proliferation and granulocyte function by microRNA-223. *Nature* **451**, 1125-1129 (2008).

13. Pulikkan, J.A., *et al.* Cell-cycle regulator E2F1 and microRNA-223 comprise an autoregulatory negative feedback loop in acute myeloid leukemia. *Blood* **115**, 1768 1778 (2010).

14. Agatheeswaran, S., *et al.* BCR-ABL mediated repression of miR-223 results in the activation of MEF2C and PTBP2 in chronic myeloid leukemia. *Leukemia* **27**, 1578-1580 (2013).

15. Homminga, I., *et al.* Integrated transcript and genome analyses reveal NKX2-1 and MEF2C as potential oncogenes in T cell acute lymphoblastic leukemia. *Cancer Cell* **19**, 484-497 (2011).

## Author contributions

NC and KD performed the experiments and wrote the manuscript; FJE, FSP and JTB supervised the experiments and writing of the manuscript.

**SUPPLEMENTARY METHODS**

**Transduction of T-ALL cells for TAL1 overexpression**

T-ALL cell lines were transduced with VSVG-pseudotyped bicistronic lentivirus driving the concomitant expression of TAL1 and GFP or with the control mock virus. The resulting cell lines expressing TAL1 or the empty vector were sorted for an

equivalent GFP expression. The viral production and transduction was performed as previously described[1].

**Transfection of T-ALL cells for TAL1 knockdown**

Nucleofection of JURKAT and PF-382 cells was performed using the Amaxa Nucleofector II (Lonza, Switzerland) according to the manufacturer's instructions. Cells (2x $10^6$) were washed in RPMI-10 medium and resuspended in 100 µl of solution V with 2 µM of a mock pool of small interfering RNAs (siRNAs) or a pool of siRNAs against TAL1 (Dharmacon, Lafayette, USA). JURKAT and PF-382 cells were nucleofected using the X-001and O-017 programs, respectively. After the nucleofection the cells were cultured for 48h in RPMI-10 medium.

**RNA extraction and microRNA expression assessment by RT-qPCR**

Total RNA was extracted using TRIZOL reagent (Life Technologies Corporation, Califor nia, USA) followed by further purification with commercially available kits that preserve the low molecular weight RNA species (miRVANA, Life Technologies Corporation, California, USA), following manufacturer's instructions. cDNA was produced with miRCURY LNA™ Universal RT kit (Exiqon, Denmark) using amounts that range from 100-200ng of total RNA. Real time PCR was performed with commercial available LNA-based primers for mature microRNA detection in SybrGreen (Exiqon, Denmark) quantitative PCR assays on the 7500 Real Time PCR system (Life Technologies Corporation, California, USA). Relative expression of the microRNAs was normalized to *SNORD38B* expression using the ddCt method.

**microRNA expression analysis**

Gene expression analysis for 372 human miRNA genes was performed in 3 independent samples of P12 mock transduced and P12 transduced with a vector driving the expression of TAL1, using a qRT-PCR based array (microRNA Ready-to-Use PCR, Human Panel I, V2.M, Exiqon). Total RNA was extracted, in 3 independent occasions, from P12-Empty and P12-TAL1 sorted cells. The RNA quality was assessed with an Agilent 2100 Bioanalyzer (Agilent Technologies, California, USA), assuring the

presence of low molecular weight RNA species and RNA integrity. A cut-off cycle threshold value of 35 was assigned and mean expression value normalization[2] used as normalization method. The p-value was calculated using a two-tailed Student's t-Test. Fold changes relative to mock transduced cells and p-values were determined by the Comparative Marker Selection suite[3]. Cut-offs for statistical significance were a p-value<0.05 and a fold change>1.5.

**Heat Map Illustration**

Heat map illustration of differentially expressed microRNAs upon TAL1 overexpression was generated with the GENE-E software (http://www.broadinstitute.org/cancer/software/GENE-E/). MicroRNAs were hierarchically clustered (rows, miRNAs; columns, experiments). Relative expression levels were normalized across the samples as described; levels greater than or less than the mean are shown in shades of red or blue, respectively. Confirmation of ChIP-seq enrichment by qPCR. Public available ChIP-seq (GEO accession number GSE29181) was analyzed with the Integrative Genomics Viewer (IGV) tool. To confirm the ChIP-seq data we performed ChIP of TAL1 in JURKAT and CCRF-CEM cells followed by qPCR for the selected genomic regions. ChIP was performed as described[4], using the following antibodies: TAL1 (Abcam), 10µg; Fibrillarin (Abcam), 10µg (Abcam). The occupancy by TAL1 of the genomic regions 9.2kb and 3.5kb upstream *miR-223* TSS was analyzedby ChIP-qPCR in the cell lines. The promoter region of LCP2[5] was used as a positive control for TAL1 binding and a random intergenic region was used as negative control. TAL1 binding was calculated as the fold enrichment relative to a mock ChIP performed against Fibrillarin.

Primers used:

*LCP2*-ChIP Fwd: AAGGCTGCTTTGGATCTTGAAA;

*LCP2*-ChIP Rev: CCTCCAGCCTGGCTGCTA;

*chip223peak*-3FWD:CCTGTTGAAGACACCAAGGGC;

*chip223 peak*-3REV:TTCCCCAGTGCTGAGCCAAC;

chip223peak-9FWD: GCAGTGGCTATTCACAGGTGACC;

*chip223peak*-9REV: CACTCCCACTATTCACATCACACCTG;

*Intergenic region* ChIP-Fwd: GGCTAATCCTCTATGGGAGTCTGTC;

*Intergenic region* ChIP Rev-CCAGGTGCTCAAGGTCAACATC

**miRNA target prediction and gene set enrichment analysis**

Prediction of microRNA putative targets was performed by MirDIP data integration portal[6], with a minimum threshold of 4 different applications. MicroRNAs experimentally validated human targets were obtained from mirTARbase 3.5, miRrecords and TarBase 6.0. Target genes without matching Entrez gene identifiers in NCBI were discarded. Graphical representation and analysis of miRNA and their cognate targets was done with Navigator software[7]. We compiled a list of high confidence TAL1 positively or negatively regulated genes from publicly available data[5, 8]. For cross-examination of congruent TAL1 regulated protein-coding and miRNA genes, we intersected the predicted targets of TAL1 downregulated microRNAs with the protein-coding gene targets previously demonstrated to be positively regulated by TAL1, and vice versa, and searched for common hits in both lists. For biological function and pathway analysis we collected T-lymphocyte and T-ALL related gene sets from Ingenuity Pathway Analysis (IPA), and from the literature[5, 8, 9]. Additional gene sets were downloaded from version 3.1 of the Molecular Signature Database (MSigDB) at the Broad Institute (http://www.broad.mit.edu/gsea/msigdb); we used three categories of gene sets from MSigDB: (C2) all curated gene sets, (C5) GO biological processes and molecular functions, and (C6) all oncogenic signatures gene sets. Gene set enrichment analysis was performed using Genomica software (http://genomica.weizmann.ac.il/). P-values were determined by a hypergeometric test, followed by a false discovery rate correction to account for multiple hypotheses (FDR < 0.05).

**SUPPLEMENTARY REFERENCES**

1. Cardoso BA, de Almeida SF, Laranjeira AB, Carmo-Fonseca M, Yunes JA, Coffer PJ , et al. TAL1/SCL is downregulated upon histone deacetylase inhibition in T-cell acute lymphoblastic leukemia cells. Leukemia : official journal of the Leukemia Society of America, Leukemia Research Fund, UK 2011 Oct; 25(10):1578-1586.

2. Mestdagh P, Van Vlierberghe P, De Weer A, Muth D, Westermann F, Speleman F, et al. A novel and universal method for microRNA RT-qPCR data normalization. Genome biology 2009; 10(6):R64.

3. Gould J, Getz G, Monti S, Reich M, Mesirov JP. Comparative gene marker selection suite. Bioinformatics 2006 Aug 1; 22(15):1924-1925.

4. Lee TI, Johnstone SE, Young RA. Chromatin immunoprecipitation and microarray based analysis of protein location. Nature protocols 2006; 1(2):729-748.

5. Palii CG, Perez-Iratxeta C, Yao Z, Cao Y, Dai F, Davison J, et al. Differential genomic targeting of the transcription factor TAL1 in alternate haematopoietic lineages. The EMBO journal 2011 Feb 2; 30(3):494-509.

6. Shirdel EA, Xie W, Mak TW, Jurisica I. NAViGaTing the micronome-using multiple microRNA prediction databases to identify signalling pathway-associated microRNAs. PloS one 2011; 6(2):e17429.

7. Brown KR, Otasek D, Ali M, McGuffin MJ, Xie W, Devani B, et al. NAViGaTOR: Network Analysis, Visualization and Graphing Toronto. Bioinformatics 2009 Dec 15; 25(24):3327-3329.

8. Sanda T, Lawton LN, Barrasa MI, Fan ZP, Kohlhammer H, Gutierrez A, et al. Core transcriptional regulatory circuit controlled by the TAL1 complex in human T cell acute lymphoblastic leukemia. Cancer cell 2012 Aug 14; 22(2):209-221.

9. Lee MS, Hanspers K, Barker CS, Korn AP, McCune JM. Gene expression profiles during human CD4+ T cell differentiation. International immunology 2004 Aug; 16(8):1109-1124.

## SUPPLEMENTARY FIGURES

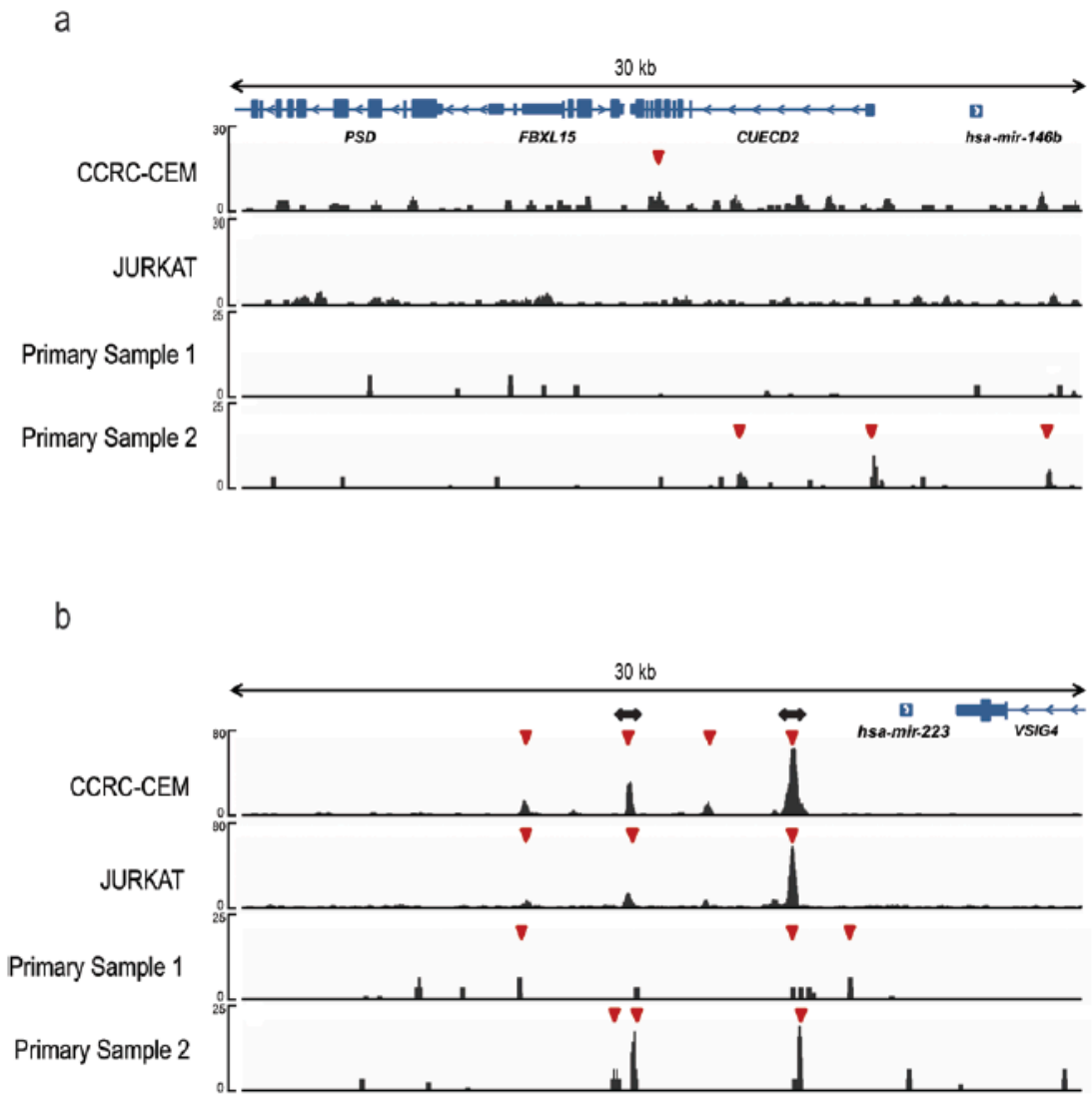


**Supplementary Figure 1: Evidence for direct binding of TAL1 to *miR-146b* and *miR-223* loci**
Analysis of publicly available ChIP-seq data for JURKAT, CCRF-CEM and two primary T-ALL samples (GEO accession number GSE29181). Representative Integrative Genomics Viewer (IGV) gene tracks show TAL1 binding peaks detected in the genomic area upstream of the *miR-146b* (**a**) and *miR-223* (**b**) TSS, whose direction of transcription is indicated by an arrow. The arrow heads indicate regions bound by TAL1. The top horizontal bars indicate the scale in kilobases (kb). The black double arrows indicate the genomic areas to which primers were designed to validate TAL1 binding by ChIP-qPCR.

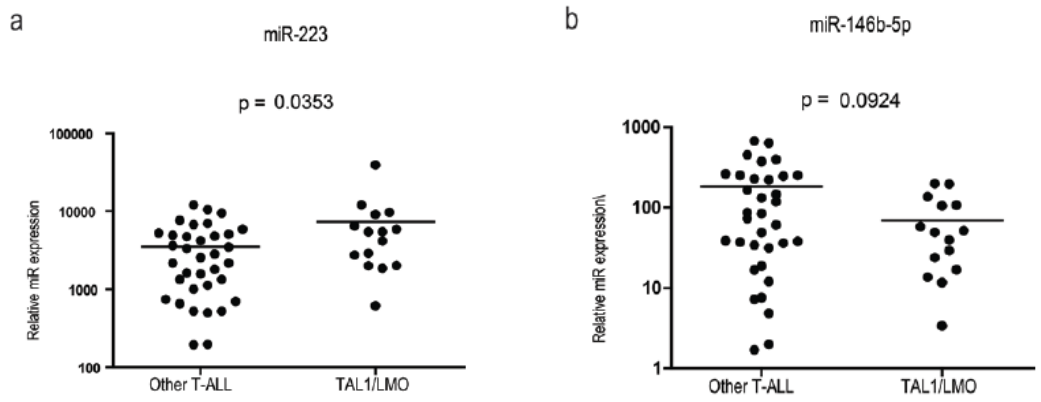


**Supplementary Figure 2. Analysis of microRNA gene expression levels in different T-ALL subsets.** *TAL/LMO* primary samples (integrating *Sil-Tal1+* and *LMO+)* display higher levels of *miR-223* **(a)** and lower levels of *miR-146b-5p* **(b)** than other T-ALL cases. Data was collected from[8]. P-values were calculated using a two-tailed Student's t-Test.

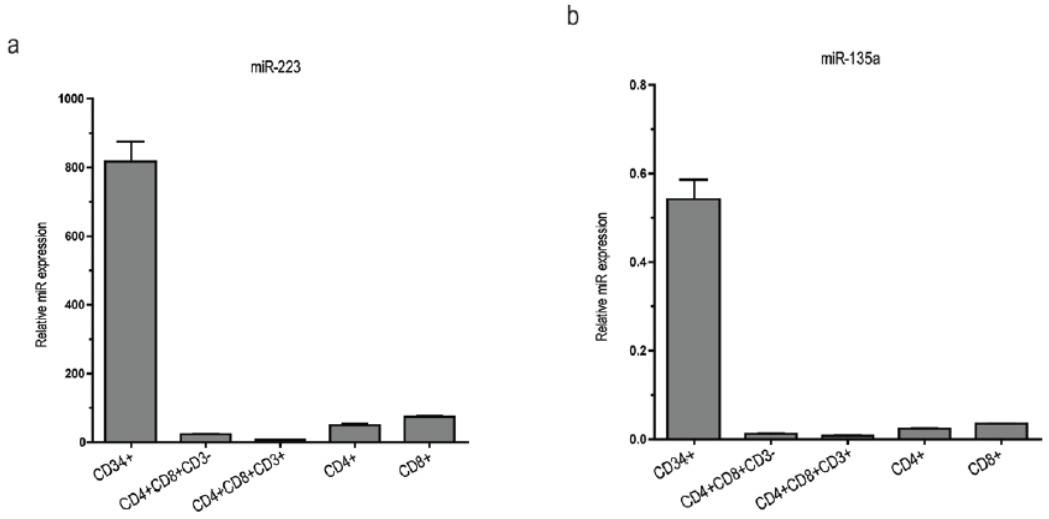


**Supplementary Figure 3. Analysis of microRNA gene expression levels in normal human thymocyte subsets.** *miR-223* **(a)** and *miR-135a* **(b)** are expressed in immature $CD34^+$ cells and their expression is dramatically downregulated in more mature $CD4^+CD8^+$ thymocytes. Data was collected from[8].

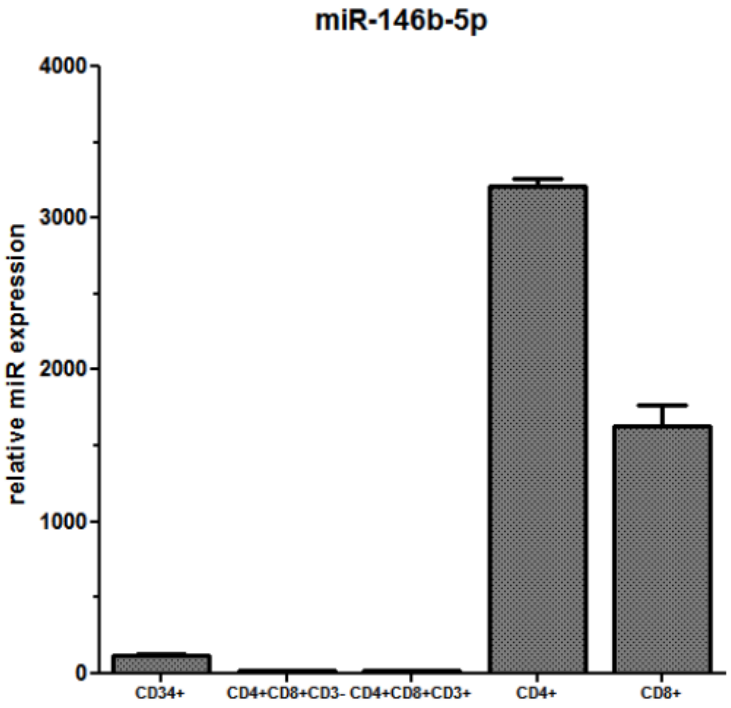


**Supplementary Figure 4. Analysis of *miR-146b-5p* gene expression levels in normal human thymocyte subsets.** *miR-146b-5p* expression is clearly upregulated in mature SP ($CD4^+$ or $CD8^+$) thymocytes. Data was collected from[8].

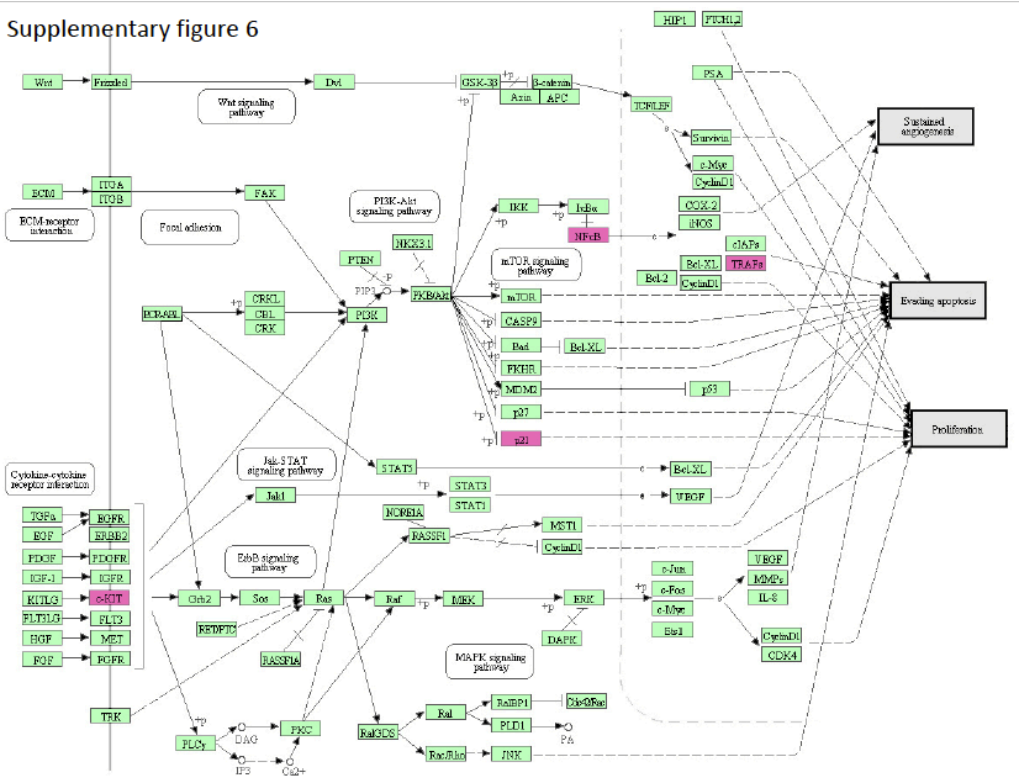


**Supplementary Figure 5. Association of *miR-146b-5p* target genes with cancer pathways.** Highlighted are experimentally validated target genes of *miR-146b-5p* (see *Supplementary Table 5*) within a zoomed representation of KEGG Pathways in Cancer.

## SUPPLEMENTARY TABLES

| Detector Name | Ct Empty 1 | Ct Empty 2 | Ct Empty 3 | Ct Tal1 1 | Ct Tal1 2 | Ct Tal1 3 | ddCT | FC | p-value |
|---|---|---|---|---|---|---|---|---|---|
| hsa-miR-135a | 3.82 | 3.45 | 4.09 | 0.20 | 0.26 | -0.16 | -3.69 | 12.90 | 0.000082 |
| hsa-miR-223 | -6.62 | -6.54 | -6.54 | -7.33 | -7.26 | -7.04 | -0.64 | 1.56 | 0.002056 |
| hsa-miR-146b-5p | 3.26 | 3.64 | 3.45 | 4.62 | 4.43 | 4.11 | 0.94 | 0.52 | 0.007100 |
| hsa-miR-503 | -0.51 | -0.66 | -0.67 | -1.18 | -0.99 | -0.93 | -0.42 | 1.34 | 0.010567 |
| hsa-miR-652 | -2.30 | -2.51 | -2.45 | -2.78 | -2.74 | -3.01 | -0.42 | 1.34 | 0.016594 |
| hsa-miR-545 | 3.65 | 3.97 | 4.11 | 4.52 | 4.37 | 4.67 | 0.61 | 0.66 | 0.019659 |
| hsa-miR-148a | -3.36 | -3.42 | -3.37 | -3.21 | -3.03 | -2.89 | 0.34 | 0.79 | 0.021373 |
| hsa-miR-20b | -2.59 | -2.67 | -2.62 | -2.78 | -2.94 | -2.78 | -0.21 | 1.15 | 0.021580 |
| hsa-miR-574-3p | 6.25 | 6.75 | 7.19 | 5.75 | 5.87 | 5.24 | -1.11 | 2.16 | 0.028828 |
| hsa-miR-20a | -8.16 | -8.27 | -8.09 | -8.02 | -7.82 | -7.90 | 0.26 | 0.84 | 0.029180 |
| hsa-miR-491-5p | 2.63 | 2.33 | 2.82 | 3.16 | 3.53 | 3.03 | 0.64 | 0.64 | 0.034590 |
| hsa-miR-375 | 3.09 | 3.34 | 3.25 | 5.56 | 3.94 | 6.06 | 1.96 | 0.26 | 0.038284 |
| hsa-miR-150 | -2.63 | -2.48 | -2.64 | -3.14 | -2.94 | -2.76 | -0.37 | 1.29 | 0.038396 |
| hsa-miR-330-3p | 2.69 | 3.11 | 2.41 | 1.97 | 2.20 | 2.12 | -0.64 | 1.55 | 0.040909 |
| hsa-miR-181a | -7.31 | -7.02 | -7.38 | -7.71 | -7.58 | -7.52 | -0.37 | 1.29 | 0.042010 |
| hsa-miR-146a | -1.19 | -0.90 | -1.12 | -1.62 | -1.30 | -1.44 | -0.38 | 1.30 | 0.042392 |
| hsa-miR-501-5p | 1.52 | 1.40 | 1.49 | 1.61 | 1.91 | 1.69 | 0.27 | 0.83 | 0.049712 |
| hsa-miR-29b-2* | 0.13 | 0.51 | 0.18 | -0.28 | 0.04 | -0.18 | -0.41 | 1.33 | 0.054029 |
| hsa-miR-153 | -4.17 | -4.06 | -4.08 | -4.25 | -4.20 | -4.18 | -0.11 | 1.08 | 0.055977 |
| hsa-miR-219-5p | 0.16 | 0.02 | -0.29 | 0.20 | 0.54 | 0.43 | 0.43 | 0.74 | 0.061502 |
| hsa-miR-30d | -1.17 | -0.85 | -1.09 | -0.33 | -0.79 | 0.09 | 0.70 | 0.62 | 0.062895 |
| hsa-miR-193b | -0.59 | 0.48 | 0.62 | 1.14 | 1.03 | 1.78 | 1.14 | 0.45 | 0.063713 |
| hsa-miR-107 | -5.49 | -5.41 | -5.38 | -5.31 | -5.06 | -5.27 | 0.21 | 0.86 | 0.063745 |
| hsa-miR-425 | -2.99 | -3.28 | -2.81 | -3.51 | -3.64 | -3.27 | -0.45 | 1.36 | 0.064679 |
| hsa-miR-130b | -1.28 | -0.99 | -1.34 | -0.98 | -0.67 | -0.89 | 0.35 | 0.78 | 0.065254 |
| hsa-miR-27b | -1.65 | -1.46 | -1.73 | -1.37 | -1.47 | -1.30 | 0.23 | 0.85 | 0.066819 |
| hsa-miR-484 | -3.67 | -3.51 | -3.66 | -3.53 | -3.28 | -3.39 | 0.22 | 0.86 | 0.067794 |
| hsa-miR-514 | 6.25 | 6.21 | 6.11 | 7.27 | 6.42 | 6.75 | 0.62 | 0.65 | 0.069056 |
| hsa-miR-590-5p | -2.13 | -2.26 | -1.92 | -1.92 | -1.81 | -1.81 | 0.26 | 0.84 | 0.069945 |
| hsa-miR-500 | 1.50 | 2.02 | 1.30 | 0.77 | 1.19 | 1.04 | -0.61 | 1.52 | 0.070630 |
| hsa-miR-425* | -0.82 | -0.53 | -0.69 | -0.43 | -0.35 | -0.54 | 0.24 | 0.85 | 0.073797 |
| hsa-miR-766 | -2.47 | -2.41 | -2.43 | -2.25 | -2.16 | -2.40 | 0.17 | 0.89 | 0.074513 |
| hsa-miR-151-5p | 0.19 | -0.07 | 0.33 | -0.70 | -0.18 | -0.16 | -0.50 | 1.41 | 0.078148 |
| hsa-miR-509-3p | 5.82 | 7.44 | 7.01 | 4.58 | 5.39 | 5.94 | -1.45 | 2.73 | 0.081093 |
| hsa-miR-362-5p | 4.26 | 3.81 | 4.09 | 3.74 | 3.67 | 3.80 | -0.32 | 1.25 | 0.082577 |
| hsa-miR-142-3p | -9.38 | -9.53 | -9.58 | -9.64 | 10.09 | -9.75 | -0.33 | 1.26 | 0.087948 |
| hsa-miR-92b | -1.62 | -1.93 | -1.75 | -0.91 | -1.50 | -1.50 | 0.46 | 0.73 | 0.103038 |
| hsa-miR-328 | 0.66 | 1.11 | 0.96 | 0.51 | 0.58 | 0.73 | -0.30 | 1.23 | 0.111700 |
| hsa-miR-450a | -0.33 | 0.06 | 0.01 | -0.24 | -0.39 | -0.50 | -0.29 | 1.22 | 0.113072 |
| hsa-miR-589 | 2.75 | 3.00 | 3.17 | 2.83 | 2.69 | 2.46 | -0.32 | 1.24 | 0.125328 |
| hsa-miR-101 | -2.58 | -2.42 | -2.54 | -2.31 | -2.49 | -2.34 | 0.14 | 0.91 | 0.129458 |
| hsa-miR-423-5p | -2.29 | -2.33 | -2.52 | -2.25 | -1.88 | -2.22 | 0.26 | 0.83 | 0.129647 |
| hsa-miR-199b-5p | 3.94 | 3.17 | 3.69 | 3.28 | 2.82 | 3.21 | -0.49 | 1.41 | 0.139039 |
| hsa-miR-760 | 4.42 | 4.29 | 3.95 | 5.25 | 6.46 | 4.38 | 1.14 | 0.45 | 0.139471 |
| hsa-miR-22* | 3.54 | 3.25 | 3.39 | 3.58 | 3.68 | 3.48 | 0.19 | 0.88 | 0.139646 |
| hsa-miR-26a-2* | 5.99 | 5.13 | 5.39 | 6.26 | 6.54 | 5.69 | 0.66 | 0.63 | 0.139965 |
| hsa-miR-361-5p | 5.62 | 5.89 | 6.11 | 6.04 | 6.99 | 6.31 | 0.57 | 0.67 | 0.142388 |
| hsa-miR-424 | -4.27 | -4.34 | -4.08 | -4.51 | -4.32 | -4.38 | -0.17 | 1.13 | 0.149796 |
| hsa-miR-194 | 2.48 | 2.27 | 2.54 | 1.27 | 1.71 | 2.44 | -0.63 | 1.54 | 0.150582 |
| hsa-miR-98 | 6.45 | 7.21 | 6.60 | 5.71 | 6.56 | 6.24 | -0.59 | 1.50 | 0.158025 |
| hsa-miR-18b | -4.71 | -5.05 | -4.97 | -4.56 | -4.73 | -4.81 | 0.21 | 0.86 | 0.170112 |

| | | | | | | | | | |
|---|---|---|---|---|---|---|---|---|---|
| hsa-miR-188-5p | 3.81 | 3.39 | 3.52 | 3.83 | 3.87 | 4.98 | 0.66 | 0.63 | 0.171733 |
| hsa-let-7g | -2.45 | -2.09 | -2.04 | -2.01 | -1.93 | -1.99 | 0.21 | 0.86 | 0.176532 |
| hsa-miR-151-3p | 1.10 | 1.11 | 2.07 | 1.67 | 2.79 | 2.07 | 0.75 | 0.59 | 0.177609 |
| hsa-miR-196b | 0.22 | 0.40 | 0.24 | 0.30 | 0.48 | 0.68 | 0.20 | 0.87 | 0.179888 |
| hsa-miR-140-3p | -1.74 | -1.58 | -1.96 | -2.27 | -2.04 | -1.81 | -0.28 | 1.21 | 0.180941 |
| hsa-miR-15b | -5.79 | -6.03 | -6.01 | -6.05 | -6.58 | -6.09 | -0.30 | 1.23 | 0.184828 |
| hsa-miR-128 | -4.52 | -4.51 | -4.24 | -4.28 | -4.14 | -4.34 | 0.17 | 0.89 | 0.185386 |
| hsa-miR-374b* | 5.79 | 5.30 | 4.54 | 5.65 | 7.51 | 5.79 | 1.11 | 0.46 | 0.187952 |
| hsa-miR-642 | 4.77 | 4.58 | 5.33 | 5.16 | 5.17 | 5.58 | 0.41 | 0.75 | 0.193765 |
| hsa-miR-365 | -0.16 | 0.07 | 0.16 | 0.20 | 0.10 | 0.80 | 0.34 | 0.79 | 0.221041 |
| hsa-miR-502-5p | -1.78 | -2.12 | -2.26 | -2.40 | -2.06 | -3.03 | -0.45 | 1.36 | 0.232702 |
| hsa-miR-181d | 1.65 | 1.26 | 1.23 | 1.56 | 1.50 | 1.75 | 0.22 | 0.86 | 0.233556 |
| hsa-miR-570 | 3.36 | 2.13 | 2.38 | 2.27 | 2.00 | 1.99 | -0.54 | 1.45 | 0.235832 |
| hsa-miR-196a | 0.31 | 0.43 | 0.42 | 0.20 | 0.42 | 0.20 | -0.11 | 1.08 | 0.256236 |
| hsa-miR-20b* | 0.34 | 0.63 | 0.47 | 0.47 | 0.82 | 0.66 | 0.17 | 0.89 | 0.267089 |
| hsa-miR-103 | -6.97 | -6.79 | -6.91 | -7.03 | -6.90 | -7.02 | -0.09 | 1.06 | 0.268748 |
| hsa-miR-30c | -5.00 | -4.78 | -5.32 | -5.23 | -5.31 | -5.18 | -0.21 | 1.15 | 0.268926 |
| hsa-miR-200c | 3.54 | 3.08 | 3.57 | 3.34 | 3.96 | 3.86 | 0.32 | 0.80 | 0.270059 |
| hsa-miR-23a | -0.85 | -0.72 | -0.43 | -1.16 | -1.04 | -0.60 | -0.27 | 1.20 | 0.271755 |
| hsa-miR-199a-3p | 4.39 | 3.74 | 3.47 | 4.54 | 4.02 | 4.22 | 0.39 | 0.76 | 0.277362 |
| hsa-miR-126 | 1.40 | 1.56 | 1.37 | 1.05 | 1.43 | 1.36 | -0.16 | 1.12 | 0.277853 |
| hsa-miR-9 | 0.27 | 0.89 | 0.94 | -0.10 | 0.80 | 0.10 | -0.44 | 1.35 | 0.278480 |
| hsa-miR-141 | 5.00 | 5.06 | 4.50 | 4.82 | 4.47 | 4.47 | -0.27 | 1.20 | 0.279235 |
| hsa-miR-30c-2* | 4.03 | 2.62 | 2.59 | 4.83 | 3.53 | 3.35 | 0.82 | 0.57 | 0.283335 |
| hsa-miR-222 | -0.48 | -1.39 | -1.35 | -1.58 | -1.35 | -1.42 | -0.38 | 1.30 | 0.284723 |
| hsa-miR-181b | -4.43 | -4.91 | -5.07 | -4.99 | -4.92 | -5.31 | -0.27 | 1.21 | 0.296664 |
| hsa-miR-193a-5p | 6.31 | 5.78 | 6.32 | 6.31 | 6.62 | 6.22 | 0.25 | 0.84 | 0.308875 |
| hsa-miR-340 | 1.61 | 1.80 | 1.26 | 1.03 | 1.14 | 1.66 | -0.28 | 1.21 | 0.326468 |
| hsa-miR-138 | 3.09 | 2.33 | 2.81 | 3.01 | 3.66 | 2.71 | 0.39 | 0.76 | 0.338066 |
| hsa-let-7f | -2.25 | -2.25 | -1.96 | -2.16 | -1.83 | -2.05 | 0.14 | 0.91 | 0.352603 |
| hsa-miR-193a-3p | 5.85 | 7.30 | 7.10 | 6.92 | 5.71 | 5.71 | -0.63 | 1.55 | 0.354666 |
| hsa-miR-18a | -3.85 | -4.01 | -4.15 | -3.81 | -3.76 | -4.05 | 0.13 | 0.91 | 0.355906 |
| hsa-miR-629 | 1.05 | 1.06 | 0.62 | 0.39 | 0.58 | 1.02 | -0.25 | 1.19 | 0.359113 |
| hsa-miR-296-5p | 6.17 | 4.98 | 7.32 | 6.35 | 4.62 | 4.81 | -0.90 | 1.86 | 0.359666 |
| hsa-miR-132 | 0.13 | 0.19 | 0.32 | 0.18 | 0.28 | 0.76 | 0.19 | 0.88 | 0.360467 |
| hsa-miR-182 | -2.53 | -2.32 | -2.34 | -2.63 | -2.48 | -2.37 | -0.10 | 1.07 | 0.370423 |
| hsa-miR-602 | 4.03 | 5.35 | 4.03 | 3.70 | 3.51 | 4.57 | -0.54 | 1.46 | 0.377500 |
| hsa-miR-96 | -2.17 | -2.02 | -2.19 | -2.16 | -1.92 | -2.04 | 0.09 | 0.94 | 0.387327 |
| hsa-miR-215 | 1.65 | 1.48 | 1.88 | 1.65 | 1.39 | 1.56 | -0.14 | 1.10 | 0.389938 |
| hsa-miR-23b | -0.83 | -0.58 | -0.58 | -0.73 | -0.33 | -0.52 | 0.13 | 0.91 | 0.391212 |
| hsa-miR-625* | 0.18 | -0.33 | -0.17 | -0.42 | 0.69 | 0.47 | 0.35 | 0.78 | 0.398829 |
| hsa-miR-374a | 0.29 | 0.26 | -0.30 | 0.32 | 0.39 | 0.11 | 0.19 | 0.88 | 0.416088 |
| hsa-miR-26a | -4.99 | -4.63 | -4.66 | -4.67 | -4.83 | -4.15 | 0.21 | 0.86 | 0.417115 |
| hsa-miR-19a | -3.73 | -3.91 | -3.89 | -3.94 | -4.43 | -3.73 | -0.19 | 1.14 | 0.418386 |
| hsa-miR-361-3p | 1.07 | 0.97 | 0.92 | 1.01 | 0.83 | 0.94 | -0.06 | 1.04 | 0.418523 |
| hsa-miR-622 | 6.03 | 4.99 | 5.29 | 6.78 | 6.14 | 5.00 | 0.53 | 0.69 | 0.429399 |
| hsa-miR-550 | 3.09 | 3.40 | 3.58 | 3.09 | 2.66 | 3.56 | -0.26 | 1.19 | 0.434541 |
| hsa-miR-31 | 2.54 | 1.31 | 2.01 | 2.66 | 2.17 | 2.06 | 0.35 | 0.79 | 0.438209 |
| hsa-miR-572 | -0.17 | 0.01 | -0.23 | 0.05 | -0.39 | 0.99 | 0.35 | 0.78 | 0.445683 |
| hsa-miR-532-5p | 1.28 | 0.50 | 0.02 | 0.25 | 0.54 | -0.01 | -0.34 | 1.26 | 0.448130 |
| hsa-miR-324-3p | -2.27 | -2.22 | -2.16 | -2.33 | -2.30 | -2.17 | -0.05 | 1.04 | 0.450359 |
| hsa-miR-30e | -1.97 | -1.35 | -1.32 | -1.74 | -1.16 | -0.95 | 0.26 | 0.83 | 0.452450 |
| hsa-miR-106a | -7.88 | -7.87 | -7.88 | -7.93 | -7.84 | -7.93 | -0.03 | 1.02 | 0.453527 |
| hsa-let-7e | 5.03 | 5.35 | 5.14 | 5.14 | 5.28 | 5.40 | 0.10 | 0.93 | 0.464845 |
| hsa-miR-663 | 2.74 | 1.94 | 1.73 | 2.67 | 2.10 | 2.47 | 0.28 | 0.83 | 0.469921 |
| hsa-miR-671-5p | 1.33 | 1.28 | 0.88 | 1.27 | 1.55 | 1.11 | 0.15 | 0.90 | 0.470775 |
| hsa-miR-221 | -2.52 | -2.48 | -1.95 | -2.71 | -2.37 | -2.38 | -0.17 | 1.13 | 0.475720 |

| | | | | | | | | | |
|---|---|---|---|---|---|---|---|---|---|
| hsa-miR-139-5p | 4.08 | 4.42 | 4.49 | 5.13 | 4.18 | 4.40 | 0.24 | 0.84 | 0.481149 |
| hsa-miR-93 | -7.09 | -6.78 | -6.95 | -7.14 | -6.93 | -7.01 | -0.08 | 1.06 | 0.481216 |
| hsa-miR-665 | 2.37 | 1.71 | 1.02 | 2.25 | 0.26 | 0.96 | -0.54 | 1.46 | 0.483505 |
| hsa-let-7d | 3.47 | 5.99 | 4.19 | 3.85 | 4.01 | 4.07 | -0.57 | 1.49 | 0.487519 |
| hsa-miR-200a | 5.96 | 7.12 | 5.21 | 6.12 | 6.66 | 6.84 | 0.45 | 0.73 | 0.497809 |
| hsa-let-7a | -0.89 | -2.12 | -2.08 | -2.04 | -1.84 | -2.14 | -0.31 | 1.24 | 0.500801 |
| hsa-miR-30e* | -0.62 | -1.31 | -0.78 | -0.78 | -0.56 | -0.86 | 0.17 | 0.89 | 0.502214 |
| hsa-miR-301b | -1.14 | -0.56 | -0.68 | -1.31 | -1.07 | -0.60 | -0.20 | 1.15 | 0.505207 |
| hsa-let-7d* | 1.33 | 1.28 | 1.09 | 1.30 | 1.15 | 1.03 | -0.08 | 1.05 | 0.513348 |
| hsa-miR-345 | 1.17 | 0.89 | 1.86 | 0.96 | 1.17 | 1.16 | -0.21 | 1.16 | 0.520043 |
| hsa-miR-197 | -2.46 | -2.37 | -2.53 | -2.67 | -2.45 | -2.43 | -0.06 | 1.05 | 0.525333 |
| hsa-miR-195 | 2.83 | 2.97 | 5.29 | 3.29 | 3.17 | 3.00 | -0.54 | 1.46 | 0.535421 |
| hsa-miR-301a | -3.82 | -3.86 | -3.88 | -4.03 | -3.65 | -3.62 | 0.09 | 0.94 | 0.542762 |
| hsa-miR-28-5p | -0.65 | -0.02 | -0.06 | -0.44 | 0.15 | 0.12 | 0.19 | 0.88 | 0.544032 |
| hsa-miR-660 | 1.28 | 1.21 | 0.89 | 2.56 | 1.14 | 0.78 | 0.37 | 0.78 | 0.546601 |
| hsa-miR-145 | 2.45 | 2.64 | 2.35 | 2.55 | 2.41 | 2.74 | 0.08 | 0.94 | 0.550921 |
| hsa-miR-16 | -6.98 | -6.93 | -6.87 | -6.18 | -6.94 | -7.11 | 0.18 | 0.88 | 0.556475 |
| hsa-miR-363* | 3.61 | 4.63 | 4.68 | 4.46 | 3.92 | 3.76 | -0.26 | 1.20 | 0.557152 |
| hsa-miR-30b* | 1.88 | 1.31 | 1.83 | 2.07 | 1.18 | 1.09 | -0.23 | 1.17 | 0.564083 |
| hsa-miR-548b-3p | 6.17 | 5.93 | 5.12 | 6.23 | 5.30 | 6.66 | 0.32 | 0.80 | 0.566582 |
| hsa-miR-615-3p | 3.87 | 4.56 | 3.85 | 4.25 | 3.89 | 4.79 | 0.21 | 0.86 | 0.573312 |
| hsa-miR-21* | 2.80 | 2.45 | 2.86 | 2.81 | 2.50 | 2.52 | -0.09 | 1.07 | 0.590173 |
| hsa-miR-106b | -3.21 | -3.50 | -3.44 | -2.82 | -3.49 | -3.46 | 0.13 | 0.91 | 0.609844 |
| hsa-miR-34c-3p | 2.27 | 2.89 | 2.61 | 2.12 | 3.17 | 1.69 | -0.26 | 1.20 | 0.612025 |
| hsa-miR-29a | -0.79 | -1.21 | -1.40 | -1.36 | -1.08 | -1.29 | -0.11 | 1.08 | 0.612360 |
| hsa-miR-190 | 3.18 | 3.05 | 3.27 | 4.06 | 2.92 | 3.11 | 0.19 | 0.88 | 0.620201 |
| hsa-miR-505 | 0.46 | 0.32 | -0.03 | 0.44 | 0.44 | 0.15 | 0.09 | 0.94 | 0.621448 |
| hsa-miR-181c | 0.68 | 0.61 | 1.18 | 0.79 | 1.06 | 0.92 | 0.10 | 0.93 | 0.622658 |
| hsa-miR-155 | -2.32 | -1.99 | -2.10 | -2.24 | -2.00 | -1.96 | 0.07 | 0.95 | 0.623293 |
| hsa-miR-216b | 5.39 | 5.15 | 5.09 | 5.38 | 5.46 | 4.08 | -0.24 | 1.18 | 0.629242 |
| hsa-miR-346 | 3.84 | 3.32 | 4.04 | 3.56 | 3.72 | 4.47 | 0.18 | 0.88 | 0.637894 |
| hsa-miR-7 | 0.51 | 0.05 | -0.41 | -0.01 | 0.59 | 0.07 | 0.17 | 0.89 | 0.639984 |
| hsa-miR-27a | -1.85 | -1.81 | -1.67 | -1.77 | -1.86 | -1.78 | -0.03 | 1.02 | 0.644751 |
| hsa-miR-148b | -3.14 | -2.85 | -2.83 | -2.93 | -3.12 | -2.95 | -0.06 | 1.04 | 0.649274 |
| hsa-miR-22 | 1.51 | 1.72 | 1.38 | 1.72 | 1.95 | 1.26 | 0.11 | 0.93 | 0.657996 |
| hsa-miR-95 | 1.43 | 1.92 | 1.19 | 1.44 | 2.73 | 1.13 | 0.25 | 0.84 | 0.662929 |
| hsa-miR-191 | -3.90 | -4.07 | -4.12 | -4.14 | -3.91 | -4.20 | -0.05 | 1.04 | 0.672211 |
| hsa-miR-140-5p | -0.77 | -1.01 | -0.92 | -1.16 | -0.84 | -0.87 | -0.06 | 1.04 | 0.675227 |
| hsa-miR-181a* | -0.41 | -0.45 | -0.50 | -0.03 | -0.64 | -1.08 | -0.13 | 1.09 | 0.692030 |
| hsa-miR-185 | -2.27 | -2.44 | -2.56 | -2.48 | -2.35 | -2.31 | 0.04 | 0.97 | 0.693710 |
| hsa-miR-720 | -5.57 | -5.08 | -5.08 | -5.76 | -5.27 | -5.03 | -0.11 | 1.08 | 0.700137 |
| hsa-miR-33a | -3.96 | -3.47 | -3.62 | -4.05 | -3.94 | -3.37 | -0.10 | 1.07 | 0.705818 |
| hsa-miR-210 | -5.12 | -4.52 | -4.56 | -4.87 | -4.99 | -3.87 | 0.15 | 0.90 | 0.723296 |
| hsa-miR-454 | -0.47 | -0.44 | -0.74 | -0.65 | -0.63 | -0.50 | -0.04 | 1.03 | 0.725827 |
| hsa-miR-26b | -2.50 | -2.58 | -2.55 | -2.47 | -2.64 | -2.45 | 0.02 | 0.98 | 0.726570 |
| hsa-miR-576-3p | 4.66 | 4.10 | 4.34 | 5.64 | 3.39 | 4.84 | 0.25 | 0.84 | 0.727678 |
| hsa-let-7i | 2.96 | 2.92 | 2.80 | 2.54 | 3.28 | 2.60 | -0.09 | 1.06 | 0.728789 |
| hsa-miR-192 | 0.38 | 0.78 | 0.32 | 0.25 | 0.51 | 0.54 | -0.06 | 1.04 | 0.742232 |
| hsa-miR-32 | -4.25 | -4.22 | -4.08 | -4.26 | -4.15 | -4.07 | 0.03 | 0.98 | 0.742343 |
| hsa-miR-25 | -4.37 | -4.59 | -4.63 | -4.69 | -4.39 | -4.37 | 0.05 | 0.97 | 0.743510 |
| hsa-let-7c | 2.30 | 3.07 | 3.35 | 2.69 | 4.12 | 2.53 | 0.21 | 0.87 | 0.747065 |
| hsa-miR-18a* | -1.20 | -1.54 | -1.64 | -1.46 | -1.46 | -1.60 | -0.05 | 1.03 | 0.753884 |
| hsa-miR-338-3p | 4.82 | 3.71 | 5.09 | 4.45 | 4.45 | 5.18 | 0.15 | 0.90 | 0.766918 |
| hsa-miR-627 | 3.40 | 3.98 | 4.07 | 4.11 | 3.43 | 4.19 | 0.10 | 0.93 | 0.775678 |
| hsa-miR-17 | -3.63 | -4.22 | -4.11 | -3.49 | -4.33 | -3.86 | 0.09 | 0.94 | 0.778927 |
| hsa-miR-199a-5p | 6.86 | 6.48 | 6.27 | 6.85 | 5.21 | 7.02 | -0.18 | 1.13 | 0.782708 |
| hsa-miR-744 | 1.37 | 1.01 | 0.67 | 1.36 | 0.91 | 0.97 | 0.07 | 0.95 | 0.800982 |

| | | | | | | | | | |
|---|---|---|---|---|---|---|---|---|---|
| hsa-miR-542-5p | 1.42 | 1.43 | 2.02 | 1.58 | 1.68 | 1.45 | -0.05 | 1.04 | 0.819452 |
| hsa-miR-421 | 0.45 | -0.26 | 0.11 | -0.03 | 0.17 | 0.00 | -0.05 | 1.04 | 0.820257 |
| hsa-miR-92a | -7.53 | -7.22 | -7.70 | -7.45 | -7.60 | -7.50 | -0.03 | 1.02 | 0.827535 |
| hsa-miR-934 | 5.67 | 5.48 | 5.09 | 5.34 | 5.28 | 5.77 | 0.05 | 0.96 | 0.833448 |
| hsa-miR-149 | 3.81 | 4.58 | 3.85 | 4.08 | 4.44 | 3.92 | 0.06 | 0.96 | 0.836850 |
| hsa-miR-33b | 0.79 | 0.65 | 2.13 | 1.97 | 1.11 | 0.87 | 0.13 | 0.92 | 0.836993 |
| hsa-miR-9* | 4.15 | 3.26 | 4.43 | 3.64 | 4.24 | 4.21 | 0.09 | 0.94 | 0.840513 |
| hsa-miR-940 | -0.47 | -0.53 | -0.64 | 0.10 | -0.94 | -0.60 | 0.07 | 0.95 | 0.841596 |
| hsa-miR-373* | 5.31 | 4.42 | 3.84 | 5.13 | 4.13 | 3.96 | -0.11 | 1.08 | 0.848090 |
| hsa-miR-877 | 1.52 | 0.67 | 0.70 | 0.96 | 0.86 | 0.91 | -0.06 | 1.04 | 0.852306 |
| hsa-miR-142-5p | -5.19 | -5.34 | -4.52 | -5.05 | -4.96 | -5.19 | -0.05 | 1.04 | 0.858633 |
| hsa-miR-1979 | -7.68 | -8.70 | -8.31 | -7.81 | -8.13 | -9.02 | -0.09 | 1.06 | 0.859521 |
| hsa-miR-21 | -5.53 | -4.41 | -4.82 | -5.43 | -4.11 | -4.96 | 0.09 | 0.94 | 0.870639 |
| hsa-miR-885-5p | 4.40 | 4.01 | 3.89 | 3.57 | 4.62 | 3.93 | -0.06 | 1.04 | 0.873436 |
| hsa-miR-431 | 4.51 | 3.70 | 3.97 | 4.50 | 4.35 | 3.52 | 0.06 | 0.96 | 0.880718 |
| hsa-let-7b | 0.30 | 0.52 | 0.06 | 0.15 | 0.67 | -0.04 | -0.04 | 1.03 | 0.886549 |
| hsa-miR-339-5p | 0.70 | 0.55 | 0.68 | 0.61 | 0.58 | 0.71 | -0.01 | 1.01 | 0.890510 |
| hsa-miR-326 | 2.80 | 2.21 | 3.45 | 3.32 | 2.50 | 2.46 | -0.06 | 1.04 | 0.903217 |
| hsa-miR-374b | -1.66 | -1.59 | -2.34 | -1.81 | -1.91 | -1.96 | -0.03 | 1.02 | 0.909933 |
| hsa-miR-331-3p | -2.90 | -2.89 | -3.02 | -3.01 | -2.98 | -2.84 | -0.01 | 1.01 | 0.910861 |
| hsa-miR-320a | -5.47 | -5.41 | -5.42 | -5.52 | -5.59 | -5.14 | 0.02 | 0.99 | 0.911347 |
| hsa-miR-324-5p | -2.77 | -2.58 | -2.56 | -2.82 | -2.55 | -2.50 | 0.01 | 0.99 | 0.919008 |
| hsa-miR-92a-1* | -0.63 | -0.48 | -0.48 | -0.77 | -0.56 | -0.30 | -0.01 | 1.01 | 0.929499 |
| hsa-miR-143 | 1.57 | 2.51 | 2.31 | 1.87 | 1.96 | 2.66 | 0.04 | 0.98 | 0.930560 |
| hsa-miR-183 | -0.41 | 0.50 | 0.40 | 0.79 | -0.41 | 0.00 | -0.04 | 1.03 | 0.938704 |
| hsa-miR-363 | -2.80 | -2.69 | -3.64 | -2.51 | -3.44 | -3.29 | -0.03 | 1.02 | 0.940303 |
| hsa-miR-31* | 3.76 | 4.15 | 5.13 | 4.48 | 4.65 | 3.80 | -0.04 | 1.02 | 0.945267 |
| hsa-miR-29c | -4.66 | -4.69 | -3.97 | -4.34 | -4.50 | -4.53 | -0.02 | 1.01 | 0.952637 |
| hsa-miR-126* | 3.84 | 5.48 | 4.67 | 4.53 | 4.18 | 5.19 | -0.03 | 1.02 | 0.955280 |
| hsa-miR-342-3p | -3.58 | -3.66 | -3.58 | -3.93 | -3.33 | -3.59 | -0.01 | 1.01 | 0.956477 |
| hsa-miR-378 | -1.75 | -2.44 | -2.57 | -2.31 | -2.06 | -2.43 | -0.01 | 1.01 | 0.963598 |
| hsa-miR-30b | -5.05 | -4.74 | -4.84 | -5.05 | -4.80 | -4.80 | -0.01 | 1.00 | 0.963711 |
| hsa-miR-15a | -7.02 | -7.21 | -7.13 | -7.16 | -7.07 | -7.14 | 0.00 | 1.00 | 0.971982 |
| hsa-miR-497 | 3.47 | 3.54 | 3.21 | 3.31 | 3.15 | 3.77 | 0.00 | 1.00 | 0.984350 |
| hsa-miR-29b | -3.24 | -2.97 | -2.94 | -2.96 | -3.01 | -3.18 | 0.00 | 1.00 | 0.984619 |
| hsa-miR-19b | -8.39 | -8.29 | -8.41 | -8.49 | -8.39 | -8.21 | 0.00 | 1.00 | 0.991189 |
| hsa-miR-24 | -1.72 | -1.59 | -1.34 | -1.87 | -1.37 | -1.42 | 0.00 | 1.00 | 0.992020 |
| hsa-miR-423-3p | -4.54 | -4.40 | -4.31 | -4.51 | -4.48 | -4.26 | 0.00 | 1.00 | 0.992399 |
| hsa-miR-130a | -0.31 | -0.39 | -0.19 | -0.22 | -0.37 | -0.31 | 0.00 | 1.00 | 0.994561 |

**Supplementary Table 1: microRNA gene expression analysis**. Columns *B-G* present the normalized CT values for each detected microRNA in the samples screened. Normalization was performed by the mean expression value normalization method. P-values were calculated using two-tailed Student's t-Test.

| Rank | Up in | Feature | score | P-value | fold change | Empty Mean | Empty Std | TAL1 Mean | TAL1 Std |
|---|---|---|---|---|---|---|---|---|---|
| 1 | TAL1 | hsa-mir-135a | -5.147 | 0.009 | 12.796 | 0.074 | 0.016 | 0.941 | 0.152 |
| 2 | TAL1 | hsa-mir-223 | -2.974 | 0.022 | 1.565 | 94.941 | 3.038 | 148.59 | 14.999 |
| 9 | TAL1 | hsa-mir-330-3p | -1.475 | 0.042 | 1.528 | 0.153 | 0.036 | 0.234 | 0.019 |
| 13 | TAL1 | hsa-mir-574-3p | -1.34 | 0.041 | 2.121 | 0.01 | 0.003 | 0.021 | 0.005 |
| 15 | Empty | hsa-mir-491-5p | 1.282 | 0.046 | 1.561 | 0.167 | 0.029 | 0.107 | 0.018 |
| 10 | Empty | hsa-mir-545 | 1.475 | 0.054 | 1.533 | 0.067 | 0.001 | 0.044 | 0.005 |
| 4 | Empty | hsa-mir-375 | 1.993 | 0.032 | 3.17 | 0.107 | 0.009 | 0.034 | 0.027 |
| 3 | Empty | hsa-mir-146b-5p | 2.11 | 0.009 | 1.906 | 0.092 | 0.012 | 0.048 | 0.009 |

**Supplementary Table 2. MicroRNAs differentially expressed upon TAL1 overexpression as determined by the Comparative Marker Selection suite**. Cutoffs for statistical significance were: 1) p-value < 0.05, and 2) fold change > 1.5.

| Gene name | KRT1 (cytokeratin-1) | RAPGEF5 | JAZF1 | FAM64A |
|---|---|---|---|---|
| Function | Keratin 1 gene; upregulation of KRT1 could result in increased of drug resistance in nasopharyngeal carcinoma cell lines cell lines. The cytokeratin 1-Src complex was found to be associated with the molecular scaffolder RACK1 in neuroblastoma. | It activates Ras oncogene family members RAP1A and RAP1B. Guanine nucleotide exchange factor (GEF) for RAP1A, RAP2A and MRAS/M-Ras-GTP. Its association with MRAS inhibits Rap1 activation . | Potential transcription factor. A chromosomal aberration ( Translocation t(7;17)(p15;q21) with SUZ12.) involving JAZF1 may be a cause of endometrial stromal tumors. The translocation generates the JAZF1-SUZ12 oncogene consisting of the N-terminus part of JAZF1 and the C-terminus part of SUZ12. It is frequently found in all cases of endometrial stromal tumors. Single nucleotide polymorphisms in this gene are associated with altered risk for type 2 diabetes and prostate cancer. 2 isoforms of the human protein are produced by alternative splicing. | family with sequence similarity 64, member A |
| Role in Cancer | Potential oncogene | Potential oncogene | Potential oncogene | Not Determined |
| References | 1: Tang S, Huang W, Zhong M, Yin L, Jiang H, Hou S, Gan P, Yuan Y. Identification Keratin 1 as a cDDP-resistant protein in nasopharyngeal carcinoma cell lines. J Proteomics. 2012 Apr 18;75(8):2352-60. doi: 10.1016/j.jprot.2012.02.003. Epub 2012 Feb 12. PubMed PMID: 22348822.<br><br>2: Attallah AM, El-Far M, Abdel Malak CA, Zahran F, Farid K, Omran MM, Zagloul H, El-Deen MS. Evaluation of cytokeratin-1 in the diagnosis of hepatocellular carcinoma. Clin Chim Acta. 2011 Nov 20;412(23-24):2310-5. doi: 10.1016/j.cca.2011.08.029. Epub 2011 Sep 7. PubMed PMID: 21924253.<br><br>3: Chuang NN, Huang CC. Interaction of integrin beta1 with cytokeratin 1 in neuroblastoma NMB7 cells. Biochem Soc Trans. 2007 Nov;35(Pt 5):1292-4. Review. PubMed PMID: 17956333. | WEB reference: http://www.genecards.org/cgi-bin/carddisp.pl?gene=RAPGEF5 | 1: Amador-Ortiz C, Roma AA, Huettner PC, Becker N, Pfeifer JD. JAZF1 and JJAZ1 gene fusion in primary extrauterine endometrial stromal sarcoma. Hum Pathol. 2011 Jul;42(7):939-46. doi: 10.1016/j.humpath.2010.11.001. Epub 2011 Feb 11. PubMed PMID: 21316079.<br><br>2: Li H, Wang J, Mor G, Sklar J. A neoplastic gene fusion mimics trans-splicing of RNAs in normal human cells. Science. 2008 Sep 5;321(5894):1357-61. doi: 10.1126/science.1156725. PubMed PMID: 18772439.<br><br>3: Koontz JI, Soreng AL, Nucci M, Kuo FC, Pauwels P, van Den Berghe H, Dal Cin P, Fletcher JA, Sklar J. Frequent fusion of the JAZF1 and JJAZ1 genes in endometrial stromal tumors. Proc Natl Acad Sci U S A. 2001 May 22;98(11):6348-53.<br><br>4: Stevens VL, Ahn J, Sun J, Jacobs EJ, Moore SC, Patel AV, Berndt SI, Albanes D, Hayes RB. HNF1B and JAZF1 genes, diabetes, and prostate cancer risk. Prostate. 2010 May 1;70(6):601-7. doi:10.1002/pros.21094. | |

| Gene name | CD53 | ARID3A (DRIL1) | SCML1 | TLE4 |
|---|---|---|---|---|
| Function | Leukocyte surface antigen of the as the tetraspanin family. In CD53- stimulated cells there is a significant reduction in caspase activation, as a reduction in the fragmentation of DNA. CD53-stimulated cells also have an increase in the level of bcl-X(L) and a reduction of bax protein, changing their ratio by 24-fold in the direction of survival. This survival signal appears to be mediated by activation of the AKT, as detected by its phosphorylation in Ser473 upon CD53 ligation. | AT-rich interaction domain DNA-binding transcription factor. DRIL1 renders primary murine fibroblasts unresponsive to RAS(V12)-induced anti-proliferative signalling by p19(ARF)/p53/p21(CIP1), as well as by p16(INK4a). DRIL1 induces the E2F1 target Cyclin E1, overexpression of which is sufficient to trigger escape from senescence. | Polycomb group protein. | Novel Groucho-transcription factor, regulates the repressive activity of PAX5 in human B-lymphocytes. Knockdown of TLE1 or TLE4 levels increased the rate of cell division of the AML1-ETO-expressing Kasumi-1 cell line, whereas forced expression of either TLE1 or TLE4 caused apoptosis and cell death. |
| Role in Cancer | Anti-apoptotic (in Jurkat cells) | Oncogene | Not Determined | Pro-apoptotic |
| References | 1: Yunta M, Lazo PA. Apoptosis protection and survival signal by the CD53 tetraspanin antigen. Oncogene. 2003 Feb 27;22(8):1219-24. PubMed PMID: 12606948. | Peeper DS, Shvarts A, Brummelkamp T, Douma S, Koh EY, Daley GQ, Bernards R. A functional screen identifies hDRIL1 as an oncogene that rescues RAS-induced senescence. Nat Cell Biol. 2002 Feb;4(2):148-53. | | Dayyani F, Wang J, Yeh JR, Ahn EY, Tobey E, Zhang DE, Bernstein ID, Peterson RT, Sweetser DA. Loss of TLE1 and TLE4 from the del(9q) commonly deleted region in AML cooperates with AML1-ETO to affect myeloid cell proliferation and survival. Blood. 2008 Apr 15;111(8):4338-47. doi: 10.1182/blood-2007-07-103291. |

| Gene name | ETS-1 | CD28 |
|---|---|---|
| Function | Member of the ETS family of transcription factors involved in stem cell development, cell senescence and death, and tumorigenesis. cortical thymic maturation arrest in T-ALLs that overexpress TLX1 or TLX3 is due to binding of TLX1/TLX3 to ETS1, leading to repression of T cell receptor α enhanceosome activity and blocked TCR-Jα rearrangement. | TCR co-stimulatory signal receptor for T cell activation. Involved in induction of cell proliferation and cytokine production and promotion of T-cell survival; CD28 co-stimulation directly controls T cell cycle progression by down-regulating the cdk inhibitor p27kip1, which actually integrates mitogenic MEK and P13K-dependent signals from both TCR and CD28. |
| Role in Cancer | Oncogene | Pro-proliferative |
| References | 1: Wei W, et al. MicroRNA-1 and microRNA-499 downregulate the expression of the ets1 proto-oncogene in HepG2 cells. Oncol Rep.2012 Aug;28(2):701-6. doi: 10.3892/or.2012.1850. Epub 2012 Jun 1.<br>2: Pallai R, Bhaskar A, Sodi V, Rice LM. Ets1 and Elk1 transcription factors regulate cancerous inhibitor of protein phosphatase 2A expression in cervical and endometrial carcinoma cells. Transcription. 2012 Nov 1;3(6). [Epub ahead of print] PubMed PMID: 23117818.<br>3: Dadi S, et al. TLX homeodomain oncogenes mediate T cell maturation arrest in T-ALL via interaction with ETS1 and suppression of TCRα gene expression. Cancer Cell. 2012 Apr 17;21(4):563-76. doi: 10.1016/j.ccr.2012.02.013. PubMed PMID: 22516263.<br>4: Wang C, et al. Gambogic acid-loaded magnetic Fe(3)O(4) nanoparticles inhibit Panc-1 pancreatic cancer cell proliferation and migration by inactivating transcription factor ETS1. Int J Nanomedicine.2012;7:781-7. doi: 10.2147/IJN.S28509. Epub 2012 Feb 14. PubMed PMID: 22393285;<br>5: Shaikhibrahim Z, Wernert N. ETS transcription factors and prostate cancer: the role of the family prototype ETS-1 (review). Int J Oncol. 2012 Jun;40(6):1748-54. doi: 10.3892/ijo.2012.1380. Epub 2012 Feb 21. Review. PubMed PMID: 22366814.<br>6: Smith AM, et al. ETS1 transcriptional activity is increased in advanced prostate cancer and promotes the castrate-resistant phenotype. Carcinogenesis. 2012 Mar;33(3):572-80. doi: 10.1093/carcin/bgs007. Epub 2012 Jan 9.<br>7: Kato T, et al. ETS1 promotes chemoresistance and invasion of paclitaxel-resistant, hormone-refractory PC3 prostate cancer cells by up-regulating MDR1 and MMP9 expression. Biochem Biophys Res Commun. 2012 Jan 20;417(3):966-71. doi: 10.1016/j.bbrc.2011.12.047. Epub 2011 Dec 20.<br>8: Singh AK, Swarnalatha M, Kumar V. c-ETS1 facilitates G1/S-phase transition by up-regulating cyclin E and CDK2 genes and cooperates with hepatitis B virus X protein for their deregulation. J Biol Chem. 2011 Jun 24;286(25):21961-70. doi: 10.1074/jbc.M111.238238. Epub 2011 Apr 22. PubMed PMID: 21515670;<br>9: Khanna A, et al. ETS1 mediates MEK1/2-dependent overexpression of cancerous inhibitor of protein phosphatase 2A (CIP2A) in human cancer cells. PLoS One. 2011 Mar 22;6(3):e17979. doi:10.1371/journal.pone.0017979.<br>10: Zhang Y, et al. miR-125b is methylated and functions as a tumor suppressor by regulating the ETS1 proto-oncogene in human invasive breast cancer. Cancer Res. 2011 May 15;71(10):3552-62. doi: 10.1158/0008-5472.CAN-10-2435. | 1: Appleman LJ, van Puijenbroek AA, Shu KM, Nadler LM, Boussiotis VA. CD28 costimulation mediates down-regulation of p27kip1 and cell cycle progression by activation of the PI3K/PKB signaling pathway in primary human T cells. J Immunol. 2002 Mar 15;168(6):2729-36.<br>2: Takeda K, Harada Y, Watanabe R, Inutake Y, Ogawa S, Onuki K, Kagaya S, Tanabe K, Kishimoto H, Abe R. CD28 stimulation triggers NF-kappaB activation through the CARMA1-PKCtheta-Grb2/Gads axis. Int Immunol. 2008 Dec;20(12):1507-15. doi: 10.1093/intimm/dxn108. Epub 2008 Oct 1. |

| Gene name | UBE3C | MYB |
|---|---|---|
| Function | E3 ubiquitin-protein ligase | Myb proto-oncogene protein is a member of the MYB (myeloblastosis) family of transcription factors. C-MYB locus is involved in chromosomal translocation and genomic duplications in human T-cell acute leukemia. |
| Role in Cancer | Not Determined | Oncogene |
| References | | 1: Sanda T, Lawton LN, Barrasa MI, Fan ZP, Kohlhammer H, Gutierrez A, Ma W, Tatarek J, Ahn Y, Kelliher MA, Jamieson CH, Staudt LM, Young RA, Look AT. Core transcriptional regulatory circuit controlled by the TAL1 complex in human T cell acute lymphoblastic leukemia. Cancer Cell. 2012 Aug 14;22(2):209-21. doi: 10.1016/j.ccr.2012.06.007. PubMed PMID: 22897851;<br>2: Kawamata N, Zhang L, Ogawa S, Nannya Y, Dashti A, Lu D, Lim S, Schreck R, Koeffler HP. Double minute chromosomes containing MYB gene and NUP214-ABL1 fusion gene in T-cell leukemia detected by single nucleotide polymorphism DNA microarray and fluorescence in situ hybridization. Leuk Res. 2009 Apr;33(4):569-71. doi: 10.1016/j.leukres.2008.07.030. Epub 2008 Sep 16.<br>3: O'Neil J, Tchinda J, Gutierrez A, Moreau L, Maser RS, Wong KK, Li W, McKenna K, Liu XS, Feng B, Neuberg D, Silverman L, DeAngelo DJ, Kutok JL, Rothstein R, DePinho RA, Chin L, Lee C, Look AT. Alu elements mediate MYB gene tandem duplication in human T-ALL. J Exp Med. 2007 Dec 24;204(13):3059-66. Epub 2007 Dec 10. PubMed PMID: 18070937; PubMed Central PMCID: PMC2150982.<br>4: Clappier E, Cuccuini W, Kalota A, Crinquette A, Cayuela JM, Dik WA, Langerak AW, Montpellier B, Nadel B, Walrafen P, Delattre O, Aurias A, Leblanc T, Dombret H, Gewirtz AM, Baruchel A, Sigaux F, Soulier J. The C-MYB locus is involved in chromosomal translocation and genomic duplications in human T-cell acute leukemia (T-ALL), the translocation defining a new T-ALL subtype in very young children. Blood. 2007 Aug 15;110(4):1251-61. Epub 2007 Apr 23. PubMed PMID: 17452517.<br>5: Lahortiga I, De Keersmaecker K, Van Vlierberghe P, Graux C, Cauwelier B,nLambert F, Mentens N, Beverloo HB, Pieters R, Speleman F, Odero MD, Bauters M, Froyen G, Marynen P, Vandenberghe P, Wlodarska I, Meijerink JP, Cools J. Duplication of the MYB oncogene in T cell acute lymphoblastic leukemia. Nat Genet. 2007 May;39(5):593-5. Epub 2007 Apr 15. PubMed PMID: 17435759.<br>6: Venturelli D, Mariano MT, Szczylik C, Valtieri M, Lange B, Crist W, Link M, Calabretta B. Down-regulated c-myb expression inhibits DNA synthesis of T-leukemia cells in most patients. Cancer Res. 1990 Nov 15;50(22):7371-5. PubMed PMID: 2224864.<br>7: Mavilio F, Sposi NM, Petrini M, Bottero L, Marinucci M, De Rossi G, Amadori S, Mandelli F, Peschle C. Expression of cellular oncogenes in primary cells from human acute leukemias. Proc Natl Acad Sci U S A. 1986 Jun;83(12):4394-8. PubMed PMID: 3520570; PubMed Central PMCID: PMC323739. |

| Gene name | ETV5 | MED12L |
|---|---|---|
| Function | ETS oncogenic family member of transcription factors (like ETS-1). The proto-oncogenes ETV1, ETV4 and ETV5 includes the most frequently rearranged and overexpressed genes in prostate cancer; ETV5 is a target for the Ras/Raf-1/MAPK pathway and can also be activated through the protein kinase A. Is overexpressed in metastatic human breast cancer cells and mouse mammary tumors and might therefore play an important role in mammary oncogenesis; up-regulation of ETV5 in B-CLL and MCL suggests this gene as a new candidate for the pathomechanism of B-cell lymphomas. | The protein encoded by this gene is part of the Mediator complex, which is involved in transcriptional coactivation of nearly all RNA polymerase II-dependent genes. Exome sequencing identified recurrent MED12 mutations in prostate cancer; MED12 suppression results in activation of TGF-βR signaling, which is both necessary and sufficient for drug resistance. |
| Role in Cancer | Oncogene | Potencial tumor suppressor |
| References | 1: T'sas F, et al. Expression of the Ets transcription factor Erm is regulated through a conventional PKC signaling pathway in the Molt4 lymphoblastic cell line. FEBS Lett. 2005 Jan 3;579(1):66-70. PubMed PMID: 15620692.<br>2: Planagumà J, et al. Up-regulation of ERM/ETV5 correlates with the degree of myometrial infiltration in endometrioid endometrial carcinoma. J Pathol. 2005 Dec;207(4):422-9. PubMed PMID: 16175655.<br>3: Monge M, et al. ERM/ETV5 up-regulation plays a role during myometrial infiltration through matrix metalloproteinase-2 activation in endometrial cancer. Cancer Res. 2007 Jul 15;67(14):6753-9. PubMed PMID: 17638886.<br>4: Helgeson BE, et al. Characterization of TMPRSS2:ETV5 and SLC45A3:ETV5 gene fusions in prostate cancer. Cancer Res. 2008 Jan 1;68(1):73-80. doi: 10.1158/0008-5472.CAN-07-5352. PubMed PMID: 18172298.<br>5: Firlej V, et al. Reduced tumorigenesis in mouse mammary cancer cells following inhibition of Pea3- or Erm-dependent transcription. J Cell Sci. 2008 Oct 15;121(Pt 20):3393-402. doi: 10.1242/jcs.027201. Epub 2008 Sep 30. PubMed PMID: 18827017.<br>6: Charfi C, et al. Gene profiling of Graffi murine leukemia virus-induced lymphoid leukemias: identification of leukemia markers and Fmn2 as a potential oncogene. Blood. 2011 Feb 10;117(6):1899-910. doi: 10.1182/blood-2010-10-311001. Epub 2010 Dec 6. PubMed PMID: 21135260.<br>7: Yu H, Zhang Y, Ye L, Jiang WG. The FERM family proteins in cancer invasion and metastasis. Front Biosci. 2011 Jan 1;16:1536-50. Review. PubMed PMID: 21196246.<br>8: Llauradó M, et al. ETV5 transcription factor is overexpressed in ovarian cancer and regulates cell adhesion in ovarian cancer cells. Int J Cancer. 2012 Apr 1;130(7):1532-43. doi: 10.1002/ijc.26148. Epub 2011 Aug 12. PubMed PMID: 21520040.<br>9: Vitari AC, et al. COP1 is a tumour suppressor that causes degradation of ETS transcription factors. Nature. 2011 May 15;474(7351):403-6. doi:10.1038/nature10005. PubMed PMID: 21572435.<br>10: Oh S, Shin S, Janknecht R. ETV1, 4 and 5: An oncogenic subfamily of ETS transcription factors. Biochim Biophys Acta. 2012 Aug;1826(1):1-12. doi:10.1016/j.bbcan.2012.02.002. Epub 2012 Mar 8. PubMed PMID: 22425584; PubMed Central PMCID: PMC3362686.<br>11: Korz C, et al. Evidence for distinct pathomechanisms in B-cell chronic lymphocytic leukemia and mantle cell lymphoma by quantitative expression analysis of cell cycle and apoptosis-associated genes. Blood. 2002 Jun 15;99(12):4554-61. | 1: Huang S, Hölzel M, Knijnenburg T, Schlicker A, Roepman P, McDermott U, Garnett M, Grernrum W, Sun C, Prahallad A, Groenendijk FH, Mittempergher L, Nijkamp W, Neefjes J, Salazar R, Ten Dijke P, Uramoto H, Tanaka F, Beijersbergen RL, Wessels LF, Bernards R. MED12 controls the response to multiple cancer drugs through regulation of TGF-β receptor signaling. Cell. 2012 Nov 21;151(5):937-50. doi: 10.1016/j.cell.2012.10.035.<br><br>2: Barbieri CE, Baca SC, Lawrence MS, Demichelis F, Blattner M, Theurillat JP, White TA, Stojanov P, Van Allen E, Stransky N, Nickerson E, Chae SS, Boysen G, Auclair D, Onofrio RC, Park K, Kitabayashi N, MacDonald TY, Sheikh K, Vuong T, Guiducci C, Cibulskis K, Sivachenko A, Carter SL, Saksena G, Voet D, Hussain WM, Ramos AH, Winckler W, Redman MC, Ardlie K, Tewari AK, Mosquera JM, Rupp N, Wild PJ, Moch H, Morrissey C, Nelson PS, Kantoff PW, Gabriel SB, Golub TR, Meyerson M, Lander ES, Getz G, Rubin MA, Garraway LA. Exome sequencing identifies recurrent SPOP, FOXA1 and MED12 mutations in prostate cancer. Nat Genet. 2012 May 20;44(6):685-9. doi: 10.1038/ng.2279. |

| Gene name | C18ORF1 | PDE3B | TSPAN2 | RBL2 |
|---|---|---|---|---|
| Function | Uncharacterized protein C18orf12 | Cyclic nucleotide phosphodiesterase with a dual-specificity for the second messengers cAMP and cGMP; promotes survival of CLL and T-ALL cells, and associates with resistance to cisplatin in head & neck carcinoma; is positively regulated by Akt; is positively involved in insulin signaling | Tetraspanin 2. Cell-surface proteins that are characterized by the presence of four hydrophobic domains. The proteins mediate signal transduction events that play a role in the regulation of cell development, activation, growth and motility. Tetraspanins protect MT1-MMP from lysosomal degradation and support its delivery to the cell surface. MT1-MMMP is a metalloproteinase that supports tumor cell invasion through extracellular matrix barriers containing fibrin, collagen, fibronectin, and other proteins. | pRb2/p130 belongs to the retinoblastoma (RB) family of proteins. pRb2/p130 acts as a tumor suppressor and it is a potent inhibitor of E2F-mediated trans-activation. |
| Role in Cancer | Not Determined | Oncogene | Supports tumor cell invasion | Potencial tumor suppressor |
| References | | 1: Moon E, Lee R, Near R, Weintraub L, Wolda S, Lerner A. Inhibition of PDE3B augments PDE4 inhibitor-induced apoptosis in a subset of patients with chronic lymphocytic leukemia. Clin Cancer Res. 2002 Feb;8(2):589-95. PubMed PMID: 11839681.<br><br>2: Yamano Y, Uzawa K, Saito K, Nakashima D, Kasamatsu A, Koike H, Kouzu Y, Shinozuka K, Nakatani K, Negoro K, Fujita S, Tanzawa H. Identification of cisplatin-resistance related genes in head and neck squamous cell carcinoma. Int J Cancer. 2010 Jan 15;126(2):437-49. doi: 10.1002/ijc.24704. PubMed PMID:19569180.<br><br>3: Dong H, Zitt C, Auriga C, Hatzelmann A, Epstein PM. Inhibition of PDE3, PDE4 and PDE7 potentiates glucocorticoid-induced apoptosis and overcomes glucocorticoid resistance in CEM T leukemic cells. Biochem Pharmacol. 2010 Feb 1;79(3):321-9. doi:10.1016/j.bcp.2009.09.001. Epub 2009 Sep 6. PubMed PMID: 19737543. | Mol Biol Cell. 2009 Apr;20(7):2030-40. doi: 10.1091/mbc.E08-11-1149. Epub 2009 Feb 11. Tetraspanin proteins regulate membrane type-1 matrix metalloproteinase-dependent pericellular proteolysis. Lafleur MA, Xu D, Hemler ME. SourceDepartment of Cancer Immunology and AIDS, Dana-Farber Cancer Institute, Boston, MA 02115, USA. | Li Y, Graham C, Lacy S, Duncan AM, Whyte P. The adenovirus E1A-associated 130-kD protein is encoded by a member of the retinoblastoma gene family and physically interacts with cyclins A and E. Genes Dev. 1993 Dec;7(12A):2366-77. |

| Gene name | CAMK2D | SPRED1 | ZNRF1 | WIBG |
|---|---|---|---|---|
| Function | Calcium/calmodulin-dependent protein kinase II delta | Spred-1 is a member of the Sprouty family of proteins and is phosphorylated by tyrosine kinase in response to several growth factors, inhibits growth-factor-mediated. Legius syndrome is caused by germline loss-of-function SPRED1 mutations, resulting in overactivation of the RAS-MAPK signal transduction cascade. Loss of function mutations appear to predispose to leukemia. | E3 ubiquitin-protein ligase that mediates the ubiquitination of AKT1 and GLUL, thereby playing a role in neuron cells differentiation | Key regulator of the exon junction complex (EJC); Interferes with nonsense-mediated mRNA decay and enhances translation of spliced mRNAs, probably by antagonizing EJC functions. |
| Role in Cancer | Not Determined | Potencial tumor suppressor | Not Determined | Not Determined |
| References | | 1: Batz C, Hasle H, Bergsträsser E, van den Heuvel-Eibrink MM, Zecca M, Niemeyer CM, Flotho C; European Working Group of Myelodysplastic Syndromes in Childhood (EWOG-MDS). Does SPRED1 contribute to leukemogenesis in juvenile myelomonocytic leukemia (JMML)? Blood. 2010 Mar 25;115(12):2557-8. doi: 10.1182/blood-2009-12-260901.<br><br>2: Brems H, Pasmant E, Van Minkelen R, Wimmer K, Upadhyaya M, Legius E, Messiaen L. Review and update of SPRED1 mutations causing Legius syndrome. Hum Mutat. 2012 Nov;33(11):1538-46. doi: 10.1002/humu.22152. | web reference: http://www.uniprot.org/uniprot/Q8ND25 | web reference: http://www.uniprot.org/uniprot/Q9BRP8 |

| Gene name | DOCK10 | AKAP2 | TFP1 | PPP1R16B |
|---|---|---|---|---|
| Function | Guanine nucleotide exchange factor (GEF). Dock10 expression is upregulated in B-lymphocytes and Chronic Lymphocytic Leukemia (CLL) cells in response to the cytokine IL-4; Dock10 is overexpressed in some aggressive papillary thyroid carcinomas; Activated Cdc42 mediated by DOCK10 induces a mesenchymal-amoeboid transition and increases cell invasion of melanoma cells. | A kinase anchoring protein 2, binds to the regulatory subunit of protein kinase A and is found associated with the actin cytoskeleton; AKAP2 plays a key role in CTR-mediated oncogenic actions by targeting cyclic AMP-dependent protein kinase PKA to CTR within a localized sub-region of the tight junctions complex. | Transferrin pseudogene | Regulator of protein phosphatase 1; acts as a positive regulator of pulmonary endothelial cell barrier function. May be a downstream target for TGF-beta1 signaling cascade in endothelial cells; in a large-scale insertional mutagenesis in Eμ-c-myc mice model pp1r16b was identified at common insertion sites and is bona fide cellular oncogene. |
| Role in Cancer | Oncogenic | Potential oncogene | Not Determined | Oncogene |
| References | 1: Yelo E, Bernardo MV, Gimeno L, Alcaraz-García MJ, Majado MJ, Parrado A. Dock10, a novel CZH protein selectively induced by interleukin-4 in human B lymphocytes. Mol Immunol. 2008 Jul;45(12):3411-8. doi: 10.1016/j.molimm.2008.04.003. Epub 2008 May 21. PubMed PMID: 18499258.<br><br>2: Gadea G, Sanz-Moreno V, Self A, Godi A, Marshall CJ. DOCK10-mediated Cdc42 activation is necessary for amoeboid invasion of melanoma cells. Curr Biol. 2008 Oct 14;18(19):1456-65. doi: 10.1016/j.cub.2008.08.053. Epub 2008 Oct 2. PubMed PMID: 18835169.<br><br>3: Humtsoe JO, Koya E, Pham E, Aramoto T, Zuo J, Ishikawa T, Kramer RH. Transcriptional profiling identifies upregulated genes following induction of epithelial-mesenchymal transition in squamous carcinoma cells. Exp Cell Res. 2012 Feb 15;318(4):379-90. doi: 10.1016/j.yexcr.2011.11.011. Epub 2011 Nov 29. PubMed PMID: 22154512.<br><br>4: Fluge Ø, Bruland O, Akslen LA, Lillehaug JR, Varhaug JE. Gene expression in poorly differentiated papillary thyroid carcinomas. Thyroid. 2006 Feb;16(2):161-75. PubMed PMID: 16676402. | web reference: http://www.labome.org/grant/r01/ca/calcitonin/in/calcitonin-in-prostate-growth-and-neplasia-7737843.html | | Mendrysa SM, Akagi K, Roayaei J, Lien WH, Copeland NG, Jenkins NA, Eisenman RN. An Integrated Genetic-Genomic Approach for the Identification of Novel Cancer Loci in Mice Sensitized to c-Myc-Induced Apoptosis. Genes Cancer. 2010 May;1(5):465-479. |

| Gene name | TGFBR1 | SPTBN1 | LYSMD2 | MGAT4 |
|---|---|---|---|---|
| Function | Transforming growth factor beta receptor 1, involved in the regulation of cellular processes, including cell division, differentiation, motility, adhesion and death. A pro-oncogenic role for TGF-beta has been proposed. Once cells lose their sensitivity to TGF-beta1-mediated growth inhibition, autocrine TGF-beta signaling can promote tumorigenesis. Elevated levels of TGF-beta1 are often observed in advanced carcinomas, and have been correlated with increased tumor invasiveness and disease progression; TGFBR1*6A enhances the migration and invasion of MCF-7 breast cancer cells through RhoA activation; Oncogenic mutations in TGFBR1 were detected in several benign or malignant skin tumors. | Spectrin is an actin crosslinking and molecular scaffold protein that links the plasma membrane to the actin cytoskeleton; it contributes to contribute to platinum anticancer drug resistance in ovarian serous adenocarcinoma; is found as part of oncogenic fusions in atypical myeloproliferative disorder | LysM, putative peptidoglycan-binding, domain containing 2 | Glycosyltransferase that regulates the formation of tri- and multiantennary branching structures in the Golgi apparatus; Oncogenic signaling in cancer cells up-regulates the transcription and activities of MGAT4. Oncogenic activation of PI3K and Erk/Ets increases Mgat4 expression and it's N-glycan products; |
| Role in Cancer | Potential oncogene | Involded in anticancer drug resistance | Not Determined | Potential oncogene |
| References | 1: Arnault JP, Mateus C, Escudier B, Tomasic G, Wechsler J, Hollville E, Soria JC, Malka D, Sarasin A, Larcher M, André J, Kamsu-Kom N, Boussemart L, Lacroix L, Spatz A, Eggermont AM, Druillennec S, Vagner S, Eychène A, Dumaz N, Robert C. Skin tumors induced by sorafenib; paradoxic RAS-RAF pathway activation and oncogenic mutations of HRAS, TP53, and TGFBR1. Clin Cancer Res. 2012 Jan 1;18(1):263-72. doi: 10.1158/1078-0432.CCR-11-1344. Epub 2011 Nov 17.<br><br>2: Rosman DS, Phukan S, Huang CC, Pasche B. TGFBR1*6A enhances the migration and invasion of MCF-7 breast cancer cells through RhoA activation. Cancer Res. 2008 Mar 1;68(5):1319-28. doi: 10.1158/0008-5472.CAN-07-5424.<br><br>3: Bian Y, Terse A, Du J, Hall B, Molinolo A, Zhang P, Chen W, Flanders KC, Gutkind JS, Wakefield LM, Kulkarni AB. Progressive tumor formation in mice with conditional deletion of TGF-beta signaling in head and neck epithelia is associated with activation of the PI3K/Akt pathway. Cancer Res. 2009 Jul 15;69(14):5918-26. doi:10.1158/0008-5472.CAN-08-4623. Epub 2009 Jul 7. | 1: Maeda O, Shibata K, Hosono S, Fujiwara S, Kajiyama H, Ino K, Nawa A, Tamakoshi K, Kikkawa F. Spectrin αII and βII tetramers contribute to platinum anticancer drug resistance in ovarian serous adenocarcinoma. Int J Cancer. 2012 Jan 1;130(1):113-21. doi: 10.1002/ijc.25983. Epub 2011 Apr 25. PubMed PMID: 21328338.<br><br>2: Gallagher G, Horsman DE, Tsang P, Forrest DL. Fusion of PRKG2 and SPTBN1 to the platelet-derived growth factor receptor beta gene (PDGFRB) in imatinib-responsive atypical myeloproliferative disorders. Cancer Genet Cytogenet. 2008 Feb;181(1):46-51. doi:10.1016/j.cancergencyto.2007.10.021. PubMed PMID: 18262053.<br><br>3: Grand FH, Iqbal S, Zhang L, Russell NH, Chase A, Cross NC. A constitutively active SPTBN1-FLT3 fusion in atypical chronic myeloid leukemia is sensitive to tyrosine kinase inhibitors and immunotherapy. Exp Hematol. 2007 Nov;35(11):1723-7. Epub 2007 Aug 30. PubMed PMID: 17764812. | | 1: Lau KS, Dennis JW. N-Glycans in cancer progression. Glycobiology. 2008 Oct;18(10):750-60. doi: 10.1093/glycob/cwn071. |

**Supplementary Table 3: List of known TAL1 upregulated genes that are potentially targeted by TAL1 downregulated microRNAs, as in Figure 2a**. Described function(s), putative role in cancer and corresponding relevant references are presented for each gene. For gene assessment details see supplemental methods.

| Gene name | SKI | IKZF3 | DOLPP1 | SH2D3C |
|---|---|---|---|---|
| Function | Nuclear protooncoprotein; negatively regulates TGFb; A dual role of SKI has been observed in different malignancies. The human SKI gene is located at chromosome 1p36, a potential tumor suppressor locus that is frequently deleted in various human cancers including neuroblastoma, melanoma, colorectal carcinoma and leukemia. | AILOS Ikaros family of zinc-finger proteins; transcription factors involved in the regulation of lymphocyte development; Ikaros inactivation is a recurrent event in human T-ALL; it's also is also a major tumor suppressor in human B-ALL. | Dolichyl pyrophosphate (Dol P-P) phosphatase, Required for efficient N-glycosylation | SH2 domain containing 3C, adaptor protein involved in cell migration. |
| Role in Cancer | Potencial tumor suppressor | Tumor suppressor | Not determined | Not determined |
| References | 1:Shinagawa T, Nomura T, Colmenares C, Ohira M, Nakagawara A, Ishii S. Increased susceptibility to tumorigenesis of ski-deficient heterozygous mice. Oncogene. 2001 Dec 6;20(56):8100-8..<br><br>2: Colmenares C, Heilstedt HA, Shaffer LG, Schwartz S, Berk M, Murray JC, Stavnezer E: Loss of the SKI proto-oncogene in individuals affected with 1p36 deletion syndrome is predicted by strain-dependent defects in Ski-/- mice.Nat Genet 2002, 30:106-109.<br><br>3: Wang P, Chen Z, Meng ZQ, Fan J, Luo JM, Liang W, Lin JH, Zhou ZH, Chen H, Wang K, Shen YH, Xu ZD, Liu LM. Dual role of Ski in pancreatic cancer cells: tumor-promoting versus metastasis-suppressive function. Carcinogenesis. 2009 Sep;30(9):1497-506. doi: 10.1093/carcin/bgp154. Epub 2009 Jun 22. | 1: Philippe Kastner and Susan Chan. Role of Ikaros in T-cell acute lymphoblastic leukemia. World J Biol Chem. 2011 June 26; 2(6): 108–114.<br><br>2: Nakase K, Ishimaru F, Avitahl N, Dansako H, Matsuo K, Fujii K, Sezaki N, Nakayama H, Yano T, Fukuda S, Imajoh K, Takeuchi M, Miyata A, Hara M, Yasukawa M, Takahashi I, Taguchi H, Matsue K, Nakao S, Niho Y, Takenaka K, Shinagawa K, Ikeda K, Niiya K, Harada M. Dominant negative isoform of the Ikaros gene in patients with adult B-cell acute lymphoblastic leukemia. Cancer Res. 2000 Aug 1;60(15):4062-5. | | |

| Gene name | SRGAP3 | TOX | IGF1R |
|---|---|---|---|
| Function | Member of the Slit-Robo sub-family of Rho GTPase-activating proteins implicated in repulsive axon guidance and neuronal migration through Slit-Robo-mediated signal transduction; has tumor suppressor-like activity in HMECs, likely through its activity as a negative regulator of Rac1 | Thymocyte selection-associated high mobility group box protein; it's required for T-Cell diferentiation; TAL1 binds to Tox genomic region in leukaemic T cells,and negatively regulates it's expression | The Insulin-like Growth Factor 1 Receptor is a transmembrane tyrosine kinase receptor that is activated by IGF-1 and IGF-2. |
| Role in Cancer | Tumor suppressor | Promotes T-Cell diferentiation | Oncogene |
| References | Lahoz A, Hall A. A tumor suppressor role for srGAP3 in mammary epithelial cells. Oncogene. 2012 Oct 29. doi: 10.1038/onc.2012.489 | 1: Aliahmad P, Kaye J (2008) Development of all CD4 T lineages requires nuclear factor TOX. J Exp Med 205: 245–256.<br><br>2: Palii CG, Perez-Iratxeta C, Yao Z, Cao Y, Dai F, Davison J, Atkins H, Allan D, Dilworth FJ, Gentleman R, Tapscott SJ, Brand M. Differential genomic targeting of the transcription factor TAL1 in alternate haematopoietic lineages. EMBO J. 2011 Feb 2;30(3):494-509. doi: 10.1038/emboj.2010.342. Epub 2010 Dec 21. | Medyouf H, Gusscott S, Wang H, Tseng JC, Wai C, Nemirovsky O, Trumpp A, Pflumio F, Carboni J, Gottardis M, Pollak M, Kung AL, Aster JC,Holzenberger M, Weng AP. High-level IGF1R expression is required for leukemia-initiating cell activity in T-ALL and is supported by Notch signaling. J Exp Med. 2011 Aug 29;208(9):1809-22. doi: 10.1084/jem.20110121. Epub 2011 Aug 1. |

| Gene name | LRP12 | ID1 | MX2 | BTG2 |
|---|---|---|---|---|
| Function | Low-density lipoprotein receptor; The level of this protein was found to be lower in tumor derived cell lines compared to normal cells; may act as tumor suppressor | Although it does not bind directly to DNA, by binding basic helix-loop-helix transcription factors through its HLH motif, ID1 may control tissue-specific genes related to cell growth, proliferation, differentiation and angiogenesis; ID1 is a common downstream target of oncogenic tyrosine kinases in leukemic cells; | Interferon-induced GTP-binding protein; is upregulated by interferon-alpha | TG family member 2 or NGF-inducible anti-proliferative protein PC3; has been shown to inhibit medulloblastoma, by inhibiting the proliferation and triggering the diffentiation of the precursors of cerebellar granule neurons. It is involved in the regulation of the G1/S transition of the cell cycle. Btg2 act as transcriptional cofactor of the Hoxb9 protein, and suggest that this interaction may mediate it's antiproliferative function. |
| Role in Cancer | Potencial tumor suppressor | Oncogene | Not determined | Tumor suppressor |
| References | web reference: http://refgene.com/gene/29967 | 1: Tam WF, Gu TL, Chen J, Lee BH, Bullinger L, Fröhling S, Wang A, Monti S, Golub TR, Gilliland DG. Id1 is a common downstream target of oncogenic tyrosine kinases in leukemic cells. Blood. 2008 Sep 1;112(5):1981-92. doi: 10.1182/blood-2007-07-103010.<br><br>2: Perk J, Iavarone A, Benezra R. Id family of helix-loop-helix proteins in cancer. Nat Rev Cancer. 2005 Aug;5(8):603-14. | | 1: Farioli-Vecchioli S, Tanori M, Micheli L, Mancuso M, Leonardi L, Saran A, Ciotti MT, Ferretti E, Gulino A, Pazzaglia S, Tirone F. Inhibition of medulloblastoma tumorigenesis by the antiproliferative and pro-differentiative gene PC3. FASEB J. 2007 Jul;21(9):2215-25. Epub 2007 Mar 19.<br><br>2: Prévôt D, Voeltzel T, Birot AM, Morel AP, Rostan MC, Magaud JP, Corbo L. The leukemia-associated protein Btg1 and the p53-regulated protein Btg2 interact with the homeoprotein Hoxb9 and enhance its transcriptional activation. J Biol Chem. 2000 Jan 7;275(1):147-53 |

**Supplementary Table 4: List of known TAL1 downregulated genes that are potentially targeted by TAL1 upregulated microRNAs, as in Figure 2b**. Described function(s), putative role in cancer and corresponding relevant references are presented for each gene. For gene assessment details see supplemental methods.

| microRNA | Modulation by TAL1 | Validated Target Genes | Top Enriched Gene Sets (Selection) |
|---|---|---|---|
| hsa-miR-135a | UP | APC, JAK2, NR3C2, FLAP | ___ |
| hsa-miR-223 | UP | RHOB, NFIX, E2F1, MEF2C, NFIA,LMO2, STMN1, Arid4b, Il6, Lpin2, CHUK, FBXW7, IGF1R, S100B, LIF, SP3, EPB41L3, SLC2A4, IRS1 | Genes down-regulated in MEF cells upon TGFB1 stimulation |
| hsa-mir-330-3p | UP | VEGFA, E2F1, NTRK3, CDC42, CD44 | Pathways in cancer |
| hsa-miR-545 | DOWN | LRP1 | ___ |
| hsa-miR-146b-5p | DOWN | NFKB1, CDKN1A, MMP16, KIT, Card10, Scube2, TRAF6, IRAK1 | NF-kB Signaling Pathway<br>IL1/IL1R Signaling Pathway<br>Pathways in cancer |

**Supplementary table 5: Validated microRNAs regulated by TAL1 and their experimentally validated human targets**. These where obtained from mirTARbase 3.5, miRrecords and TarBase 6.0. Gene set enrichment analysis was performed as described in supplemental methods.

| microRNA | Modulation by TAL1 | Enriched Set | Description | Pvalue | Set Hits | Targets of the individual miR | Set Size | Set Hits (%) | Total Hits | Total Size | Total Hits (%) |
|---|---|---|---|---|---|---|---|---|---|---|---|
| hsa-miR-146b-5p | Down | BIOCARTA_NFKB_PATHWAY | NF-kB Signaling Pathway | 5,22E-08 | 3 | IRAK1, NFKB1, TRAF6 | 6 | 50 | 23 | 15958 | 0,15 |
| | | BIOCARTA_IL1R_PATHWAY | Signal transduction through IL1R | 1,60E-07 | 3 | IRAK1, NFKB1, TRAF6 | 6 | 50 | 33 | 15958 | 0,21 |
| | | PID_IL1PATHWAY | IL1-mediated signaling events | 1,76E-07 | 3 | IRAK1, NFKB1, TRAF6 | 6 | 50 | 34 | 15958 | 0,22 |
| | | BIOCARTA_TOLL_PATHWAY | Toll-Like Receptor Pathway | 2,28E-07 | 3 | IRAK1, NFKB1, TRAF6 | 6 | 50 | 37 | 15958 | 0,24 |
| | | KEGG_LEISHMANIA_INFECTION | Leishmania infection | 1,74E-06 | 3 | IRAK1, NFKB1, TRAF6 | 6 | 50 | 72 | 15958 | 0,46 |
| | | KEGG_PATHWAYS_IN_CANCER | Pathways in cancer | 2,54E-06 | 4 | CDKN1A, KIT, NFKB1, TRAF6 | 6 | 66,67 | 328 | 15958 | 2,06 |
| | | KEGG_TOLL_LIKE_RECEPTOR_SIGNALING_PATHWAY | Pathways in cancer | 5,00E-06 | 3 | IRAK1, NFKB1, TRAF6 | 6 | 50 | 102 | 15958 | 0,64 |
| | | KEGG_NEUROTROPHIN_SIGNALING_PATHWAY | Neurotrophin signaling pathway | 9,45E-06 | 3 | IRAK1, NFKB1, TRAF6 | 6 | 50 | 126 | 15958 | 0,79 |
| | | REACTOME_SIGNALLING_BY_NGF | Genes involved in Signalling by NGF | 4,81E-05 | 3 | IRAK1, NFKB1, TRAF6 | 6 | 50 | 217 | 15958 | 1,36 |
| | | LI_INDUCED_T_TO_NATURAL_KILLER_UP | Genes up-regulated in ITNK cells (T-lymphocyte progenitors (DN3 cells) reprogrammed to natural killer (NK) cells by ablation of BCL11B [GeneID=64919] gene), compared to the parental DN3 cells. | 9,43E-05 | 3 | CDKN1A, NFKB1, KIT | 6 | 50 | 272 | 15958 | 1,71 |
| hsa-miR-223 | UP | PLASARI_TGFB1_TARGETS_10HR_DN | Genes down-regulated in MEF cells (embryonic fibroblast) upon stimulation with TGFB1 [GeneID=7040] for 10 h. | 2,29E-06 | 5 | IRS1, STMN1, MEF2C, NFIA, NFIX | 16 | 31,25 | 230 | 15958 | 1,45 |
| | | RIZ_ERYTHROID_DIFFERENTIATION_CCNE1 | Selected gradually up-regulated genes whose expression profile follows that of CCNE1 [GeneID=898] in the TLX1 [GeneID=3195] Tet On IEBHX15-4 cells (pro-erythroblasts). | 7,99E-06 | 3 | E2F1, NFIX, SP3 | 16 | 18,75 | 40 | 15958 | 0,26 |
| | | STARK_PREFRONTAL_CORTEX_22Q11_DELETION_UP | Genes up-regulated in prefrontal cortex (PFC) of mice carrying a hemizygotic microdeletion in the 22q11.2 region. | 2,40E-05 | 4 | MEF2C, NFIX, SP3, IGF1R, Lpin2 | 16 | 25 | 177 | 15958 | 1,11 |
| | | KEGG_ADIPOCYTOKINE_SIGNALING_PATHWAY | Adipocytokine signaling pathway | 3,81E-05 | 3 | CHUK, IRS1, SLC2A4 | 16 | 18,75 | 67 | 15958 | 0,42 |
| | | PID_P75NTRPATHWAY | p75(NTR)-mediated signaling | 4,16E-05 | 3 | RHOB, CHUK, E2F1 | 16 | 18,75 | 69 | 15958 | 0,44 |
| | | WESTON_VEGFA_TARGETS_3HR | Genes up-regulated in MMEC cells (myometrial endothelium) at 3 h after VEGFA | 4,73E-05 | 3 | RHOB, LMO2, SP3 | 16 | 18,75 | 72 | 15958 | 0,46 |
| | | REACTOME_NFKB_AND_MAP_KINASES_ACTIVATION_MEDIATED_BY_TLR4_SIGNALING_REPERTOIRE | Genes involved in NFkB and MAP kinases activation mediated by TLR4 signaling repertoire | 4,73E-05 | 3 | MEF2C, CHUK, S100B | 16 | 18,75 | 72 | 15958 | 0,46 |
| | | REACTOME_TRIF_MEDIATED_TLR3 SIGNALING | Genes involved in TRIF mediated TLR3 signaling | 5,13E-05 | 3 | MEF2C, CHUK, S100B | 16 | 18,75 | 74 | 15958 | 0,47 |
| | | RIZ_ERYTHROID_DIFFERENTIATION | Selected gradually up-regulated genes in the TLX1 [GeneID=3195] Tet On IEBHX15-4 cells (pro-erythroblasts). | 5,78E-05 | 3 | E2F1, NFIX, SP3 | 16 | 18,75 | 77 | 15958 | 0,49 |
| | | REACTOME_TRAF6_MEDIATED_INDUCTION_OF_NFKB_AND_MAP_KINASES_UPON_TLR7_8_OR_9_ACTIVATION | Genes involved in TRAF6 mediated induction of NFkB and MAP kinases upon TLR7/8 or 9 activation | 5,78E-05 | 3 | MEF2C, CHUK, S100B | 16 | 18,75 | 77 | 15958 | 0,49 |
| | | REACTOME_MYD88_MAL_CASCADE_INITIATED_ON_PLASMA_MEMBRANE | Genes involved in MyD88:Mal cascade initiated on plasma membrane | 7,24E-05 | 3 | MEF2C, CHUK, S100B | 16 | 18,75 | 83 | 15958 | 0,53 |
| | | KEGG_PROSTATE_CANCER | Prostate cancer | 8,91E-05 | 3 | IGF1R, CHUK, E2F1 | 16 | 18,75 | 89 | 15958 | 0,56 |
| | | REACTOME_ACTIVATED_TLR4_SIGNALLING | Genes involved in Activated TLR4 signalling | 1,02E-04 | 3 | MEF2C, CHUK, S100B | 16 | 18,75 | 93 | 15958 | 0,59 |
| | | MCCLUNG_CREB1_TARGETS_UP | Genes up-regulated in the nucleus accumbens (a major reward center in the brain) 8 weeks after induction of CREB1 | 1,12E-04 | 3 | MEF2C, FBXW7, STMN1 | 16 | 18,75 | 96 | 15958 | 0,61 |
| | | WESTON_VEGFA_TARGETS | Genes up-regulated in MMEC cells (myometrial endothelium) by VEGFA | 1,50E-04 | 3 | RHOB, LMO2, SP3 | 16 | 18,75 | 106 | 15958 | 0,67 |
| hsa-mir-330-3p | UP | KEGG_PANCREATIC_CANCER | Pancreatic cancer | 8,03E-07 | 3 | CDC42, E2F1, VEGFA | 5 | 60 | 70 | 15958 | 0,44 |
| | | KEGG_PATHWAYS_IN_CANCER | Pathways in cancer | 8,34E-05 | 3 | CDC42, E2F1, VEGFA | 5 | 60 | 328 | 15958 | 2,06 |

**Supplementary Table 6: Gene set enrichment analysis for the experimentally validated targets of TAL1 regulated microRNAs.** Analysis was performed using Genomica software (http://genomica.weizmann.ac.il/). P-values were determined by a hypergeometric test, followed by a false discovery rate correction to account for multiple hypotheses (FDR < 0.05).

## Chapter 3: Results

# The Notch driven long non-coding RNA repertoire in T-cell acute lymphoblastic leukemia

Kaat Durinck[1*], Annelynn Wallaert[1*], Inge Van de Walle[2], Wouter Van Loocke[1], Pieter-Jan Volders[1], Suzanne Vanhauwaert[1], Ellen Geerdens[3], Yves Benoit[1], Nadine Van Roy[1], Bruce Poppe[1], Jean Soulier[4], Jan Cools[3], Pieter Mestdagh[1], Jo Vandesompele[1], Pieter Rondou[1], Pieter Van Vlierberghe[1], Tom Taghon[2**] and Frank Speleman[1**]

[1]*Center for Medical Genetics, Ghent University, Ghent, Belgium*

[2]*Department of Clinical Chemistry, Microbiology and Immunology, Ghent University, Ghent, Belgium;*

[3]*Laboratory for the Molecular Biology of Leukemia, Center for Human Genetics, KU Leuven and Center for the Biology of Disease, VIB, Leuven, Belgium*

[4]*Genome Rearrangements and Cancer Laboratory, U944 INSERM, University Paris Diderot and Hematology Laboratory, Saint-Louis Hospital, Paris, France*

**shared first authorship*

**Haematologica. 2014 Dec;99(12):1808-16**

## Chapter 3: Results

### ABSTRACT

Genetic studies in T-cell acute lymphoblastic leukemia have uncovered a remarkable complexity of oncogenic and loss-of-function mutations. Amongst this plethora of genetic changes, *NOTCH1* activating mutations stand out as the most frequently occurring genetic defect, identified in more than 50% of T-cell acute lymphoblastic leukemias, supporting a role as an essential driver for this gene in T-cell acute lymphoblastic leukemia oncogenesis. In this study, we aimed to establish a comprehensive compendium of the long non-coding RNA transcriptome under control of Notch signaling. For this purpose, we measured the transcriptional response of all protein coding genes and long non-coding RNAs upon pharmacological Notch inhibition in the human T-cell acute lymphoblastic leukemia cell line CUTLL1 using RNA-sequencing. Similar Notch dependent profiles were established for normal human $CD34^+$ thymic T-cell progenitors exposed to Notch signaling activity *in vivo.* In addition, we generated long non-coding RNA expression profiles (array data) from *ex vivo* isolated Notch active $CD34^+$ and Notch inactive $CD4^+CD8^+$ thymocytes and from a primary cohort of 15 T-cell acute lymphoblastic leukemia patients with known *NOTCH1* mutation status. Integration of these expression datasets with publicly available Notch1 ChIP-sequencing data resulted in the identification of long non-coding RNAs directly regulated by Notch activity in normal and malignant T cells. Given the central role of Notch in T-cell acute lymphoblastic leukemia oncogenesis, these data pave the way for the development of novel therapeutic strategies that target hyperactive Notch signaling in human T-cell acute lymphoblastic leukemia.

# Chapter 3: Results

## INTRODUCTION

The Notch pathway comprises a highly conserved signaling pathway that regulates various cellular processes in all metazoans, including stem cell maintenance, regulation of cell fate decisions, cellular proliferation, differentiation, cell death and adult tissue homeostasis.[1] As such, Notch signaling is critically involved in many different tissues including epithelial, neuronal, blood, bone, muscle and endothelial cells.[2] Precise regulation and duration of Notch signaling activity is of critical importance to ensure appropriate execution of the various developmental cues and cellular processes. Consequently, constitutive or acquired perturbation of Notch signaling frequently leads to human disease and cancer.[1-4]

Notch signaling plays multiple roles in hematopoiesis and is essential for the establishment of definitive hematopoiesis through the generation of hematopoietic stem cells,[5] as well as for their subsequent differentiation in an expanding number of blood cell types.[6-9] The role of Notch signaling has been particularly well documented in T-cell development where Notch1/Dll4 interactions are crucial to induce T-lineage differentiation at the expense of other hematopoietic lineages.[10-14] Subsequently, Notch signaling is implemented in TCR-rearrangements,[15,16] modulation of TCR-αb versus-γδ development,[17-21] and in the support of proliferation during β-selection.[22-24] Sustained activation of Notch1 signaling beyond this developmental checkpoint has been shown to cause T-cell acute lymphoblastic leukemia (T-ALL) and *NOTCH1* activating mutations are amongst the most frequently observed genetic alterations in T-ALL.[25,26] Importantly, γ-secretase inhibitors (GSIs) that block S3 cleavage of the Notch1 receptor and subsequent release of the intracellular signaling domain (ICN) are the subject of intensive investigation as novel drugs to combat T-ALL. However, single compound therapies almost invariably lead to resistance. Therefore, a deeper understanding of Notch signaling in normal thymocyte maturation[27] and in Notch1 activated T-ALLs could yield novel insights that could make treatment more effective.

Activation of Notch1 converts the intracellular domain (ICN1) of the Notch1 receptor into a transcriptional activator and ICN1 subsequently acts as a direct regulator of multiple target genes.[28] However, despite intensive investigation, the nature of these genes, as well as their context-dependent activation, remains largely elusive.

## Chapter 3: Results

In general, oncogenic Notch signaling promotes leukemic T-cell growth through direct transcriptional upregulation of multiple anabolic genes involved in ribosome biosynthesis, protein translation, and nucleotide and amino acid metabolism. Furthermore, Notch1 positively regulates G1/S cell cycle progression in T-ALL[29-31] and upregulates several cyclins and CDKs,[30] in addition to the recurrent oncogene MYC. Furthermore, Notch signaling regulates cell size, glucose uptake and PI3K-AKT activated glycolysis through HES1-mediated *PTEN* repression. Besides direct regulation of *HES1*, Notch1 is also implicated in the control of essential early T-cell genes such as *pre-TCRα* (*PTCRA*) and *IL7R*.[32-34] Taken together, these genes and pathways, as well as a further expanding list controlled by Notch1 in T-ALL and normal T-cell development, illustrate the complexity and vastness of the Notch1 controlled regulatory program.

Recent transcriptome-wide profiling efforts have uncovered an unanticipated pervasiveness of transcription of the human genome, most of which is not translated into protein.[35-38] Evidence is now emerging that more than 60% of the entire genome is transcribed.[39] In addition to previously well-characterized untranslated RNA molecules such as tRNAs, snoRNAs and microRNAs (miRNAs), thousands of so-called long non-coding RNAs (lncRNAs) have been annotated to the human genome.[40, 41] Although functional studies still need to be carried out on the vast majority of these lncRNA sequences, important cellular functions are rapidly being attributed to some of them, including roles in disease processes such as cancer.[42] In contrast to microRNAs, a picture is emerging in which lncRNAs can exhibit a myriad of different functions. These include various regulatory mechanisms of gene transcription, splicing, post-transcriptional control, protein activity and nuclear architecture.[43-45] Despite this initial progress, mechanisms of upstream regulation of lncRNAs have so far remained largely unexplored.

In this study, we investigate the role of Notch in the control of lncRNA transcription in the context of normal T-cell development and T-ALL. To this end, lncRNA expression was measured following modulation of Notch signaling in the T-ALL cell line CUTLL1 as well as in normal human thymocytes, and the recently published data

on genome-wide Notch1 binding sites was used to reveal the potential for direct regulation.[34] Using this approach, we identified a total of 40 Notch-driven lncRNAs, thereby revealing a novel layer in the molecular machinery that mediates Notch signaling.

## METHODS

### GSI treatment of T-ALL cell lines

HPB-ALL, TALL-1, ALL-SIL and CUTLL1 cells (see also Online Supplementary Methods) were seeded at a density of $1x10^6$ cells/mL and treated with either DMSO or 1 µM of Compound E (Enzo Life Sciences). Cells were harvested 12 and 48 h after treatment.

### Human thymocytes and OP9-DLL1 co-cultures

Pediatric thymus samples were obtained and used according to the guidelines of the Medical Ethical Commission of the Ghent University Hospital, Belgium. $CD34^+$ thymocytes were purified using magnetic activated cell sorting (MACS, Miltenyi Biotec) to a purity of more than 98% and seeded onto confluent OP9-GFP or OP9-DLL1 plates for 48h in α-MEM media supplemented with 20% heat-inactivated FCS plus 100 U/mL penicillin, 100 µg/mL streptomycin, 2 mM L-glutamine and the T-lineage supporting cytokines SCF, Flt3-L and IL-7 at 5 ng/mL each.[20] Following 48 h of OP9 co-culture, cells were harvested by forceful pipetting and stained with CD45-PE (Miltenyi) to purify $CD45^+$ human thymocytes through sorting to remove contaminating OP9 stromal cells. For validation of selected lncRNAs, CD34 MACS purified thymocytes were labeled with CD34, CD1 and CD4 to sort $CD34^+CD1^-CD4^-$ uncommitted and $CD34^+CD1^+CD4^-$ committed early thymocytes, while $CD4^+CD8^+CD3^-$ and $CD4^+CD8^+CD3^+$ double positive thymocytes were sorted following CD4, CD8 and CD3 labeling of a total thymus suspension[20]. Sorted cells were lysed in 700 µl QIAzol (Qiagen) and stored at -70°C prior to RNA isolation.

## Chapter 3: Results

### Clinical samples

Diagnostic blood samples of 15 individuals with T-ALL were acquired after informed consent from the Department of Pediatric Hemato-Oncology at Ghent University Hospital, Belgium. This cohort includes 8 wild-type *NOTCH1* cases and 7 mutant *NOTCH1* cases (all *FBXW7* wild type). Sequencing was performed as described by Mavrakis et al.[46] Correlation analysis was performed on bone marrow lymphoblast samples from 64 T-ALL patients (unknown *NOTCH1* mutation status), which were collected after informed consent according to the Declaration of Helsinki from Saint-Louis Hospital, Paris, France. The study was approved by the Institut Universitaire d'Hématologie Institutional Review Board. This primary T-ALL cohort had been previously investigated[47] and the high-quality RNA samples from this cohort were used for lncRNA micro-array based expression profiling.

### RNA sequencing

RNA samples from the CUTLL1 cells treated with GSI and thymocytes cultured on OP9-GFP/DLL1 were prepared (see also *Supplementary Methods*). RNA-seq was performed after unstranded poly-A library prep with an average coverage of $130x10^6$ paired-end reads. Reads were mapped to the hg19 reference genome using Tophat and transcript assembly was performed with Cufflinks. Differential expression analysis was carried out with DESeq2 in R. The design formula was adjusted to take into account the paired nature of the data.

### Micro-array based gene expression profiling

RNA samples (see also *Supplementary Methods*) were profiled on a custom designed Agilent micro-array covering all protein coding genes and 12,000 lncRNAs (23,042 unique lncRNA probes) as described by Volders et al.[48] The data-analysis workflow can be found in the *Supplementary Methods*. The data discussed in this publication have been deposited in the NCBI Gene Expression Omnibus[49] and are accessible through GEO Series accession number GSE62006. Complete details of study methods can be found in the *Online Supplementary Appendix*.

## RESULTS

### Pharmacological Notch inhibition followed by RNA-sequencing reveals a set of Notch regulated lncRNAs in T-ALL.

To identify lncRNAs that are regulated through Notch signaling activity in the context of T-ALL, we used the γ-secretase (GSI) inhibitor responsive T-ALL cell line CUTLL1 as a model system, since genome-wide information on this cell line is available with respect to Notch1 binding[34] and the Notch dependent expression of coding genes.[50] CUTLL1 T-ALL cells were treated with GSI for 12h and 48h in triplicate. Genome-wide transcriptional changes determined by performing differential expression analysis on the RNA-seq data (see alignment summary in **Supplementary Table S1**) with DESeq2 using Ensembl (release 75) as a reference, showed robust downregulation of several of the canonical Notch1 protein coding target genes (e.g. *DTX1*, *NRARP*, *NOTCH3*) upon GSI treatment (**Figure 1A**). A decrease in ICN1 protein levels was shown by western blot analysis and downregulation of the canonical Notch1 target gene *DTX1* upon GSI treatment was further validated by RT-qPCR (**Supplementary Figure S1**). Amongst previously annotated lncRNAs[48] we could detect significant differential expression (adjusted P-value <0.05) for 83 lncRNAs, using a basemean cut off of 100 (**Figure 1B**). In total, 50 out of the 83 differentially expressed lncRNAs were downregulated after GSI treatment.

Besides previously annotated lncRNAs, we also detected differential expression of non-coding transcripts that had not been previously annotated in other databases (Gencode, lncRNAdb, Broad Institute and Ensembl release 64).[48] Differentially expressed lncRNA loci with a basemean higher than 100 and identified as “unknown, intergenic transcript” or “transfrag falling entirely within a reference intron” by Cuffcompare were retained for further analysis. This led to a selection of 134 lncRNA loci of which 74 were downregulated upon GSI treatment.

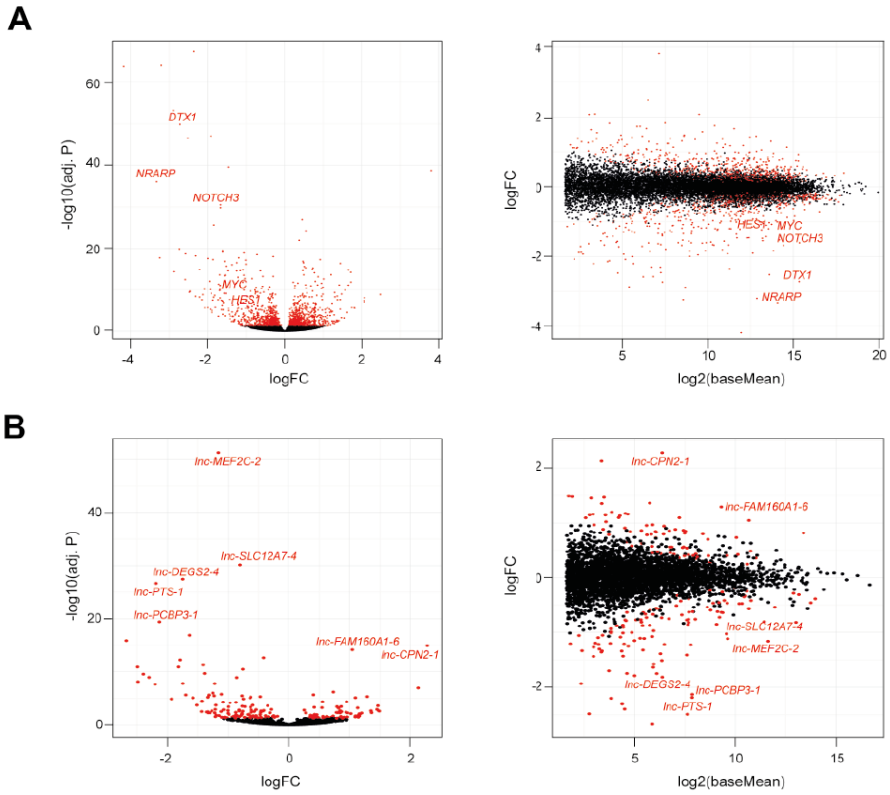


**Figure 1: Pharmacological Notch inhibition followed by RNA-sequencing identifies a set of Notch regulated lncRNAs in T-ALL**. (**A**) Volcano (left) and MA plot (right) representation of the differential expression of protein coding genes in CUTLL1 cells upon GSI treatment. Red dots represent the significant differentially expressed genes (adjusted P-value <0.05). (**B**) Volcano (left) and MA plot (right) representation of the differential expression of previously annotated lncRNAs in CUTLL1 cells upon GSI treatment. Red dots represent the significant differentially expressed genes (adjusted P-value<0.05; n=2). LncRNAs names depicted in the plots are the top differentially regulated lncRNAs.

## Transcriptional regulation of Notch regulated lncRNAs in immature normal human thymocytes

Physiological levels of Notch signaling are essential during the earliest stages of T-cell development, but no information is available on the Notch dependent expression of lncRNAs in these cells.[27] Therefore, and in order to have an independent screening method in addition to the CUTLL1 cell line to identify Notch dependent lncRNAs, we used the in *vitro* OP9-DLL1 co-culture system (**Figure 2A**). Here, *ex vivo* purified $CD34^+$ thymocytes from healthy human donors (n=2) were cultured on a feeder layer of stromal OP9 cells either expressing GFP (as a negative control) or the Notch1 ligand DLL1 to trigger Notch signaling. $CD34^+$ progenitor cells were collected after

48h of co-culture and deep RNA-sequencing was performed (*see alignment summary in Supplementary Table S2*). The set of differentially expressed protein coding genes and lncRNAs was defined as above for the CUTLL1 cells. Detection of differentially expressed protein coding genes known to be regulated by Notch signaling in early human thymocytes,[20,27] also validated our approach in this model system (**Figure 2B**). Differential expression analysis for previously annotated lncRNAs revealed 131 significantly upregulated lncRNAs as a consequence of Notch activation (**Figure 2C**). From these 131 lncRNAs, 27 overlapped with the set of downregulated lncRNAs upon GSI treatment of the CUTLL1 cell line (**Figure 2D and Supplementary Table S3**). Furthermore, we identified 156 unannotated lncRNA loci (base mean >100; adjusted P-value <0.05) in $CD34^+$ thymocytes that were upregulated by the Notch ligand DLL1. In total, 13 unique unannotated lncRNA loci were identified to be positively regulated by Notch in both normal and malignant T-cell development (**Figure 2E and Supplementary Table S4**). Amongst the set of 13 overlapping Notch lncRNA loci, the recently described *LUNAR1*[51] was present, thus supporting the validity of our approach. In addition, we also identified 33 annotated lncRNAs to be upregulated upon GSI treatment of CUTLL1 cells by RNA-seq, 18 of them overlapping with the set of lncRNAs downregulated in $CD34^+$ T-cell progenitors upon DLL1 exposure in the OP9 *in vitro* culture system (366 in total) (**Supplementary Table S5 and Figure S2A**). In a similar manner, 7 of 57 previously unannotated lncRNAs upregulated upon GSI treatment of CUTLL1 cells overlapped with the set of 320 unannotated lncRNAs downregulated in $CD34^+$ thymocytes with DLL1 exposure (**Supplementary Table S6 and Figure S2B**). Furthermore, we hypothesize that the Notch dependent lncRNAs (both annotated and unannotated) that are not shared between CUTLL1 T-ALL cells and normal human thymocytes can be assumed to have very context-specific functions and should be regarded as potentially interesting for further exploration in future studies. For example, lncRNAs expressed exclusively in T-ALL cells could be restrictively connected to a malignant context. To evaluate the putative protein coding potential of all unannotated lncRNA loci identified by RNA-seq in CUTLL1 T-ALL cells and $CD34^+$ T-cell progenitors cultured on OP9 stromal cells, Phylogenetic Codon Substitution Frequency (PhyloCSF) scores for all loci were calculated and we could confirm that more than 90% of all unannotated lncRNA loci determined are

truly ‘non-coding’ (**Supplementary Figure S3**). Putative unannotated lncRNA loci with a PhyloCSF score higher than the determined threshold score are listed and thus predicted to be ‘coding’ (*Supplementary Tables S7 and S8*) (*see also Supplementary Methods*).

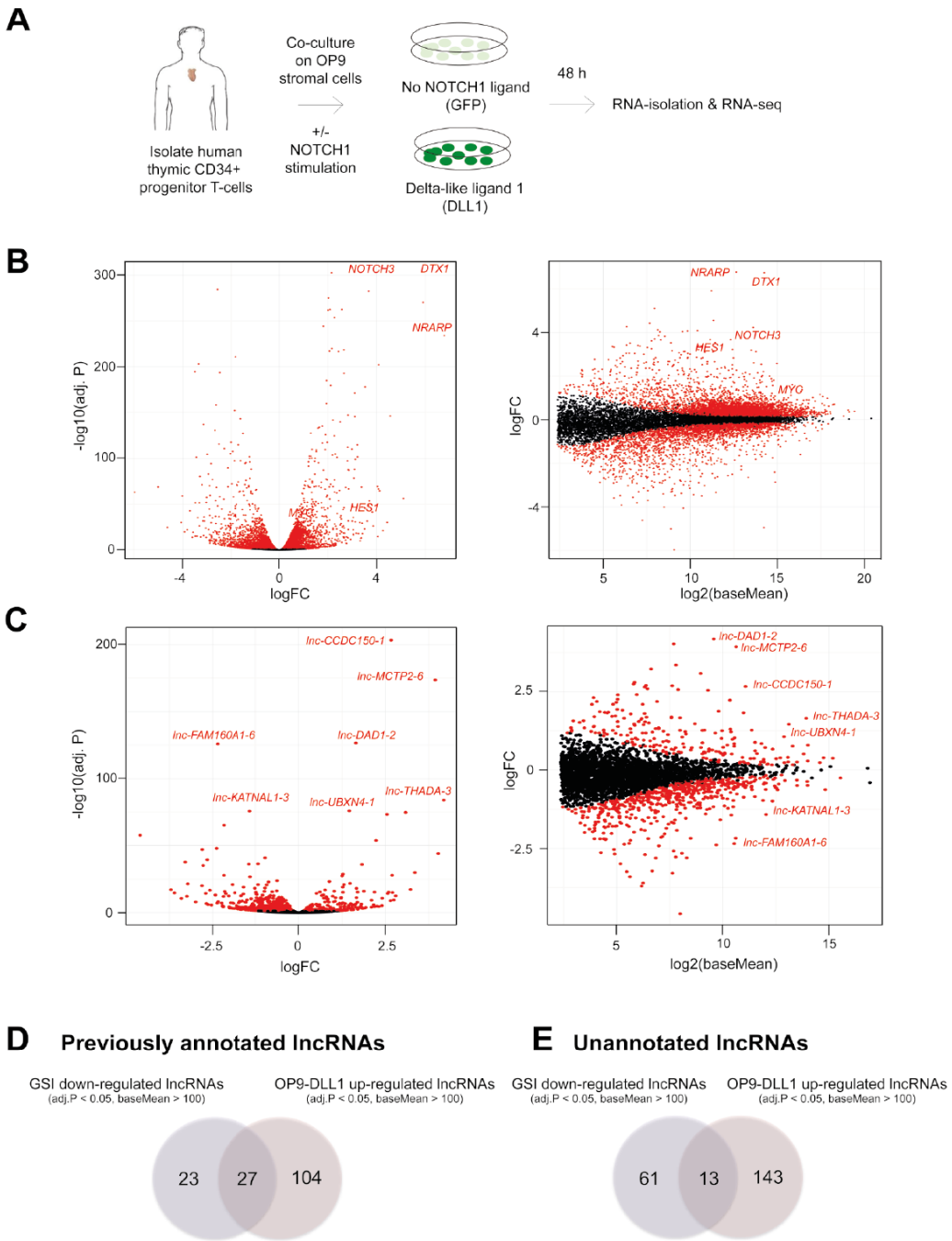


**Figure 2: Transcriptional regulation of Notch regulated lncRNAs in immature normal human thymocytes.** (**A**) Schematic overview of the OP9-control and OP9-DLL1 co-culture system used to manipulate Notch signaling in healthy human immature CD34$^+$ thymocytes. (**B**) Volcano (left) and MA plot (right) representation of the differential expression of protein coding genes in CD34$^+$ cells upon Notch signaling induction by an OP9-DLL1 feeder layer. Red dots represent the significant differentially expressed genes (adjusted P-value <0.05; n=2). (**C**) Volcano (left) and MA plot (right) representation of the differential expression of previously annotated lncRNAs in CD34$^+$ cells upon Notch activation by an OP9-DLL1 feeder layer. LncRNA names depicted in the figure are the top differentially regulated lncRNAs. (**D**) Venn diagram depicting the overlap between previously annotated lncRNAs that are downregulated upon GSI treatment of the CUTLL1 cell line and up-regulated upon co-culturing of CD34$^+$ thymocytes on the OP9-DLL1 feeder layer. (**E**) Venn diagram depicting the overlap between previously unannotated lncRNAs that are downregulated upon GSI treatment of the CUTLL1 cell line and upregulated upon co-culturing of CD34$^+$ thymocytes on OP9-DLL1 stromal cells.

**Validation of Notch regulated lncRNAs in an extended panel of T-ALL cell lines, normal T-cell subsets and primary T-ALLs**

To further validate our data, we used a custom designed Agilent micro-array[48] developed in house that contains probes for 15 of the 27 previously annotated lncRNAs and the recently identified *LUNAR1* lncRNA that were shown to be regulated by Notch in the above described RNA-seq data from the T-ALL and normal thymocyte models. First, we treated the T-ALL cell lines ALL-SIL, TALL-1, HPB-ALL and DND-41 with GSI (*Supplementary Figure S4A and B*) and carried out gene expression profiling after 12 hand 48 h. Inclusion of the GSI-treated CUTLL1 cell line samples and the samples of 4 donors of $CD34^+$ thymocytes cultured on OP9 stromal cells, revealed that there was a significant overlap between the RNA-sequencing data and the micro-array data as validated by overlapping the protein-coding signatures derived from both datasets by Gene Set Enrichment Analysis (GSEA) (*Supplementary Figure S4C and D*). Nevertheless, few lncRNAs were significantly Notch dependent over all samples of the extended panel of T-ALL cell lines (ALL-SIL, HPB-ALL, DND-41 and TALL-1), probably related to the difference in the T-ALL genetic subgroup and concomitant differences in maturation arrest of the different cell lines evaluated (**Figure 3A**). From our selection, only *lnc-PLEKHB2-1* and *lnc-UBXN4-1* were differentially expressed at a significant level, while *lnc-GSDMC-2* and *lnc-CA7-2* narrowly failed to reach significance. As we were able to detect the previously unannotated and recently described lncRNA *LUNAR1*[51] on our custom designed micro-array platform, this lncRNA was one of the strongest overlapping and significantly differentially expressed lncRNAs amongst the four GSI-treated T-ALL cell lines screened. Secondly, we validated the Notch dependency of selected lncRNAs in normal thymocytes by analyzing their expression in the most immature Notch dependent $CD34^+$ stages in comparison to the Notch independent $CD4^+CD8^+$ double positive stages of human T-cell development. As is evident from the profiles of the Notch target gene *DTX1*, we could show that in these two T-cell subpopulations *LUNAR1* follows the expression pattern of this canonical Notch target (**Figure 3B**). Remarkably, 9 out of 15 lncRNAs (and *LUNAR1*) from this selection significantly correlated with *DTX1* expression (Spearman rho correlation), supporting their

regulation by Notch during early stages of normal T-cell development (**Figure 3C and Supplementary Table S9**).

Moreover, we also had access to 15 primary T-ALL samples of which 7 harbored activating *NOTCH1* mutations while 8 were wild type (all cases are *FBXW7* wild type). There was a significant difference in expression of *LUNAR1* and *lnc-FAM120AOS-1* between *NOTCH1* wildtype and mutant cases (**Figure 3D and Supplementary Tables S10 and S11**). By implying an additional dataset of 64 primary T-ALL patient samples, we could correlate the expression of lncRNAs *lnc-PGBD5-2*, *lnc-FAM120AOS-1*, *lnc-c2orf55-1* and *LUNAR1* with the Notch1 positively regulated gene set Vilimas_NOTCH1_targets_up[52] by GSEA (**Figure 3E**). Overall, these independent experiments confirm the Notch dependent regulation of the selected lncRNAs, thereby validating the RNA-seq data from the GSI treated CUTLL1 T-ALL cell line and the Notch perturbed normal human thymocytes.

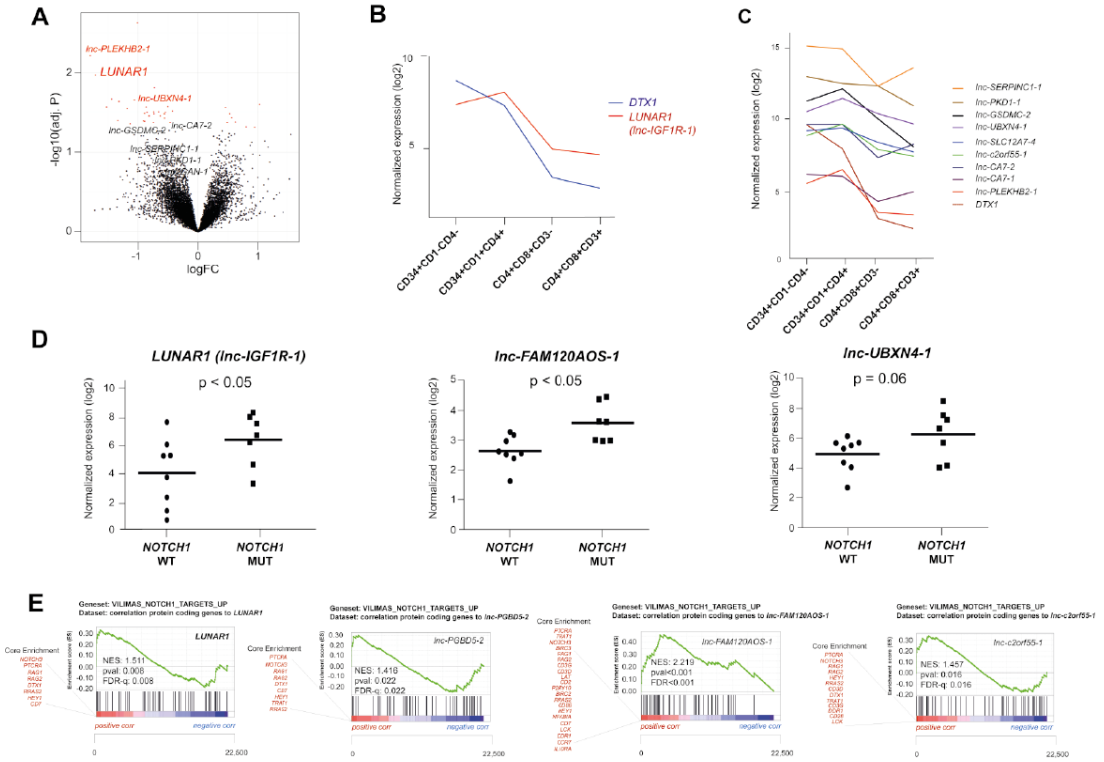


**Figure 3: Screening expression of Notch regulated lncRNAs in an extended panel of T-ALL cell lines, normal T-cells subsets and primary T-ALLs.** (**A**) Volcano plot representation of the differential expression of lncRNAs upon GSI treatment of ALL-SIL, TALL-1, HPB-ALL and DND-41 cells. Red dots represent the significant differentially expressed genes (adjusted P-value <0.05). *LUNAR1* was amongst the top-differentially expressed lncRNAs across the panel of GSI-treated T-ALL cell lines. The other lncRNA names depicted in the figure are some of the selected lncRNAs from the CUTLL1 GSI treatment and the OP9-DLL1 co-culture system. (**B**) Plot representing the expression of lncRNAs in selected Notch-dependent and -independent stages of normal T-cell development for one healthy donor. *LUNAR1* expression is significantly correlated with the expression of *DTX1* (see also *Supplementary Table S6*) and the data are representative for 4 independent donors. (**C**) Similar analysis as in (**B**) for the other lncRNAs that are significantly correlated with the expression of *DTX1* (see also *Supplementary Table S6*); data are representative for 4 independent donors. (**D**) Expression of *LUNAR1*, *lnc-FAM120AOS-1* and *lnc-UBXN4-1* in *NOTCH1* wildtype (WT) versus *NOTCH1* mutant (MUT) primary T-ALL samples. (**E**) Gene set enrichment analysis (GSEA) using the public gene set 'VILIMAS_NOTCH1_TARGETS_UP'[52] and the Spearman correlations between all protein coding genes and the set of 15 selected annotated candidate Notch lncRNAs was performed. This NOTCH1 signature was significantly enriched within the set of protein coding genes positively correlated to the expression of *lnc-PGBD5-2*, *lnc-FAM120AOS-1* and *lnc-c2orf55-1*. This enrichment was also found for lncRNA *LUNAR1*.

### Genome-wide analysis reveals direct Notch1 binding to selected lncRNAs

To further validate the direct regulation of selected lncRNAs by Notch, publically available ChIP sequencing (ChIP-seq) data from the CUTLL1 cell line were analyzed for Notch1 binding at specific loci.[34] From the Notch-driven annotated lncRNAs that overlapped between normal and malignant thymocytes (**Figure 2D**), 13 out of the 27 lncRNAs were bound by ICN1 (*Supplementary Table S12*) as illustrated for *lnc-UBXN4-1* and *lnc-PLEKHB2-1* (**Figure 4**). Remarkably, 12 out of the 13 lncRNAs with a

Notch1 binding peak also show Brd4 and Med1 binding. Notably, from the putative Notch regulated lncRNAs that showed correlated expression with *DTX1* in $CD34^+$ and $CD4^+CD8^+$ normal thymocytes, 6 out of 9 (**Figure 4 and Supplementary Figure S5**) showed binding of ICN1, suggesting that the majority is a direct Notch target.

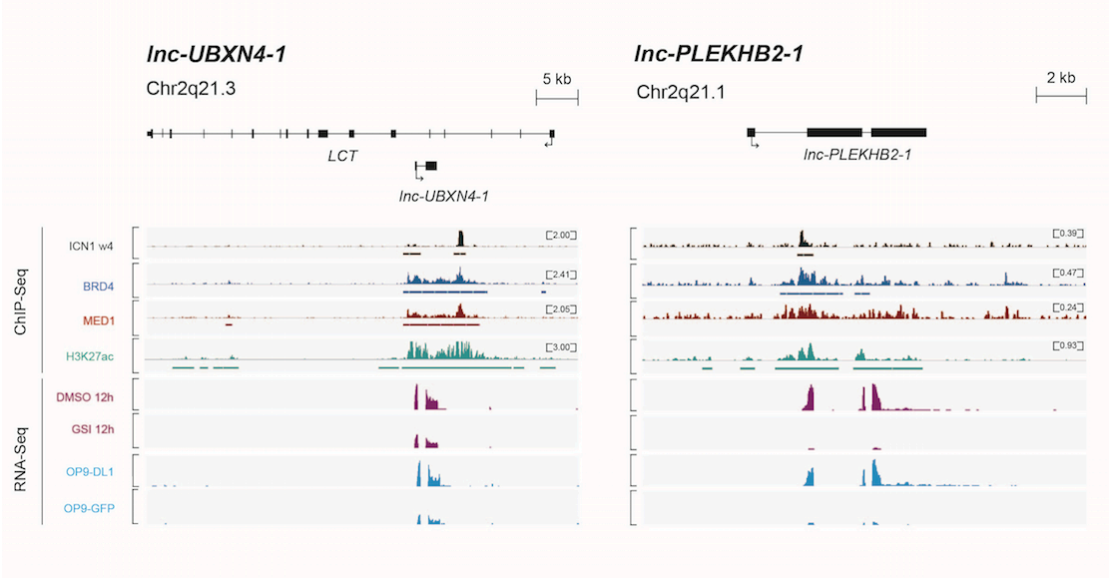


**Figure 4: Notch1 ChIP-seq reveals direct binding of Notch1 to a subset of regulated lncRNAs**. Representation of ChIP-sequencing tracks[34] for Notch1, Brd4, Med1 and H3K27ac and representative RNA-sequencing tracks for CUTLL1 DMSO/GSI treatment and OP9-GFP/DLL1 of *lnc-UBXN4-1* and *lnc-PLEKHB2-1*.

In addition, we evaluated the presence of H3K27 acetylation (H3K27ac) ChIP-seq signal at these lncRNA loci, a histone mark indicative for putative enhancer regions. For 18 out of the 27 selected lncRNAs, H3K27ac ChIP-seq signal was present in close proximity of the promoter region (*Supplementary Table S12*), suggesting the presence of enhancer sequences. Moreover, this public ChIP-seq data also showed *LUNAR1* to be directly bound by ICN1, Brd4, Med1 and H3K27ac (**Figure 5**). We also evaluated ICN1 binding at annotated lncRNA loci up-regulated upon GSI treatment of CUTLL1 T-ALL cells and downregulated in $CD34^+$ T-cell progenitors upon DLL1 exposure in the OP9 *in vitro* co-culture system. Only 4 out of the 18 overlapping annotated lncRNAs that are negatively regulated by Notch (*Supplementary Figure S2A*) showed direct binding by ICN1. The same analysis was performed on the set of 7 unannotated lncRNAs repressed by Notch1 signaling (*Supplementary Figure S2B*). Only 3 out of these 7 lncRNA loci showed ICN1 binding in the proximity of its promoter region. Given the established predominant role of Notch1 as a

transcriptional activator, lncRNAs that are negatively affected by Notch1 signaling may actually be indirect targets.

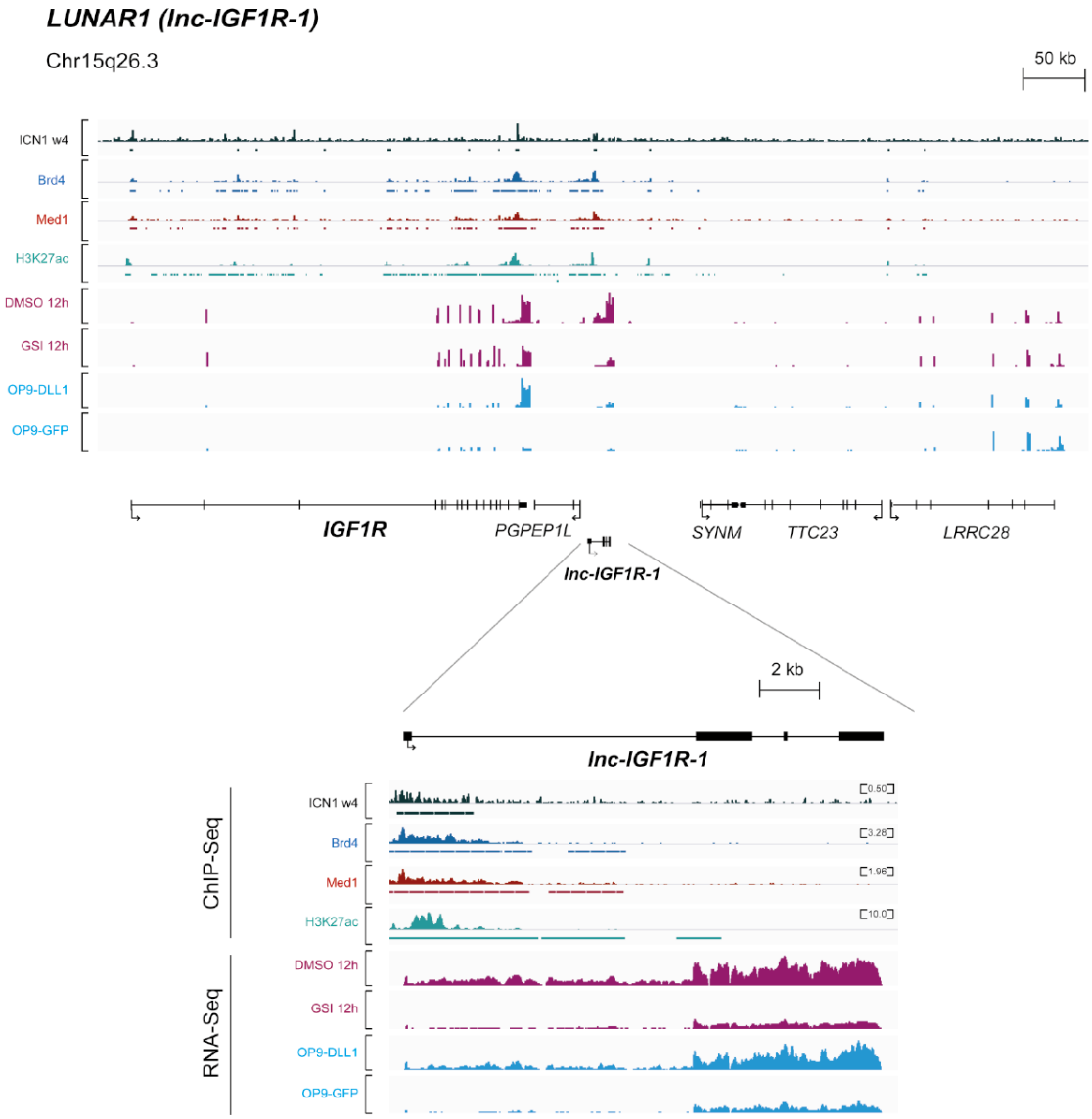


**Figure 5: Notch1 ChIP-seq reveals direct binding of Notch1 to LUNAR1.**
*LUNAR1*[51] (*lnc-IGF1R-1*) was identified amongst the top differentially expressed novel, unannotated lncRNAs in both GSI-treated CUTLL1 cells and CD34$^{+}$ thymic progenitor cells exposed to DLL1-triggered Notch signaling. Publically available ChIP-seq tracks[34] for ICN1 BRD4, MED1 and H3K27ac as well as representative in house generated RNA-seq data tracks for CUTLL1 DMSO/GSI treated cells and OP9-GFP/DLL1 are shown at the *LUNAR1* locus.

### Attributing functional annotation to Notch regulated lncRNAs through guilt-by-association analysis

As described above, we defined a core set of 27 Notch driven and previously annotated lncRNAs by considering only those differentially expressed and positively

regulated by Notch signaling in the GSI perturbation model in CUTLL1 cells and the *in vitro* OP9-DLL1 co-culture system. As a next step, we aimed to assign potential functionalities to each of these candidates. To this end, we used the 'guilt-by-association' approach (*see Supplementary Methods*). As previously mentioned, 15 out of these 27 lncRNAs (together with *LUNAR1*) were detectable by a probe on our custom designed micro-array platform. In a first step, we calculated the Spearman correlation coefficients between the lncRNAs-of-interest and all protein-coding genes using the expression data of a primary T-ALL cohort of 64 patients from which we profiled all samples on the custom designed Agilent array.[48] These correlations were subsequently used as an input for a GSEA pre-ranked analysis. Next, the output of this GSEA analysis was further refined into functional clusters of enriched gene sets using the Cytoscape plug-in enrichment mapping. This analysis yielded markedly different functional clustering patterns for each of the 16 lncRNAs analyzed (including *LUNAR1*). Important putative functionalities were represented in each of the networks as exemplified by TCR-signaling and phospholipid metabolism for *lnc-PLEKHB2-1*, DNA replication and DNA repair for *lnc-UBXN4-1* and splicing and cell cycle regulation for *LUNAR1* (**Figure 6A-C** *and Supplementary Figure S6A-M*).

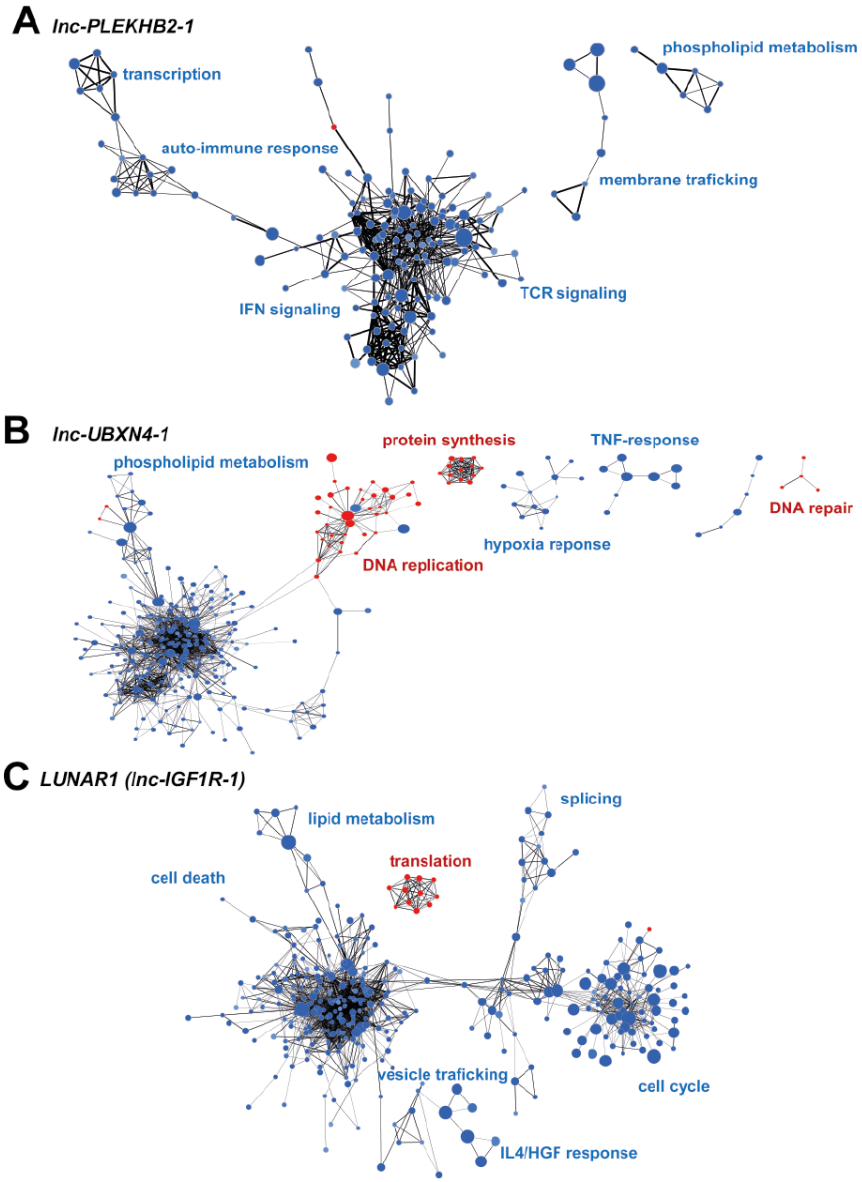


**Figure 6: Attributing functional annotation to selected, annotated lncRNAs through guilt-by-association analysis.**
Enrichment maps of gene sets correlated with the expression of (**A**) *lnc-PLEKHB2-1*, (**B**) *lnc-UBXN4-1* and (**C**) *LUNAR1*. Red nodes represent the positively correlated gene sets to the lncRNA of interest, blue nodes the negatively correlated gene sets. The size of the nodes depicts the size of the gene sets. Nodes that are clustered represent gene sets with the same or similar functional indication.

## DISCUSSION

Non-coding RNAs are emerging as important players in normal development and disease, including cancer. In previous studies, we investigated the role of miRNAs in T-cell acute lymphoblastic leukemia (T-ALL), thereby identifying a small set of miRNAs that is responsible for the cooperative suppression of several tumor suppressor genes.[46]

These miRNAs produced overlapping and co-operative effects with several *bona fide* T-ALL tumor suppressor genes including *IKZF1*, *PTEN*, *BIM*, *PHF6*, *NF1* and *FBXW7*, and more recently this network was expanded further with *PHF6*.[53] In order to provide some insight into the genetic components driving long non-coding RNAs in T-ALL formation, we performed an integrated analysis of lncRNA profiling data sets from GSI inhibited Notch-driven T-ALL cell lines and Notch-stimulated immature normal human thymocytes using the OP9 co-culture system, together with publically available genome-wide data on Notch1 binding and specific chromatin marks. In addition, we correlated the expression of Notch-dependent lncRNAs with the Notch-dependent stages of normal thymocytes during T-cell differentiation. Overall, our work establishes a novel lncRNA network that acts downstream of Notch during normal and malignant thymocyte development.

Our study provides a number of fundamental new insights into Notch-dependent regulation of lncRNAs in T-ALL and normal developing thymocytes. First, we unambiguously demonstrate that a significant number of lncRNAs are directly regulated by Notch signaling activity. Through RNA-sequencing, we identified 40 lncRNAs that are positively regulated by Notch in both normal and malignant T-lymphocytes (annotated as well as previously unannotated lncRNAs), supporting an important role for these lncRNAs in Notch-regulated T-cell biology. This could be related to various functions of Notch signaling, including T-cell lineage specification and commitment, proliferation and differentiation. Importantly, the recently identified lncRNA *LUNAR1*[51] was present amongst the most robustly Notch regulated long non-coding RNAs in our data sets. *LUNAR1* was shown to be required for efficient T-ALL growth as a consequence of its role in enhancing *IGF1R* mRNA expression to sustain IGF1 signaling.[51] As a prelude to assigning functional annotation to the newly assigned Notch-regulated lncRNAs in this study, we applied

the so-called 'guilt-by-association' approach in which functions are predicted based upon correlation with known protein-coding genes and subsequent gene set enrichment analysis. For the selected lncRNAs, various functions were predicted, several of which are linked to T-cell biology or processes that are perturbed in cancer. This marks these lncRNAs as prime targets for further functional studies in order to unravel their mode of action and assess to what extent they might serve as future therapeutic targets for treatment of T-ALL.

Not all of the 40 overlapping lncRNAs displayed ICN1 binding, as is evident from the publically available ChIP-seq data.[34] This may relate to the complexity of the chromosomal 3D-structures that are generated when lncRNAs act as cis-regulatory elements, as well as to the sensitivity of the Notch1 ChIP procedure. However, for the previously annotated lncRNAs directly bound by ICN1, all but one displayed Brd4 and Med1 binding. Those lncRNAs that are characterized by Brd4 and Med1 ChIP-seq signal are also characterized by the presence of H3K27ac ChIP-seq signal, which could be indicative of an enhancer activity of these loci.

A second aspect of our study involved the identification of novel, previously unannotated lncRNAs. Indeed, previous studies have shown that lncRNAs are often shown to be very restricted, but with biologically high relevant expression.[40-45] This includes expression during very specific time points during development and/or differentiation, as well as restriction to very specific cell subsets. Typically, these lncRNAs are expressed at significant levels in these cells whereas in other cell types their expression is very low or absent. Here, we identified novel lncRNAs in the CUTLL1 cell line and in the OP9-DLL1 co-culture system. Interestingly, 61 of these lncRNAs were present in T-ALL cells only, suggesting that their ectopic expression could be restricted to the malignant context. Likewise, lncRNAs only present in thymocytes may be implicated in differentiation of normal T-cells which is disrupted in T-ALL cells, or may reflect differential Notch3 activity as the DLL1 ligand, to which $CD34^{+}$ progenitor T cells are exposed in the OP9-DLL1 co-culture system, can activate both Notch1 and Notch3 (*Waegemans E, Van de Walle I and Taghon T, unpublished data on preferential Notch receptor-ligand interactions in human, 2011*) while both receptors are implicated in modulating human T-cell development.[21] Both subsets of lncRNAs may, therefore, serve as novel therapeutic targets for T-ALL treatment. It is

evident that our work, as well as the recent paper by Aifantis and colleagues,[51] strongly favors an important role for lncRNAs in normal T-cell development and T-ALL oncogenesis. Moreover, we show that the Notch1 transcription factor directly controls the transcription of many of these long non-coding RNAs. Therefore, one can predict that other oncogenic transcription factors and drivers in T-ALL, such as *TAL1*, *TLX1/TLX3*, *LMO1/2* and *HOXA* genes, as well as other transcriptional regulators of normal T-cell development, will also perform similar transcriptional control. Therefore, specific T-ALL subgroups and more distinct subsets of normal immature developing T cells need to be analyzed in human for detection of all lncRNAs. We predict that this will further dramatically expand the lncRNA landscape for T-ALL and thymocyte maturation, and thus provide an important regulatory framework for understanding some of the unique features that control human T-cell biology.[27] Finally, given the central role of oncogenic Notch1 activation in most if not all T-ALLs, and the current limitations of targeted therapy, further exploration of the new therapeutic opportunities offered by these lncRNAs in the context of their specific functionality is strongly recommended.

**FUNDING**

The authors would like to thank the following funding agencies: the Fund for Scientific Research Flanders ('FWO Vlaanderen' research projects G.0202.09, G.0869.10N, 3G055013N, 3G056413N to FS; 3GA00113N, 3G065614, G.0C47.13N to PVV and G0B2913N, G037514N, 3G002711 to TT; PhD grant to AW; postdoctoral grants to IvdW, TT, PM, PVV, and PR; BP is a senior clinical investigator), IWT Vlaanderen (PhD grant to KD), the Belgian Foundation against Cancer (FS, JVds (SCIE 2010-177)); Ghent University (GOA grant 01G01910 to FS), the Cancer Plan from the Federal Public Service of Health (FS), the Children Cancer Fund Ghent (FS) and the Belgian Program of Interuniversity Poles of Attraction (IUAP P7/03 and P7/07). We also would like to thank Aline Eggermont for excellent technical assistance.

**REFERENCES**

1. Hori K, Sen A, Artavanis-Tsakonas S. Notch signaling at a glance. J Cell Sci. 2013;126(Pt10):2135-40.

2. Aster JC. In brief: Notch signalling in health and disease. J Pathol. 2014;232(1):1-3.

3. Koch U, Radtke F. Notch signaling in solid tumors. Curr Top Dev Biol. 2010;92:411-55.

4. Ntziachristos P, Lim JS, Sage J, Aifantis I. From fly wings to targeted cancer therapies: a centennial for notch signaling. Cancer Cell. 2014;25(3):318-34.

5. Kumano K, Chiba S, Kunisato A, Sata M, Saito T, Nakagami-Yamaguchi E, et al. Notch1 but not Notch2 is essential for generating hematopoietic stem cells from endothelial cells. Immunity. 2003;18(5): 699-711.

6. Oh P, Lobry C, Gao J, Tikhonova A, Loizou E, Manent J, et al. In vivo mapping of notch pathway activity in normal and stress hematopoiesis. Cell Stem Cell. 2013;13(2):190-204.

7. Radtke F, MacDonald HR, Tacchini-Cottier F. Regulation of innate and adaptive immunity by Notch. Nat Rev Immunol. 2013;13(6):427-37.

8. Sandy AR, Maillard I. Notch signaling in the hematopoietic system. Expert Opin Biol Ther. 2009;9(11):1383-98.

9. Yuan JS, Kousis PC, Suliman S, Visan I, Guidos CJ. Functions of notch signaling in the immune system: consensus and controversies. Annu Rev Immunol. 2010;28: 343-65.

10. De Obaldia ME, Bell JJ, Wang X, Harly C, Yashiro-Ohtani Y, DeLong JH, et al. T cell development requires constraint of the myeloid regulator C/EBP-alpha by the Notch target and transcriptional repressor Hes1. Nat Immunol. 2013;14(12):1277-84.

11. Hozumi K, Mailhos C, Negishi N, Hirano K, Yahata T, Ando K, et al. Delta-like 4 is indispensable in thymic environment specific for T cell development. J Exp Med. 2008;205 (11):2507-13.

12. Koch U, Fiorini E, Benedito R, Besseyrias V, Schuster-Gossler K, Pierres M, et al. Deltalike 4 is the essential, nonredundant ligand for Notch1 during thymic T cell lineage commitment. J Exp Med. 2008;205(11): 2515-23.

13. Radtke F, Wilson A, Stark G, Bauer M, van Meerwijk J, MacDonald HR, et al. Deficient T cell fate specification in mice with an induced inactivation of Notch1. Immunity. 1999;10(5):547-58.

14. Wilson A, MacDonald HR, Radtke F. Notch1-deficient common lymphoid precursors adopt a B cell fate in the thymus. J Exp Med. 2001;194(7):1003-12.

15. De Smedt M, Hoebeke I, Reynvoet K, Leclercq G, Plum J. Different thresholds of Notch signaling bias human precursor cells toward B-, NK-, monocytic/dendritic-, or T-cell lineage in thymus microenvironment. Blood. 2005;106(10):3498-506.

16. Wolfer A, Wilson A, Nemir M, MacDonald HR, Radtke F. Inactivation of Notch1 impairs VDJbeta rearrangement and allows pre- TCR-independent survival of early alpha beta Lineage Thymocytes. Immunity. 2002;16(6):869-79.

17. Ciofani M, Knowles GC, Wiest DL, von Boehmer H, Zuniga-Pflucker JC. Stage-specific and differential notch dependency at the alphabeta and gammadelta T lineage bifurcation. Immunity. 2006;25(1):105-16.

18. Garbe AI, von Boehmer H. TCR and Notch synergize in alphabeta versus gammadelta lineage choice. Trends Immunol. 2007;28(3): 124-31.

19. Taghon T, Yui MA, Pant R, Diamond RA, Rothenberg EV. Developmental and molecular characterization of emerging beta- and gammadelta-selected pre-T cells in the adult mouse thymus. Immunity. 2006;24(1):53-64.

20. Van de Walle I, De Smet G, De Smedt M, Vandekerckhove B, Leclercq G, Plum J, et al. An early decrease in Notch activation is required for human TCR-alphabeta lineage differentiation at the expense of TCRgammadelta T cells. Blood. 2009;113(13):2988-98.

21. Van de Walle I, Waegemans E, De Medts J, De Smet G, De Smedt M, Snauwaert S, et al. Specific Notch receptor-ligand interactions control human TCR-alphabeta/gammadelta development by inducing differential Notch signal strength. J Exp Med. 2013;210(4):683-97.

22. Ciofani M, Zuniga-Pflucker JC. Notch promotes survival of pre-T cells at the betaselection checkpoint by regulating cellular metabolism. Nat Immunol. 2005;6(9):881-8.

23. Maillard I, Tu L, Sambandam A, Yashiro-Ohtani Y, Millholland J, Keeshan K, et al. The requirement for Notch signaling at the beta-selection checkpoint in vivo is absolute and independent of the pre-T cell receptor. J Exp Med. 2006;203(10):2239 45.

24. Taghon T, Van de Walle I, De Smet G, De Smedt M, Leclercq G, Vandekerckhove B, et al. Notch signaling is required for proliferation but not for differentiation at a well-defined beta-selection checkpoint during human T-cell development. Blood. 2009;113(14):3254-63.

25. Van Vlierberghe P, Ferrando A. The molecular basis of T cell acute lymphoblastic leukemia. J Clin Invest. 2012;122(10):3398-406.

26. Weng AP, Ferrando AA, Lee W, Morris JPt, Silverman LB, Sanchez-Irizarry C, et al. Activating mutations of NOTCH1 in human T cell acute lymphoblastic leukemia. Science. 2004;306(5694):269-71.

27. Taghon T, Waegemans E, Van de Walle I. Notch signaling during human T cell development. Curr Top Microbiol Immunol. 2012;360:75-97.

28. Kopan R, Ilagan MX. The canonical Notch signaling pathway: unfolding the activation mechanism. Cell. 2009;137(2):216-33.

29. Dohda T, Maljukova A, Liu L, Heyman M, Grander D, Brodin D, et al. Notch signaling induces SKP2 expression and promotes reduction of p27Kip1 in T-cell acute lymphoblastic leukemia cell lines. Exp Cell Res. 2007;313(14):3141-52.

30. Joshi I, Minter LM, Telfer J, Demarest RM, Capobianco AJ, Aster JC, et al. Notch signaling mediates G1/S cell-cycle progression in T cells via cyclin D3 and its dependent kinases. Blood. 2009;113(8):1689-98.

31. Rao SS, O'Neil J, Liberator CD, Hardwick JS, Dai X, Zhang T, et al. Inhibition of NOTCH signaling by gamma secretase inhibitor engages the RB pathway and elicits cell cycle exit in T-cell acute lymphoblastic leukemia cells. Cancer Res. 2009;69(7):3060-8.

32. Gonzalez-Garcia S, Garcia-Peydro M, Martin-Gayo E, Ballestar E, Esteller M, Bornstein R, et al. CSL-MAML-dependent Notch1 signaling controls T lineage-specific IL-7R{alpha} gene expression in early human thymopoiesis and leukemia. J Exp Med. 2009;206(4):779-91.

33. Reizis B, Leder P. Direct induction of T lymphocyte- specific gene expression by the mammalian Notch signaling pathway. Genes Dev. 2002;16(3):295-300.

34. Wang H, Zang C, Taing L, Arnett KL, Wong YJ, Pear WS, et al. NOTCH1-RBPJ complexes drive target gene expression through dynamic interactions with superenhancers. Proc Natl Acad Sci USA. 2014;111(2):705-10.

35. Carninci P, Kasukawa T, Katayama S, Gough J, Frith MC, Maeda N, et al. The transcriptional landscape of the mammalian genome. Science. 2005;309(5740):1559-63.

36. Consortium EP, Birney E, Stamatoyannopoulos JA, Dutta A, Guigo R, Gingeras TR, et al. Identification and analysis of functional elements in 1% of the human genome by the ENCODE pilot project. Nature. 2007;447(7146):799-816.

37. Djebali S, Davis CA, Merkel A, Dobin A, Lassmann T, Mortazavi A, et al. Landscape of transcription in human cells. Nature. 2012;489(7414):101-8.

38. Katayama S, Tomaru Y, Kasukawa T, Waki K, Nakanishi M, Nakamura M, et al. Antisense transcription in the mammalian transcriptome. Science. 2005;309(5740): 1564-6.

39. Okazaki Y, Furuno M, Kasukawa T, Adachi J, Bono H, Kondo S, et al. Analysis of the mouse transcriptome based on functional annotation of 60,770 full-length cDNAs. Nature. 2002;420(6915):563-73.

40. Cabili MN, Trapnell C, Goff L, Koziol M, Tazon-Vega B, Regev A, et al. Integrative annotation of human large intergenic noncoding RNAs reveals global properties and specific subclasses. Genes Dev. 2011;25(18): 1915-27.

41. Guttman M, Amit I, Garber M, French C, Lin MF, Feldser D, et al. Chromatin signature reveals over a thousand highly conserved large non-coding RNAs in mammals. Nature. 2009;458(7235):223-7.

42. Gutschner T, Diederichs S. The hallmarks of cancer: a long non-coding RNA point of view. RNA Biol. 2012;9(6):703-19.

43. Geisler S, Coller J. RNA in unexpected places: long non-coding RNA functions in diverse cellular contexts. Nat Rev Mol Cell Biol. 2013;14(11):699-712.

44. Kung JT, Colognori D, Lee JT. Long noncoding RNAs: past, present, and future. Genetics. 2013;193(3):651-69.

45. Ulitsky I, Bartel DP. lincRNAs: genomics, evolution, and mechanisms. Cell. 2013;154(1):26-46.

46. Mavrakis KJ, Van Der Meulen J, Wolfe AL, Liu X, Mets E, Taghon T, et al. A cooperative microRNA-tumor suppressor gene network in acute T-cell lymphoblastic leukemia (TALL). Nat Genet. 2011;43(7):673-8.

47. Clappier E, Gerby B, Sigaux F, Delord M, Touzri F, Hernandez L, et al. Clonal selection in xenografted human T cell acute lymphoblastic leukemia recapitulates gain of malignancy at relapse. J Exp Med. 2011; 208(4):653-61.

48. Volders PJ, Helsens K, Wang X, Menten B, Martens L, Gevaert K, et al. LNCipedia: a database for annotated human lncRNA transcript sequences and structures. Nucleic Acids Res. 2013;41(Database issue):D246-51.

49. Edgar R, Domrachev M, Lash AE. Gene Expression Omnibus: NCBI gene expression and hybridization array data repository. Nucleic Acids Res. 2002;30(1):207-10.

50. Palomero T, Lim WK, Odom DT, Sulis ML, Real PJ, Margolin A, et al. NOTCH1 directly regulates c-MYC and activates a feed-forward-loop transcriptional network promoting leukemic cell growth. Proc Natl Acad Sci USA. 2006;103(48):18261-6.

51. Trimarchi T, Bilal E, Ntziachristos P, Fabbri G, Dalla-Favera R, Tsirigos A, et al. Genomewide Mapping and Characterization of Notch-Regulated Long Noncoding RNAs in Acute Leukemia. Cell. 2014;158(3):593-606.

52. Vilimas T, Mascarenhas J, Palomero T, Mandal M, Buonamici S, Meng F, et al. Targeting the NF-kappaB signaling pathway in Notch1-induced T-cell leukemia. Nat Med. 2007;13(1):70-7.

53. Mets E, Van Peer G, Van der Meulen J, Boice M, Taghon T, Goossens S, et al. MicroRNA-128-3p is a novel oncomiR targeting PHF6 in T-cell acute lymphoblastic leukemia. Haematologica. 2014;99(8):1326-33.

## SUPPLEMENTARY METHODS

### Cell lines and compound treatment

HPB-ALL, TALL-1 and ALL-SIL cells were obtained from the DSMZ cell line repository, CUTLL1 cells were a kind gift of H.G. Wendel (Memorial Sloan Kettering Cancer Center, New York, USA). Cells were maintained in RPMI-.-1640 medium (Life Technologies, 52400-025), supplemented with 10% or 20 % (ALL-SIL and CUTLL1) fetal bovine serum (Biochrom AG, S0615), 1 % L-glutamin (Life Technologies) and 1% penicillin/streptomycin (Life Technologies). CUTLL1, HPB-ALL, TALL-1 and ALL-SIL cells were seeded at a density of $1*10^6$ cells/ml and treated with either DMSO or 1 µM of Compound E (Enzo Life Sciences). Cells were harvested 12 and 48 hours after treatment.

### RNA-isolation, cDNA synthesis and RT-qPCR

Total RNA was harvested with the miRNeasy minikit (Qiagen) with DNase treatment on-column. RNA-concentrations were measured by means of spectrophotometry (Nanodrop). cDNA was synthesized using the iScript cDNA synthesis kit (Biorad) according to the manufacturers' protocol, starting with 500ng of RNA, followed by RT-qPCR using the Light Cycler 480 (Roche). Finally, qPCR data was analyzed using the qBasePLUS software (Biogazelle) according to the ΔΔCt-method.

| Target | Forward primer | Reverse primer |
|---|---|---|
| *c-MYC* | GCCACGTCTCCACACATCAG | TGGTGCATTTTCGGTTGTTG |
| *HES1* | TGTCAACACGACACCGGATAAA | CCATAATAGGCTTTGATGACTTTCTG |
| *DTX1* | ACGAGAAAGGCCGGAAGGT | GGTGTTGGACGTGCCGATAG |
| *HPRT* | TGACACTGGCAAAACAATGCA | GGTCCTTTTCACCAGCAAGCT |
| *HMBS* | GGCAATGCGGCTGCAA | GGGTACCCACGCGAATCAC |
| *TBP* | CACGAACCACGGCACTGATT | TTTTCTTGCTGCCAGTCTGGAC |
| *B2M* | TGCTGTCTCCATGTTTGATGTATCT | TCTCTGCTCCCCACCTCTAAGT |

Reaction conditions for RT-qPCR

| Components | Amount |
|---|---|
| sSo Advanced 2x mastermix | 2,5 µl |
| Forward Primer (5 µM) | 0,25 µl |
| Reverse Primer (5 µM) | 0,25 µl |
| cDNA (2,5 ng/µl) | 2 µl |

Thermocycling parameters

| Step | Temperature | Time | Cycles |
|---|---|---|---|
| *Enzyme activation* | 95 °C | 2 min | 1 |
| *Amplification* | 95 °C | 5 sec | 44 |
| | 60 °C | 30 sec | |
| | 72 °C | 1 sec | |
| *Melting cyclus* | 95 °C | 5 sec | 1 |
| | 60 °C | 1 min | |
| | 95 °C | continuous | |
| *Cooling* | 37 °C | 3 min | 1 |

**Western blotting**

Total protein isolation was performed with RIPA-lysis buffer, supplemented with protease inhibitors and SDS-PAGE was performed according to standard protocols. For immunoblotting, the rabbit polyclonal antibody to cleaved NOTCH1 (Cell signaling) was used in a 1:500 dilution in BSA.

**Protein coding potential calculation**

We used PhyloCSF to identify putative protein coding transcripts in the unannotated, novel putative lncRNA loci obtained by RNA-seq. This algorithm employs codon substitution frequencies in whole-genome multi-species alignments to distinguish between coding and non-coding loci. Whole-genome alignments of 46 species are obtained from the UCSC website and processed using the PHAST package (version 1.3) to obtain the required input format for PhyloCSF.

To validate our workflow, we benchmarked PhyloCSF with transcripts annotated in Ensembl (version 75). Transcripts with biotype 'lincRNA' or 'antisense' (20,320 transcripts) serve as a negative set while transcripts with biotype 'protein coding' and an annotated coding sequence (36,959 transcripts) serve as a positive set. Using these sets, we have determined 41.2019 as an optimal treshold for the PhyloCSF score (precision of 95% and sensitivity of 91%).

## Chapter 3: Results

### Micro-array based gene expression profiling

RNA samples from T-ALL cells treated with GSI, $CD34^+$ thymocytes cultured on the OP9-GFP/DLL1 system, sorted T-cell subsets ($CD34^+$ and $CD4^+CD8^+$) and two primary T-ALL patient cohorts of which one cohort including samples with known *NOTCH1* mutation status (n=15) (all *FBXW7* wild type) and a larger cohort (n=64) were profiled on a custom designed Agilent micro-array covering all protein coding genes and 12,000 lncRNAs (23,042 unique lncRNA probes) as described by Volders et al.[46] Profiling was performed according to the manufacturers protocol (One-color Microarray-Based Gene Expression Analysis, Low Input Quick Amp Labeling, Agilent Technologies), with 100 ng RNA as input. Normalization of the expression data was performed with the VSN-package (BioConductor release 2.12) in R. Expression values were further subjected to background subtraction by selecting those probes detecting a 10% higher expression than the negative control probes of the array design in at least one treatment. Differential expression analysis was performed in R using Limma. A multifactorial design was used to control for batch effects.

### Correlation analysis for functional annotation of selected lncRNAs

Normalized micro-array based gene expression profiles were generated for all samples of the primary T-ALL patient cohort (n=64). Spearman's rho values were calculated between 15 out of the set of 27 overlapping annotated lncRNAs (**Figure 2E**) (and also for *LUNAR1* (*lnc-IGF1R-1*)) for which a probe on the custom micro-array[46] was available. This output was used to generate a ranked (.rnk) file and used as an input for a GSEA pre-ranked analysis using the c2v3.1 MsigDB collection as geneset database. The output files were subsequently loaded into Cytoscape. By means of the Cytoscape plug-in 'enrichment mapping' (Isserling et al., F1000Research, 2014), enrichment maps were built representing functional gene set clusters that were significantly correlated (red nodes) or anti-correlated (blue nodes) with the lncRNA-of-interest.

# Chapter 3: Results

## SUPPLEMENTARY TABLES

### Supplementary Table 1: RNA-seq alignment summary for CUTLL1 samples

| Sample name | Paired-end reads | Aligned Pairs | Aligned Pairs (%) | Multimapping pairs | Multimapping pairs (%) | Concordant aligned pairs (%) |
|---|---|---|---|---|---|---|
| DMSO 12h repl1 | 146323593 | 131275766 | 89.7 | 3216065 | 2.4 | 88.8 |
| DMSO 48h repl1 | 131215273 | 117807914 | 89.8 | 2895717 | 2.5 | 88.9 |
| GSI 12h repl1 | 159416630 | 143627829 | 90.1 | 3462073 | 2.4 | 89.3 |
| GSI 48h repl1 | 95100288 | 85514736 | 89.9 | 2019348 | 2.4 | 89.1 |
| DMSO 12h repl2 | 135554412 | 122299013 | 90.2 | 2828382 | 2.3 | 89.5 |
| DMSO 48h repl2 | 100687539 | 90796028 | 90.2 | 2110770 | 2.3 | 89.4 |
| GSI 12h repl2 | 199650982 | 180374457 | 90.3 | 4257865 | 2.4 | 89.6 |
| GSI 48h repl2 | 169001713 | 152387296 | 90.2 | 3637367 | 2.4 | 89.3 |
| DMSO 12h repl3 | 153193248 | 138567335 | 90.5 | 3389716 | 2.4 | 89.6 |
| DMSO 48h repl3 | 98349936 | 88513219 | 90.0 | 2165418 | 2.5 | 89.1 |
| GSI 12h repl3 | 117967005 | 106283685 | 90.1 | 2499311 | 2.4 | 89.2 |
| GSI 48h repl3 | 95918114 | 86593969 | 90.3 | 2058472 | 2.4 | 89.4 |

## Supplementary Table 2: RNA-seq alignment summary for OP9 samples

| Sample Name | Paired-end reads | Aligned Pairs | Aligned Pairs (%) | Multimapping pairs | Multimapping pairs (%) | Concordant aligned pairs (%) |
|---|---|---|---|---|---|---|
| OP9-GFP donor 1 | 175557925 | 157523775 | 89.7 | 3998129 | 2.5 | 88.9 |
| OP9-DLL1 donor 1 | 121468805 | 110981627 | 91.4 | 2682569 | 2.4 | 90.4 |
| OP9-GFP donor 2 | 133723750 | 119466289 | 89.3 | 3172892 | 2.5 | 88.4 |
| OP9-DLL1 donor 2 | 194441409 | 177560274 | 91.3 | 4350749 | 2.5 | 90.5 |

**Supplementary Table 3: Overview of 27 differentially expressed (baseMean > 100) and annotated Notch positively regulated lncRNAs shared between CUTLL1 T-ALL cells and CD34$^{+}$ T-cells on OP9**

| Chr | start | stop | Ensembl ID | lncipedia |
|---|---|---|---|---|
| chr1 | 113499037 | 113544813 | *ENSG00000226419* | *lnc-LRIG2-4* |
| chr1 | 173833038 | 173838020 | *ENSG00000234741* | *lnc-SERPINC1-1* |
| chr1 | 230394440 | 230404229 | *ENSG00000227006* | *lnc-PGBD5-2* |
| chr1 | 239866684 | 239893765 | *ENSG00000233355* | *lnc-GREM2-6* |
| chr2 | 87754887 | 87906324 | *ENSG00000222041* | *lnc-PLGLB2-1* |
| chr2 | 99378401 | 99388543 | *ENSG00000226791* | *lnc-c2orf55-1* |
| chr2 | 111965353 | 112252677 | *ENSG00000172965* | *lnc-AC108463.1-3* |
| chr2 | 132160474 | 132166622 | *ENSG00000223631* | *lnc-PLEKHB2-1* |
| chr2 | 136577761 | 136580657 | *ENSG00000226806* | *lnc-UBXN4-1* |
| chr5 | 987295 | 997423 | *ENSG00000215246* | *lnc-SLC12A7-4* |
| chr5 | 111496223 | 111499973 | *ENSG00000224032* | *lnc-APC-6* |
| chr6 | 86370710 | 86388451 | *ENSG00000203875* | *lnc-SYNCRIP-2* |
| chr7 | 22893875 | 22901021 | *ENSG00000228649* | *lnc-IL6-2* |
| chr8 | 130228728 | 130253496 | *ENSG00000250400* | *lnc-GSDMC-2* |
| chr9 | 96197614 | 96199403 | *ENSG00000227603* | *lnc-FAM120AOS-1* |
| chr9 | 139440664 | 139444345 | *ENSG00000237886* | *lnc-c9orf163-2* |
| chr16 | 2204798 | 2205359 | *ENSG00000260260* | *lnc-PKD1-1* |
| chr16 | 66921918 | 66922834 | *ENSG00000261705* | *lnc-CA7-1* |
| chr16 | 66923072 | 66924996 | *ENSG00000261088* | *lnc-CA7-2* |
| chr16 | 81416874 | 81424489 | *ENSG00000261609* | *lnc-GAN-1* |
| chr17 | 13932609 | 13972775 | *ENSG00000223385* | *lnc-CDRT15-2* |
| chr17 | 14113805 | 14121239 | *ENSG00000231595* | *lnc-COX10-1* |
| chr17 | 14207171 | 14208822 | *ENSG00000266709* | *lnc-COX10-3* |
| chr17 | 16342136 | 16381992 | *ENSG00000175061* | *lnc-TRPV2-1* |
| chr21 | 47013568 | 47017005 | *ENSG00000233922* | *lnc-PCBP3-1* |
| chr22 | 23804273 | 23829167 | *ENSG00000178248* | *lnc-IGLL1-2* |
| chrX | 130836678 | 130964671 | *ENSG00000213468* | *lnc-FRMD7-1* |

**Supplementary Table 4: Overview of 13 differentially expressed (baseMean > 100) and unannotated Notch positively regulated lncRNAs shared between CUTLL1 T-ALL cells and CD34$^{+}$ T-cells on OP9**

| Chr | CUTLL1_Start | CUTLL1_End | CUTLL1_Name | OP9_Start | OP9_End | OP9_Name |
|---|---|---|---|---|---|---|
| chr3 | 72762617 | 72774075 | *XLOC_032451* | 72767224 | 72773948 | *XLOC_032318* |
| chr3 | 73027441 | 73028329 | *XLOC_032454* | 73027514 | 73028331 | *XLOC_032320* |
| chr3 | 138253033 | 138254792 | *XLOC_032825* | 138252949 | 138255180 | *XLOC_032820* |
| chr5 | 81616893 | 81636923 | *XLOC_036711* | 81616441 | 81629071 | *XLOC_036960* |
| chr5 | 81667707 | 81678632 | *XLOC_036719* | 81672215 | 81678702 | *XLOC_036966* |
| chr12 | 113652353 | 113654532 | *XLOC_010851* | 113649939 | 113654123 | *XLOC_010919* |
| chr14 | 72878457 | 72906694 | *XLOC_012963* | 72875211 | 72906687 | *XLOC_012750* |
| chr15 | 99557714 | 99589675 | *XLOC_014517* | 99557739 | 99586083 | *XLOC_014390* |
| chr17 | 3577525 | 3578999 | *XLOC_019018* | 3578539 | 3578908 | *XLOC_018585* |
| chr17 | 3599783 | 3616722 | *XLOC_018313* | 3600043 | 3602985 | *XLOC_018591* |
| chr20 | 13350996 | 13368579 | *XLOC_028304* | 13350988 | 13366426 | *XLOC_027976* |
| chr21 | 46975354 | 46985114 | *XLOC_029412* | 46975468 | 46978095 | *XLOC_029330* |
| chr22 | 23874749 | 23889951 | *XLOC_029562* | 23878831 | 23890363 | *XLOC_029452* |

**Supplementary Table 5: Overview of 18 differentially expressed (baseMean > 100) and annotated Notch negatively regulated lncRNAs shared between CUTLL1 T-ALL cells and CD34$^+$ T-cells on OP9**

| Chr | start | stop | Ensembl ID | lncipedia |
|---|---|---|---|---|
| chr1 | 111196182 | 111216076 | *ENSG00000259834* | *lnc-KCNA3-1* |
| chr4 | 153021906 | 153025872 | *ENSG00000245954* | *lnc-FAM160A1-6* |
| chr4 | 174243357 | 174250845 | *ENSG00000248774* | *lnc-HMGB2-1* |
| chr6 | 114290865 | 114792869 | *ENSG00000228624* | *lnc-MARCKS-5* |
| chr6 | 71961061 | 72037787 | *ENSG00000232295* | *lnc-B3GAT2-2* |
| chr7 | 141404138 | 141438146 | *ENSG00000228775* | *lnc-KIAA1147-2* |
| chr8 | 60031599 | 60034363 | *ENSG00000167912* | *lnc-SDCBP-2* |
| chr12 | 47599681 | 47610239 | *ENSG00000247774* | *lnc-AMIGO2-1* |
| chr13 | 30914407 | 30951327 | *ENSG00000238121* | *lnc-KATNAL1-3* |
| chr14 | 98602411 | 98628990 | *ENSG00000258511* | *lnc-C14orf177-3* |
| chr15 | 58879706 | 58883875 | *ENSG00000259250* | *lnc-LIPC-1* |
| chr15 | 38794807 | 38797182 | *ENSG00000259326* | *lnc-FAM98B-1* |
| chr16 | 66441932 | 66447150 | *ENSG00000246898* | *lnc-CDH5-1* |
| chr16 | 89179583 | 89181687 | *ENSG00000261546* | *lnc-CBFA2T3-2* |
| chr17 | 67547499 | 67550002 | *ENSG00000267194* | *lnc-MAP2K6-5* |
| chr19 | 35302493 | 35305249 | *ENSG00000261754* | *lnc-ZNF599-1* |
| chr19 | 35279486 | 35323773 | *ENSG00000267767* | *lnc-ZNF599-2* |
| chr19 | 54862991 | 54864894 | *ENSG00000268802* | *lnc-LAIR1-1* |

**Supplementary Table 6: Overview of 7 differentially expressed (baseMean>100) and unannotated Notch positively regulated lncRNAs shared between CUTLL1 T-ALL cells and CD34$^+$ T-cells on OP9**

| Chr | CUTLL1_Start | CUTLL1_End | CUTLL1_Name | OP9_Start | OP9_End | OP9_Name |
|---|---|---|---|---|---|---|
| chr2 | 191439671 | 191455565 | *XLOC_026974* | 191439699 | 191456830 | *XLOC_027082* |
| chr3 | 141515902 | 141519763 | *XLOC_032844* | 141515791 | 141519759 | *XLOC_030962* |
| chr5 | 80698801 | 80702028 | *XLOC_036686* | 80699345 | 80701960 | *XLOC_036927* |
| chr14 | 53020359 | 53032577 | *XLOC_013366* | 53020411 | 53032938 | *XLOC_013224* |
| chr15 | 58731929 | 58747956 | *XLOC_015245* | 58737362 | 58747955 | *XLOC_015119* |
| chr15 | 60824624 | 60829179 | *XLOC_015269* | 60824529 | 60829869 | *XLOC_015183* |
| chr22 | 22609022 | 22620320 | *XLOC_030158* | 22615017 | 22620331 | *XLOC_029961* |

**Supplementary Table 7: Unannotated putative lncRNA loci identified in CUTLL1 by RNA-seq and predicted as 'coding' by PhyloCSF analysis (precision: 95%; sensitivity: 90%)**

| ID | Score | Chr | Start | End |
|---|---|---|---|---|
| *TCONS_00056766* | 52.15 | chr1 | 2246753 | 2251281 |
| *TCONS_00086798* | 43.68 | chr1 | 51628045 | 51630685 |
| *TCONS_00081942* | 44.76 | chr1 | 111333342 | 111342403 |
| *TCONS_00056764* | 52.15 | chr1 | 117354279 | 117370293 |
| *TCONS_00051781* | 54.1 | chr2 | 102007909 | 102010517 |
| *TCONS_00048597* | 60.08 | chr2 | 235384613 | 235389131 |
| *TCONS_00056543* | 49.11 | chr2 | 240516862 | 240526394 |
| *TCONS_00059899* | 41.56 | chr2 | 241126710 | 241128149 |
| *TCONS_00080921* | 72.2 | chr4 | 187952855 | 187953853 |
| *TCONS_00086799* | 43.68 | chr5 | 39099174 | 39103319 |
| *TCONS_00086796* | 43.68 | chr5 | 82223281 | 82226577 |
| *TCONS_00056765* | 52.15 | chr6 | 14444424 | 14450217 |
| *TCONS_00081943* | 44.76 | chr6 | 14451309 | 14514496 |
| *TCONS_00080012* | 48.79 | chr6 | 33548126 | 33551228 |
| *TCONS_00048598* | 60.08 | chr6 | 85587066 | 85588203 |
| *TCONS_00056767* | 52.15 | chr7 | 44122439 | 44135578 |
| *TCONS_00076833* | 65.01 | chr7 | 64940991 | 64949641 |
| *TCONS_00088333* | 466.21 | chr8 | 53673358 | 53694399 |
| *TCONS_00086792* | 43.68 | chr8 | 53675310 | 53676444 |
| *TCONS_00081938* | 44.76 | chr8 | 144272996 | 144280254 |
| *TCONS_00040364* | 48.99 | chr9 | 46278172 | 46282364 |
| *TCONS_00055762* | 113.61 | chr9 | 139472437 | 139475056 |
| *TCONS_00090830* | 60.61 | chr10 | 8393180 | 8395114 |
| *TCONS_00055763* | 112.45 | chr10 | 89871096 | 89872775 |
| *TCONS_00077100* | 103.42 | chr10 | 125757085 | 125759130 |
| *TCONS_00081941* | 44.76 | chr11 | 134570645 | 134576828 |
| *TCONS_00048600* | 60.08 | chr12 | 10472892 | 10473695 |
| *TCONS_00086793* | 43.68 | chr13 | 87409766 | 87431966 |
| *TCONS_00086794* | 43.68 | chr13 | 87441562 | 87444206 |
| *TCONS_00051777* | 86.28 | chr13 | 105817944 | 105838505 |
| *TCONS_00086795* | 43.68 | chr13 | 110359240 | 110360897 |
| *TCONS_00088327* | 117.61 | chr14 | 97646784 | 97665870 |
| *TCONS_00077099* | 103.42 | chr14 | 106837417 | 106838015 |
| *TCONS_00022415* | 43.96 | chr14 | 106856726 | 106857157 |

| | | | | |
|---|---|---|---|---|
| *TCONS_00056483* | 65.43 | chr14 | 107161628 | 107161912 |
| *TCONS_00087227* | 86.57 | chr14 | 107164554 | 107166077 |
| *TCONS_00062955* | 46.92 | chr15 | 46675349 | 46676557 |
| *TCONS_00083990* | 45.3 | chr16 | 13337081 | 13337749 |
| *TCONS_00040365* | 48.35 | chr17 | 3599782 | 3616722 |
| *TCONS_00088325* | 117.61 | chr17 | 63491521 | 63501505 |
| *TCONS_00088330* | 117.61 | chr17 | 72486556 | 72487602 |
| *TCONS_00081939* | 44.76 | chr18 | 10298402 | 10305837 |
| *TCONS_00056542* | 61.16 | chr18 | 10319095 | 10322466 |
| *TCONS_00086797* | 43.68 | chr18 | 76390627 | 76397128 |
| *TCONS_00091468* | 158.24 | chr18 | 76393073 | 76397128 |
| *TCONS_00086800* | 43.68 | chr18 | 76393688 | 76397128 |
| *TCONS_00038764* | 42.54 | chr18 | 76423717 | 76444074 |
| *TCONS_00080917* | 46.34 | chr18 | 76525660 | 76529323 |
| *TCONS_00091467* | 158.49 | chr20 | 24688672 | 24707491 |
| *TCONS_00088326* | 466.21 | chr20 | 39373455 | 39385194 |
| *TCONS_00088328* | 50 | chr20 | 39373455 | 39383151 |
| *TCONS_00088332* | 117.61 | chr20 | 56293787 | 56304682 |
| *TCONS_00081940* | 44.76 | chr20 | 56293787 | 56304682 |
| *TCONS_00058284* | 85.71 | chr20 | 56414001 | 56415852 |
| *TCONS_00021977* | 58.74 | chr21 | 47037435 | 47038182 |
| *TCONS_00059898* | 41.56 | chr21 | 47045984 | 47059169 |
| *TCONS_00022416* | 43.96 | chr21 | 47372575 | 47376597 |
| *TCONS_00021976* | 85.3 | chr22 | 23874748 | 23889951 |
| *TCONS_00088331* | 117.61 | chr22 | 46544029 | 46545743 |
| *TCONS_00088329* | 466.21 | chrX | 18902412 | 18903831 |
| *TCONS_00087753* | 186.24 | chrX | 63985367 | 64002448 |
| *TCONS_00056486* | 95.4 | chrX | 78606175 | 7861790 |
| *TCONS_00087636* | 70.65 | chrX | 130828109 | 130829871 |

**Supplementary Table 8: Unannotated putative lncRNA loci identified in CD34$^+$ thymocytes cultured on an OP9 stromal feeder layer by RNA-seq and predicted as 'coding' by PhyloCSF analysis (precision: 95%; sensitivity: 90%)**

| ID | Score | Chr | Start | End |
|---|---|---|---|---|
| *TCONS_00072393* | 44.47 | chr1 | 59763517 | 59766075 |
| *TCONS_00000024* | 71.81 | chr1 | 94482764 | 94483785 |
| *TCONS_00049576* | 119.44 | chr1 | 184071088 | 184080918 |
| *TCONS_00018092* | 49.19 | chr1 | 201492686 | 201496026 |
| *TCONS_00013282* | 57.67 | chr1 | 204579092 | 204583098 |
| *TCONS_00005447* | 74.64 | chr1 | 206266987 | 206269412 |
| *TCONS_00028199* | 47.43 | chr2 | 8578376 | 8582043 |
| *TCONS_00056874* | 57.99 | chr2 | 47765920 | 47769139 |
| *TCONS_00052880* | 192.83 | chr2 | 75488665 | 75490774 |
| *TCONS_00008149* | 71.82 | chr2 | 75944631 | 75947096 |
| *TCONS_00006489* | 53.11 | chr2 | 89074227 | 89074933 |
| *TCONS_00059446* | 73.91 | chr2 | 102979438 | 102980995 |
| *TCONS_00036912* | 58.06 | chr2 | 128352279 | 128353933 |
| *TCONS_00037996* | 44.64 | chr2 | 129448171 | 129449912 |
| *TCONS_00007201* | 51.59 | chr2 | 173364320 | 173364905 |
| *TCONS_00025943* | 65.72 | chr2 | 197044762 | 197046167 |
| *TCONS_00061061* | 99.23 | chr3 | 16005716 | 16014366 |
| *TCONS_00006917* | 203.31 | chr3 | 18572889 | 18574386 |
| *TCONS_00046453* | 72.11 | chr3 | 45844195 | 45846999 |
| *TCONS_00009952* | 43.38 | chr3 | 45854323 | 45856659 |
| *TCONS_00029725* | 42.29 | chr3 | 72767223 | 72773948 |
| *TCONS_00050097* | 130.58 | chr3 | 107844588 | 107860198 |
| *TCONS_00041198* | 54.4 | chr3 | 129325763 | 129327842 |
| *TCONS_00009908* | 98.04 | chr3 | 167462678 | 167466894 |
| *TCONS_00071913* | 41.51 | chr3 | 185543397 | 185547711 |
| *TCONS_00024054* | 385.19 | chr3 | 194355573 | 194360483 |
| *TCONS_00050052* | 113.61 | chr3 | 194356984 | 194360483 |
| *TCONS_00023792* | 46.54 | chr4 | 25171054 | 25176183 |
| *TCONS_00062252* | 43.52 | chr4 | 25213770 | 25219660 |
| *TCONS_00019745* | 42.84 | chr4 | 40187190 | 40191932 |
| *TCONS_00071014* | 138.77 | chr4 | 123200409 | 123200928 |
| *TCONS_00064666* | 45.23 | chr5 | 345191 | 345528 |
| *TCONS_00029210* | 73.7 | chr5 | 5315687 | 5317724 |
| *TCONS_00062251* | 43.52 | chr5 | 65386257 | 65389744 |
| *TCONS_00024695* | 55.93 | chr5 | 86362230 | 86371165 |
| *TCONS_00007271* | 57.61 | chr5 | 89774583 | 89776807 |

| | | | | |
|---|---|---|---|---|
| *TCONS_00011164* | 49.19 | chr5 | 133376357 | 133393098 |
| *TCONS_00062270* | 49.32 | chr5 | 150606606 | 150631743 |
| *TCONS_00057599* | 66.44 | chr5 | 179890063 | 179891602 |
| *TCONS_00052572* | 57.74 | chr6 | 2403148 | 2406370 |
| *TCONS_00050701* | 47.74 | chr6 | 3304830 | 3310274 |
| *TCONS_00026406* | 90.5 | chr6 | 5072922 | 5073683 |
| *TCONS_00064968* | 68.85 | chr6 | 6702961 | 6704251 |
| *TCONS_00047535* | 48.93 | chr6 | 14398440 | 14401713 |
| *TCONS_00064969* | 68.85 | chr6 | 14452366 | 14452809 |
| *TCONS_00064967* | 68.85 | chr6 | 14511669 | 14512993 |
| *TCONS_00013283* | 57.67 | chr6 | 14661252 | 14662655 |
| *TCONS_00013983* | 87.82 | chr6 | 15744959 | 15749318 |
| *TCONS_00045206* | 66.38 | chr6 | 29850640 | 29852333 |
| *TCONS_00006709* | 61.13 | chr6 | 37009596 | 37012118 |
| *TCONS_00029415* | 50.56 | chr6 | 106277928 | 106340820 |
| *TCONS_00052342* | 50.46 | chr6 | 130516350 | 130518701 |
| *TCONS_00066073* | 79.81 | chr6 | 130519728 | 130521019 |
| *TCONS_00045196* | 49.01 | chr6 | 130538723 | 130540284 |
| *TCONS_00068680* | 78.18 | chr6 | 149453055 | 149454182 |
| *TCONS_00028198* | 52.78 | chr6 | 150206104 | 150207553 |
| *TCONS_00066074* | 79.81 | chr6 | 156149206 | 156204567 |
| *TCONS_00007518* | 47.02 | chr6 | 157795798 | 157802109 |
| *TCONS_00068988* | 94.15 | chr6 | 161585933 | 161586608 |
| *TCONS_00049704* | 82.1 | chr7 | 1549453 | 1560923 |
| *TCONS_00057036* | 51.44 | chr7 | 23562289 | 23569431 |
| *TCONS_00052257* | 66.33 | chr7 | 99822288 | 99824735 |
| *TCONS_00023996* | 48.35 | chr10 | 88159462 | 88162084 |
| *TCONS_00013280* | 57.67 | chr10 | 98774668 | 98775476 |
| *TCONS_00039798* | 49.01 | chr11 | 36618167 | 36618905 |
| *TCONS_00029745* | 61.14 | chr11 | 64098670 | 64099428 |
| *TCONS_00023407* | 51.88 | chr11 | 127920833 | 128057011 |
| *TCONS_00029266* | 125.21 | chr11 | 127921365 | 127931679 |
| *TCONS_00019744* | 42.84 | chr12 | 2853698 | 2858699 |
| *TCONS_00029267* | 125.21 | chr12 | 2862395 | 2865432 |
| *TCONS_00050031* | 69.4 | chr12 | 9756644 | 9758808 |
| *TCONS_00029209* | 73.7 | chr12 | 12881631 | 12883860 |
| *TCONS_00018582* | 172.63 | chr12 | 92032126 | 92039218 |
| *TCONS_00056635* | 46.92 | chr12 | 113649938 | 113654123 |
| *TCONS_00064971* | 43.71 | chr12 | 113671963 | 113673219 |
| *TCONS_00050079* | 72.43 | chr12 | 117254966 | 117257189 |
| *TCONS_00059445* | 73.91 | chr13 | 49105331 | 49107037 |

| | | | | |
|---|---|---|---|---|
| *TCONS_00028236* | 57.24 | chr13 | 100065629 | 100070089 |
| *TCONS_00064970* | 49.99 | chr14 | 23437727 | 23438969 |
| *TCONS_00013979* | 180.78 | chr14 | 53068696 | 53069630 |
| *TCONS_00007335* | 42.33 | chr14 | 65420816 | 65423040 |
| *TCONS_00067832* | 284.96 | chr14 | 72893256 | 72906687 |
| *TCONS_00062629* | 47.14 | chr14 | 72893256 | 72906552 |
| *TCONS_00036913* | 58.06 | chr14 | 72900554 | 72900967 |
| *TCONS_00049502* | 51.09 | chr14 | 72991218 | 72992231 |
| *TCONS_00034745* | 42.14 | chr14 | 73032380 | 73033337 |
| *TCONS_00029813* | 69.45 | chr14 | 100528647 | 100529255 |
| *TCONS_00009953* | 43.98 | chr14 | 106969092 | 106969523 |
| *TCONS_00024694* | 55.93 | chr15 | 40338297 | 40342680 |
| *TCONS_00036185* | 49.23 | chr15 | 56939054 | 56939702 |
| *TCONS_00063288* | 47.57 | chr15 | 56942051 | 56942536 |
| *TCONS_00013977* | 46.88 | chr15 | 66761087 | 66770639 |
| *TCONS_00050927* | 52.15 | chr15 | 69117878 | 69120611 |
| *TCONS_00057832* | 48.94 | chr15 | 70551056 | 70553387 |
| *TCONS_00050925* | 52.15 | chr15 | 90597897 | 90599313 |
| *TCONS_00059609* | 215.5 | chr15 | 99557738 | 99574337 |
| *TCONS_00034744* | 42.54 | chr15 | 99569810 | 99574337 |
| *TCONS_00063770* | 88.29 | chr16 | 2469884 | 2470738 |
| *TCONS_00063304* | 49.76 | chr16 | 49672974 | 49674445 |
| *TCONS_00048613* | 42.52 | chr16 | 67602034 | 67603724 |
| *TCONS_00059447* | 73.91 | chr16 | 68428413 | 68430973 |
| *TCONS_00052256* | 41.29 | chr16 | 72260597 | 72265505 |
| *TCONS_00047337* | 74.83 | chr16 | 83976427 | 83979066 |
| *TCONS_00029774* | 63.28 | chr16 | 85495679 | 85496270 |
| *TCONS_00071013* | 138.77 | chr16 | 87931351 | 87934262 |
| *TCONS_00033907* | 63.44 | chr17 | 26218043 | 26218928 |
| *TCONS_00067628* | 142.98 | chr17 | 29042829 | 29051874 |
| *TCONS_00024062* | 248.12 | chr17 | 37314134 | 37315360 |
| *TCONS_00072724* | 53.63 | chr17 | 43277314 | 43281145 |
| *TCONS_00029705* | 64.89 | chr17 | 45023736 | 45030864 |
| *TCONS_00018205* | 59.56 | chr17 | 62396691 | 62407826 |
| *TCONS_00050080* | 53.87 | chr17 | 66361368 | 66363633 |
| *TCONS_00059448* | 73.91 | chr17 | 75842425 | 75847375 |
| *TCONS_00008150* | 71.82 | chr18 | 3696263 | 3697848 |
| *TCONS_00014925* | 41.49 | chr19 | 16259690 | 16259996 |
| *TCONS_00067730* | 47.41 | chr19 | 21714994 | 21717673 |
| *TCONS_00063275* | 119.25 | chr19 | 54878348 | 54879779 |
| *TCONS_00057833* | 45.18 | chr20 | 4185348 | 4187974 |

| | | | | |
|---|---|---|---|---|
| *TCONS_00026403* | 42.58 | chr20 | 13770520 | 13773490 |
| *TCONS_00063302* | 44.62 | chr21 | 45614432 | 45619053 |

**Supplementary Table 9: Correlation of selected annotated lncRNAs with *DTX1* expression in T-cell subsets of 4 healthy donors**

| Spearman correlation lncRNA with *DTX1* | r | p (two-tailed) | p-value summary |
|---|---|---|---|
| *LUNAR1* | 0.9386 | 0,0165 | * |
| *lnc-SYNCRIP-2* | 0.2912 | 0.3344 | ns |
| *lnc-SLC12A7-4* | 0.7308 | 0,0045 | ** |
| *lnc-PLEKHB2-1* | 0.8022 | 0,0010 | *** |
| *lnc-c2orf55-1* | 0.7033 | 0,0073 | ** |
| *lnc-UBXN4-1* | 0.6154 | 0,0252 | * |
| *lnc-PGBD5-2* | 0.3681 | 0,2159 | ns |
| *lnc-FAM120AOS-1* | -0.06593 | 0,8305 | ns |
| *lnc-COX10-1* | -0.2692 | 0,3737 | ns |
| *lnc-SERPINC1-1* | 0.7857 | 0,0015 | ** |
| *lnc-c9orf163-2* | 0.01099 | 0,9716 | ns |
| *lnc-GSDMC-2* | 0.7582 | 0,0027 | ** |
| *lnc-PKD1-1* | 0.7527 | 0,0030 | ** |
| *lnc-CA7-2* | 0.7967 | 0,0011 | ** |
| *lnc-GAN-1* | 0.3242 | 0,2799 | ns |
| *lnc-CA7-1* | 0.7198 | 0,0055 | ** |

**Supplementary Table 10: *NOTCH1* mutation status of primary T-ALL samples**

| | ***NOTCH1*** **WT** | ***NOTCH1*** **MUT PEST** | ***NOTCH1*** **MUT HD** | ***NOTCH1*** **MUT PEST+HD** |
|---|---|---|---|---|
| n | 8 | 3 | 2 | 2 |

**Supplementary Table 11: Differential expression and significance level of selected annotated lncRNAs in primary T-ALL samples of 8 *NOTCH1* WT and 7 *NOTCH1* MUT cases**

| **lncRNA** | **logFC** | **P** |
|---|---|---|
| *LUNAR1* | 2.376 | 0.0290 |
| *lnc-SYNCRIP-2* | 0.3544 | 0.4765 |
| *lnc-SLC12A7-4* | -0.0466 | 0.9400 |
| *lnc-PLEKHB2-1* | 0.3689 | 0.5840 |
| *lnc-c2orf55-1* | 0.3275 | 0.6443 |
| *lnc-UBXN4-1* | 1.3274 | 0.0600 |
| *lnc-PGBD5-2* | 0.2793 | 0.3982 |
| *lnc-FAM120AOS-1* | 0.9387 | 0.0072 |
| *lnc-COX10-1* | 0.3860 | 0.5047 |
| *lnc-SERPINC1-1* | 0.2643 | 0.4333 |
| *lnc-c9orf163-2* | 0.5812 | 0.0982 |
| *lnc-GSDMC-2* | 2.2868 | 0.1052 |
| *lnc-PKD1-1* | 0.2334 | 0.6461 |
| *lnc-CA7-2* | 0.1776 | 0.6448 |
| *lnc-GAN-1* | 0.3355 | 0.4639 |
| *lnc-CA7-1* | 0.0539 | 0.8577 |

**Supplementary Table 12: Notch1, Brd4, Med1 and H3K27ac ChIP-sequencing peaks for the selected annotated lncRNAs**

| lncRNA | Notch1 | Brd4 | Med1 | H3K27ac |
|---|---|---|---|---|
| *lnc-SYNCRIP-2* | X | X | X | X |
| *lnc-SLC12A7-4* | - | X | X | X |
| *lnc-PLEKHB2-1* | X | X | - | X |
| *lnc-c2orf55-1* | X | X | X | X |
| *lnc-UBXN4-1* | X | X | X | X |
| *lnc-PGBD5-2* | - | X | - | X |
| *lnc-FAM120AOS-1* | - | - | - | - |
| *lnc-COX10-1* | - | - | - | - |
| *lnc-SERPINC1-1* | X | X | X | X |
| *lnc-c9orf163-2* | X | X | X | X |
| *lnc-GSDMC-2* | X | X | X | X |
| *lnc-PKD1-1* | X | X | X | X |
| *lnc-CA7-2* | - | - | - | - |
| *lnc-GAN-1* | - | - | - | - |
| *lnc-CA7-1* | - | - | - | - |
| *lnc-AC108463.1-3* | - | - | - | - |
| *lnc-TRPV2-1* | X | X | X | X |
| *lnc-IGLL1-2* | - | X | X | X |
| *lnc-FRMD7-1* | - | - | - | - |
| *lnc-PLGLB2-1* | - | - | - | - |
| *lnc-CDRT15-2* | - | X | X | X |
| *lnc-APC-6* | X | X | X | X |
| *lnc-LRIG2-4* | X | X | X | X |
| *lnc-IL6-2* | X | X | X | X |
| *lnc-GREM2-6* | X | X | X | X |
| *lnc-PCBP3-1* | - | X | - | X |
| *lnc-COX10-3* | - | - | - | - |

X: presence of a ChIP-sequencing peak, -: absence of a ChIP-sequencing peak

# Chapter 3: Results

## SUPPLEMENTARY GRAPHICAL ABSTRACT

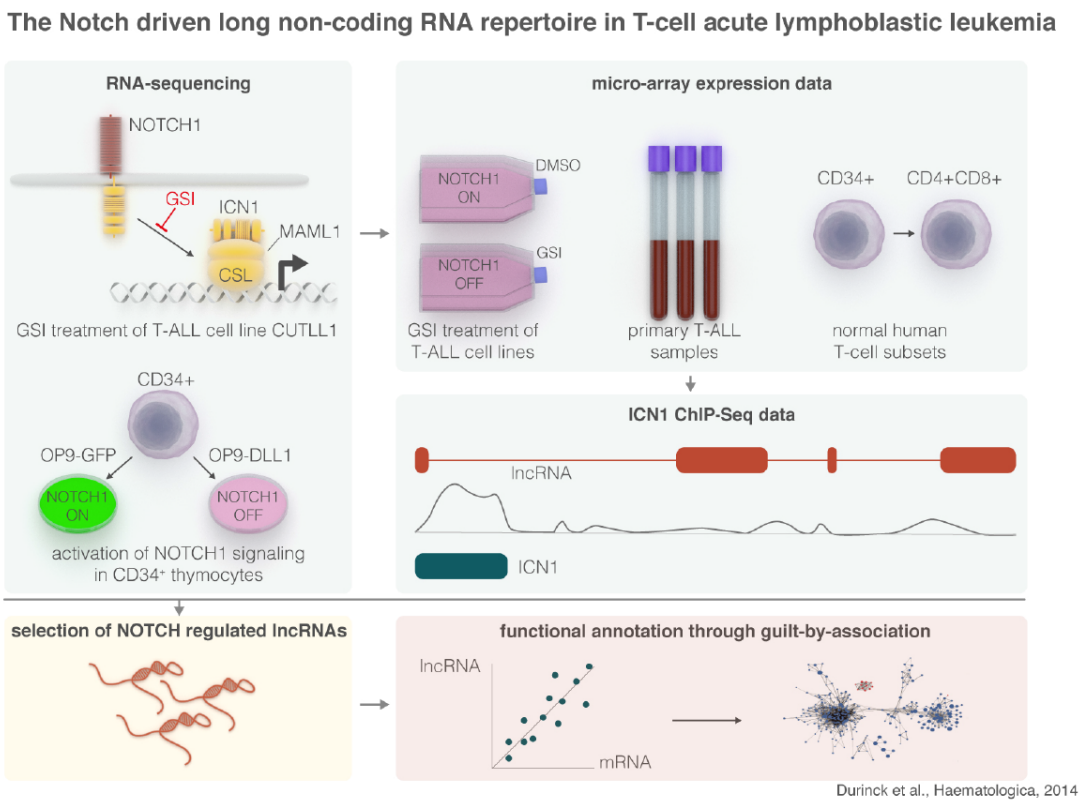

# Chapter 3: Results

## SUPPLEMENTARY FIGURES

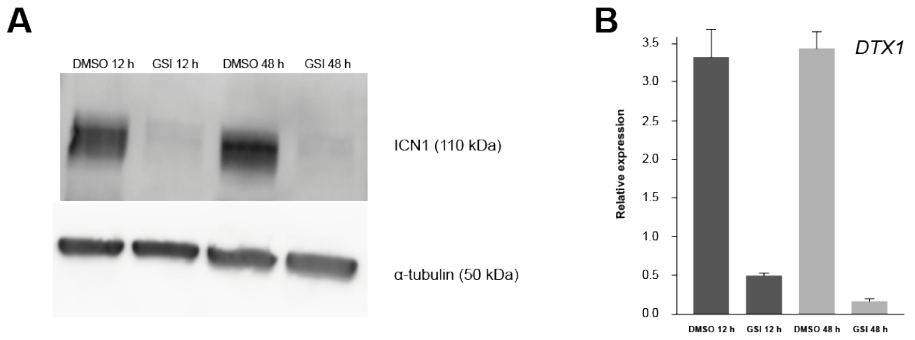


**Supplementary Figure 1: Validation of the pharmacological Notch inhibition model in CUTLL1.**
(**A**) Down-regulation of ICN1 protein levels upon GSI treatment for 12h and 48h in CUTLL1 was validated by western blot analysis. (**B**) RT-qPCR could confirm down-regulation of *DTX1* expression upon GS Itreatment of CUTLL1 T-ALL cells.

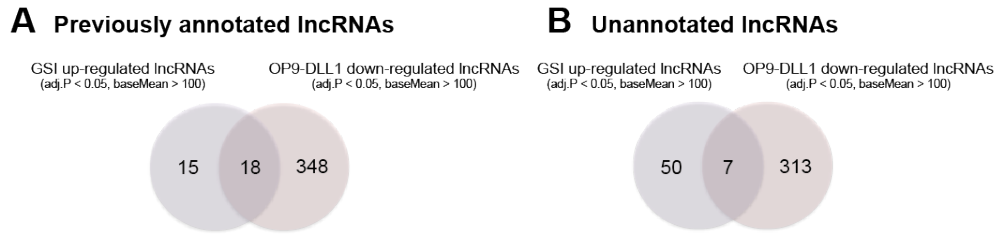


**Supplementary Figure 2: Overlap between lncRNAs that are negatively correlated with Notch signaling in GSI treatment of CUTLL1 cells and co-culturing of CD34$^+$ thymocytes on the OP9-DLL1 feeder layer.**
(**A**) Venn diagram depicting the overlap between previously annotated lncRNAs that are upregulated upon GSI treatment of the CUTLL1 cell line and down-regulated upon co-culturing of CD34$^+$ thymocytes on the OP9-DLL1 feeder layer. (**B**) Venn diagram depicting the overlap between previously unannotated lncRNAs that are upregulated upon GSI treatment of the CUTLL1 cell line and downregulated upon co-culturing of CD34$^+$ thymocytes on the OP9-DLL1 feeder layer.

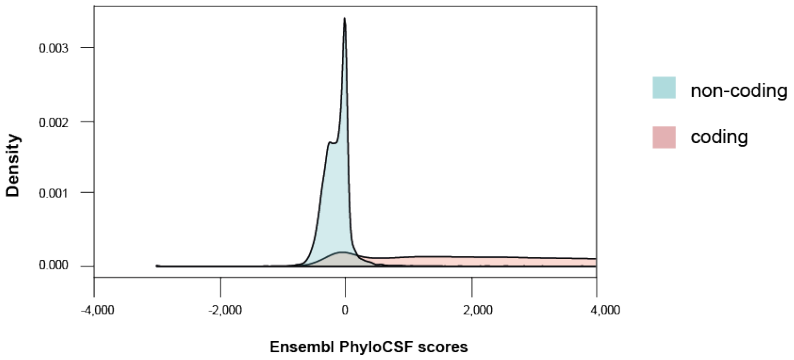


**Supplementary Figure 3: PhyloCSF density plot to evaluate the protein-coding potential of novel, unannotated lncRNA loci by RNA-seq.**
The putative protein coding potential of unannotated lncRNA loci in CUTLL1 T-ALL cells and $CD34^{+}$ T-cell progenitors cultured on an OP9 stromal feeder layer was calculated using the PhyloCSF algorithm. The optimal treshold for the PhyloCSF score was determined as 41.2019 to obtain a precision of 95% and sensitivity of 90%.

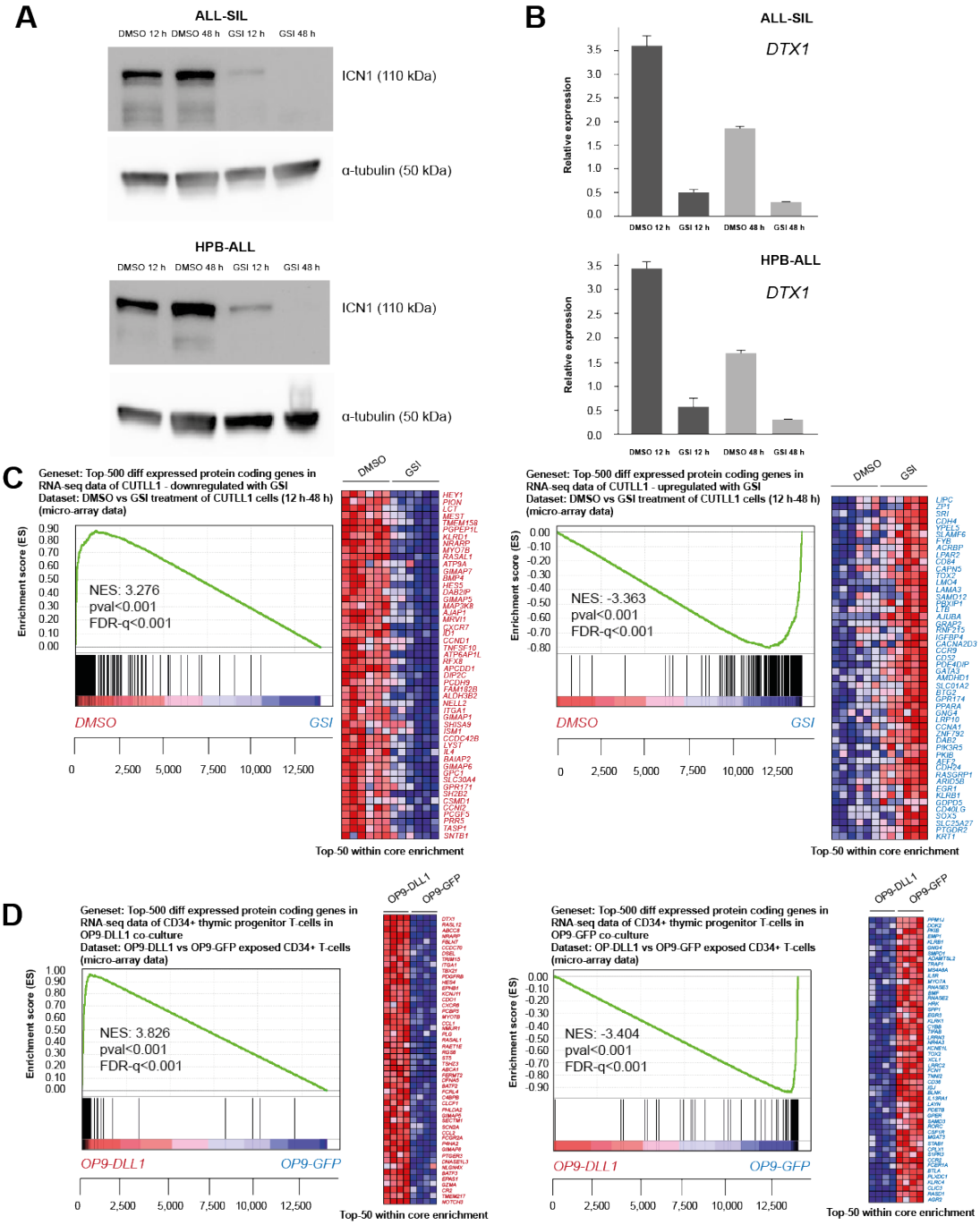


**Supplementary Figure 4: Validation of Notch regulated lncRNAs in other model systems.**
(**A**) Western blot analysis confirms down-regulation of ICN1 in HPB-ALL and ALL-SIL cells upon GSI treatment for 12 h and 48 h. (**B**) RT-qPCR shows *DTX1* downregulation upon GSI treatment of HPB-ALL and ALL-SIL T-ALL cells. GSEA shows significant overlap for differentially expressed protein-coding genes found by RNA-seq and micro-array data of (**C**) GSI-treated CUTLL1 cells and (**D**) $CD34^{+}$ T-cell progenitor on OP9-DLL1/GFP co-cultures.

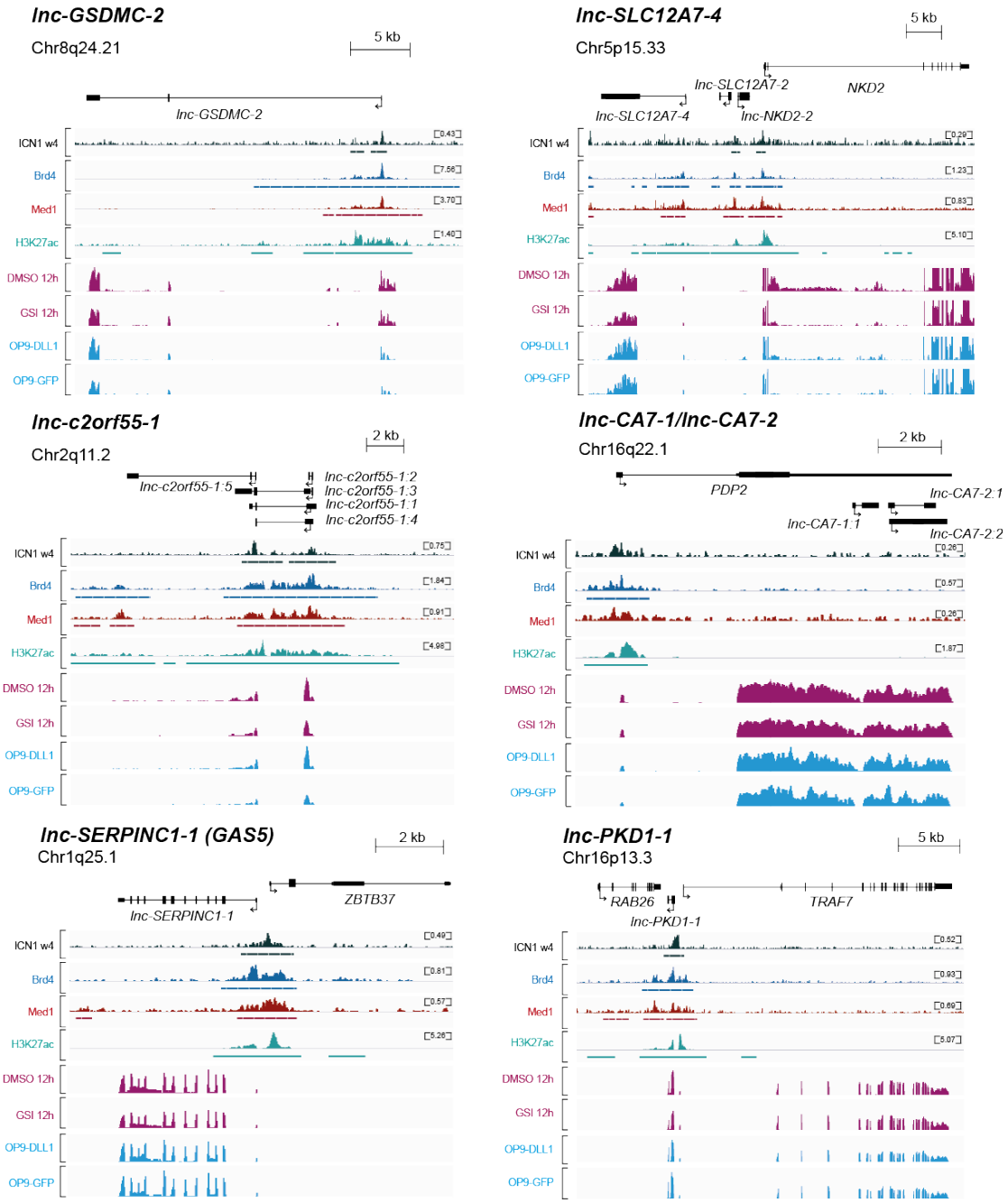


**Supplementary Figure 5: Validation of direct regulation of selected lncRNAs by Notch1.**
ChIP-seq tracks in CUTLL1 cells of Notch1, Brd4, Med1 and H3K27ac are depicted for the selection of annotated lncRNAs that were identified as overlapping Notch1 driven lncRNAs in CUTLL1 cells and $CD34^{+}$ progenitor cells cultured on OP9 stromal cells. Representative RNA-seq tracks are shown for both *in vitro* model systems.

**A** *lnc-SYNCRIP-2*

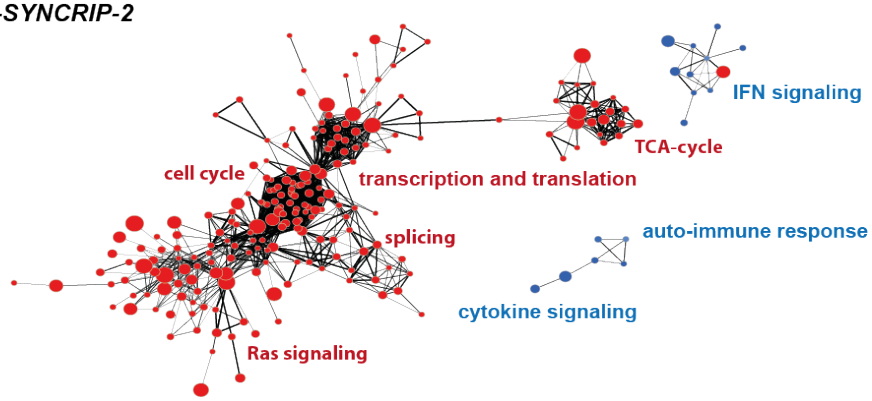


**B** *lnc-SLC12A7-4*

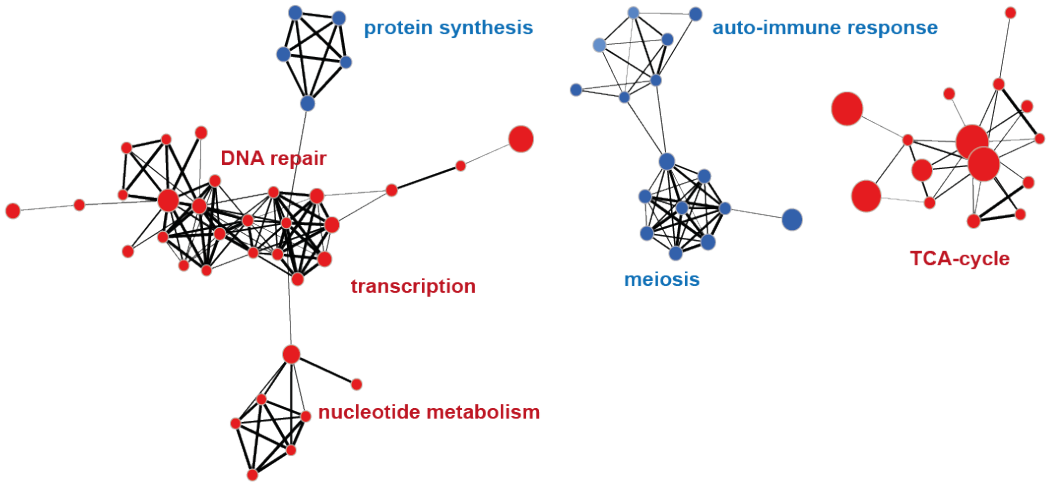


**C** *lnc-CA7-2*

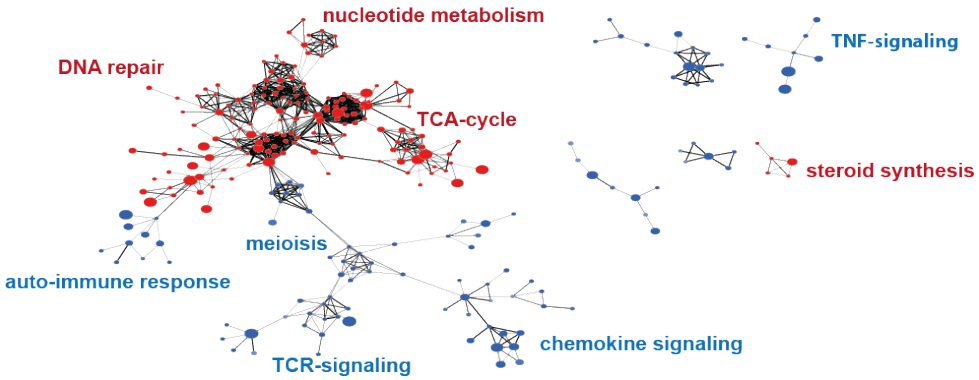

**D** *lnc-c2orf55-1*

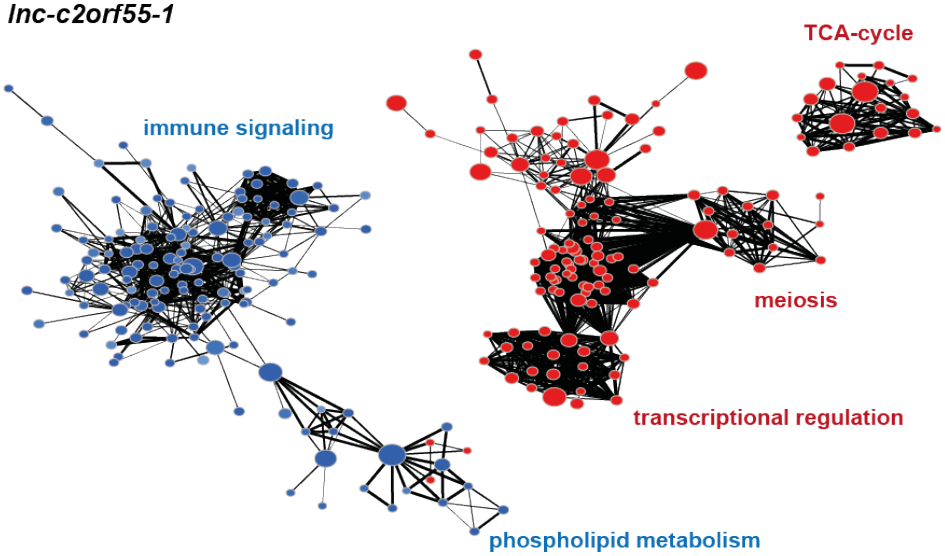


**E** *lnc-GSDMC-2*

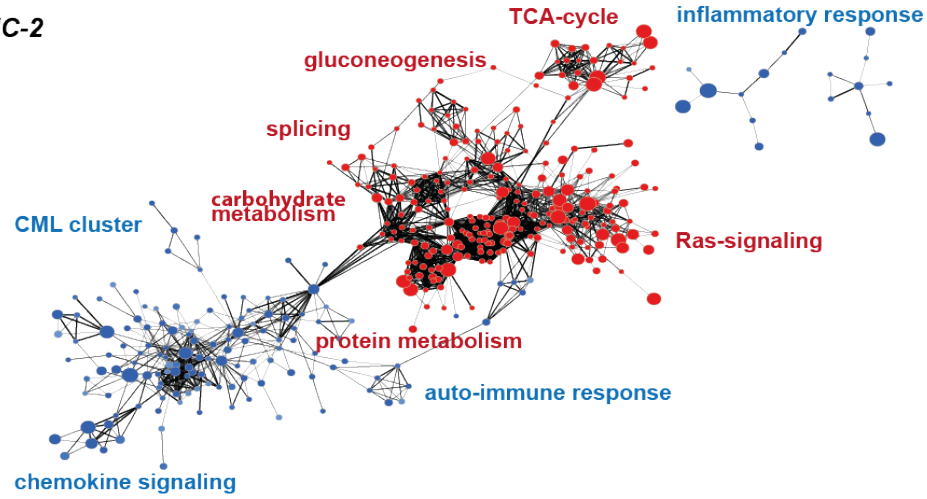


**F** *lnc-PGBD5-2*

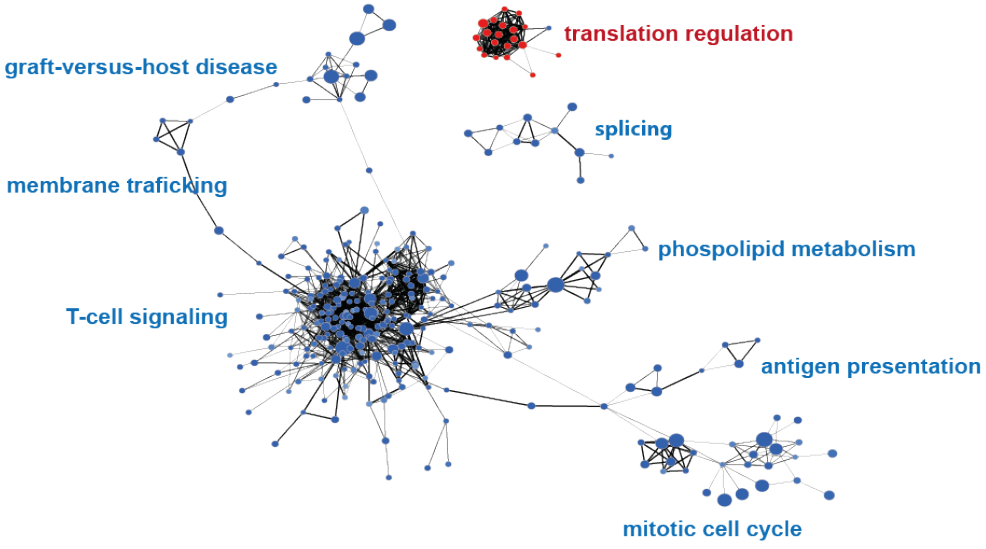

**G** *lnc-FAM120AOS-1*

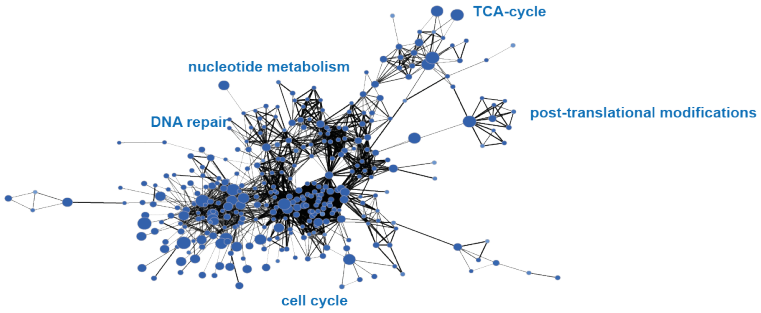


**H** *lnc-COX10-1*

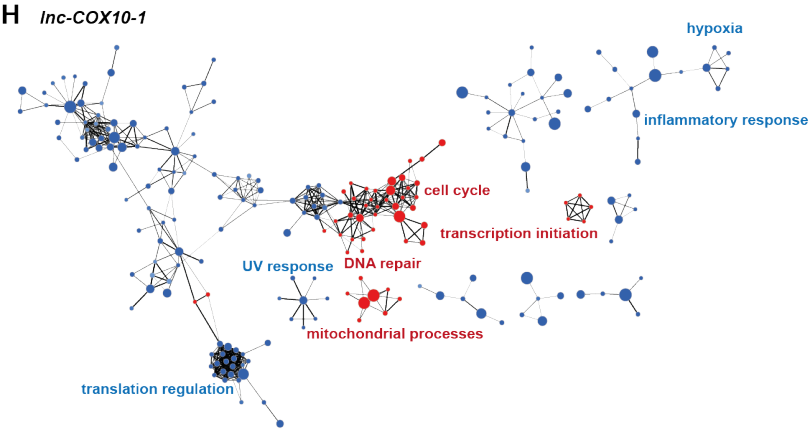


**I** *lnc-c9orf163-2*

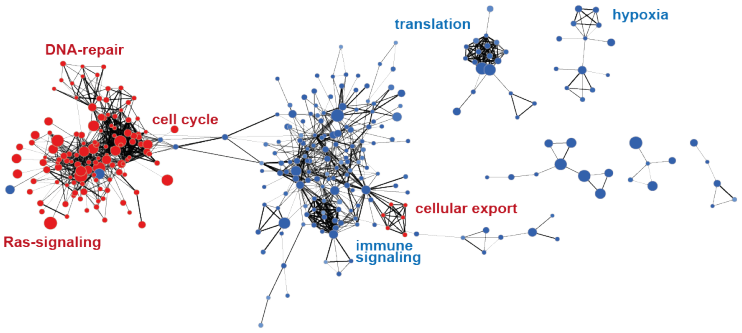

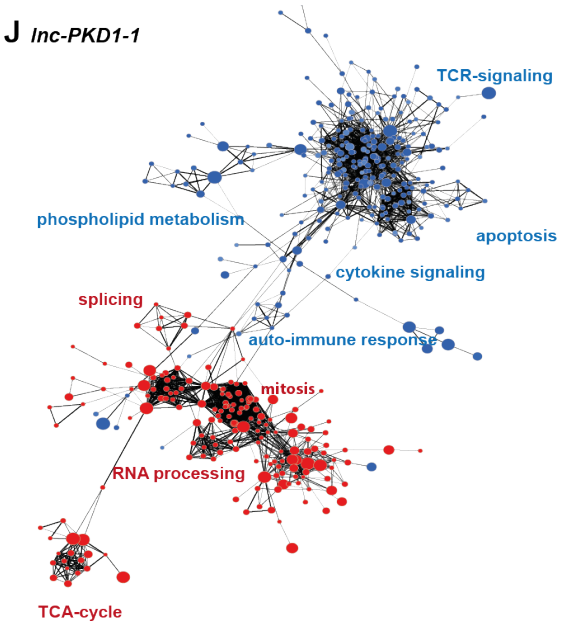
J lnc-PKD1-1
TCR-signaling
phospholipid metabolism
apoptosis
cytokine signaling
splicing
auto-immune response
mitosis
RNA processing
TCA-cycle

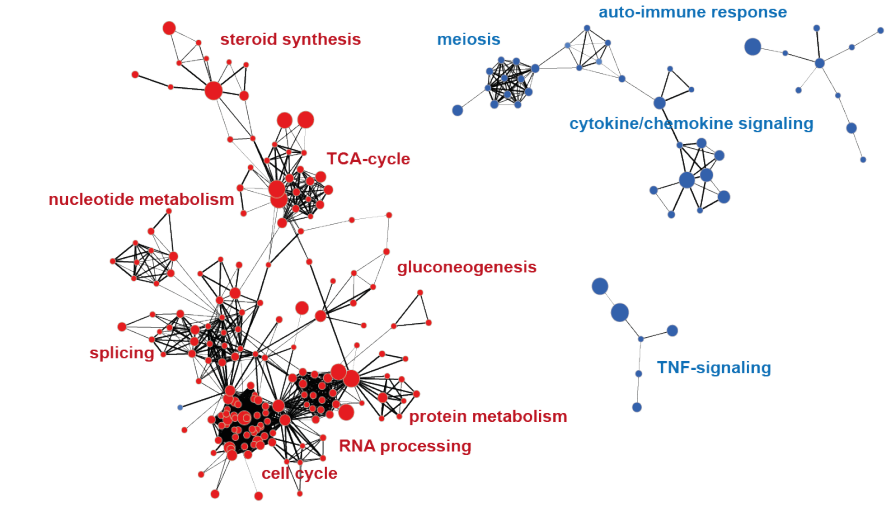
K lnc-GAN-1
steroid synthesis
meiosis
auto-immune response
cytokine/chemokine signaling
TCA-cycle
nucleotide metabolism
gluconeogenesis
splicing
TNF-signaling
protein metabolism
RNA processing
cell cycle

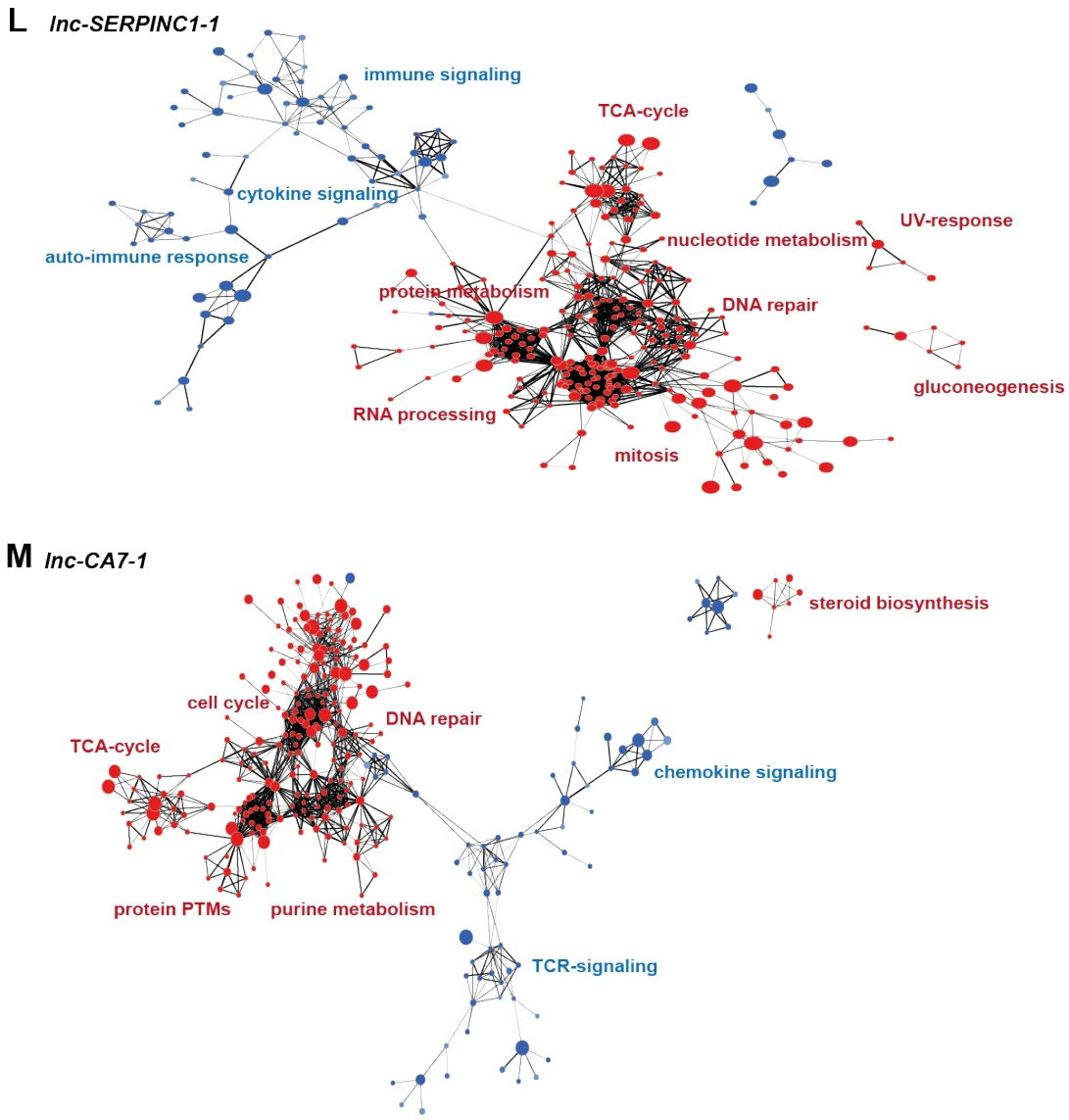


**Supplementary Figure 6: Functional annotation of candidate Notch driven lncRNAs in CUTLL1 T-ALL cells and CD34$^{+}$ thymic progenitor T-cells through enrichment mapping.**
(**A-M**) Pairwise Spearman's rho correlations were calculated between the selected Notch driven lncRNAs (with probes on the custom array) and all protein-coding genes and used for functional annotation of each of the candidate lncRNAs by GSEA. Followingly, enrichment maps were generated in Cytoscape for all selected Notch driven lncRNAs and indicates potential clusters of functionalities linked to each of the candidate lncRNAs such as involvement in the TCA-cycle, meiosis, TCR-signaling, ....

## Chapter 3: Results

# The T-ALL oncogene TLX1 represses expression of the long non-coding RNA *lnc-DAD1-2* in T-ALL

Kaat Durinck[1], Wouter Van Loocke[1], Filip Matthijssens[1], Karen Verboom[1], Inge Van de Walle[2], Christian Valdes[3], Annelynn Wallaert[1], Ellen Geerdens[2], Jan Cools[2], Wouter de Laat[3], Tom Taghon[2], Jean Soulier[4], Pieter Van Vlierberghe[1], Frank Speleman[1]

[1]*Center for Medical Genetics, Ghent University, Ghent, Belgium*

[2]*Laboratory for the Molecular Biology of Leukemia, Center for Human Genetics, KU Leuven and Center for the Biology of Disease, VIB, Leuven, Belgium*

[3]*Hubrecht Institute, Utrecht, The Netherlands*

[4]*Genome Rearrangements and Cancer Laboratory, U944 INSERM, University Paris Diderot and Hematology Laboratory, Saint-Louis Hospital, Paris, France*

**In preparation**

# Chapter 3: Results


## ABSTRACT

For a long time, proteins were considered to be the sole hubs that could support a regulatory network. Technological advances have recently contributed to the recognition and understanding of the central role of RNA species in homeostasis and malignant transformation. More in particular, lncRNAs have now proven to be versatile and key players in transcriptional control, mainly acting in concert with epigenetic modifier proteins. TLX1 is a transcription factor that is critically involved in the multi-step pathogenesis of T-cell acute lymphoblastic leukemia (T-ALL), an aggressive blood cancer mainly diagnosed in children. Although the oncogenic transcriptional program downstream of TLX1 has been extensively characterized at the level of protein coding genes, a comprehensive overview of lncRNAs that are regulated by this transcription factor oncogene remains to be established. Here, we identified and functionally dissected the role of lncRNAs downstream of TLX1 in the context of malignant T-cell transformation. These include amongst others, *lnc-THADA-1* as the top-scoring super-enhancer associated lncRNA located *in cis* to *ZFP36L2*, a recently identified novel T-ALL tumor suppressor gene and *lnc-DAD1-2* residing within the TCRα locus and putatively involved in the interference of TLX1 with TCRα function. Locked nucleic acid (LNA)-mediated *lnc-DAD1-2* knockdown revealed a core set of commonly regulated genes as compared to TLX1, including important genes in differentiation and cell proliferation such as *RAG1* and *TERT*. This study thus provides the first in depth landscaping of the TLX1 lncRNAome providing novel insights for further exploration of lncRNAs involved in T-cell transformation and normal thymocyte maturation and also offers novel targets for therapeutic intervention.

# Chapter 3: Results

## INTRODUCTION

T-cell acute lymphoblastic leukemia (T-ALL) is an aggressive hematological malignancy arising from uncontrolled proliferation (clonal expansion) and arrested differentiation of immature precursor T-cells. Genetic and epigenetic studies in T-ALL have uncovered a remarkable complexity of oncogenic and loss-of-function mutations over the past decade. Distinct molecular-cytogenetic subgroups can be defined and are associated with a specific gene expression signature. So far, these profiles have only been defined at the level of protein coding genes. Considering that the proportion of the whole genome with protein coding potential only constitutes about 2%, while up to 70-90% is transcribed, the complexity of regulatory mechanisms involved in normal development and disease can only be fully understood when also considering the non-coding part of the genome[1].

For acute T-cell leukemia, we previously identified a set of microRNAs acting in a cooperative manner to regulate key transcription factors with a tumor suppressor role in T-ALL[2]. Long non-coding RNAs (lncRNAs) are now a newly emerging class of non-coding RNAs. These transcripts are more than 200 nucleotides in length and are rather poorly evolutionary conserved in contrast to other types of non-coding RNAs[3]. The mechanisms by which they regulate gene expression or cellular functions more broadly are not yet fully understood, but a significant portion of lncRNAs is considered to act in concert with chromatin modifier enzymes. In this way, three main modes-of-action can be defined: they can act as 'guides' (eg recruitment of epigenetic regulatory protein complexes), 'decoys' (eg titrate proteins away from their DNA binding site) or 'scaffolds' (eg assist in the formation of multi-ribonucleoprotein complexes). The level of lncRNA-mediated gene regulation can also differ, acting either locally on the same chromosome from which the lncRNA itself is transcribed (*in cis*) or affecting multiple genes located at other chromosomes (*in trans*). The role for lncRNAs as crucial transcriptional regulators in many cancer types including malignant hematopoiesis is now emerging. LncRNAs are also considered to be essential components of normal development as has been shown amongst other for normal haematopoiesis[4,5]. Thusfar, the role and expression patterns of lncRNAs in T-ALL and the regulatory networks in which they take part are

still poorly defined. In a recent effort, we and others identified a subset of lncRNAs that act in concert with NOTCH1 in both normal T-cell development and malignant T-cell transformation[6,7]. Besides NOTCH1, another key driver in T-ALL is the '*T-cell leukemia homeobox 1*' (*TLX1*, *HOX11*) transcription factor.

TLX1 is involved in spleen organogenesis and is normally not expressed in developing thymocytes. In T-ALL, TLX1 is ectopically expressed in 5-10% of pediatric patients and 30% of adult cases due to either of two chromosomal translocations, t(7;10) or t(10;14), involving the TCR-δ or TCR-β regulatory regions respectively. The molecular subgroup defined by *TLX1* overexpression shows a gene expression profile that is indicative for a leukemic arrest at the early cortical stage of T cell development and TLX1-positive T-ALL cases are generally associated with a favorable prognostic outcome[8,9]. The TLX1 regulatory network in terms of co-factors and downstream protein-coding gene targets has been extensively studied[10]. Recently, we proposed that the long latency in TLX1-driven leukemia can at least be partly explained by a transcriptional antagonism between TLX1 and NOTCH1 during pre-leukemic stages, establishing a large dependency for these T-ALL blasts to acquire activating *NOTCH1* mutations as a prerequisite to further evolve towards full malignant transformation[11]. Here, we implemented an integrative genomics approach to identify and functionally characterize TLX1 regulated lncRNAs in the context of human T-ALL and identify several TLX1 driven lncRNAs with a putative role in normal T-cell development and T-cell oncogenesis.

# Chapter 3: Results

## METHODS

### Cell lines

ALL-SIL cells were obtained from the DSMZ cell line repository. Cells were maintained in RPMI-1640 medium (Life Technologies) supplemented with 20% fetal bovine serum, 1% of L-glutamine (Life Technologies) and 1% penicillin/streptomycin (Life Technologies).

### Clinical samples

Bone marrow lymphoblast samples from 64 T-ALL patients (15 immature, 25 *TAL/LMO*, 17 *TLX1/TLX3* and 7 *HOXA*) were collected with informed consent according to the declaration of Helsinki from Saint-Louis Hospital (Paris, France) and the study was approved by the Institut Universitaire d'Hématologie Institutional Review Board.

### siRNA-mediated knockdown TLX1, RNA-isolation, cDNA synthesis and RT-qPCR

ALL-SIL cells were electroporated (250 V, 1000 µF) using a Genepulser Xcell device (Biorad) with 400 nM of Silencer Select Negative Control 1 siRNA (Ambion) or siRNAs targeting *TLX1* (Silencer Select, Ambion, #4392420, s6746 and s6747). ALL-SIL cells were collected 24h post-electroporation. Total RNA was isolated using the miRNeasy mini kit (Qiagen) with DNA digestion on-column. By means of spectrophotometry, RNA concentrations were measured (Nanodrop 1000) and RNA integrity was evaluated (Experion, Bio-Rad). Next, cDNA synthesis was performed using the iScript cDNA synthesis Kit (Bio-Rad) followed by RT-qPCR using the LightCycler 480 (Roche). Finally, qPCR data was analyzed according to the ΔΔCt-method using the qBasePLUS software (Biogazelle).

## Chapter 3: Results

### LNA-mediated knockdown *lnc-DAD1-2*

ALL-SIL cells were electroporated (300 V, 1 mF) using a Genepulser Xcell device (Biorad) with 400 nM of negative control LNA (Exiqon, antisense LNA GapmeR, Premium, 300611-00, sequence: AACACGTCTATACGC) or LNAs targeting *lnc-DAD1-2* (custom designed LNAs, Exiqon, LNA1 (sequence: ATAGAATCAAGATCAC en LNA2 (sequence: GTAATTCAGTGTAAGT)), ALL-SIL cells were collected 48h post-electroporation. RNA-isolation, cDNA synthesis and qPCR were performed as described above.

### Cell fractionation assay

This cell fractionation protocol has been adapted from previous studies[12]. In brief, 10*10e6 ALL-SIL cells were collected, resuspended in lysis buffer (0.5% NP-40, 60 mM KCl, 15 mM NaCl, 0.15 mM spermine, 0.5 mM spermidine, 15 mM 2-mercapto-ethanol, 15 mM Tris-HCl (pH 7.4)) and centrifugated (3000 rpm, 5 min., 4°C). The resulting supernatant is the cytoplasmic fraction and was kept aside. The resulting pellet was resuspended in 1 ml lysis buffer, with incubation on ice for 30 min. The resulting lysate was centrifugated (3000 rpm, 10 min.) and through a 350 ul cushion of 20% sucrose (W/W) in lysis buffer. The resulting supernatant was discarded and the resulting pellet was respuspended in 1 ml lysis buffer. The resulting lysate was centrifugated (3000 rpm, 10 min.) and through a 350 ul cushion of 30% sucrose (W/W) in lysis buffer. The resulting pellet was resuspended in 500 ul lysis buffer. RNA-isolation from the cytoplasmic fraction was performed using the Qiagen RNeasy mini protocol for isolation of cytoplasmic RNA from animal cells (Qiagen). RNA-isolation from the nuclear fraction was performed using the Qiagen miRNeasy mini kit. cDNA synthesis was performed using the iScript cDNA synthesis Kit (Bio-Rad) followed by RT-qPCR using the LightCycler 480 (Roche).

### Gene expression profiling and Gene Set Enrichment Analysis

RNA samples from ALL-SIL cells were profiled on a custom designed Agilent micro-array covering all protein coding genes (33,128 mRNA probes, Human Sureprint G3

8x60k micro-arrays (Agilent)) and 12,000 lncRNAs (23,042 unique lncRNA probes). Expression data were normalized using the VSN-package (Bioconductor release 2.12) in R. Differential expression analysis was performed in R using Limma. Gene expression profiling data from TLX1 siRNA mediated knockdown and JQ1 treatment in ALL-SIL cells were previously published and deposited in the GEO database (GSE62144). Gene Set Enrichment analysis was performed against the c2 MSigDB collections (curated gene sets).

**polyA RNA-sequencing**

In this study, RNA-sequencing by poly-A capture (unstranded) was performed using 100 ng of RNA as input material (Biogazelle, Belgium). The sequencing read depth comprised for all samples 100 million reads, which were aligned to the reference genome hg38 with STAR-2.4.2a and default settings. Differential expression analysis was performed with DESeq2. Scrambled siRNA was used as control and compared with 2 independent TLX1 targeting siRNAs (3 replicates). A multifactorial design was used to control for batch effects.

**Motif enrichment**

TLX1 ChIP-seq reads were aligned with bowtie2 and peak calling was performed with MACS1.4 using input DNA as control. BEDTools was used to make a fasta file 500bp centered to the TLX1 peak summits. MEME-ChIP was used to perform motif enrichment analysis on this file.

**Super-enhancer analysis**

ROSE software (Young Lab) was used to identify superenhancers. BEDtools overlap was used to assign genes to enhancers.

# Chapter 3: Results

## RESULTS and DISCUSSION

### TLX1 regulated lncRNAs are located within the vicinity of T-ALL tumor suppressor genes

To elucidate the lncRNA repertoire under control of the TLX1 transcription factor, we perfomed RNA-sequencing by polyA-capture from ALL-SIL cells with transient knockdown of TLX1 using two independent siRNAs (**Fig. 1A**). In total, 119 long non-coding RNAs of the biotype 'lincRNA' or 'antisense' were significantly (adjusted p-value<0.05) downregulated versus 77 upregulated upon TLX1 knockdown (**Fig. 1A and 1B**). Notably, the ratio of significantly up- and downregulated lncRNA transcripts is opposite as compared to the effect of TLX1 knockdown on protein-coding genes (881 downregulated and 1294 upregulated upon TLX1 knockdown) (**Fig. 1C**). Interestingly, some of the identified TLX1 regulated lncRNAs are *in cis* to a known T-ALL tumor suppressor gene, as exemplified by *lnc-PTPN2* (**Fig. 1D and 1E**), suggesting that certain TLX1-driven lncRNAs might be involved in the regulation of TLX1 repressed tumor suppressor genes. Our results thus indicate that TLX1 can act both as an activator or repressor of lncRNA expression. To understand which co-factors might potentially be involved in lncRNA expression regulation together with TLX1, we performed *de novo* motif analysis on the set of differentially regulated lncRNAs upon TLX1 knockdown and found significant enrichment for ETS family and RUNX family transcription factor motifs (**Fig. 1F**), similar as to what we previously found for TLX1 regulated protein-coding genes as identified by ChIP-sequencing[11].

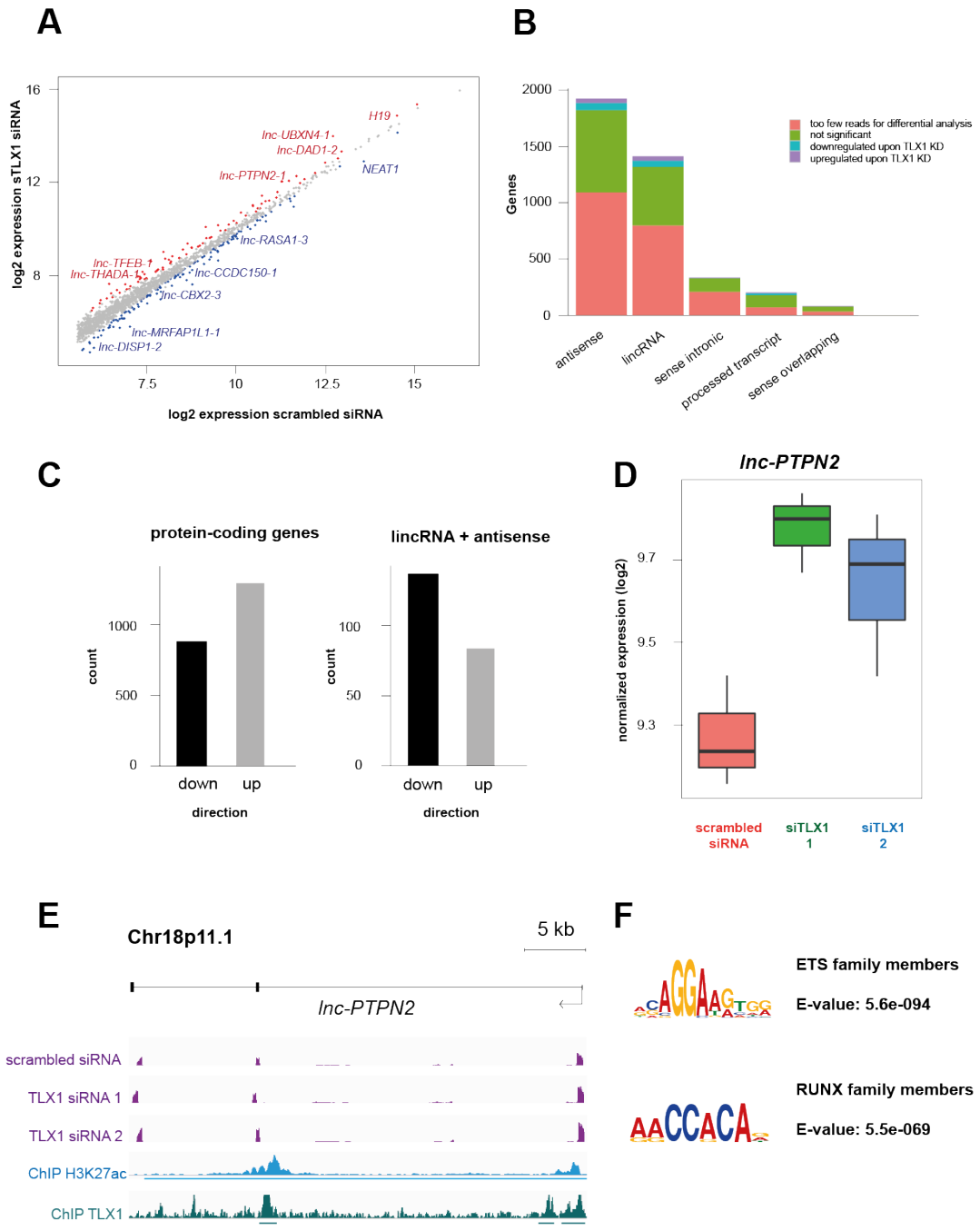


**Figure 1: Identification of TLX1 regulated long non-coding RNAs using an *in vitro* TLX1 knockdown model system in ALL-SIL lymphoblasts.** (**A**) Diagonal plot showing significantly (p-adjusted<0.05) downregulated (blue) and upregulated (red) lncRNAs upon TLX1 knockdown in ALL-SIL as determined by polyA RNA-seq, (**B**) Bar plot indicating the numbers of differentially expressed lncRNAs per biotype, (**C**) Bar plot showing the numbers of significantly differentially expressed protein-coding genes (left) and lncRNAs (biotype: lincRNA or antisense) upon TLX1 knockdown in ALL-SIL (right), (**D**) Box plot showing the average log2-expression of *lnc-PTPN2* across triplicate samples of ALL-SIL cells electroporated with either scrambled siRNA (pink box), TLX1 targeting siRNA 1 (green box) and TLX1 targeting siRNA 2 (blue), (**E**) IGV screenshot of the *lnc-PTPN2* locus with the corresponding RNA-seq profiles of representative samples of scrambled or TLX1 targeting siRNA electroporated ALL-SIL cells (purple tracks), H3K27ac (blue) and TLX1 (green) ChIP-seq profiles at the *lnc-PTPN2* locus, (**F**) Motif enrichment analysis on the set of TLX1 regulated lncRNAs using the MEME-ChIP suite identifies significant enrichment of the DNA binding motifs of the ETS and RUNX family of transcription factors.

Next to the screening in ALL-SIL T-ALL cells *in vitro*, we also aimed to retrieve *TLX1/3* driven lncRNAs from a primary T-ALL patient cohort, including 5 *TLX1+* and 12 *TLX3+* cases (**Fig. 2A, 2B and 2C**). Notably and similar to what we observed in our *in vitro TLX1* knockdown model, more protein-coding genes were significantly upregulated upon TLX1 knockdown, whereas the opposite was true for lncRNAs (**Fig. 2C**). In addition, we could identify 199 lncRNAs that are higher expressed in the *TLX1/3* genetic subgroup in comparison to the other T-ALL subtypes represented in the cohort of study (*TAL1+*, *immature*, *HOXA+*), amongst others also *lnc-PTPN2* (**Fig. 2D**).

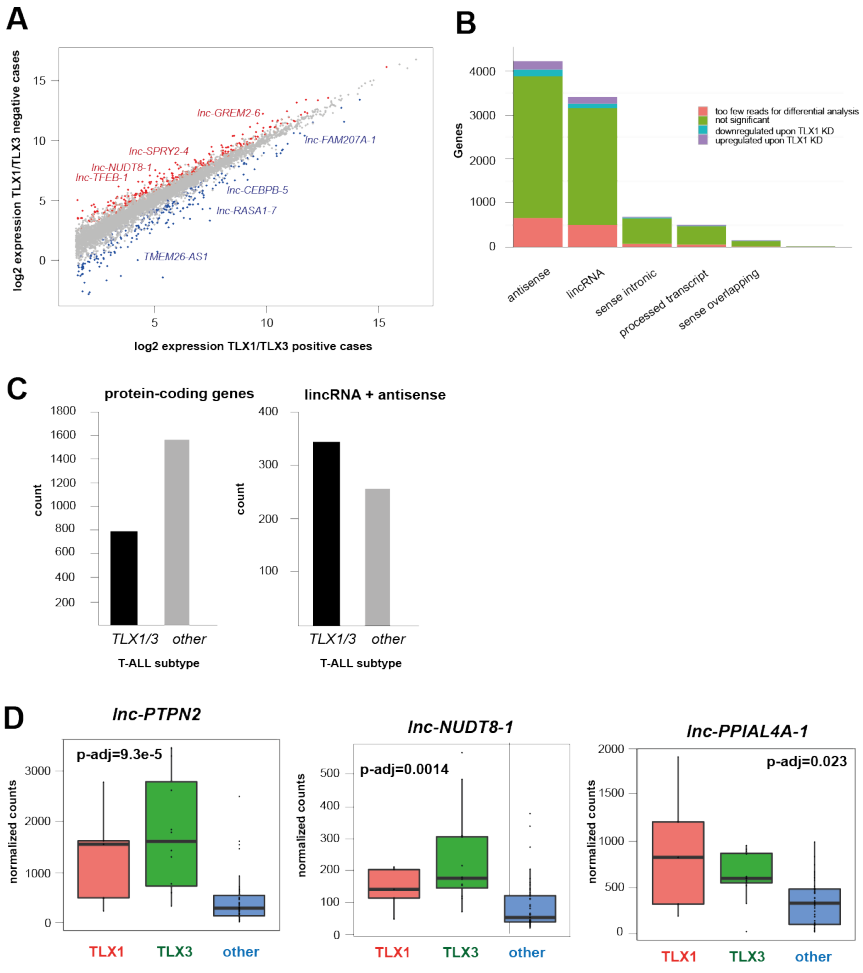


**Figure 2: Identification of TLX1/3 regulated lncRNAs in a primary T-ALL cohort.** (**A**) Diagonal plot based on the RNA-seq dataset from a primary cohort of T-ALL patients (see method section) showing lncRNAs that are significantly (p-adjusted value<0.05) higher (red) or lower (blue) expressed in TLX1/3 subgroup T-ALLs compared to T-ALL patients belonging to other T-ALL subtypes (TAL1+, immature, HOXA), (**B**) Bar plot indicating the numbers of differentially expressed lncRNAs per biotype, (**C**) Bar plot showing the numbers of significantly differentially expressed protein-coding genes (left) and lncRNAs (biotype: lincRNA or antisense) (right) between the TLX1/3 genetic subgroup and the other T--ALL subtypes of the studied primary patient cohort, (**D**) Boxplots showing lncRNAs that are significantly higher expressed in the TLX1/3 genetic subtypes compared to the other T-ALL subtypes.

A fascinating question arising from the current data is how TLX1 controlled repression of protein coding tumor suppressor genes is linked to the nearby located TLX1 putative cis-regulatory lncRNAs. At least part of these TLX1 lncRNA loci have features of enhancers (so-called eRNAs) and are enriched for H3K4me1 and H3K27ac enhancer marks. To study this interrelationship in more detail, chromatin conformation studies are ongoing while further functional dissection e.g. using CRIPSR-Cas9 technology is mandatory. An exciting therapeutic perspective from these novel findings is the possibility to reveal TLX1 controlled repression of multiple tumor suppressor genes through modulation of their functionally connected enhancer RNAs.

**Super-enhancer associated long non-coding RNAs under control of TLX1**

We have previously shown that TLX1 significantly associates with super-enhancers near protein-coding genes with a key role in normal and malignant T-cell development[11]. In this study, we aimed to identify (super)-enhancer associated lncRNAs that could be regulated by TLX1. To this end, we treated ALL-SIL lymphoblast cells with the small molecule inhibitor JQ1, interfering with BRD4 activity and thereby known to affect major context-specific enhancer sites (**Fig. 3A**). This set of differentially expressed lncRNAs upon JQ1 treatment of ALL-SIL was then compared to overlap with the lncRNA expression signatures obtained upon TLX1 in the same cellular context (**Fig. 3B**). In total, 20 lncRNAs downregulated upon TLX1 knockdown and 21 lncRNAs upregulated upon TLX1 knockdown were overlapping with those lncRNAs downregulated upon JQ1 exposure. To identify in more detail super-enhancer associated lncRNAs from this set, we integrated previously generated H3K27ac ChIP-seq data from ALL-SIL cells[11] and ordered TLX1 regulated lncRNAs according to their overlapping signal and rank of H3K27ac ChIP-seq peak clusters (**Fig. 3C**). From this analysis, we identified *lnc-THADA-1* as the top-scoring super-enhancer associated lncRNA under control of TLX1 (**Fig. 3D**). Interestingly, this lncRNA resides *in cis* to *ZFP36L2*, a recently identified novel T-ALL tumor suppressor gene[14]. By means of cellular fractionation[12], we could show that *lnc-THADA-1* is enriched four times more in the nuclear fraction than in the cytoplasmic fraction, to

the same extent as the positive control for the nuclear fraction lncRNA *MALAT1* (*GADPH* as a positive control for the cytoplasmic fraction) (**Fig. 3E**).

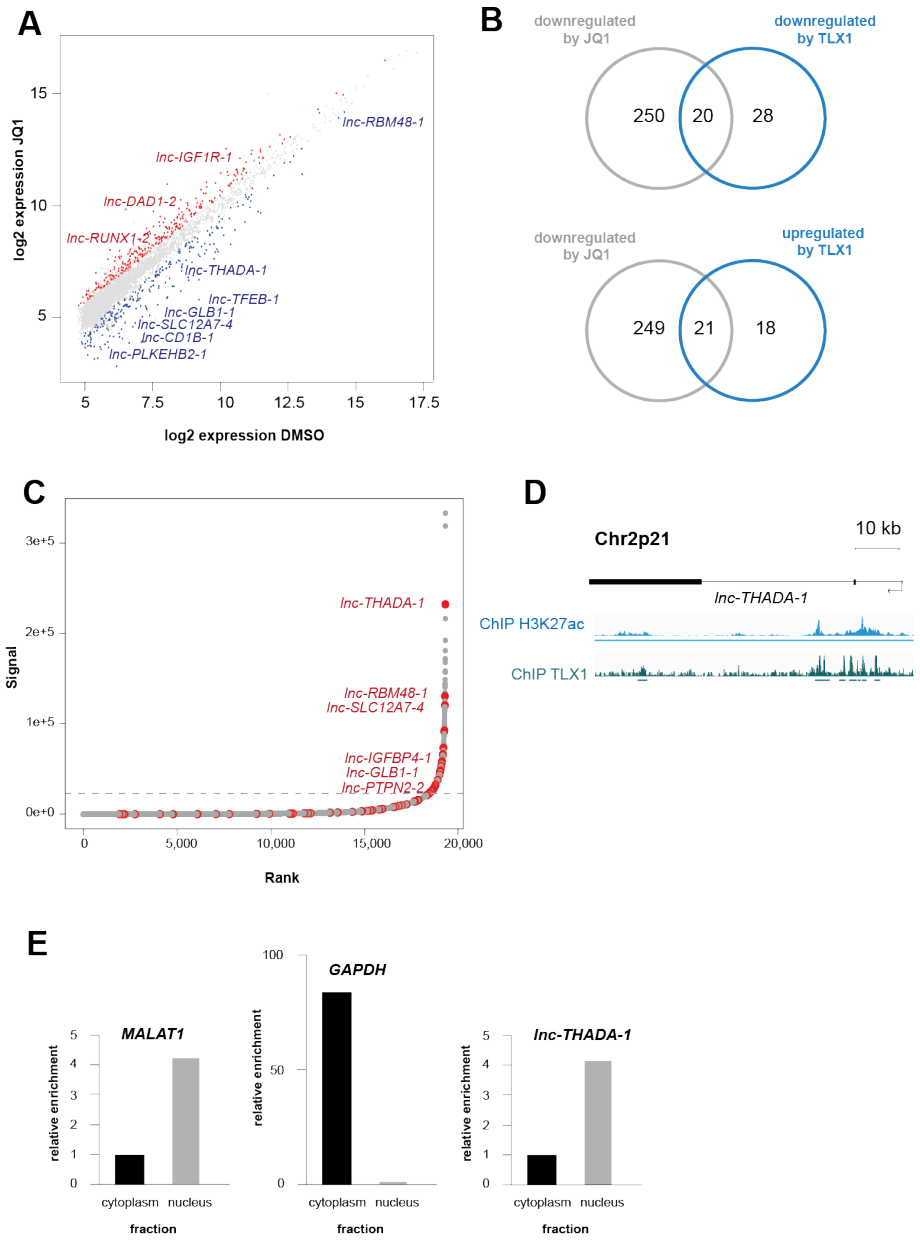


**Figure 3: Identification of super-enhancer associated lncRNAs under control of TLX1.** (**A**) Diagonal plot showing significantly (p-adjusted<0.05) down- (blue) or upregulated lncRNAs (red) upon JQ1 treatment of ALL-SIL cells, (**B**) Diagrams showing overlapping lncRNAs significantly downregulated upon JQ1 treatment of ALL-SIL cells with lncRNAs significantly downregulated (upper diagram) or upregulated (lower diagram) upon TLX1 knockdown, (**C**) Hockey-stick plot representing the normalized rank and cluster signal of clusters of H3K27ac peaks at lncRNA transcripts that are significantly differentially expressed upon TLX1 knockdown in ALL-SIL cells (red dots), (**D**) Screenshot of the *lnc-THADA-1* locus in ALL-SIL cells as the top-scoring super-enhancer associated lcnRNAs that is differentially expressed upon TLX1 knockdown in the same model system, (**E**) Cell fractionation of ALL-SIL cells followed by RT-qPCR analysis shows that *lnc-THADA-1* is a putative nuclear expressed lncRNA, with a similar enrichment as the positive control lncRNA *MALAT1* for the nuclear fraction, while *GAPDH* was used as a positive control for the cytoplasmic fraction.

## Chapter 3: Results

### Functional landscaping of *lnc-DAD1-2*, a TCRα-locus associated lncRNA

Previous studies on the transcriptional regulatory networks of TLX1 showed that ectopic expression of TLX1 in developing thymocytes causes a developmental arrest at the early cortical T-cell differentiation stage by binding with ETS1, with the formation of a repressor complex at the TCRα enhanceosome[15]. From our *in vitro* TLX1 knockdown model system, we identified *lnc-DAD1-2* as one of the repressed lncRNAs by TLX1 (**Fig. 1A and 4A**). Notably, this lncRNA resides within the TCRα locus and might thus be involved in the interference of TLX1 with TCRα function. In this study, we further scrutinized the potential function of *lnc-DAD1-2* by transient knockdown applying 'locked nucleic acids' (LNAs) targeting this lncRNA. We identified two very potent LNAs, resulting in up to 90% reduction of *lnc-DAD1-2* expression, as verified by RT-qPCR (**Fig. 4B**). We performed knockdown of *lnc-DAD1-2* in triplicate using both LNAs in ALL-SIL lymphoblasts, followed by micro-array based gene expression profiling. Using 'Gene Set Enrichment Analysis' (GSEA), we identified various significantly enriched gene sets from the C2 Molecular signature database (MSigDB) (**Fig. 4C**). Amongst others, a signature of genes high in immature stages of T-cell development (*LEE_EARLY_THYMOCYTES_UP*) compared to later stages is significantly upregulated upon knockdown *of lnc-DAD1-2*. Furthermore, genes downregulated in the immature B-cell stages are also upregulated with *lnc-DAD1-2* depletion. Interestingly, we also found a set of EZH2 target genes that are significantly upregulated upon *lnc-DAD1-2* knockdown, suggesting a potential functional interaction between *lnc-DAD1-2* and the PRC2 complex, given that many recent studies show interaction between EZH2 and a variety of lncRNAs[16].

In order to verify a putative overlap of downstream target genes between TLX1 and lncRNA *lnc-DAD1-2*, we compared the gene signatures related to TLX1 and *lnc-DAD1-2* knockdown by GSEA. Notably, we found that a core set of genes is shared amongst both, including amongst others *RAG1* and *TERT*. We hypothesize that *lnc-DAD1-2* might be a key lncRNA involved in TCR-rearrangements. In order to further landscape the functional role of this lncRNA in normal T-cell development, we are currently setting up functional studies using the *in vitro* model system OP9-DLL1. From the first LNA 'passive uptake' experiments, we could reach about 80%

knockdown of *lnc-DAD1-2* in CD34$^{+}$ cord blood progenitor cells (data not shown). This will allow us to further evaluate the phenotypic implications of *lnc-DAD1-2* on normal hematopoietic lineage development and by directed PCR-assays to the TCR loci, we will be able to further monitor the functional implications of *lnc-DAD1-2* in TCR-rearrangements.

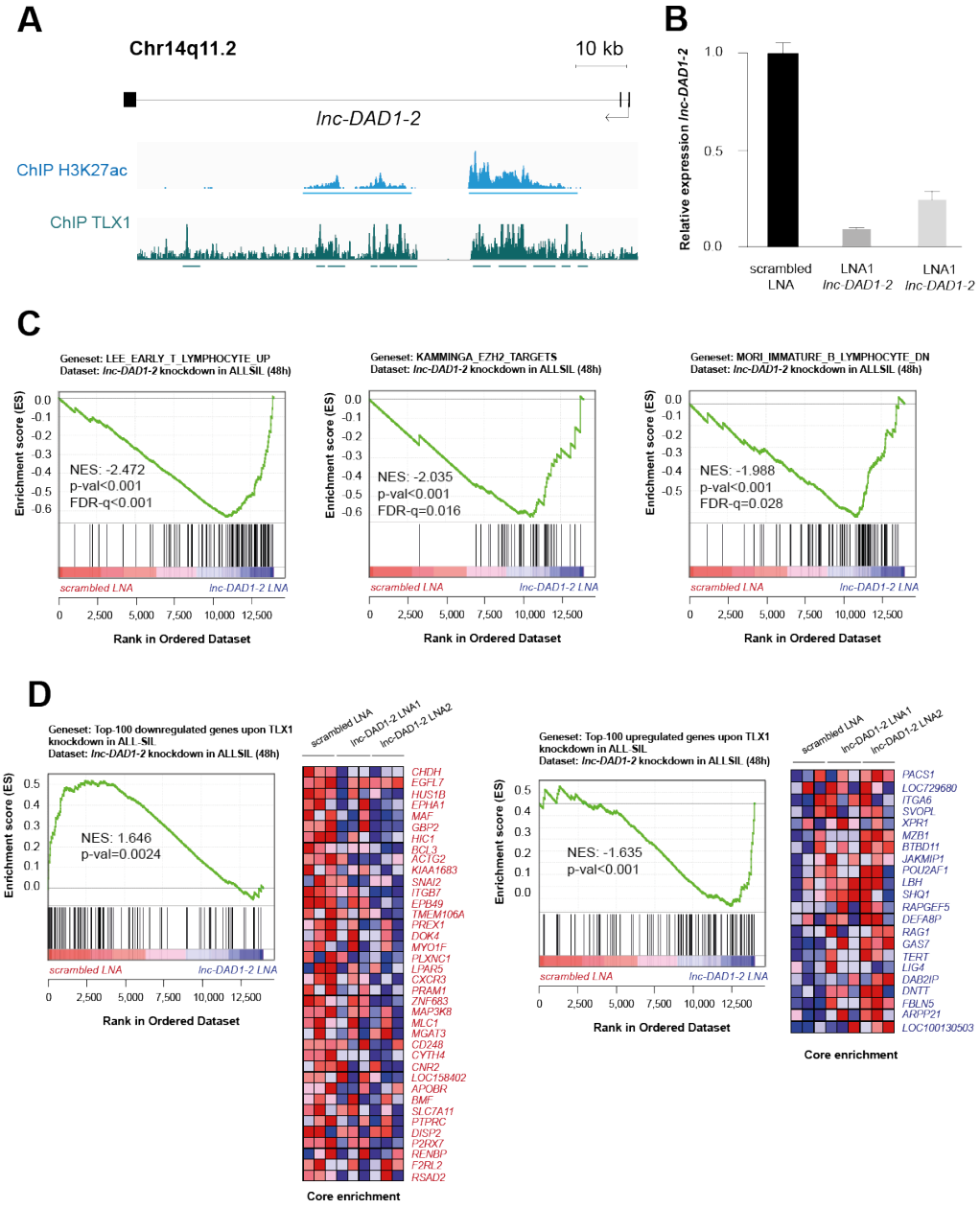


**Figure 4: Identification of *lnc-DAD1-2*, a TLX1 regulated lncRNA within the TCRα locus**. (**A**) Screenshot of the *lnc-DAD1-2* locus in ALL-SIL lymphoblast, (**B**) RT-qPCR validation of LNA-mediated downregulation of *lnc-DAD1-2* in ALL-SIL using 2 independent LNAs, (**C**) Gene Set Enrichment Analysis showing significantly enriched gene sets of the C2 MSigDB database within the gene signature upregulated upon *lnc-DAD1-2* knockdown in ALL-SIL cells, (**D**) Gene Set Enrichment Analysis shows significant overlap between genes differentially expressed upon TLX1 knockdown and its downstream lncRNA *lnc-DAD1-2* in ALL-SIL lymphoblasts.

### TLX1 regulates multiple previously unannotated lncRNAs

In the last part of this study, we searched for previously unnanotated lncRNAs in the ALL-SIL genome and evaluated which of those are directly under control of TLX1. In total, we identified 35 TLX1 activated and 20 TLX1 repressed unannotated lncRNAs (basemean>100), p-adjusted<0.05)(**Fig. 5A**), with *XLOC_023952* as an example of one of the top-downregulated unannotated lncRNA upon TLX1 knockdown (**Fig. 5B**). Secondly, we evaluated whether a set of these unannoted lncRNA transcripts could act as potential enhancer RNAs. To this end, we again matched the H3K27ac ChIP-seq data[11] to the respective lncRNA loci and scored them based on their rank-signal ratio for H327ac ChIP-seq peaks (**Fig. 5C**). We identified *XLOC_1477* to be associated with the strongest super-enhancer site of all identified unannotated lncRNAs that are significantly differentially expressed upon TLX1 knockdown (**Fig. 5D**). Further studies will include the analysis of these novel lncRNA during the various stages of thymocyte maturation and in other genetic subsets of T-ALL. Ultimately, further selected lncRNAs will be functionally analysed in order to unravel their normal function and role in transformation.

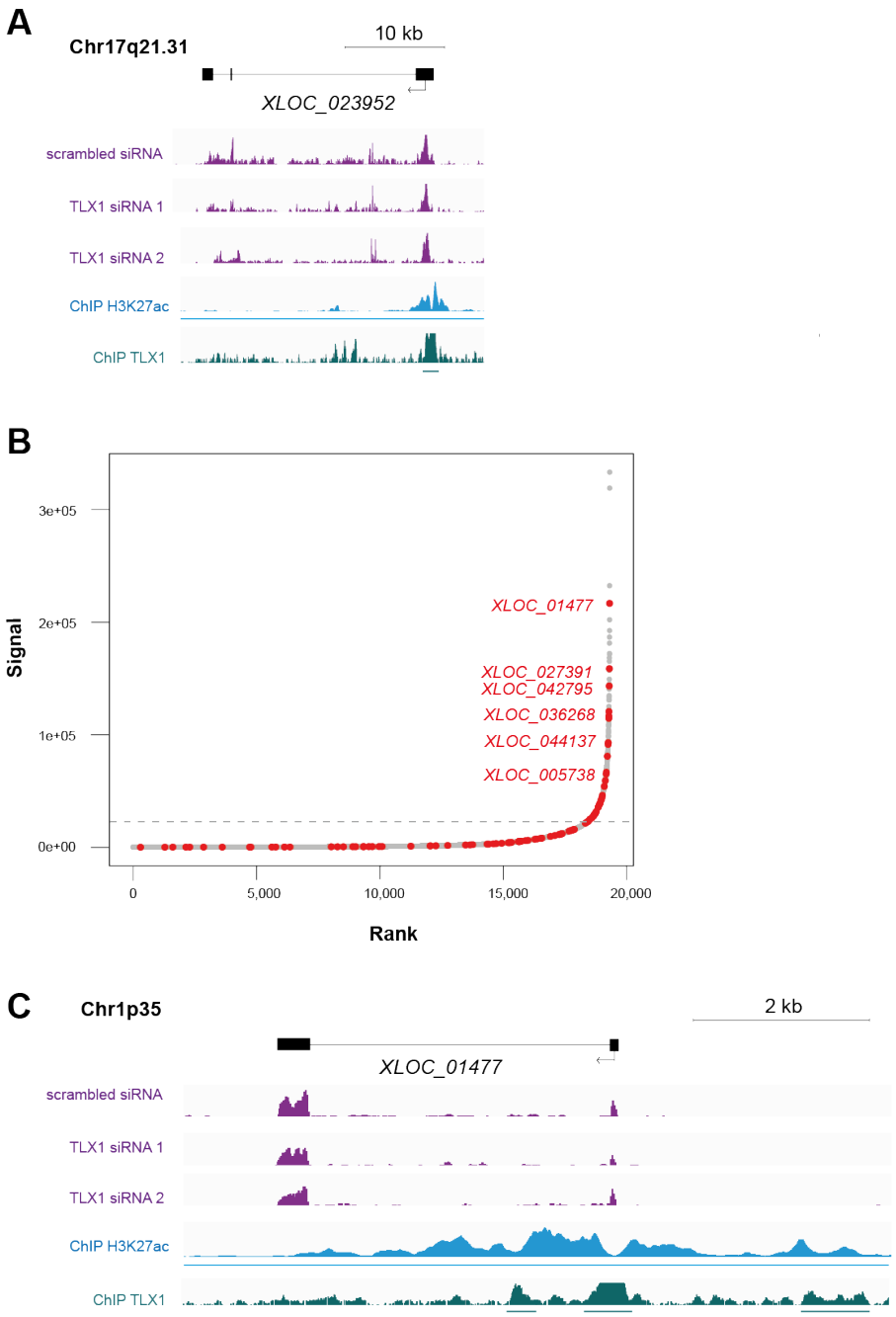


**Figure 5: Scrutinizing the set of unannoted lcnRNAs under control of TLX1 regulation**. (**A**) Screenshot of the RNA-seq tracks (purple) and ChIP-seq tracks (blue and green) for *XLOC_023952* locus as one of the top-downregulated unannotated lncRNAs upon TLX1 knockdown in ALL-SIL lymphoblasts, (**B**) Hockey-stick plot representing the normalized rank and cluster signal of clusters of H3K27ac peaks at the set of unannotated lncRNA transcripts that are significantly differentially expressed upon TLX1 knockdown in ALL-SIL cells (red dots), (**C**) Screenshot of the RNA-seq (purple) and ChIP-seq data tracks for H3K27ac (blue) and TLX1 (green) for the *XLOC_01477* locus identified as one of the top-scoring super-enhancer associated unannotated lncRNAs upon TLX1 knockdown in ALL-SIL lymphoblasts

## Author contributions

KD, KVB, FM, IvdW performed the experiments; KD wrorte the manuscript; JC, WL, TT, PVV and FS supervised the experiments and writing of the manuscript.

**REFERENCES**

1. Mattick, J.S. & Rinn, J.L. Discovery and annotation of long noncoding RNAs. *Nat Struct Mol Biol* **22**, 5-7 (2015).

2. Mavrakis, K.J.*, et al.* A cooperative microRNA-tumor suppressor gene network in acute T-cell lymphoblastic leukemia (T-ALL). *Nat Genet* **43**, 673-678 (2011).

3. Guttman, M.*, et al.* Chromatin signature reveals over a thousand highly conserved large non-coding RNAs in mammals. *Nature* **458**, 223-227 (2009).

4. Han, B.W. & Chen, Y.Q. Potential pathological and functional links between long noncoding RNAs and hematopoiesis. *Sci Signal* **6**, re5 (2013).

5. Alvarez-Dominguez, J.R., Hu, W., Gromatzky, A.A. & Lodish, H.F. Long noncoding RNAs during normal and malignant hematopoiesis. *Int J Hematol* **99**, 531-541 (2014).

6. Trimarchi, T.*, et al.* Genome-wide mapping and characterization of Notch-regulated long noncoding RNAs in acute leukemia. *Cell* **158**, 593-606 (2014).

7. Durinck, K.*, et al.* The Notch driven long non-coding RNA repertoire in T-cell acute lymphoblastic leukemia. *Haematologica* **99**, 1808-1816 (2014).

8. Bergeron, J.*, et al.* Prognostic and oncogenic relevance of TLX1/HOX11 expression level in T-ALLs. *Blood* **110**, 2324-2330 (2007).

9. Riz, I. & Hawley, R.G. G1/S transcriptional networks modulated by the HOX11/TLX1 oncogene of T-cell acute lymphoblastic leukemia. *Oncogene* **24**, 5561-5575 (2005).

10. Della Gatta, G.*, et al.* Reverse engineering of TLX oncogenic transcriptional networks identifies RUNX1 as tumor suppressor in T-ALL. *Nat Med* **18**, 436-440 (2012).

11. Durinck, K.*, et al.* Characterization of the genome-wide TLX1 binding profile in T-cell acute lymphoblastic leukemia. *Leukemia* **29**, 2317-2327 (2015).

12. Carneiro, M. & Schibler, U. Accumulation of rare and moderately abundant mRNAs in mouse L-cells is mainly post-transcriptionally regulated. *J Mol Biol* **178**, 869-880 (1984).

13. Lee, T.I., Johnstone, S.E. & Young, R.A. Chromatin immunoprecipitation and microarray-based analysis of protein location. *Nat Protoc* **1**, 729-748 (2006).

14. Hodson, D.J*., et al.* Deletion of the RNA-binding proteins ZFP36L1 and ZFP36L2 leads to perturbed thymic development and T lymphoblastic leukemia. *Nat Immunol* **11**, 717-724 (2010).

15. Dadi, S*., et al.* TLX homeodomain oncogenes mediate T cell maturation arrest in T-ALL via interaction with ETS1 and suppression of TCRalpha gene expression. *Cancer Cell* **21**, 563-576 (2012).

16. Davidovich, C. & Cech, T.R. The recruitment of chromatin modifiers by long noncoding RNAs: lessons from PRC2. *RNA* **21**, 2007-2022 (2015).

## Chapter 3: Results

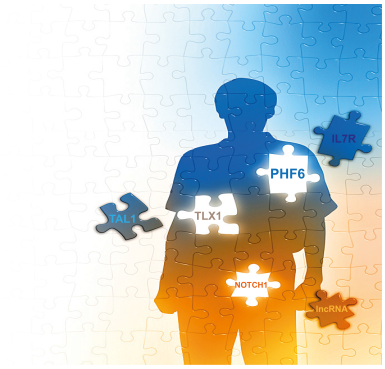


# CHAPTER 4

## Discussion and Future perspectives

## Chapter 4: Discussion and Future Perspectives

# Chapter 4: Discussion and Future Perspectives

## Discussion and future perspectives

In the field of T-ALL research, the aim for a comprehensive and in depth understanding of the genetic landscape that underlies the oncogenic rewiring of the transcriptional circuitries that govern normal thymopoiesis has already made a significant leap forward over the past decade, mainly driven by technological advances in the field of next-generation sequencing, but is still very much work in progress. One of the major challenges that we still face today is a profound understanding of the mechanism-of-action for many of these known and novel drivers in T-ALL and how they work in concert to establish malignant T-cell transformation.

To this end, I aimed during my PhD mandate to perform a comprehensive functional analysis for some of the key transcriptional regulators (TLX1, NOTCH1, PHF6) implicated in normal T-cell development and T-ALL and landscape their interconnection at the level of gene expression networks. In summary, this work has amongst others resulted in intruiging novel insights on the molecular mechanism of oncogene cooperativity between two important T-ALL drivers NOTCH1 and TLX1. More specifically, I could demonstrate a crucial cooperative role for PHF6 as a novel and important epigenetic regulator in the genetic crosstalk with NOTCH1 and TLX1. In addition, my work uncovers a key regulatory role for PHF6 in normal hematopoiesis. The TLX1 and NOTCH1 cellular model systems developed during this investigation also opened initially unanticipated possibilities to study the impact on lncRNAomes in their respective transcriptional networks. In this part of the thesis, I will elaborate on the novel insights that were retrieved in this PhD thesis with respect to the functional evaluation of the transcriptional networks that underlie T-ALL formation, evaluate the therapeutic potential of our findings and discuss how these results can be exploited as novel entry points for further studies, both in the context of T-ALL and other cancer entities.

# Chapter 4: Discussion and Future Perspectives

## 1. Dissection of interconnected transcriptional networks in T-ALL pathogenesis

Throughout the past decades, a key set of transcriptional regulators has been identified that act as individual hubs in the context of a larger transcriptional network underlying normal hematopoietic lineage development. This knowledge has broadened our understanding how their individual mechanism-of-action and the set of dowstream target genes they regulate is driving lineage commitment and differentiation in a hierarchical biological system. Nevertheless, we are now only taking the first leap forward in our understanding and insights in the global architecture in which these individually studied factors are embedded and how these organisational maps contribute to the complexity of gene regulation. In this PhD thesis, I anticipated to address the question how TLX1, as an ectopically expressed transcription factor in developing thymocytes, can rewire individual regulatory subnetworks of the T-cell developmental path and how these events collectively contribute to leukemic transformation. I have learned that TLX1 hijacks the intrinsic regulatory machinery, that normally drives thymocytes into a T-cell differentiation path, in a genome-wide manner and that a large part of this deregulation can be atributed by its interfere with super-enhancer sites that are associated with critical nodes in normal T-cell programming. In this study, we could also show for the first time that this ectopically expressed factor is partially hampering full-blown leukemia formation through its repression of the NOTCH1 driven transcriptional program, explaining why *NOTCH1* activating mutations are significantly enriched in the TLX1 subtype of T-ALL patients. However, in order to fully grasp the complete transcriptional map that underlies the transforming capacity of ectopically induced TLX1 in thymocytes, we also needed to further functionally characterize other genetic events that co-occur with a TLX1 translocation. One of the most obvious candidate genes for a follow-up study was *PHF6*, as *PHF6* loss-of-function mutations are predominantly enriched in the TLX1-driven T-ALL subtype. We studied the functionalities of PHF6 in several *in vitro* model systems. Evaluation of the gene signatures under control of PHF6 in these different model systems revealed some interesting but nevertheless complex insights that we now only start to understand and which will require further investigation. First, the overlap

between the gene signatures obtained in Jurkat T-ALL lymphoblasts and $CD34^+$ thymocyte progenitors was significant. This implies that with respect to the transcriptional network connected to PHF6 in these cellular contexts, not much has changed. In both systems we could find a functional connection to the NOTCH1 driven program. In contrast, when comparing the transcriptional profiles upon PHF6 knockdown between Jurkat and ALL-SIL lymphoblast as well as in the comparison of $CD34^+$ T-cell progenitors and ALL-SIL cells with PHF6 perturbation (not shown in this thesis), we could hardly find any overlap between the PHF6 imposed gene signatures. We propose that this is attributed to an intricate connectivity of the transcriptional networks governed by TLX1 and PHF6. As long as TLX1 is not present (like in Jurkat and $CD34^+$) progenitors, it will drive part of the NOTCH1 transcriptional program. Notably, we could not find a significant enrichment of the NOTCH1 signature in the PHF6 expression dataset with *PHF6* knockdown in ALL-SIL cells, probably because TLX1 is there to intervene with NOTCH1 signature genes. Instead, if PHF6 resides in a cellular context where TLX1 is active, the PHF6 downstream network will probably get rewired. An interesting and remarkable shared target gene between PHF6 en TLX1 is *IL7R*. We propose that TLX1-driven T-ALLs will impose loss of PHF6 expression as a way to upregulate IL7R coupled JAK-STAT signaling (see also point 2 of this discussion section).

In the second part of this thesis, I elaborated on the functional implications of non-coding RNAs embedded as an additional and key layer of the multidimensional networks in hematopoietic development and malignant leukemic transformation. We have identified NOTCH1 and TLX1 regulated lncRNAs. Notably, there is a core set of lncRNAs that are positively regulated by NOTCH1 and repressed by TLX1, in line to what we found at the level of protein-coding genes. We thus propose that further study is required to evaluate the potential involvement of these novel identified lncRNAs in the functional antagonism between TLX1 and NOTCH1.

## Chapter 4: Discussion and Future Perspectives

### 2.. The IL7R signaling pathway as a therapeutic entry point in *PHF6* mutated T-ALL

Our findings indicate the IL7R-JAK-STAT signaling cascade as a crucial node at the crossroads of the NOTCH1-TLX1-PHF6 regulatory axis in T-ALL. Interleukin-7 (IL-7) is an important trophic factor in the hematopoietic system, especially for the T-cell lineage. A functional IL-7 receptor (IL7R) is composed as a heterodimer of the IL7Rα and the common γ-chain (γc) and surface expression is tightly regulated and coordinated with T-cell maturation[1]. Receptor heterodimerization is triggered by IL-7 ligand binding, with subsequent downstream activation of the JAK-STAT pathway. Under normal physiological conditions, the JAK kinase family (JAK1, JAK2, JAK3 and TYK2) is activated following receptor phosphorylation (eg IL7R) upon ligand binding[2]. Although *IL7R* was already for a long time recognized as a key NOTCH1 target in both normal and malignant T-cell development, its inherent driver role in T-ALL blast formation was only rather recently underscored by the identification of activating *IL7R* mutations in about 10% of all T-ALL cases[3]. Intriguingly, we could show that TLX1-driven T-ALL blasts are hampered for full leukemic transformation through aberrant suppression of the NOTCH1 gene signature, most notably *IL7R* expression, by ectopic TLX1 at pre-leukemic T-ALL stages (**paper 1**). First, this provided us with an essential lead to understand why, amongst all T-ALL subgroups, especially TLX1-positive T-ALL cases are significantly enriched for *NOTCH1* activating mutations (90% of all cases). Secondly, during this PhD mandate, we identified *IL7R* as one of the most robust PHF6 negatively regulated downstream targets in both developing T-cell precursors and T-ALL blasts (**paper 2 and 3**). Given that *PHF6* mutations are significantly associated with ectopic *TLX1/3* expression, this discovery puts functional loss of PHF6 forward a second mechanism to upregulate *IL7R* expression and the downstream JAK-STAT signaling cascade in this leukemia subtype. Oncogenic mutations in the JAK-STAT pathway occur in both various hematological malignancies and solid cancer types such as breast and lung cancer (**Figure 1**)[4]. Interestingly, a recent study conducted by Vicente and co-workers[5] revealed not only a significant burden (27%) in T-ALL of oncogenic aberrations in *IL7R*, *JAK1*, *JAK3* and *STAT5*, but also an unrecognized association between IL7R-JAK and epigenetic

regulator gene mutations, most notably in 35% of all cases with *PHF6* inactivating mutations, further underscoring the relevance of our findings.

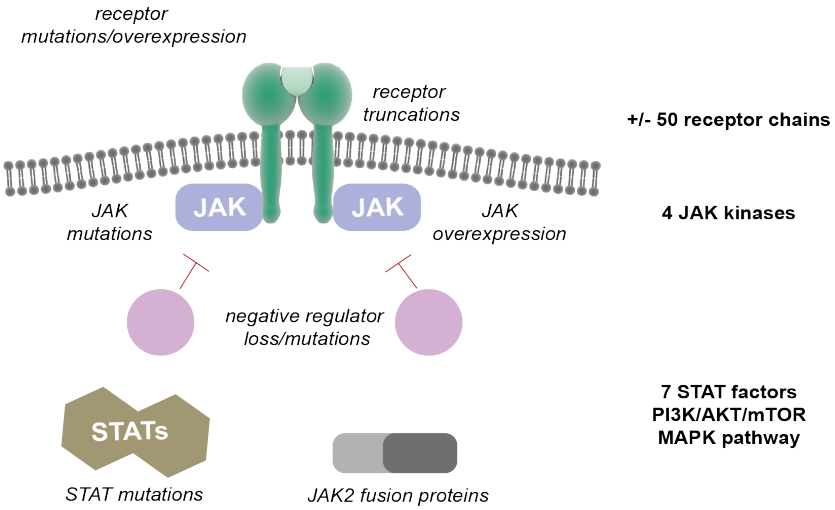


**Figure 1**: Overview of the JAK-STAT pathway mutational repertoire in various hematological cancers often indicative for a poor prognosis. Novel small molecule compounds and combination therapies are readily evaluated to improve therapeutic efficacy of targeting this pathway frequently overactivated in many hematological cancers (adapted from Springuel et al., Haematologica, 2015)[4].

Current treatment regiments in T-ALL reach survival rates of 50-60% in adults and up to 80% in pediatric patients[6,7]. Nevertheless, this success rate is currently still hampered due to therapy resistance in 25% of pediatric and 50% of adult cases[8-10]. The JAK-STAT pathway is in T-ALL amongst the potent pathways for targeted therapy, together with the Wnt-signaling, MAPK and NOTCH1 pathway amongst other[11]. Taken together, our results further warrant the therapeutic relevance of JAK inhibitors, such as tofacitinib and ruxolitinib, in treatment of *PHF6* mutated T-ALL. Ruxolitinib has already been approved for treatment of myelofibrosis patients and is currently being tested for many hematological cancers[2]. For instance, ruxolitinib treatment has already been shown efficacious for immature T-ALL in pre-clinical studies[12]. To further test the role of *PHF6* loss in counteracting TLX1 mediated *IL7R* repression *in vivo*, we performed *Phf6* gene inactivation by injection of gRNAs and Cas9 protein into one-cell stage zebrafish embryos yielding varying out-of-frame in/dels (unpublished data). Next, we will investigate the genetic interaction between

TLX1 and PHF6 either by crossing PHF6 deficient and *Rag2-TLX1* overexpressing stable lines or injection of *Rag2-TLX1* constructs into PHF6 deficient embryos.

**3. Deciphering the role of PHF6 as an epigenetic regulator in neuroblastoma**

In this PhD thesis, we have revealed PHF6 as a novel master regulator of human hematopoietic lineage development using the OP9-DLL1 *in vitro* model system. To validate these observations in a relevant *in vivo* context, we are currently investigating the phenotypic and molecular consequences of Phf6 knockdown/knock-out during zebrafish hematopoiesis. Preliminary results demonstrate marked increased expression of *LMO2*, a marker for erythropoiesis and primitive hematopoiesis by *in situ* hybridization upon morpholino-mediated knock down of Phf6 and CRISPR-mediated Phf6 knockout (unpublished data). Interestingly, a significant increase in thymus development and size could be observed in Phf6 deficient *Rag2:GFP* zebrafish, in line with the *in vitro* observed accelerated $CD4^+CD8^+$ T-cell stage progression of human $CD34^+$ thymocytes cultured on an OP9 stromal feeder layer (**paper 2**).

The identification of PHF6 as an important lineage switch in the blood system could serve as a prelude to trigger further functional analysis of the role of PHF6 in other tissue types. Notably, besides its expression in the hematopoietic system, PHF6 is also abundantly expressed in neuronal tissue. In neuronal cells, PHF6 has already been shown to functionally act in concert with the PAF1 complex to regulate neuron migration[13] and with *miR-128* to control neuronal morphology[14]. Many well-established tumor suppressor genes were formerly identified from familial cancer syndromes, suggestive for their role in malignant transformation in specific tissue types. Notably, *PHF6* germline mutations were previously linked to the Börjeson-Forssman-Lehman[15], Coffin-Siris and Nicolaides-Baraitser syndromes[16], in which patients suffer amongst others from intellectual disability. Given the prominent somatic mutation rate of *PHF6* in T-ALL[17] and to a minor extent also in AML, hepatocellular carcinoma, CML in blast crisis and bladder cancer[18,19], it could be speculated that PHF6 loss could also play a critical role in neuronal cancer types.

## Chapter 4: Discussion and Future Perspectives

Given the significant track record of our research team in the study of neuroblastoma, a rare childhood neuroendocrine tumor arising from neuroblasts of the sympatho-adrenal lineage, I will study the functional role of PHF6 in this malignancy as a follow-up of this PhD mandate. In the 'Cancer cell line Encyclopedia' (CCLE), neuroblastoma is one of the top-ranked tumor entities with high *PHF6* expression besides T-ALL. In addition, preliminary data from our research team indicate that stable overexpression of PHF6 in neuroblastoma cell lines leads to a significant induction of anchorage independent growth in a soft agar assay (unpublished data), hinting towards an oncogenic role for PHF6 in this malignancy. Recent work by Meacham and co-workers already proposed a role for *PHF6* as a potential B-ALL oncogene[20]. The dual and lineage-specific role for PHF6 as either a tumor suppressor or oncogene depending on the type of cancer is an intruiging aspect that I will further investigate.

### 4. The SWI/SNF complex regulatory network in T-ALL and neuroblastoma

The mammalian SWI/SNF remodeling complex has 12 possible subunits, with the constellation of the complex changing depending on the specialized function required in a specific context[21]. This complex binds to DNA in a sequence-independent manner, but likely associates with its target sites upon recruitment by other tissue-specific transcriptional regulators[22]. This is nicely illustrated by a study of Bakshi and co-workers showing that the ATPase subunit BRG1 associates with RUNX1 to control gene expression in the hematopoietic system[23]. Most notably, in murine model systems the role of Brg1 as a critical regulator of the T-cell compartment is already established[24]. Following this PhD mandate, I will further elaborate on the functional implications of several of the SWI-SNF complex members in human normal and malignant T-cell development. To this end, we have already established stable knockdown of BRG1 in human $CD34^+$ progenitors cultured on an OP9 stromal feeder layer. Preliminary data indicate massive induction of apoptosis and a differentiation block at early T-cell stages for BRG1 deficient thymocytes in comparison to controls (**paper 3**). Moreover, we have performed initial experiments evaluating the transcriptional program of BRG1 in human T-ALL blasts, hinting

towards overlap with a PHF6/TLX1 gene signature (**paper 3**). Interestingly, mutations in *PHF6* have been recently identified in Coffin-Siris syndrome cases that normally typically harbor germline mutations in genes encoding SWI-SNF complex members (*BRG1*, *ARID1A/1B*, *SMARCB1* and *SMARCE1*). First, this observation could further underscore a functional link between PHF6 and BRG1 in T-ALL. Notably, using arrayCGH analysis, we very recently identified in our T-ALL cohort one patient with a focal *ARID1A* deletion and one with a *SMARCA4* (*BRG1*) deletion (unpublished data), strongly suggesting the potential implication of the SWI-SNF complex as a novel tumor supppressor in T-ALL, in contrast to its known oncogenic role in AML[22]. Most recently, Mullighan and colleagues identified *SMARCA4* mutations in 3% of a pediatric T-ALL cohort (online communication abstracts ASH meeting 2015). This finding further triggers our interest to explore the role of SMARCA4 and other SWI-SNF components in T-ALL.

Similar to PHF6, also BRG1 has proven a key role in neuronal differentiation[25]. The mutational association between *SOX11* and the SWI-SNF complex in Coffin-Siris syndrome could also in that respect be of broader relevance, given that our research team has identified *SOX11* as a novel oncogene in neuroblastoma (unpublished data). From the CCLE-database, T-ALL and neuroblastoma cell lines show amongst other entities the highest levels of *BRG1* expression. Moreover, it has been shown that in AML cells BRG1 occupies a distal c-*MYC* enhancer region, regulating its interaction with other transcriptional regulators and chromatin looping towards the c-*MYC* promoter[22]. Both MYC and MYCN have a central role in neuroblastoma tumor biology and it could thus be speculated that functional interaction of BRG1 with MYC/MYCN/MAX in the context of neuroblastoma could be relevant in the context of transcriptional deregulation (**Figure 2**)[26]. To this end, we will further evaluate the transcriptional networks of BRG1 both in T-ALL and neuroblastoma context using a genome-wide approach combining RNA-sequencing and ChIP-sequencing amongst others.

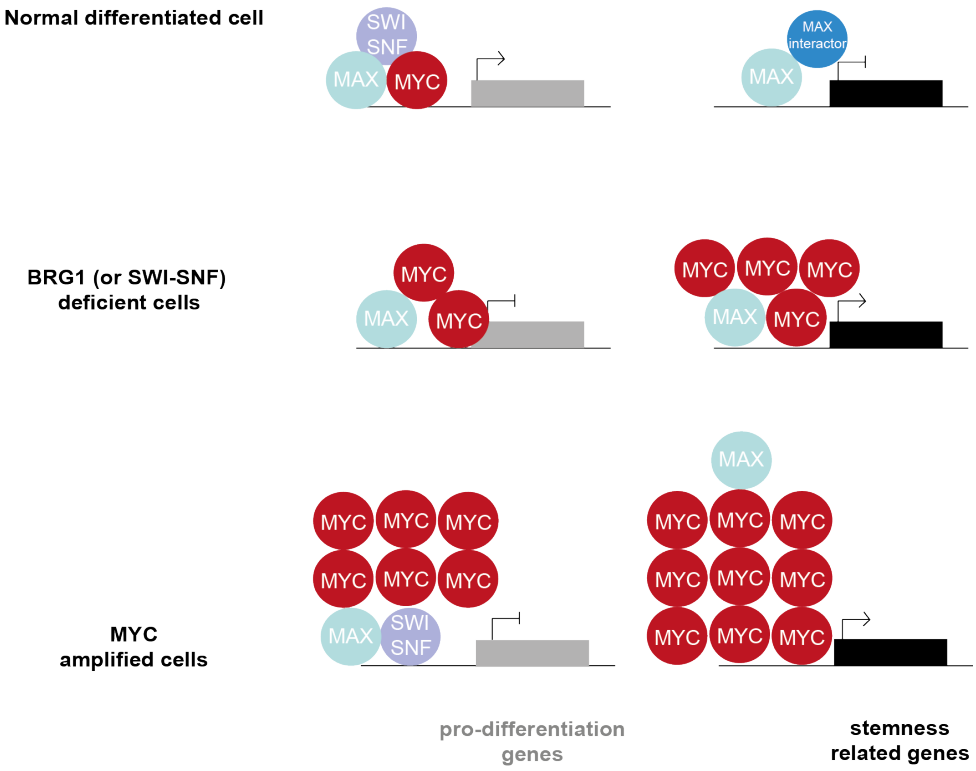


**Figure 2**: Schematic overview of possible interactions between BRG1, MYC and its co-factor MAX. The physical interaction between MYC and BRG1 (SWI-SNF) is required for regulating the expression of MYC and MYC target genes and antagonizes MYC activity to induce cell differentiation in the context of malignant transformation, thereby acting as a tumor suppressor gene (**upper panel**). In case of *BRG1* mutations, this regulatory loop is distorted and will lead to a switch from differentation towards cell growth (proliferation) (**middle pannel**). In case of *MYC* amplification (mutually exclusive with *BRG1* mutations) MYC will repress pro-differentiation genes and induce a proliferative state (**lower panel**) (adapted from Romero et al., Cancer Discovery, 2014)[26]

Chromatin modifier enzymes have been proven to be the main interactors of long non-coding RNAs both in development and in the process of malignant transformation, as exemplified by their recognized role in both normal hematopoiesis and leukemia[27,28] (**Figure 3**). The ENCODE consortium now estimates that the human genome encodes approximately 28,000 distinct lncRNAs[29]. A well-known example is the lncRNA *ANRIL*, exerting its function by guiding the PRC2 complex to silence the expression of the tumor suppressor genes *p15* (*INK4A*), *p14* (*ARF*) and *p16* (*INK4B*), eventually contributing to uncontrolled tumor growth (**Figure 3**, right)[27]. In the meantime, many cancer types have been identified with *ANRIL* overexpression such as breast, lung and ovarian cancer. The PRC2 complex is

currently the prototype chromatin modifier complex that is known for its interaction with various lncRNAs such as *XIST* to mediate X-chromosome inactivation for gene dosage compensation. Interestingly, a recent study by Yildirim and co-workers identified *XIST* as a novel tumor suppressor in hematological cancer, affecting both the myeloid and the lymphoid blood lineages[30].

Recent studies now show that also other chromatin remodeling complexes, including the SWI-SNF complex interacts with lncRNAs to exert is function. In many cancer types, the function of the SWI-SNF complex is directly affected in one or more of its core components. In prostate cancer however, it seems that SWI-SNF mutations are much less frequent. Nevertheless, SWI-SNF complex function is deregulated in prostate cancer cases due to the overexpression of the lncRNA *SChLAP1*, binding to the SNF5 component of the complex and thereby interfering with association to its target genes[31]. Also in the context of plant development (*Arabidopsis Thaliana*), the SWI-SNF complex was recently shown to take part in complex formation with lncRNAs in concert with other lncRNA binding proteins and in that way facilitate lncRNA mediated gene silencing[32]. In follow-up of this PhD mandate, I will evaluate whether also in the context of normal and malignant T-cell development either association between the SWI-SNF complex and lncRNAs or direct regulation of lncRNA expression by BRG1 amongst other takes place.

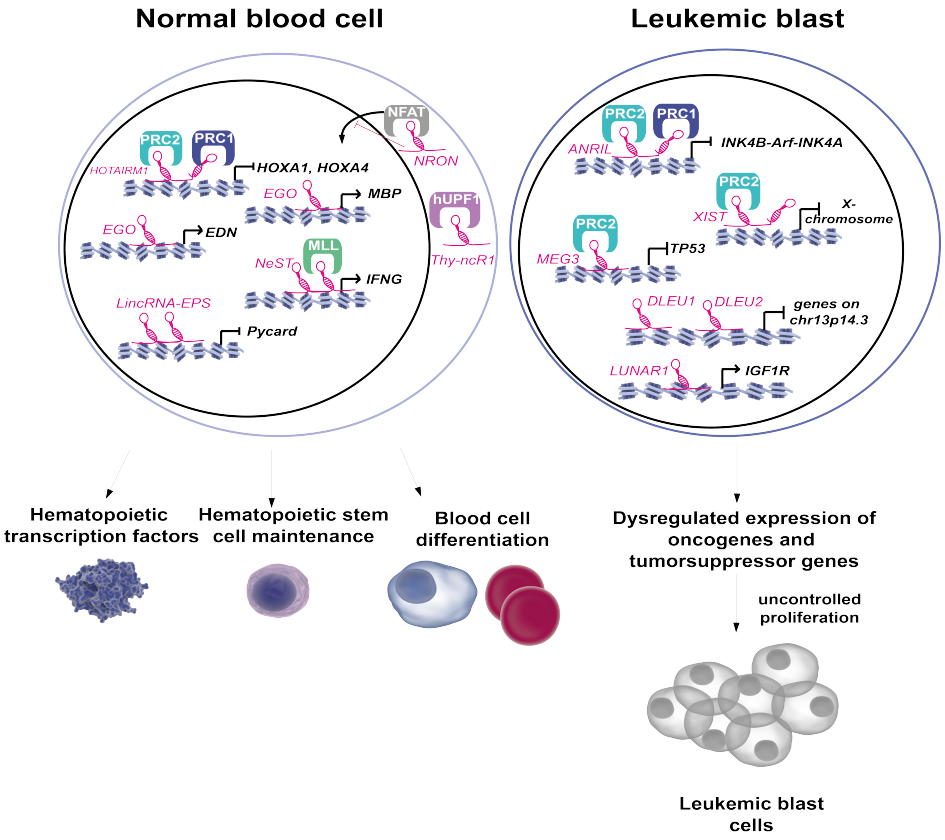


**Figure 3**: Schematic overview of lncRNAs known so far to be involved in normal and malignant hematopoiesis. This set of lncRNAs will actively participate in the gene regulatory networks that govern normal hematopoietic development or malignant leukemic transformation either through their interaction with chromatin remodeler complexes or guidance/sequestration of key master regulators that are involved in hematopoietic lineage commitment and differentiation (adapted from Han and Chen, Science Signaling, 2013)[27].

### 1.4 Non-coding RNAs as novel therapeutic targets in T-ALL

Our research team has previously, in collaboration with the team of Hans-Guido Wendel (Memorial Sloan Kettering, New York, USA), identified five novel oncogenic miRNA (*miR-19b*, *miR-20a*, *miR-26a*, *miR-92* and *miR-223*), that were capable of inducing T-ALL in a NOTCH1-induced mouse model, linked to their cooperative suppression of several known T-ALL tumor suppressor genes (*PHF6*, *BIM*, *IKZF1*, *FBXW7*, *PTEN* and *NF1*)[33]. Later, Gusscott and co-workers showed that NOTCH1 itself is capable of regulating miRNA-expression in T-ALL blasts. More specifically, it was shown that NOTCH1 represses the expression of *miR-223* to counteract the negative regulation of IGF1R signaling by *miR-223*[34]. During this PhD mandate, we have

identified, in parallel with the study of Trimarchi and colleagues[35], *LUNAR1* as the most robustly regulated NOTCH1 lncRNA, both in thymocyte progenitors and T-ALL blasts (**paper 6**). The contribution of *LUNAR1* to malignant transformation was shown to be linked to its direct induction of IGF1R expression and signaling. We have also extended the TLX1 regulome towards long non-coding RNAs, landscaping the implication of these non-coding RNAs in this T-ALL subtype (**paper 5**). In addition, we scrutinized the set of miRNAs implicated in the TAL1 downstream network in T-ALL (**paper 4**). Altogether, these findings indicate that the pool of non-coding RNAs, both miRNAs and lncRNAs, are a novel class of targets in the future for innovative therapeutic strategies in T-ALL treatment.

MiRNA-directed therapeutic strategies offer the advantage of the ability to affect the expression of multiple genes at a time, but this may also cause at the same time potential off-target effects[36]. Effective targeting of oncogenic miRNAs such as those identified in T-ALL by Mavrakis and colleagues[33] can be reached by the use of anti-miRs or modified versions such as 'locked nucleic acids' (LNAs), which are currently evaluated for clinical application[37], but also by using miRNA sponges, that harbour binding sites for the miRNA to be targeted through complementarity with the heptamer sequence of its seed site[38].

Although the function of many lncRNAs is still poorly characterized so far, a plethora of recent studies underscore their key role in malignant transformation such as in T-ALL and various aspects make them attractive for targeted therapeutic applications. Some lncRNAs are involved in many cancer types, such as *MALAT1*, which is overexpressed in lung cancer, gastric cancer and colorectal cancer amongst others and this is associated with overall poor survival[39]. However, many lncRNAs display tissue-specific expression patterns, making them attractive for biomarker development and targeted treatment (**Table 1**)[40,41]. A prototypical example is the lncRNA *PCA3* which is specifically overexpressed in prostate cancer[42]. The detection of *PCA3* in urine is currently used as a diagnostic tool for prostate cancer and turned out to be more specific than the previously used 'prostate-specific antigen' (PSA)[41,43]. Various strategies can be applied to downregulate oncogenic lncRNAs such as by antisense oligonucleotides (ASOs), small interfering RNAs (siRNAs) or short-hairpin

RNAs (shRNAs) as well as genome-editing tools like CRISPR-Cas9 and these have been successfully applied in various *in vitro* models. The challenge remains however to perform lncRNA targeting *in vivo*. Another interesting aspect of lncRNAs that can be exploited to target them is that many lncRNAs exert their function by interactions with various chromatin-remodeling complexes. Small molecule compounds, designed to disrupt these interactions could be very potent[44].

| Cancer Type | lncRNA | Biological Sample | Fold-Change to Normal Control | Number of Patients | Specificity | Sensitivity | AUC |
|---|---|---|---|---|---|---|---|
| Lung cancer | MALAT1 | Peripheral blood cells | ↓ 0.30 | 45 | 96% | 56% | 0.79 |
| Colorectal cancer | HOTAIR | Peripheral blood cells | ↑ 5.22 | 84 | 92.5% | 67% | 0.87 |
| Prostate cancer | PCA3 | Urine | n/a | 3245 | 75% | 62% | 0.75 |
| | | | ↑ 2.58 * | 407 | 60.1% | 94.9% | 0.87 |
| | | | ↑ n/a | 3073 | 75% | 53% | 0.69 |
| | MALAT1 | Plasma | ↑ n/a | 87 | 58.6% | 84.8% | 0.84 |
| Hepatocellular carcinoma | RP11-160H22.5<br>XLOC_014172<br>LOC149086 | Plasma | ↑ 2.5<br>↑ 67.7<br>↑ 4.6 | 467 | 73% | 82% | 0.896 |
| Bladder cancer | UCA1 | Urine | ↑ n/a | 94 | 91.8% | 80.9% | 0.88 |
| | | | ↑ 32.9 | 117 | 79.7% | 79.5% | 0.86 |
| Gastric cancer | AA174084 | Tissue Gastric juice | ↓ 3.18 | 134 | 73% | 57% | 0.68 |
| | AA174084 | | ↑ n/a | 39 | 93% | 46% | 0.85 |
| | LINC00152 | Plasma/plasma exosomes | ↑ n/a | 79 | 85.2% | 48.1% | 0.66 |

Arrows represent the up-regulation (↑) or down-regulation (↓) of the transcript. * Fold-change of PCA3 score, as determined by PROGENSA PCA3 assay. n/a, not available, since data is presented only in graphical format in the original report.

**Table 1:** Long non-coding RNAs as biomarkers for different cancer types[41]

Nevertheless, advances in the field of lncRNA directed therapy development are currently hampered amongst others by the lack of knowledge on the *in vivo* function for many of the identified lncRNAs[44]. Profound functional and structural analysis of lncRNAs will be required to drive the therapeutic potential of this novel pool of non-coding RNAs towards clinical application[45].

## Chapter 4: Discussion and Future Perspectives

### References


1. Munitic, I.*, et al.* Dynamic regulation of IL-7 receptor expression is required for normal thymopoiesis. *Blood* **104**, 4165-4172 (2004).

2. Quintas-Cardama, A. & Verstovsek, S. Molecular pathways: Jak/STAT pathway: mutations, inhibitors, and resistance. *Clin Cancer Res* **19**, 1933-1940 (2013).

3. Zenatti, P.P.*, et al.* Oncogenic IL7R gain-of-function mutations in childhood T-cell acute lymphoblastic leukemia. *Nat Genet* **43**, 932-939 (2011).

4. Springuel, L., Renauld, J.C. & Knoops, L. JAK kinase targeting in hematologic malignancies: a sinuous pathway from identification of genetic alterations towards clinical indications. *Haematologica* **100**, 1240-1253 (2015).

5. Vicente, C.*, et al.* Targeted sequencing identifies associations between IL7R-JAK mutations and epigenetic modulators in T-cell acute lymphoblastic leukemia. *Haematologica* **100**, 1301-1310 (2015).

6. Van Vlierberghe, P., Pieters, R., Beverloo, H.B. & Meijerink, J.P. Molecular-genetic insights in paediatric T-cell acute lymphoblastic leukaemia. *Br J Haematol* **143**, 153-168 (2008).

7. Pui, C.H., Robison, L.L. & Look, A.T. Acute lymphoblastic leukaemia. *Lancet* **371**, 1030-1043 (2008).

8. Barrett, A.J.*, et al.* Bone marrow transplants from HLA-identical siblings as compared with chemotherapy for children with acute lymphoblastic leukemia in a second remission. *N Engl J Med* **331**, 1253-1258 (1994).

9. Barrett, A.J. Bone marrow transplantation for acute lymphoblastic leukaemia. *Baillieres Clin Haematol* **7**, 377-401 (1994).

10. Van Vlierberghe, P. & Ferrando, A. The molecular basis of T cell acute lymphoblastic leukemia. *J Clin Invest* **122**, 3398-3406 (2012).

11. Neumann, M.*, et al.* Mutational spectrum of adult T-ALL. *Oncotarget* **6**, 2754-2766 (2015).

12. Maude, S.L.*, et al.* Efficacy of JAK/STAT pathway inhibition in murine xenograft models of early T-cell precursor (ETP) acute lymphoblastic leukemia. *Blood* **125**, 1759-1767 (2015).

13. Zhang, C.*, et al.* The X-linked intellectual disability protein PHF6 associates with the PAF1 complex and regulates neuronal migration in the mammalian brain. *Neuron* **78**, 986-993 (2013).

14. Franzoni, E.*, et al.* miR-128 regulates neuronal migration, outgrowth and intrinsic excitability via the intellectual disability gene Phf6. *Elife* **4**(2015).

15. Lower, K.M.*, et al.* Mutations in PHF6 are associated with Borjeson-Forssman-Lehmann syndrome. *Nat Genet* **32**, 661-665 (2002).

16. Wieczorek, D.*, et al.* A comprehensive molecular study on Coffin-Siris and Nicolaides-Baraitser syndromes identifies a broad molecular and clinical spectrum converging on altered chromatin remodeling. *Hum Mol Genet* **22**, 5121-5135 (2013).

17. Van Vlierberghe, P.*, et al.* PHF6 mutations in T-cell acute lymphoblastic leukemia. *Nat Genet* **42**, 338-342 (2010).

18. Yoo, N.J., Kim, Y.R. & Lee, S.H. Somatic mutation of PHF6 gene in T-cell acute lymphoblatic leukemia, acute myelogenous leukemia and hepatocellular carcinoma. *Acta Oncol* **51**, 107-111 (2012).

19. Kandoth, C.*, et al.* Mutational landscape and significance across 12 major cancer types. *Nature* **502**, 333-339 (2013).

20. Meacham, C.E.*, et al.* A genome-scale in vivo loss-of-function screen identifies Phf6 as a lineage-specific regulator of leukemia cell growth. *Genes Dev* **29**, 483-488 (2015).

21. Ho, L. & Crabtree, G.R. Chromatin remodelling during development. *Nature* **463**, 474-484 (2010).

22. Shi, J.*, et al.* Role of SWI/SNF in acute leukemia maintenance and enhancer-mediated Myc regulation. *Genes Dev* **27**, 2648-2662 (2013).

23. Bakshi, R.*, et al.* The human SWI/SNF complex associates with RUNX1 to control transcription of hematopoietic target genes. *J Cell Physiol* **225**, 569-576 (2010).

24. Gebuhr, T.C.*, et al.* The role of Brg1, a catalytic subunit of mammalian chromatin-remodeling complexes, in T cell development. *J Exp Med* **198**, 1937-1949 (2003).

25. Seo, S., Richardson, G.A. & Kroll, K.L. The SWI/SNF chromatin remodeling protein Brg1 is required for vertebrate neurogenesis and mediates transactivation of Ngn and NeuroD. *Development* **132**, 105-115 (2005).

26. Romero, O.A.*, et al.* MAX inactivation in small cell lung cancer disrupts MYC-SWI/SNF programs and is synthetic lethal with BRG1. *Cancer Discov* **4**, 292-303 (2014).

27. Han, B.W. & Chen, Y.Q. Potential pathological and functional links between long noncoding RNAs and hematopoiesis. *Sci Signal* **6**, re5 (2013).

28. Morlando, M., Ballarino, M. & Fatica, A. Long Non-Coding RNAs: New Players in Hematopoiesis and Leukemia. *Front Med (Lausanne)* **2**, 23 (2015).

29. Huarte, M. The emerging role of lncRNAs in cancer. *Nat Med* **21**, 1253-1261 (2015).

30. Yildirim, E.*, et al.* Xist RNA is a potent suppressor of hematologic cancer in mice. *Cell* **152**, 727-742 (2013).

31. Lee, R.S. & Roberts, C.W. Linking the SWI/SNF complex to prostate cancer. *Nat Genet* **45**, 1268-1269 (2013).

32. Zhu, Y., Rowley, M.J., Bohmdorfer, G. & Wierzbicki, A.T. A SWI/SNF chromatin-remodeling complex acts in noncoding RNA-mediated transcriptional silencing. *Mol Cell* **49**, 298-309 (2013).

33. Mavrakis, K.J.*, et al.* A cooperative microRNA-tumor suppressor gene network in acute T-cell lymphoblastic leukemia (T-ALL). *Nat Genet* **43**, 673-678 (2011).

34. Gusscott, S., Kuchenbauer, F., Humphries, R.K. & Weng, A.P. Notch-mediated repression of miR-223 contributes to IGF1R regulation in T-ALL. *Leuk Res* **36**, 905-911 (2012).

35. Trimarchi, T.*, et al.* Genome-wide mapping and characterization of Notch-regulated long noncoding RNAs in acute leukemia. *Cell* **158**, 593-606 (2014).

36. Rothschild, S.I. microRNA therapies in cancer. *Mol Cell Ther* **2**, 7 (2014).

37. Stenvang, J., Silahtaroglu, A.N., Lindow, M., Elmen, J. & Kauppinen, S. The utility of LNA in microRNA-based cancer diagnostics and therapeutics. *Semin Cancer Biol* **18**, 89-102 (2008).

38. Ling, H., Fabbri, M. & Calin, G.A. MicroRNAs and other non-coding RNAs as targets for anticancer drug development. *Nat Rev Drug Discov* **12**, 847-865 (2013).

39. Zhang, J., Zhang, B., Wang, T. & Wang, H. LncRNA MALAT1 overexpression is an unfavorable prognostic factor in human cancer: evidence from a meta-analysis. *Int J Clin Exp Med* **8**, 5499-5505 (2015).

40. Gloss, B.S. & Dinger, M.E. The specificity of long noncoding RNA expression. *Biochim Biophys Acta* (2015).

41. Silva, A., Bullock, M. & Calin, G. The Clinical Relevance of Long Non-Coding RNAs in Cancer. *Cancers (Basel)* **7**, 2169-2182 (2015).

42. Bussemakers, M.J.*, et al.* DD3: a new prostate-specific gene, highly overexpressed in prostate cancer. *Cancer Res* **59**, 5975-5979 (1999).

43. Lee, G.L., Dobi, A. & Srivastava, S. Prostate cancer: diagnostic performance of the PCA3 urine test. *Nat Rev Urol* **8**, 123-124 (2011).

44. Fatemi, R.P., Velmeshev, D. & Faghihi, M.A. De-repressing LncRNA-Targeted Genes to Upregulate Gene Expression: Focus on Small Molecule Therapeutics. *Mol Ther Nucleic Acids* **3**, e196 (2014).

45. Sanchez, Y. & Huarte, M. Long non-coding RNAs: challenges for diagnosis and therapies. *Nucleic Acid Ther* **23**, 15-20 (2013).

## Chapter 4: Discussion and Future Perspectives

# Summary

T-cell acute lymphoblastic leukemia (T-ALL) is a highly aggressive malignant disorder. While originally associated with poor prognosis, more recent intensified T-ALL therapy has led to remarkable improvements in survival of these patients. Unfortunately, these therapeutic schemes are associated with severe acute and long-term toxicities, thus demanding for further research in order to design more precision medicine oriented treatment. Importantly, for T-ALL patients with relapsed and refractory T-ALL, outcome remains extremely poor, thus urging further investigations to design therapies with further reduced relapse risk and/or novel treatment to cure relapsed cases. To shift towards this personalized medicine approach, a more profound understanding of the molecular basis of T-ALL progression is required. Several decades of genetic studies in T-ALL have uncovered a remarkable heterogeneous and complex landscape of combined oncogenic and loss-of-function mutations that contribute to malignant thymocyte transformation. One of the major challenges in T-ALL research is to unravel in detail how the diverse complement of oncogenes and tumor suppressors functionally contribute to T-ALL pathogenesis and response to therapy. To this end, I have studied the functional properties and cooperation of several key players that participate in normal and malignant T-cell development at the level of transcriptional regulatory networks.

*TLX1* is a major driver oncogene causing transformation of immature thymocytes towards T-ALL. Previous pioneering work partly uncovered its mode of action in relation to T-ALL formation, showing that ectopic overexpression of TLX1 in immature thymocytes causes repression of multiple T-ALL tumor suppressor genes. The study performed during this doctoral mandate, led to the observation of an unexpected antagonism between the TLX1 and NOTCH1 oncogenes, with activated TLX1 suppressing *NOTCH1* and key NOTCH1 target genes. Based on this finding, we hypothesized that this unique interaction between both oncogenes could explain the presence of *NOTCH1* mutations in most TLX1 driven T-ALL. Furthermore, the required cooperativity of *NOTCH1* (pathway) activating mutations can also explain the very long latency of T-ALL development in a TLX1 driven leukemia mouse model

## Summary

(**paper 1**). In addition to *NOTCH1* mutations, *PHF6* loss-of-function mutations are also frequently observed, pointing at a further putative required cooperative genetic lesion for full-blown TLX1 driven T-ALL formation. Given the lack of insight into the normal cellular function of the epigenetic reader protein PHF6, I investigated its role during normal hematopoiesis and observed a profound effect of PHF6 loss on hematopoietic lineage development (**paper 2**). Moreover, in the context of *TLX1* driven T-ALL formation, I identified the tyrosine kinase '*interleukine-7 receptor*' (*IL7R*) as a robustly upregulated gene upon PHF6 knockdown. Given the role of IL7R signaling in survival of maturing thymocytes, this observation opens an exciting perspective that PHF6 loss is required as an essential cooperative event in TLX1 driven T-ALL pathogenesis by re-installment of TLX1 repressed IL7R expression. Importantly, in addition to paving the way for further animal modeling and mechanistic studies, this finding is also highly relevant in the context of design of novel therapies targeting IL7R downstream JAK-STAT signaling (**paper 3**).

Until recently, transcriptional regulatory networks were mainly studied from a 'gene-protein coding' genomic viewpoint. Several studies have challenged this central dogma based on the proven role of non-coding RNAs in control of normal cellular behavior. Given this exciting new perspective on further expanding complexity of gene regulation during normal development and malignant transformation, I decided to study the role of such micro-RNAs (miRNAs) and long non-coding RNAs (lncRNAs) in T-ALL perturbed transcriptional networks. More specifically, I studied the role of miRNAs under control of TAL1 (**paper 4**), unraveled the landscape of lncRNAs implicated in the NOTCH1 signaling pathway (**paper 5**) and performed the first landscaping of the TLX1 lncRNAome (**paper 6**).

In conclusion, my work has contributed to novel insights into transcriptional networks in normal and malignant T-cell development, revealing several novel nodes for therapeutic intervention in the pursuit of personalized medicine development in the field of T-ALL research.

# Samenvatting

T-cel acute lymfoblastische leukemie (T-ALL) is een uiterst agressieve, maligne aandoening. Hoewel dit type kanker voorheen gekenmerkt werd door een slechte prognose, heeft de evolutie naar geïntensifieerde therapie geleid tot een enorme verbetering in de huidige overlevingskansen van T-ALL patiënten. Deze behandelingsstrategieën zijn echter geassocieerd met heel wat toxische neveneffecten, zowel op korte als lange termijn. Verder onderzoek is daarom vereist om de overgang naar gepersonaliseerde en gerichte behandeling mogelijk te maken. Voornamelijk voor T-ALL patiënten die hervallen of resistent zijn voor de huidige behandelingsprotocollen, blijft de kans op genezing enorm gering, wat de sterke nood aan behandelingsmethodes waarbij geen herval kan optreden of die in staat zijn patiënten met herval van ziekte te genezen verder onderstreept. Om de transitie naar dergelijke gepersonaliseerde behandeling mogelijk te maken is een grondigere kennis van de moleculaire basis van T-ALL progressie van uitermate belang. Verscheidene decennia van genetische studies omtrent T-ALL hebben geleid tot de ontrafeling van een onwaarschijnlijk heterogene en complexe constellatie van oncogene en verlies-van-functie mutaties die bijdragen tot de maligne transformatie van voorloper T-cellen. Eén van de huidige uitdagingen in het onderzoek naar T-ALL, omvat het ontrafelen van de manier waarop het geheel aan oncogenen en tumor-suppressor genen functioneel bijdragen tot T-ALL pathogenese en de respons op therapie. In dit opzicht heb ik de functionele eigenschappen en de samenwerking tussen verschillende belangrijke factoren in normale en maligne T-cel ontwikkeling bestudeerd op het niveau van transcriptionele netwerken.

De transcriptiefactor TLX1 is één van de voornaamste ‘driver’ oncogenen die maligne transformatie van ontwikkelende T-cellen naar T-ALL lymfoblasten veroorzaakt. Baanbrekend werk heeft reeds eerder aangetoond dat de ectopische expressie van TLX1 van belang is in T-ALL vorming door de werking als repressor eiwit voor heel wat gekende T-ALL tumor suppressor genen in voorloper T-cellen. Het onderzoek in dit doctoraatsproefschrift heeft aangetoond dat een functioneel antagonisme zich voordoet tussen de oncogenen TLX1 en NOTCH1 in pre-leukemische T-ALL stadia,

waarbij TLX1 de expressie van *NOTCH1* en een aantal van zijn belangrijke doelwitgenen onderdrukt. Op basis van deze bevinding stellen we als hypothese voorop dat deze unieke antagonistische interactie tussen twee oncogenen de uiterst hoge frequentie van activerende *NOTCH1* mutaties in TLX1-gedreven T-ALL kan verklaren. Daarnaast vormen de vereiste activerende mutaties in de NOTCH1 signaalcascade een mogelijke verklaring voor de uiterst lange latentieperiode van T-ALL ontwikkeling in het eerder beschreven TLX1 gedreven T-ALL muismodel (**manuscript 1**). Naast mutaties in *NOTCH1*, komen ook vaak verlies-van-functie mutaties voor in het *PHF6* gen in TLX1-positieve T-ALL patiënten, wat aangeeft dat bijkomende coöperatieve genetische veranderingen nodig zijn om te evolueren naar een mature, TLX1-gedreven T-ALL vorming. De normale cellulaire functie van de epigenetische regulator PHF6 is tot op heden ongekend. In mijn proefschrift heb ik de rol van PHF6 in normale humane hematopöese bestudeerd. Dit heeft tot het inzicht geleid dat verlies van PHF6 expressie de vorming van de verschillende types hematopoiëtische cellen sterk verstoort (**manuscript 2**). Daarnaast heeft dit onderzoek geleid tot de identificatie van de '*interleukine 7 receptor*' (*IL7R*) als één van de sterkst opgereguleerde genen bij PHF6 neerregulatie in de context van TLX1-gedreven T-ALL. IL7R-signalisatie is van uiterst belang in de overleving van ontwikkelende T-cellen. Deze observatie postuleert dus dat verlies van PHF6 een cruciale coöperatieve genetische wijziging is in TLX1-gedreven T-ALL vorming, om zo de onderdrukking van IL7R expressie door TLX1 te kunnen herstellen (**manuscript 3**).

Transcriptionele regulatorische netwerken werden tot recent nog voornamelijk vanuit het 'gen-eiwit' genetisch perspectief benaderd. Verschillende studies hebben dit centrale dogma nu in vraag gesteld op basis van de huidig aangetoonde cruciale rol van niet-coderende RNA species in de regulatie van normale cellulaire ontwikkeling. In het kader van deze nieuwe, evoluerende inzichten in de complexiteit van genregulatie tijdens normale ontwikkeling en maligne transformatie, bestudeerde ik tijdens dit doctoraatsmandaat de rol van micro-RNAs en lange niet-coderende RNAs in de verstoorde transcriptionele netwerken die T-ALL vorming onderbouwen. In het bijzonder hebben deze studies geleid tot de identificatie van micro-RNAs die gereguleerd worden door de transcriptiefactor TAL1

(**manuscript 4**), de ontdekking van lange niet-coderende RNAs die deel uitmaken van de NOTCH1 signaalcascade (**manuscript 5**) en de ontrafeling van het complement van lange niet-coderende RNAs onder controle van TLX1 (**manuscript 6**).

Samenvattend heeft het onderzoek uitgevoerd in het kader van dit doctoraatsproefschrift bijgedragen tot nieuwe inzichten in de transcriptionele netwerken van belang in normale en maligne T-cel ontwikkeling, waarbij verschillende nieuwe aanknopingspunten voor de ontwikkeling van nieuwe therapeutische strategieën werden blootgelegd, in het kader van het streven naar gepersonaliseerde en doelgerichte behandeling in het T-ALL onderzoeksgebied.

# Dankwoord

Ik herinner me nog goed de eerste gesprekken met mijn promotor prof. Frank Speleman voor de aanvang van dit doctoraat: 'Denk er nog eens goed over na of je dit zeker wil doen, 4 jaar is een lange tijd'. Voor mij was er geen twijfel, de kans om me als wetenschapper te vormen in een sterk en gemotiveerd onderzoeksteam wou ik zo graag grijpen. De tijd is voorbij gevlogen, we zijn ondertussen vijf jaar verder en ik kan terugkijken op een fantastische periode. De stimulerende en warme groep van collega's waarin ik heb mogen vertoeven is uitzonderlijk en daar ben ik enorm dankbaar voor. De boeiende en uitdagende projecten waar ik mocht aan meewerken, de talrijke binnen- en buitenlandse meetings waaraan ik heb deelgenomen, de samenwerkingen met binnen- en buitenlandse onderzoeksgroepen, … zijn allen een enorme leerschool geweest tijdens dit doctoraatstraject, niet alleen als onderzoeker maar ook als persoon.

In de eerste plaats wil ik in dit dankwoord dan ook voor dit alles mijn promotor prof. Frank Speleman bedanken. Je eindeloze enthousiasme en passie voor wetenschappelijk onderzoek zijn zo aanstekelijk, dat ik onder jouw begeleiding de spirit vond om te blijven doorgaan, ook al waren sommige projecten een enorme uitdaging. Frank, je was mijn supervisor, mentor, coach in schrijf- en presentatie-skills, mental coach, … in al deze aspecten als promotor was je uitmuntend en heb je een sfeer en omgeving gecreëerd waarin ik me als wetenschapper ten volle heb kunnen ontplooien en daar ben ik je enorm dankbaar voor. Ik kijk dan ook met vol enthousiasme uit naar onze verdere samenwerking.

Verder wil ik ook mijn co-promotoren prof. Pieter van Vlierberghe en prof. Tom Taghon heel erg bedanken. Pieter, onze samenwerking heeft een vliegende start genomen nadat je terug was uit New York en is gegroeid tot een belangrijke leerschool voor mij tijdens dit doctoraat. Brainstormen over talrijke projecten, samen werken om een manuscript te vormen en te schrijven tot het goed zit, … samen met Frank was je steeds paraat om me te helpen en ondersteuning te bieden waar nodig, enorm bedankt daarvoor. Tom, de samenwerking met jouw lab gaf me

de opportuniteit om mee te proeven van onderzoek in de context van normale hematopoëse en ervaar ik dan ook als een enorme meerwaarde van dit doctoraat. Samen met Inge zijn we verschillende uitdagingen tijdens dit doctoraat aangegaan, waarbij ik van jullie beide veel heb geleerd en de samenwerking met jullie heeft ook een erg motiverende invloed gehad tijdens deze volledige periode.

Daarnaast wil ik ook graag dr. Pieter Rondou bedanken voor de leerrijke begeleiding en ondersteuning. Van bij de start van mijn master thesis tot op heden zijn we er samen voor gegaan om de rol van PHF6 in normale en maligne T-cel ontwikkeling te bestuderen. Je stond altijd paraat om me te helpen, bedankt daarvoor!

Een speciaal woordje van dank wil ik heel graag richten tot Aline. Van bij de start van mijn master thesis hebben we elkaar leren kennen en dit is echt kunnen uitgroeien tijdens deze doctoraatsperiode tot een duo-samenwerking die draait als een tandem. Ik bewonder je inzet en enthousiasme waarmee je elke dag er weer voor gaat, ook al moesten we soms moeilijke en uitdagende experimenten tegemoet, merci Aline!

Tijdens de periode van deze PhD thesis, heb ik ook met heel wat andere onderzoekers mogen kennis maken en samenwerken, een zeer verrijkende en boeiende ervaring. Ik had dit PhD traject dan ook nooit kunnen vervolledigen zonder de hulp van heel wat mensen buiten het lab en ik wil hier dan ook een aantal van hen in de aandacht brengen. Van bij de aanvang van dit doctoraat tot het einde heb in het L3 lab van prof. Bruno Verhasselt de kans gekregen om me te ontplooien in de wondere wereld van 'virusproductie en transductie', bedankt aan het volledige L3-team. In samenwerking met het lab onder leiding van prof. Jan Cools, kreeg ik de kans om onderzoek te verrichten onder andere samen met dr. Charles de Bock, van wie ik de eerste mouse handling skills heb aangeleerd gekregen en die steeds paraat stond tijdens onze samenwerkingen, bedankt Charley!

Daarnaast wil ik ook een grote 'dankjewel' richten naar mijn vroegere en huidige bureaugenootjes waar ik altijd heb op kunnen rekenen en vele leuke momenten heb

## Dankwoord

mogen beleven (ik hoop dat ik hier niemand vergeet): Nadine, Pieter R, Sofie, Evelien, Joni, Suzanne, Hetty, Fary, Aline, Jolien, Annelynn, Bruce, Karen, Frank. Superbedankt voor de grappige (en soms hilarische) momenten, de sappige roddels en de leuke sfeer! Verder wil ik uiteraard ook een heel dikke merci richten aan alle andere collega's, iedereen staat steeds paraat om elkaar te helpen en dankzij jullie is er steeds een 'warme' wersksfeer in het lab.

Een speciaal dankwoord ook aan mijn familie en vrienden. Mijn ouders, broer en zus hebben in dit volledige traject een warm nest van onuitputtelijke steun en aanmoediging betekend, what a family! Ook de schoonfamilie verdient hiervoor zeker ook een hartelijke merci. Daarnaast wil ik de sGKC, de dames van het 'thesis hokje' en andere vriendenkringen enorm bedanken voor de vele leuke en gezellige momenten samen. Last but not least wil ik mijn liefste, Sven, bedanken om er altijd te zijn voor mij en de zalige momenten samen.

## Curriculum Vitae

# Kaat Durinck

## Personalia

Address: Antwerpsesteenweg 72
Postal code/City: 9000 Gent
Country: Belgium
Phone: 0032 474916573
Date of birth: 07/02/1987
E-mail address: kaat.durinck@ugent.be
Nationality: Belgian

## Experience

**9 months Faculty grant of the Faculty of Medicine and Health Sciences**

- **Period**: January 1st, 2016 to September 30th, 2016

**1 year PhD grant of VLK Emmanuel van der Schueren sholarship**

- **Period**: 2014 – 2015
  **Institute**: Ghent University, Center for Medical Genetics, Ghent, Belgium
  **Thesis**: Unraveling the role of PHF6 in normal T-cell development and T-cell acute lymphoblastic leukemia
  **Promotor**: Prof. dr. Frank Speleman & **co-promotors** prof. dr. ir. Pieter van Vlierberghe and prof. dr. Tom Taghon

**Doctoral research Assistant, 4 years PhD grant of IWT, Flanders**

- **Period**: 2011 – 2014
  **Institute**: Ghent University, Center for Medical Genetics, Ghent, Belgium
  **Thesis**: Unraveling the role of PHF6 in normal T-cell development and T-cell acute lymphoblastic leukemia
  **Promotor**: Prof. dr. Frank Speleman & **co-promotors** prof. dr. ir. Pieter van Vlierberghe and prof. dr. Tom Taghon

## Curriculum Vitae

# Education

**Master of Science in Biochemistry and Biotechnology**

- **Period**: 2005-2010
  **Institute**: Ghent University
  **Thesis**: Ontrafelen van de rol van PHF6 in normale T-cel ontwikkeling en acute T-cel leukemie
  **Promotor**: Prof. dr. Frank Speleman & co-promotor dr. Pieter Rondou

# Scientific Achievements

**Publications, oral presentations, posters, conferences and supervision of students**

## Publications:

1. Durinck K, Goossens S, Peirs S, Wallaert A, Van Loocke W, Matthijssens F, Pieters T, Milani G, Lammens T, Rondou P, Van Roy N, De Moerloose B, Benoit Y, Haigh J, Speleman F, Poppe B, Van Vlierberghe P. **Novel biological insights in T-cell acute lymphoblastic leukemia**. Exp Hematol. 2015 Aug;43(8):625-39. (*IF: 2.746, ranking: Q3*)

2. Durinck K, Loocke WV, Van der Meulen J, Van de Walle I, Ongenaert M, Rondou P, Wallaert A, de Bock CE, Van Roy N, Poppe B, Cools J, Soulier J, Taghon T, Speleman F, Van Vlierberghe P. **Characterization of the genome-wide TLX1 binding profile in T-cell acute lymphoblastic leukemia**. Leukemia. 2015 Dec;29(12):2317-27 (*IF: 10.431, ranking: Q1*)

3. Goossens S, Radaelli E, Blanchet O, Durinck K, Van der Meulen J, Peirs S, Taghon T, Tremblay CS, Costa M, Farhang Ghahremani M, De Medts J, Bartunkova S, Haigh K, Schwab C, Farla N, Pieters T, Matthijssens F, Van Roy N, Best JA, Deswarte K, Bogaert P, Carmichael C, Rickard A, Suryani S, Bracken LS, Alserihi R, Canté-Barrett K, Haenebalcke L, Clappier E, Rondou P, Slowicka K, Huylebroeck D, Goldrath AW, Janzen V, McCormack MP, Lock RB, Curtis DJ, Harrison C, Berx G, Speleman F, Meijerink JP, Soulier J, Van Vlierberghe P, Haigh JJ. **ZEB2 drives immature T-cell lymphoblastic leukaemia development via enhanced tumour-initiating potential and IL-7 receptor signalling**. Nat Commun. 2015 Jan 7;6:5794. (*IF: 11.47, ranking Q1*)

4. Durinck K*, Wallaert A*, Van de Walle I, Van Loocke W, Volders PJ, Vanhauwaert S, Geerdens E, Benoit Y, Van Roy N, Poppe B, Soulier J, Cools J, Mestdagh P, Vandesompele J, Rondou P, Van Vlierberghe P, Taghon T, Speleman F. The Notch driven long non-coding RNA repertoire in T-cell acute lymphoblastic leukemia. Haematologica. 2014 Dec;99(12):1808-16. (*IF: 5.814, ranking: Q1*)

5. Bethuyne J, De Gieter S, Zwaenepoel O, Garcia-Pino A, Durinck K, Verhelle A, Hassanzadeh-Ghassabeh G, Speleman F, Loris R, Gettemans J. **A nanobody modulates the p53 transcriptional program without perturbing its functional architecture**. Nucleic acids research. 2014;42(20):12928-38 (*IF: 8.867, ranking: Q1*)

6. Van der Meulen J, Sanghvi V, Mavrakis K, Durinck K, Fang F, Matthijssens F, Rondou P, Rosen M, Pieters T, Vandenberghe P, Delabesse E, Lammens T, De Moerloose B, Menten B, Van Roy N, Verhasselt B, Poppe B, Benoit Y, Taghon T, Melnick AM, Speleman F, Wendel HG, Van Vlierberghe P. T**he H3K27me3 demethylase UTX is a gender-specific tumor suppressor in T-cell acute lymphoblastic leukemia**. Blood. 2015;125(1):13-21 (*IF: 10.452, ranking: Q1*)

7. Atak ZK, Gianfelici V, Hulselmans G, De Keersmaecker K, Devasia AG, Geerdens E, Mentens N, Chiaretti S, Durinck K, Uyttebroeck A, Vandenberghe P, Wlodarska I, Cloos J, Foà R, Speleman F, Cools J, Aerts S. C**omprehensive analysis of transcriptome variation uncovers known and novel driver events in T-cell acute lymphoblastic leukemia**. PLoS genetics. 2013;9(12):e1003997 (*IF: 8.167,ranking: Q1*)

8. Bustin SA, Benes V, Garson J, Hellemans J, Huggett J, Kubista M, Mueller R, Nolan T, Pfaffl MW, Shipley G, Wittwer CT, Schjerling P, Day PJ, Abreu M, Aguado B, Beaulieu JF, Beckers A, Bogaert S, Browne JA, Carrasco-Ramiro F, Ceelen L, Ciborowski K, Cornillie P, Coulon S, Cuypers A, De Brouwer S, De Ceuninck L, De Craene J, De Naeyer H, De Spiegelaere W, Deckers K, Dheedene A, Durinck K, Ferreira-Teixeira M, Fieuw A, Gallup JM, Gonzalo-Flores S, Goossens K, Heindryckx F, Herring E, Hoenicka H, Icardi L, Jaggi R, Javad F, Karampelias M, Kibenge F, Kibenge M, Kumps C, Lambertz I, Lammens T, Markey A, Messiaen P, Mets E, Morais S, Mudarra-Rubio A, Nakiwala J, Nelis H, Olsvik PA, Pérez-Novo C, Plusquin M, Remans T, Rihani A, Rodrigues-Santos P, Rondou P, Sanders R, Schmidt-Bleek K, Skovgaard K, Smeets K, Tabera L, Toegel S, Van Acker T, Van den Broeck W, Van der Meulen J, Van Gele M, Van Peer G, Van Poucke M, Van Roy N, Vergult S, Wauman J, Tshuikina-Wiklander M, Willems E, Zaccara S, Zeka F, Vandesompele J. T**he need for transparency and good practices in the qPCR literature.** Nature methods. 2013;10(11):1063-7 (*IF: 25.953, ranking: Q1*)

9. Correia NC, Durinck K, Leite AP, Ongenaert M, Rondou P, Speleman F, Enguita FJ, Barata JT. **Novel TAL1 targets beyond protein-coding genes: identification of TAL1-regulated microRNAs in T-cell acute lymphoblastic leukemia**. Leukemia. 2013 Jul;27(7):1603-6. (*IF: 10.431, ranking: Q1*)

## Curriculum Vitae

Oral presentations:

- **Unraveling a NOTCH1-lncRNA-miRNA regulatory network in acute T-cell lymphoblastic leukemia and normal T-cell development**. Durinck K, Mestdagh P, Taghon T, Van der Meulen J, Van de Walle I, Volders PJ, Pattyn F, Van Roy N, Benoit Y, Poppe B, Van Vlierberghe P, Menten B, Vandesompele J, Rondou P, Speleman F. 12th BeSHG meeting, March 2nd, 2012, Liège, Belgium

- **Functional interplay of NOTCH1 and PHF6: balancing between normal T-cell development and T- ALL.** Durinck K, Van der Meulen J, Pattyn F, Ongenaert M, Verhasselt B, Taghon T, Van Roy N, Poppe B, Van Vlierberghe P, Rondou P, Speleman F. 1st Oncopoint meeting, May 23th, 2012, Ghent, Belgium

- **Unraveling a NOTCH1-lncRNA-miRNA regulatory network in acute T-cell lymphoblastic leukemia and normal T-cell development.** Durinck K, Mestdagh P, Taghon T, Van der Meulen J, Van de Walle I, Volders PJ, Pattyn F, Van Roy N, Benoit Y, Poppe B, Van Vlierberghe P, Menten B, Vandesompele J, Rondou P, Speleman F. 17th Congress of the European Hematology Association, June 14-17th, 2012, Amsterdam, The Netherlands

- **Expanding the TLX1-regulome in T-cell acute lymphoblastic leukemia towards long non-coding RNAs.** Durinck K, Van der Meulen J, Ongenaert M, Volders PJ, Wallaert A, Van Roy N, Benoit Y, Poppe B, Mestdagh P, Vandesompele J, Rondou P, Soulier J, Van Vlierberghe P, Speleman F. 55th ASH Annual Meeting and Exposition, December 5-10th, 2013, New Orleans, USA

- **Expanding the TLX1-regulome in T-cell acute lymphoblastic leukemia towards long non-coding RNAs.** Durinck K, Van der Meulen J, Ongenaert M, Volders PJ, Wallaert A, Van Roy N, Benoit Y, Poppe B, Mestdagh P, Vandesompele J, Rondou P, Soulier J, Van Vlierberghe P, Speleman F. 2nd Oncopoint meeting, February 6th, 2014, Ghent, Belgium

- **PHF6 loss causes IL7R upregulation and sensitization to JAK inhibitors**. Durinck K, Van de Walle I*, De Bock C*, Rondou P*, Van Roy N, Benoit Y, Poppe B, Soulier J, Taghon T,Cools J, Van Vlierberghe P and Speleman F. Pre-EHA workshop, June 10-11th, 2014, Amsterdam, The Netherlands

- **Expanding the TLX1 regulome towards long non-coding RNAs**. Durinck K, Van der Meulen J, Ongenaert M, Volders PJ, Wallaert A, Van Roy N, Benoit Y, Poppe B, Mestdagh P, Vandesompele J, Rondou P, Soulier J, Van Vlierberghe P, Speleman F. Non-coding RNA meeting, June 22nd-25th, Heidelberg, Germany

- **Functional genomic dissection of the PHF6-TLX1 regulatory axis in T-ALL**. Durinck K, Van de Walle I*, De Bock C*, Rondou P*, Van Roy N, Benoit Y, Poppe B, Soulier J, Taghon T,Cools J, Van Vlierberghe P and Speleman F. re-EHA workshop, June 9-10th, 2014, Rotterdam, The Netherlands

Posters:

- **Unraveling a NOTCH1-lncRNA-miRNA regulatory network in acute T-cell lymphoblastic leukemia and normal T-cell development.** Durinck K, Mestdagh P, Taghon T, Van der Meulen J, Van de Walle I, Volders PJ, Pattyn F, Van Roy N, Benoit Y, Poppe B, Van Vlierberghe P, Menten B, Vandesompele J, Rondou P, Speleman F. Keystone Symposia: non-coding RNAs, March 31st-April 5th, 2012, Utah, USA

- **Unraveling a NOTCH1-lncRNA-miRNA regulatory network in acute T-cell lymphoblastic leukemia and normal T-cell development.** Durinck K, Mestdagh P, Taghon T, Van der Meulen J, Van de Walle I, Volders PJ, Pattyn F, Van Roy N, Benoit Y, Poppe B, Van Vlierberghe P, Menten B, Vandesompele J, Rondou P, Speleman F. Cell Symposia: Angiogenesis, Metabolic Regulation and Cancer Biology in association with VIB, July 6-8th, 2012, Leuven, Belgium

- **Integrative analysis of the NOTCH1 regulatory network identifies key downstream lncRNAs in acute T-cell lymphoblastic leukemia and normal T-cell development.** Durinck K, Mestdagh P, Volders PJ, Taghon T, Van de Walle I, Ongenaert M, Van der Meulen J, Vanhauwaert S, Wallaert A, Soulier J, Van Roy N, Benoit Y, Poppe B, Menten B, Vandesompele J, Van Vlierberghe P, Rondou P, Speleman F. Keystone Symposia: noncoding RNAs in Development and Cancer, January 20th-25th, 2013, Vancouver, Canada

- **NOTCH1 driven miRNAs implicated in normal and malignant T-cell development.** Durinck K, Van der Meulen J, Van de Walle I, Pipelers P, Mestdagh P, Ongenaert M, Van Roy N, Benoit Y, Poppe B, Vandesompele J, De Preter K, Thas O, Van Vlierberghe P, Rondou P, Soulier J, Speleman F*, Taghon T*. EHA-ESH: Second Scientific Workshop: T-cell acute lymphoblastic leukemia, March 22nd-24th, 2013, Lisbon, Portugal

- **NOTCH1 signaling induces global transcriptional changes in long non-coding RNA expression in T-cell acute lymphoblastic leukemia and normal T-cell development.** Durinck K, Mestdagh P, Volders PJ, Taghon T, Van de Walle I, Ongenaert M, Van der Meulen J, Vanhauwaert S, Wallaert A, Soulier J, Van Roy N, Benoit Y, Poppe B, Menten B, Vandesompele J, Van Vlierberghe P, Rondou P, Speleman F. EHA-ESH: Second Scientific Workshop: T-cell acute lymphoblastic leukemia, March 22nd-24th, 2013, Lisbon, Portugal

## Curriculum Vitae

- **Phf6 deficiency causes defective primitive and definitive hematopoiesis during zebrafish development.** Vanhauwaert S, Janssens E, Willaert A, Durinck K, De Paepe A, Vandesompele J, Van Vlierberghe P, Rondou P, Speleman F. 8th European Zebrafish Meeting, July 9-13th, 2013, Barcelona, Spain

- **The plant homeodomain (PHD)-like finger protein PHF6 chromatin binding pattern and transcriptional regulation indicates a functional link with NOTCH1 in T-cell acute lymphoblastic leukemia.** Durinck K, Van der Meulen J, Ongenaert M, Verhasselt B, Taghon T, Van de Walle I, Van Roy N, Poppe B, Benoit Y, Gevaert K, Van Vlierberghe P, Rondou P, Speleman F. Cell symposia: Cancer Epigenomics, October 6-8th, 2013, Sitges, Spain

- **Characterization of the NOTCH1 driven miRNA network that controls normal human T- cell development.** Van der Meulen J, Durinck K, Van de Walle I, Mestdagh P, De Preter K, Van Peer G, Van Roy N, Poppe B, Ongenaert M, Vandesompele J, Rondou P, Van Vlierberghe P, Speleman F, Taghon T. 2nd Oncopoint Meeting, February 6th, 2014, Ghent, Belgium

- **Phf6 plays a role in hematopoiesis and thymopoiesis in zebrafish.** Janssens E., Vanhauwaert S, Willaert A, Durinck K, De Paepe A, Vandesompele J, Van Vlierberghe P, Rondou P, Speleman F. 2nd Oncopoint Meeting, February 6th, 2014, Ghent, Belgium

- **Expanding the TLX1-regulome in T-cell acute lymphoblastic leukemia towards long non-coding RNAs.** Durinck K, Van der Meulen J, Ongenaert M, Volders PJ, Wallaert A, Van Roy N, Benoit Y, Poppe B, Mestdagh P, Vandesompele J, Rondou P, Soulier J, Van Vlierberghe P, Speleman F. 14th BeSHG meeting, February 7th, 2014, Antwerp, Belgium

- **Unique lncRNA signatures mark the major T-ALL genetic subgroups.** Wallaert A, Durinck K, Vanloocke W, Volders PJ, Benoit Y, Poppe B, Mestdagh P, Vandesompele J, Soulier J, Cools J, Van Vlierberghe P, Rondou P, Speleman F. 14th BeSHG meeting, February 7th, 2014, Antwerp, Belgium

- **PHF6 loss drives IL7R oncogene addiction in T-ALL.** Durinck K, Rondou P*, Van de Walle I*, De Bock C, Van Roy N, Benoit Y, Poppe B, Taghon T, Soulier J, Cools J, Van Vlierberghe P and Speleman F. 19th congress of EHA, June 12-15th, Milan, Italy

- **Transcriptional antagonism between the cooperative oncogenes NOTCH1 and TLX1 in T-cell acute lymphoblastic leukemia.** Durinck K, Van Loocke W, Van der Meulen J, Van de Walle I, Rondou P, de Bock CE, Poppe B, Cools J, Soulier J, Taghon T, Speleman F and Van Vlierberghe P. AACR meeting Hematological Malignancies, September 20-23th, Philadelphia, Pennsylvania, USA

- ***PHF6* loss compensates for TLX1 mediated repression of IL7R expression and shows a functional interplay with the SWI-SNF remodeling complex during T-ALL formation.** Durinck K, Van de Walle I*, De Bock C*, Rondou P*, Van Roy N, Benoit Y, Poppe B, Soulier J, Taghon T,Cools J, Van Vlierberghe P and Speleman F. Keystone meeting, January 24-30th, Denver, USA

- **Functional genomic dissection of the TLX1 regulome in T-ALL.** Durinck K, Van Loocke W, Van der Meulen J, Van de Walle I, Rondou P, de Bock CE, Poppe B, Cools J, Soulier J, Taghon T, Speleman F and Van Vlierberghe P. FASEB meeting, July 26th-31st, Vermont, Saxtons River, USA

- **The T-ALL oncogene TLX1 controls enhancer lncRNA expression.** Durinck K, Van Loocke W, Matthijssens F, Verboom K, Van de Walle I, Wallaert A, Volders PJ, Van Roy N, Benoit Y, Poppe B, Rondou P, Mestdagh P, Vandesompele J, De Laat W, Taghon T, Soulier J, Van Vlierberghe P, Speleman F. AACR meeting Epigenetics, September 24-27th, Atlanta, USA

## Conferences:

- 7th European Zebrafish Meeting, July 5th-9th, 2011, Edinburgh, Scotland
- 53th ASH Annual Meeting and Exposition, December 10th-13th, 2011, San Diego, USA
- 12th BeSHG Meeting, March 2nd, 2012, Liège, Belgium
- 1st Oncopoint Meeting, May 23th, 2012, Ghent, Belgium
- 17th Congress of the European Hematology Association, June 14-17th, 2012, Amsterdam, The Netherlands
- Cell Symposia: Angiogenesis, Metabolic Regulation and Cancer Biology in association with VIB, July 6th-8th, 2012, Leuven, Belgium
- Keystone Symposia: noncoding RNAs in Development and Cancer, January 20-25th, 2013, Vancouver, Canada
- EHA-ESH: Second Scientific Workshop: T-cell acute lymphoblastic leukemia, March 22nd-24th, 2013, Lisbon, Portugal
- Cell symposia: Cancer Epigenomics, October 6th-8th, 2013, Sitges, Spain
- 55th ASH Annual Meeting and Exposition, December 5th-10th, 2013, New Orleans, USA

- 2nd Oncopoint Meeting, February 6th, 2014, Ghent, Belgium
- 14th BeSHG meeting, February 7th, 2014, Antwerp, Belgium
- 1st Masterclass Hematology meeting, 9-10th June, 2014, Amsterdam, The Netherlands
- EMBL meeting on Non-coding RNAs in development and disease, 22nd-25th June, 2014, Heidelberg, Germany
- 56th Annual ASH meeting, December 6-9th, 2014, San Francisco, USA
- Keystone epigenetics meeting, January 24-30th, 2015, Denver, USA
- 2nd Masterclass Hematology meeting, 9-10th June, 2015, Rottterdam The Netherlands
- FASEB meeting, July 26th-31st, Vermont, Saxtons River, USA
- AACR meeting on Epigenetics, September 24-27th, 2015, Atlanta, USA

## Courses

- **Felasa C certificate for Laboratory Anima science**, academic year 2011-2012 Ghent University, Belgium
- **BITS course, RNA-seq analysis for differential expression,** April 22nd and 24th, 2014, VIB, Leuven, Belgium
- **Wellcome Trust Advanced Course on Epigenetics**, November 10-19th, 2014, Sanger Institute, Cambridge, UK

## Training

- **Training in 4C-sequecing**, host lab Wouter de Laat, Hubrecht Institute, February 2nd - 6th, Utrecht, The Netherlands

## Supervision of students:

**Z-lijn paper, 2nd Bachelor of Medicine 2010-2011:** Sofie Demoen, Het kankerepigenoom: potentieel doelwit voor nieuwe therapeutische strategieën. Supervision: Kaat Durinck, promotor: prof. Frank Speleman

**Master Thesis, 2nd Master of Biomedical Sciences 2011-2012**: Maaike Van Hoecke, Functionele analyse van PHF6 als tumor suppressor in T-cel acute lymfoblastische leukemie. Supervision: Kaat Durinck and Pieter Rondou, promotor: prof. Frank Speleman

**Z-lijn paper, 2nd Bachelor of Medicine 2011-2012**: Tomas Paquet, Deregulatie van het epigenetisch landschap in oncogenese als potentieel doelwit voor nieuwe

therapeutische strategieën. Supervision: Kaat Durinck, promotor: prof. Frank Speleman

**Master Thesis 2nd Master of Biomedical Sciences 2012-2013**: Hannelore Haemerlinck, Functionele analyse van PHF6 als tumor suppressor in T-cel acute lymfoblastische leukemie. Supervision: Kaat Durinck and Pieter Rondou, promotor: prof. Frank Speleman

**Z-lijn paper, 2nd Bachelor of Medicine 2012-2013:** Björn Tuytens, Toepassing van epigenetische therapeutica in hematologische maligniteiten. Supervision: Kaat Durinck, promotor: prof. Frank Speleman

**Z-lijn paper, 2nd Bachelor of Medicine 2012-2013:** Zander Macharis, Toepassing van epigenetische therapeutica in hematologische maligniteiten. Supervision: Kaat Durinck, promotor: prof. Frank Speleman

**Z-lijn paper, 2nd Bachelor of Medicine 2013-2014:** Siska Van den Hautte, Toepassing van epigenetische therapeutica in hematologische maligniteiten. Supervision: Kaat Durinck, promotor: prof. Frank Speleman

**Z-lijn, 2nd Bachelor of Medicine, 2014-2015**: Tessa Berben, Interleukine 7 receptor signalisatie als therapeutisch doelwit in T-cel leukemie. Supervision: Kaat Durinck, promotor: prof. Frank Speleman

**Z-lijn, 2nd Bachelor of Medicine, 2015-2016:** Elise de Cuyper, Bromodomein-inhibitoren als nieuwe epigenetische therapie in kanker. Supervision: Kaat Durinck, promotor: prof. Frank Speleman

**Z-lijn, 2nd Bachelor of Medicine, 2015-2016:** Tim Krols, Bromodomein-inhibitoren als nieuwe epigenetische therapie in kanker. Supervision: Kaat Durinck, promotor: prof. Frank Speleman

## List of main abbreviations

## List of main abbreviations

| | |
|---|---|
| AID | Activation Induced cytidine Deaminase |
| AML | Acute myeloid leukemia |
| ASO | antisense oligonucleotide |
| BFLS | Börjeson-Forssman-Lehmann syndrome |
| CD | Cluster of Differentiation |
| ceRNA | competing endogenous RNA |
| CHD | Chromodomain helicase |
| ChIP | Chromatin immunoprecipitation |
| CRISPR | Clustered regularly interspaced short palindromic sequences |
| CSS | Coffin-Siris syndrome |
| DNA | DeoxyriboNucleic Acid |
| DDR | DNA damage response |
| DNMT | DNA methyltransferase |
| EMT | Epithelial-mesenchymal transition |
| ETP | Early T-cell precursor |
| FACS | Fluorescence activated cell sorting |
| FCS | Fetal Calf Serum |
| GFP | Green Fluorescent Protein |
| GRAALL | Group for Research in Adult Acute Lymphoblastic Leukemia |
| GREAT | Genomic Regions Enrichment of Annotations |
| GSEA | Gene Set Enrichment Analysis |
| GSI | gamma-secretase inhibitor |
| HSC | Hematopoietic stem cell |
| ICN1 | Intracellular NOTCH1 fragment |
| IGF1R | Insulin Growth factor Receptor 1 |
| ING | Inhibitor of Growth |
| IL7R | Interleukin 7 receptor |
| INO80 | Inositol requiring 80 |
| KDM6A | Lysine-specific (K) demethylase 6A |
| lncRNA | long non-coding RNA |
| miRNA | micro-RNA |
| NCBRS | Nicolaides-Baraitser syndrome |

## List of main abbreviations

| | |
|---|---|
| NLS | Nuclear Localization Signal |
| NurD | Nucleosome Remodeling and Deacetylation |
| MAML | Mastermind-like |
| MBD | Methyl-Binding Domain |
| PHD | Plant Homeodomain |
| PRC2 | Polycomb group protein complex 2 |
| shRNA | short hairpin RNA |
| SWI-SNF | Switching defective/Sucrose Non-Fermenting |
| PHF6 | Plant Homeodomain zinc finger protein 6 |
| PTM | post-translational modification |
| qPCR | quantitative polymerase chain reaction |
| TAL1 | T-cell acute Lymphocytic Leukemia 1 |
| T-ALL | T-cell acute lymphoblastic leukemia |
| TCR | T-cell receptor |
| TDG | thymine DNA glycosylase |
| TET | Ten Eleven Translocation |
| TLX1 | T-cell leukemia homeobox 1 |
| UBF | Upstream Binding factor |
| ZEB2 | Zinc finger E-box binding homeobox 2 protein |